THE UNIVERSITY OF HULL

Physical and chemical properties of sporopollenin exine particles

being a Thesis submitted for the Degree of

Doctor of Philosophy

in the University of Hull

by

Sylvain Barrier, M.Eng. M.Sc.

July 2008

« *Un homme ne vit pas une seconde sans être influencé par quelque chose.*
On n'invente rien tout seul, bien sûr. » Georges Brassens.

Acknowledgements

This work would never have been successful without the help and support of many people. First of which stand my always optimistic and enthusiastic supervisor, Grahame Mackenzie, as well as my co-supervisor Steve Atkin, both to whom I owe the biggest debt of gratitude.

May other members of Sporomex and the SporoTeam, past and present, receive my deepest gratefulness. Many thanks to Steve Beckett, Lisa Blackwell and Matthew Thomasson, muchas gracias a Alberto Diego Taboada, merci beaucoup à Laurent Maillet, vielen Dank Andreas Löbbert.

A special thought goes to my predecessors on this project. Thanks to Sarah Kettley, Alia Boasman and Lesley Galbraith, merci à Bertrand Dinneweth, Aurélia Maulny, Ludovic Coutable, Aurélie Cointre, Cédric Desplanques et William Bienstman.

I would also like to acknowledge my academic co-workers for our fruitful collaboration. Thanks to Andrew Boa, Paul Fletcher, Leigh Madden, Tom Brown and Alan Rigby.

Technical staff must certainly not be forgotten. Thanks to Carol Kennedy, Bob Knight, Tony Sinclair, Ian Dobson and Jan Halder.

Finally I would like to thank the numerous project students and trainees for there motivation and the nice working atmosphere they established in the lab. Thanks to Ben Bateson, Jon Finch, Chris Moriarty, Chris Pinder and Simon Wright, ευχαριστώ Παναυιότα Ανδρέου (Panayiota Andreou), Μαρία Λειγη (Maria Leigh) και Μαρία Μιχαηλίδου (Maria Michaelidou), merci à Véronique Marzec, Ludovic Vanneville, Jean-Baptiste Rapinel, Vincent Panel, Adeline Ranoux, Antoine Favière, Alexandra Biance, Sophie Trettel, Aïcha Ouattou, Amandine Guidi, David Genest, Étienne Baco, Mélanie Burlion, Céline Nowak, Romain Tenchon, Stéphan Bielski et Vanessa Le Poupon.

Thanks to Tom, Dick and Harry. Merci à Pierre, Paul, Jacques et les autres.

Abstract

The chemical structure of sporopollenin was extensively reviewed, along with some considerations pertaining to its physical and biological properties. A comparative study is presented of extraction protocols to isolate exines from *L. clavatum*, in particular, but with extension to spores from other species, namely, *Lycopodium* spec., *Ambrosia trifida*, *Aspergillus niger* and *Chlorella vulgaris*. Physical aspects of the materials extracted were studied, including size (highlighting large and small types of commercial "Lycopodium"), wall thickness, mechanical resistance and density.

Encapsulation of a wide variety of compounds in sporopollenin microcapsules was investigated using passive, vacuum, compression and centrifugation methods. Diverse products, with molecular weights ranging from less than 1kDa to 464kDa, were successfully encapsulated in exines, including both polar (e.g. dyes, proteins, carbohydrates and oligonucleotides) and non-polar products (e.g. oils and waxes). It was shown that a protein, alkaline phosphatase, does not lose its initial activity after it has been encapsulated in exines and subsequently released.

Sporopollenin was found to grant oils protection against photooxidation triggered by UV light and the extinction coefficient of sporopollenin was determined (20,000-40,000m^{-1}). Protective abilities offered by exines to oils against aerial oxidation, and refining effects of sporopollenin on rancid fats, were studied, completed by a preliminary investigation of sporopollenin's redox characteristics. A flavour test on 20 volunteers showed that exines mask the taste of encapsulated cod liver oil up to a 1/1 (w/w) loading level.

Sporopollenin was also used in solid-phase organic synthesis. It was established that the reaction of ammonia, primary aliphatic amines and aniline with sporopollenin formed an amide bond on a carboxylic group of the sporopollenin. A short diamine was attached to sporopollenin in order to construct a spacer arm by further reaction between the free amino end and succinic anhydride. Sporopollenin was derivatised with bromine and chlorine by addition to the unsaturated functional groups, substitution of the hydroxyl groups and chloromethylation of the aromatic rings. The attached halogen atoms were then successfully substituted by azide and thiols. The thiol availability to nucleophilic substitution and formation of disulphide bridges was assessed.

Contents

J Solid-state NMR spectra of sporopollenin derivatives

Abbreviations

Note: For scientific names of species and abbreviations of the botanists, see Glossary under entry "Binary name".

AcS: Acetolysed Sporopollenin (following Erdtman's method)

AHS: Acid-Hydrolysed Sporopollenin

ALP: Alkaline Phosphatase

BHS: Base-Hydrolysed Sporopollenin

BHT: Butylated HydroxyToluene

Bn: Benzyl

CP-MAS NMR: Cross Polarisation-Magic Spinning Angle Nuclear Magnetic Resonance

Cys: Cysteine

DCM: Dichloromethane

DDAO: 1,3-dichloro-9,9-dimethyl-acridine-2-one-7-yl

DFS: Defatted Sporopollenin

DMSO: Dimethyl Sulfoxide

DTNB: Dithionitrobenzoic acid *or* Ellman's reagent *or* 3-carboxy-4-nitrophenyl disulfide

Extr.: Extraction

FTIR: Fourier Transform Infra-Red

GC: Gas Chromatography

GI: Gastro-Intestinal

HPLC: High-Performance Liquid Chromatography

ICP-OES: Inductively Coupled Plasma-Optical Emission Spectrometry

IR: Infrared

LAH: Lithium Aluminium Hydride

LSCM: Light Confocal Scanning Microscopy

LM: Light Microscopy

MS: Mass Spectrometry

N/a: Not applicable

N/d: Not determined

NMR: Nuclear Magnetic Resonance

Oct: *n*-Octyl

OIT: Oxidative Induction Time

PBS: Phosphate-Buffered Saline solution

PMMA: Polymethyl Methacrylate

Por.: porosity grade

PS: Polystyrene

ptcl: particles

PV: Peroxide Value

Ref.: Reference

resp.: respectively

RT: Room Temperature

s.d.: standard deviation

SEM: Scanning Electron Microscopy

STM: Scanning Tunnelling Microscopy

Sp.: Sporopollenin

TBAF: Tetrabutylammonium fluoride

TEM: Transmission Electron Microscopy

Temp.: Temperature

TFA: Trifluoroacetic Acid

THF: Tetrahydrofuran

TLC: Thin-Layer Chromatography

TSAO-T: [1-[2',5'-bis-*O*-(*tert*-butyldimethylsilyl)-β-D-ribofuranosyl]thymine]-3'-spiro-5'-(4"-amino-1",2"-oxathiole-2',2'-dioxide)

UV: Ultraviolet

UV/Vis: Ultraviolet/Visible

WE41: Water/Ethanol (4/1 (v/v))

XPS: X-ray Photoelectron Spectroscopy

A. Sporopollenin

1 Spores & pollen

1.1 Definitions

Spores are the mobile reproductive particles of plants.[1-7] They generally consists of one or two cells (*sporoplasm*) containing all sorts of fats, many vitamins and some proteins and carbohydrates. Spores are produced by *sporangia*, the sexual organs of plants, within the *loculus*, their internal cavity. They originate from a tissue called *tapetum* that carpets the inside of each sporangium, and mature grouped in a growing unit, typically by four (a growing unit of four spores is called a *tetrad*). Their role is to disperse away haploid nuclei (*i.e.* containing only one set of chromosomes), constituting the fragile genetic information which is fundamental for reproduction. The fact that spores constitute a moveable stage of the sexual cycle of the organism has led to specialised mechanisms for dispersal and to a specific morphology. They are usually between 1 – 250µm and are protected by a remarkably complex and robust double-layered wall. The inner layer of this wall, *intine*, is mainly composed of cellulose and a few other polysaccharides. The outer shell, *exine*, consists largely of sporopollenin, one of the most resistant natural organic material known.

Different types of spores are distinguished:

- in seed-bearing plants (spermatophytes), *microspores* are the precursors of male gametophytes (pollen grains) and *megaspores* of female gametophytes (ovules);[1]
- in algae, ferns, mosses and fungi (cryptogams), *spores* constitute the final dispersal phase for sexual or asexual reproduction;[1-5]
- *endospores* are the dormant stage and resistant form of some bacteria (e.g. *Bacillus anthracis* and *Clostridium tetani* respectively responsible for anthrax and tetanus diseases).[1,6]

To avoid any confusion, the word “spore” never refers to “endospore” in this study. In most cases, the use of the term “spore” was reserved to cryptogams, while “pollen” was used for spermatophytes. Once mature, spores of ferns, mosses, fungi and algae are either blown away by the wind or carried by water currents, or they simply fall

on the soil for a new organism to sprout when good conditions are reached.[1-5]

Pollen grains are the mature state of *microspores* in seed-bearing plants (*spermatophytes*).[1-5,7,8] They contain the male gametophyte. Flowering plants hold their pollen in the male sporangia (*anthers*) of flowers; pollen grains, once ready, are exposed for insects and winds to carry them on the tip (*stigma*) of the female organ (*pistil*) of another flower of the same species; there, they achieve their maturation by growing, through the *apertures* of exine, a *pollen tube* that eventually enters the ovary; fecundation happens then, forming a fruit. Sporangia of non-flowering seed-bearing plants (mainly conifers) are *cones*; male cones produce pollen, transported by wind, once ripe, to fecundate female cones.

Spores and pollen grains have a size comprised between a few micrometers (e.g. pollen grain of forget-me-not, *Myosotis* spec. L., is 5µm) and a few hundreds micrometers (e.g. pollen grain of pumpkin, *Cucurbita maxima* Duchesne, is 250µm).[7] Their features are characteristic of a plant group or even a species.[2] Under high-magnification microscopy, spores can be categorized in function of: their global shape (ratio between polar and equatorial diameters); the presence of scars (*laesurae*) on the proximal face, or *sacci* on the sides; the presence, position and shape of apertures; the external ornamentations (tectal elements); or the sculpturing of the layers (sexine).

1.2 Spores and pollen used in this study

Different species of spores and pollen were used in this study as they show different properties and could be used for different purposes and applications.

1.2.1 *Lycopodium* spec.

Provider	Country	Price (£/kg) in 2007
Fluka	UK	90
Post Apple Scientific	USA	60
Unikem	Denmark	42
G. Baldwin & Co	UK	42
Cedar Vale	USA	25
Tibrewala International	Nepal	10

Table 1 – Providers of "Lycopodium"

Spores of *Lycopodium clavatum* L. (common club moss) were purchase from several companies and plant growers, for a price varying from £10 (€15) to £90 (€143) per kg at the time of writing this thesis (see Table 1).

"Lycopodium" has been used as a cheap flammable powder for pyrotechnics since the 19th century[1] and has also been largely utilised as a drying and dusting agent, both in worldwide folk medicine and modern pharmacy.[9]

Commercial providers sell these spores under the only trade name of "Lycopodium". Unfortunately, this lacks of scientific precision. From the point of view of botanical taxonomy, club mosses should be named using the binomial or the trinomial nomenclatures. It was initially believed that the spores purchased belonged to the plant *Lycopodium clavatum* L. However, in the past few years, two types of spores have been discovered in various batches of commercial "Lycopodium" exhibiting different morphologies and sizes, as checked by LM, SEM and LSCM. Based on size consideration, one type has been named S (for "small") and the other one L (for "large"). Incidentally, it is noteworthy that Kremp[10] already mentioned the presence of a foreign spore in a batch of *L. clavatum*: the particle he described was ca. 44µm in diameter amongst smaller spores (ca. 25µm).

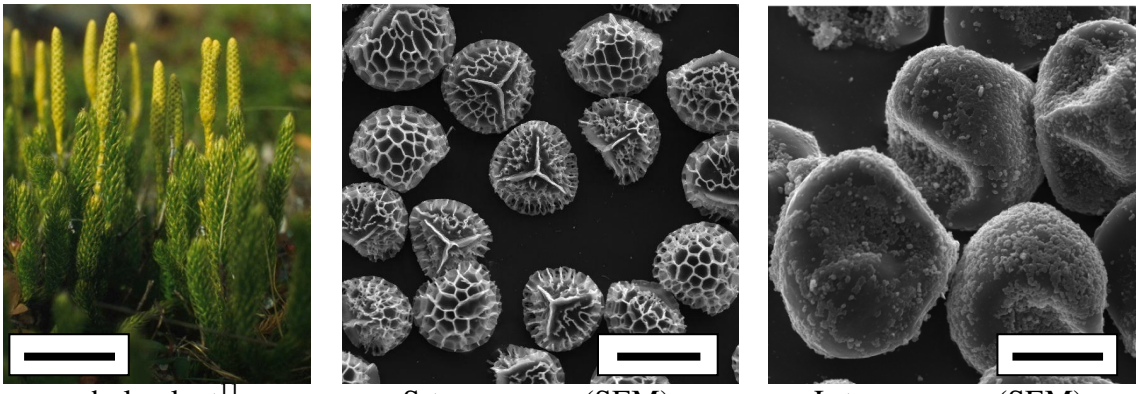

whole plant[11] *scale bar = 10cm* | S-type spores (SEM) *scale bar = 25µm* | L-type spores (SEM) *scale bar = 20µm*

Figure 1 – *Lycopodium* spp.

As explained in the next sections, the S type has been recognised as belonging to *L. clavatum* L., whereas it is still impossible to determine the exact origin of the L type. Therefore, the plant the latter originates from has been named *Lycopodium* spec., as botanical nomenclature suggests. Images of club moss plant and spores are gathered in Figure 1.

1.2.1.1 S-type spores, from *Lycopodium clavatum* L.

S-type spores correspond to most descriptions found in the literature[12-15] for *Lycopodium clavatum* L. (common club moss *or* ground pine) spores, to which they were unequivocally identified. The plant is a worldwide-spread 20-50cm high fern ally

whose strobili produce abundant anæmophilous (airborne) spores illustrated and described in Figure 2 and Table 2.[16]

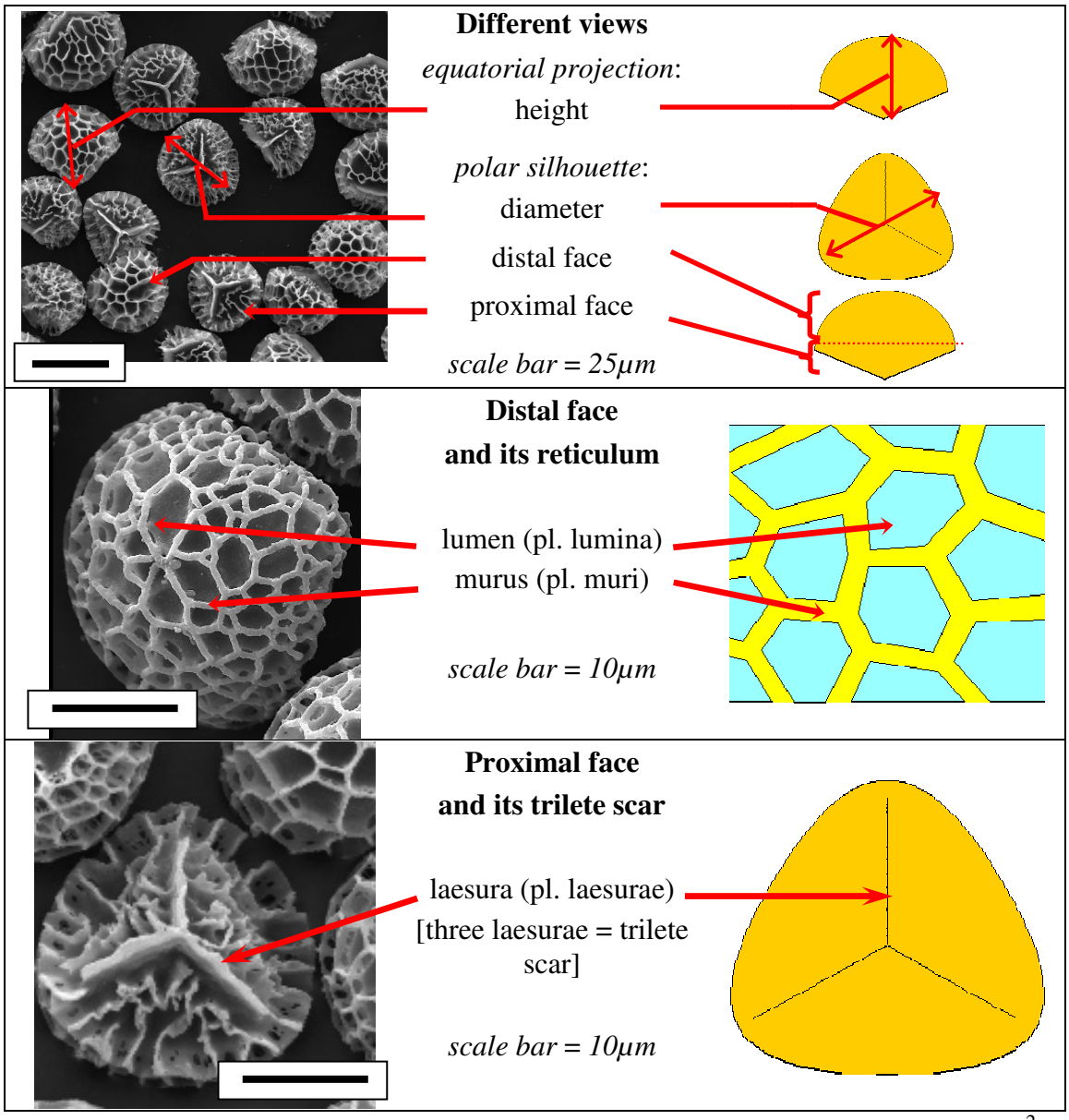

schemes from Punt *et al.*[2]

Figure 2 – *Lycopodium clavatum* L. spores

L. clavatum L. spore morphology and size have already been studied by various workers, although with a constant lack of precision. Now, the high monodispersity pertaining to spores within one single species[7,12] must apply to *Lycopodium* spp. as well. This property is also emphasised by their being free-flowing powders and their ability to form even suspensions, especially smokes or clouds, and thus their use for pyrotechnics.[17] Large imprecision in size determination is therefore suspected to come from the confusion and mixing of the two types of spores described before.

A short review of descriptions found in the literature is summarised in Table 2.

Description in the main literature sources[10,12-15]		
diameter (µm):	25-30	
shape:	ratio height/diameter	suboblate (height ≈ 0.8 × diameter)
	equatorial projection	trilete
decorations: (tectal elements)	distal face	reticulum
	proximal face	laesurae (trilete scar)

Description in detailed source[15]		
diameter (µm)	27-39	
shape:	polar silhouette	subtriangular
	equatorial projection	trilete
decorations: (tectal elements)	distal face	reticulum ↳muri shape: narrow, irregular ↳muri height: 3µm ↳muri width: 0.5µm ↳lumina shape: irregular ↳lumina size: 0-5µm
	proximal face	reduced reticulum laesurae (trilete scar) ↳ridges shape: narrow, undulated ↳ridges length: 0.5-0.7 × spore radius ↳ridges height: 0-3µm ↳ridges width: 0.5µm
	micro-ornamentation	small granules, short baculae

Table 2 – Description of *Lycopodium clavatum* L. spores

Further characterisations were necessary to tackle the large imprecision in the diameter measurement. The whole study is gathered in Section B-2.1.

1.2.1.2 L-type spores, from *Lycopodium* spec.

L-type spores have not yet been identified since it is only sold under the trade name “Lycopodium”. They are believed to come from another type of club moss, although it has yet been impossible to check whether they belonged to a genetic variant, a subspecies, a variety, a form or even another species of the genus *Lycopodium*. In consequence, the plant is designated under the imprecise name *Lycopodium* spec.

The nomenclature of *Lycopodiaceae* is indeed not homogeneous amongst botanists and the plant genus *Lycopodium* exhibits a variable extension. For example, Øllgaard[18] counted nine sections and around 40 species; under *L.* sect. *Lycopodium*, he counted ca. 15 species, and reported one subspecies other than *L. clavatum* subsp.

clavatum L., namely *L. clavatum* subsp. *contiguum* B. Øllg.; furthermore, he noticed a genetic variation between populations of *L. clavatum* L. from Old World and from Tropical America. More recently, at least 10 European species of *Lycopodium* have been reckoned by Jérôme.[19,20] The official list of the International Code of Botanical Nomenclature[21] exhibits as well another subspecies, *L. clavatum* subsp. *megastachyon* Á.Löve & D.Löve, and many varieties, subvarieties and forms, although some being synonyms.[22]

These novel particles might have been described in the literature, but since the plant they belong to has not been clearly identified, it is impossible to find any reliable reference. By LM and SEM, they were found to be ca. 40µm-large, psilate ("smooth"), suboblate, trilete spores.

1.2.2 *Ambrosia trifida*

A development of the study was envisaged on pollen of *Ambrosia trifida* L. (giant ragweed), bought from Sigma (£5/g to £10/g in 2007). *A. trifida* is a noxious 1-3m high weed (See Figure 3), nowadays considered as a menace in many tempered countries (e.g. in the United States and in continental Europe) as its anæmophilous pollen causes hay fever.[23,24] On the other hand, as it grows freely, it may not be difficult to cultivate it in greenhouses so that its price may drop significantly if we happen to prove it could be useful to human beings.

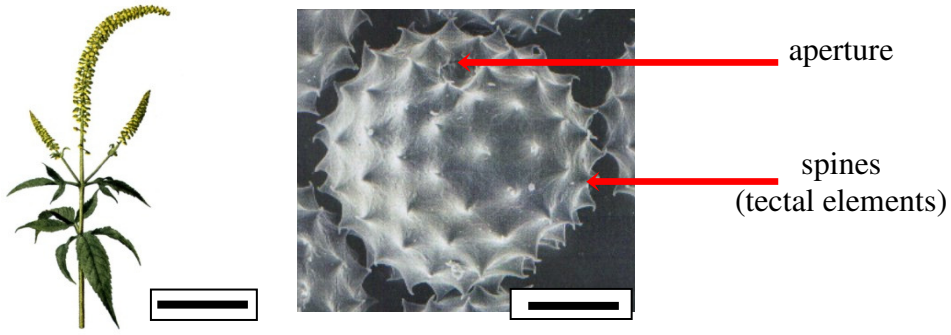

whole plant[25] *scale bar = 25cm*

pollen grain (SEM) *scale bar = 5µm*

Figure 3 – *Ambrosia trifida* L.

Ambrosia trifida pollen, illustrated in Figure 3, is spheroidal, echinate, tricolporate and ca. 15µm-large in diameter.[24]

1.2.3 *Aspergillus niger*

A commencing study of spores from *Aspergillus niger* Tiegh. further enlarged this work. That filamentous fungus grows as a mould on many organic products in decay, especially food waste.[26-28] It is also frequently used in food industry, for instance to produce citric acid (E330) or gluconic acid (E574).

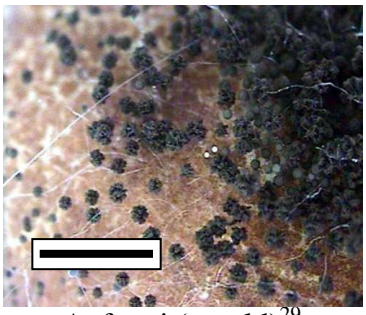

A. fungi (mould)[29]
scale bar = 1mm

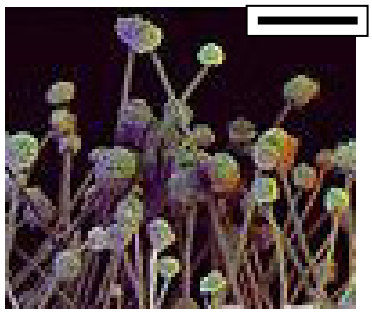

B. fungi filaments [*hyphae*] (SEM)[30]
scale bar = 15µm

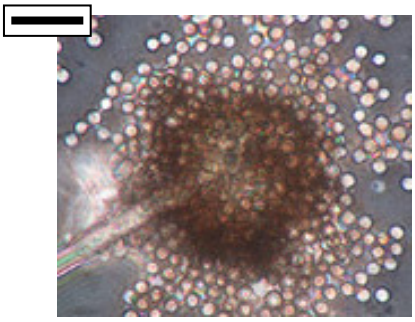

C. filament head [*conidial head*] sprouting spores [*conidia*] (LM)[31]
scale bar = 25µm

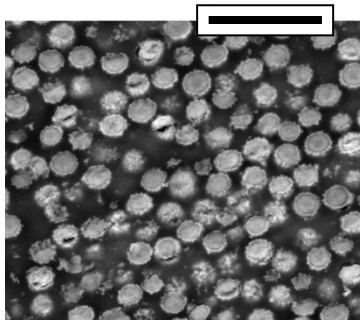

D. spores filled with acrylic resin (microtome sections, SEM)
scale bar = 25µm

Figure 4 – *Aspergillus niger* Tiegh.

During its saprophytic growth, it sprouts millions of very small *conidia* (*i.e.* non-motile spores).[32] Those spores are brownish, verrucate and regulate. They have greatly heterogeneous sizes, their diameter ranging from 3.5 to 6µm, the majority having diameter within 4.1-5.0µm.[28,33] Shaw and his team[34,35] reported the presence of sporopollenin in *A. niger* spores. Additionally, they estimated the amounts of cellulose [6% (w/w) of the total spore dry weight] and sporopollenin (5%) in conidial walls.[36,37] However, no method of analysis was identified. On the other hand, a recent study[33] mention none of these elements and only focused on a polymeric complex composed of chitin [5-6% (w/w) of the total spore dry weight] and glucan (3-4%).

Those conidia are easily inhaled and readily enter the body down to the most remote parts of the lungs.[26,27] Usually harmless to human beings, *Aspergillus* spores can

sometimes be toxic, and even mortal, to fragile people, which develop different kinds of diseases called *aspergilloses*. *A. niger* and its spores are illustrated in Figure 4.

Aspergillus niger used in this work was grown by Tate & Lyle PLC (Selby, UK) and generously provided by them. It was initially cultivated on a cotton seeds brew. However, cotton fibres in the resulting extracts of *Aspergillus* pleaded for a change of medium. Better conditions were found with ground maize cob as a support and soy flour as nutrient, although maize cob fibres still remained. Incidentally, while the normal strain, used in citric acid production, is coloured in black by melanin,* the strain used for this microcapsule study was paler.[27]

1.2.4 *Chlorella vulgaris*

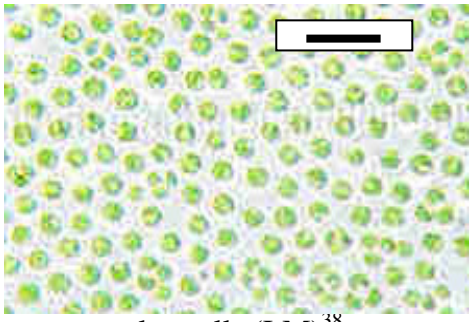

alga cells (LM)[38]
scale bar = 10µm

food complement pills[39]

Figure 5 – *Chlorella vulgaris* Beij.

Chlorella vulgaris Beij. is widely used in herb-therapy and food complements, as a source of chlorophyll, vitamin B and regenerative, moisturizing, anti-free-radicals proteins (See Figure 5).[38,39] It is sold in specialised health shop, pharmacies or online for a price varying from £20/kg (loose powder) up to £300/kg (tablets), in 2007. The unique cell of this microscopic green alga has a size comprised between 2 and 8µm. *C. vulgaris* reproduces asexually, by direct mitosis; ergo it produces no spore.[40] Its micro-sized cells develop a resistant inclusion (cyst) strengthened with a resistant biomacromolecules, probably an algaenan.[41] This polymer has often been regarded as a sporopollenin[35,42,43] hence the cysts are generally called (erroneously) spores.

For the present study, *C. vulgaris* was provided by maBitec Gmbh (Bruckmühl, Germany).

* Hence its specific name: *niger*, Latin for "black".

2 Exine and sporopollenin

2.1 Pollen grain and spore wall

Palynolderm and *sporoderm* are the names of the pollen grain wall and the spore wall respectively.[2] In vascular plants, they are identical and have a multi-layered structure as can be seen on Figure 6. In certain species, some layers may not be present; tectum or footlayer, for instance, are commonly absent.[44] In fungi and algae, sporoderm is generally not layered.[45]

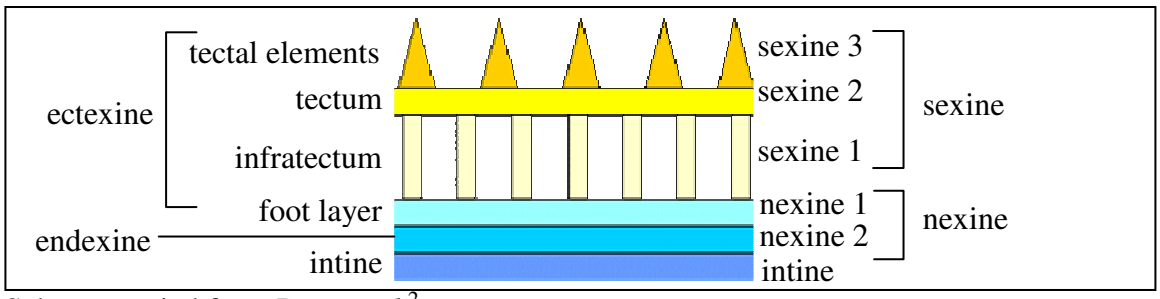

Scheme copied from Punt *et al.*[2]

Figure 6 – Spore wall scheme – maximal number of layers

The *intine* is the innermost of the major layers of the pollen grain wall, underlying the exine and bordering the surface of the cytoplasm.[2] It consists mainly of cellulose and some other polysaccharides. Thus it is not acetolysis resistant and therefore absent in conventionally prepared palynological material. The intine is sometimes called the *endospore*, in spore walls. The intine can be divided in two sub-layers: *endintine*, the inner, thicker, cellulosic zone which is adjacent to the cytoplasm and stains positively with iodine in sulphuric acid or with Calcofluor white; and *exintine*, the outer, thinner, pectic one, which stains positively with Alcian blue.

Exine is the other major, outer layer of the pollen grain wall.[2,46] The exine of spores is sometimes called the *exospore*. On purely morphological criteria, the exine is subdivided into an outer, sculptured zone, *sexine*, which lies above an inner, non-sculptured part, *nexine*. Another two different divisions of exine can be highlighted, taking into account their staining properties, development stages and texture: the outer part, *ectexine*, and the inner zone, *endexine*; the first one stains positively with basic fuchsine in optical microscopy and has higher electron density in conventionally prepared TEM sections, compared with the second one. Ectexine is highly resistant to

strong acids and bases, and is considered the *sporopollenin* part of exine, whereas endexine is a thin heterogeneous lamellated layer interpreted as remnant of unincorporated sporopollenin precursors or as terminal accretions.[44]

To sum up, from the innermost to the outermost, the sub-layers of exine are:[2]

- *nexine 2* or *endexine* (thin and not always present);
- *nexine 1* or *foot layer* (not always present);
- *sexine 1* or *infratectum*;
- *sexine 2* or *tectum* (more or less perforated, or even absent sometimes);
- *sexine 3* or *tectal elements* or sculpture elements, that vary in number, size and shape.

A few species have an even outer layer called *perine* or *perispore* that does not always resist acetolysis.[2] Then, entomophilous (insect-borne) pollen grains are covered in an acetolysis-sensitive, natural cement: the *pollenkitt*. This most external layer is mainly composed of waxes and more volatile lipids secreted by the tapetum. It makes the grains stick together in the dispersal unit or to a pollinator insect. This coat actually contains many different products (flavonoids, steroids, phenolics and aliphatics) that attract insects by their odours and colours and that could also play roles of protectors against UV radiations and/or microbial attack.[47-49] Finally when sporangia ripen, all pollen grains and spores are coated with *tryphine*,[2,49] a deposit of proteic and lipidic debris from the senescent tapetum. Both tryphine and pollenkitt are readily removed by the extraction protocols (See Section A-2.4).

By extension, all entities that have the same structure as pollen or spores are called palynomorphs or sporomorphs.[2] The terms encompass some special entities used in palynology.

2.2 Sporopollenin

A wide range of resistant natural biopolymers are found in modern vegetable, fungal and algal species.[41,50] Given their physical strength, they have structural roles in plants. The chemical nature of some of them is known. Cellulose, for instance, is a well-known polysaccharide. Tannins, lignins and lignans are polyphenols; cutins are polyesters of fatty acids, while suberins are mixed polymers with aromatic and aliphatic moieties. Four biomacromolecules are especially resistant to most chemical treatments apart from oxidative ones: lignins, cutans, algaenans and sporopollenins.

Lignins, main structural consistuents of wood, are now virtually fully characterised.[41,51] Cutans, mixed with cutins in leaf and stem cuticles, are now considered to be polyethers of hydroxy fatty acids. Algaenans, found in algal cell walls, are more ill-defined although they are believed to be polyesters and polyethers of mono- and dihydroxy fatty acids. However, the most resistant natural biomaterials are most certainly *sporopollenins*, found in spores and pollen wall and yet chemically poorly characterised because of their inertness.

The first reported chemical study on exines of pollen grains were done by John[52] in 1814. He commented on the inertness of the exine of tulips, when compared to the rest of the pollen wall, and introduced the term "pollenin" to name the matter of which it was made. In 1829, Braconnot[17] confirmed those results with pollen from bulrush. The term "sporonin" was invented almost one century later by Zetzsche[53-56] to describe the resistant exine material obtained from the asexual spores of *Lycopodium clavatum* L. (club moss). By 1931, Zetzsche *et al.*[55,56] had associated those words in the collective name "sporopollenin" to describe the resistant exine material forming both spore and pollen grain walls, since they appeared to be of the same chemical character.

Sporopollenin is a chemical concept (as opposed to biological), defined as "the resistant non-soluble material left after acetolysis".[5] The exact chemical nature of sporopollenin still remains mysterious and may depend on the development stage and the source, due to differences in the degrees of polymerisation, saturation or cross-linking, or the proportion and order of monomers. Since differences are appreciated from species to species, the word "sporopollenin" actually refers to the family of natural polymeric compounds that noticeably prevail in pollen and spores exines.[14,57] The phylogenetic parenting between sporopollenins probably follows that of plants: vascular plants (spermatophytes and ferns) originating from a common fern ancestor, pollen grains and fern spores must exhibit a similar sporopollenin, while resistant polymers from resting fungal spores are not evolutionarily linked to the ones from higher plants.[5] Their similarities must then be coincidental and due to the fact that sporopollenins are the unique chemical materials to fulfil the requirements of spores and pollen grains.

The resistant biomacromolecules of resting cysts have often been called sporopollenins although their actual identification to sporopollenin was highly questioned in several algal and fungal species (*Botryococcus braunii*,[58-60] *Scenedesmus obliquus*,[58] *Chlamydomonas monoica*,[61] *Mucor mucedo*,[62] lichens[63]…). The confusion may come from the biological similarities between vegetative algal cysts, dormant

spores and zygospores. Finally, van Bergen *et al.*[41,64] suggested that such structural biomaterials in algal cell walls (including that of algal zygospores) should always be called algaenans whereas sporopollenin should be restricted to the chemically resistant biopolymers in spore walls of non-algal species excluding fungal spores.

Some workers suggested the sporopollenin part of exine was ectexine[14,44] and that endexine might contain lignin.[14] Ectexine is amorphous, granular and highly consolidated, and stains positively with basic fuchsine, while endexine is laminated and does not react to fuchsine.[7] These histochemical and ultrastructural divergences tend to prove the chemical difference of their sporopollenins.

Wiermann and Gubatz[47] noticed that sporopollenin could be found in other parts of plants, precisely some organelles involved in its deposition into exine. Those are:

- orbicules (or Ubisch bodies), initially composed of precursors and in which sporopollenin eventually concretes;
- tapetal wall itself, finally covered in sporopollenin at the end of spore or pollen maturation;
- and viscin threads, cord-shaped structures linking some pollen grains to the tapetum.

2.3 Ontogeny of exines

No other biological process seems as peculiar as the exine formation.[14] It has been thoroughly investigated in vascular plants, and scientists now agree on the main steps.[7,8,14,35,65-70] Mother cells, present in the sporangia, undergo meiosis to produce *microspores*, gathered by four in a growing cluster called *tetrad*. They are enclosed within a callose wall. Inside this filtering shell, a polysaccharide-protein fibrillar template (*glycocalyx*)[71] holding the main features of exine is set. A thick cellulose layer soon carpets the callose wall, except where apertures are to develop. And then, rod-like lipoprotein elements (*probacula)* radially traverse this matrix. Their heads and feet start to connect to form the future tectum and foot layer, respectively. Sporopollenin deposition begins at this stage on the growing structures (*primexine*).[7,14,44]

Microspores are then released from the thick callose wall of their tetrad and swell.[7,14] This causes the primexine to stretch and slim, and shreds and disperses the cellulose matrix in which probacula are embedded. Sporopollenin deposition continues in parallel, thickening tectum, infratectum and foot layer. Formation of endexine starts

just before the tetrad break-up, from sporopollenin-covered lamellae, similar to probacula but laid tangentially.

Callose being impermeable to lipidic precursors of sporopollenin, primexine and endexine originate from inside the haploid spore.[7,14] On the opposite, after dissolution of the callose wall, precursors are secreted massively by the tapetum: this is the main source of sporopollenin-to-be. During the maturation phase of some angiosperms, orbicules (or Ubisch bodies) sometimes appear on the tapetum of anthers: some claim that these small granules store sporopollenin precursors, cross the loculus to deposit it onto the growing spore where polymerisation occurs.[8,35,65,66,68,72] Brooks and Shaw[72,73] described precisely this post-tetrad phase from a chemical point of view: they claimed orbicules would transport carotenoids onto the polysaccharide template while they polymerise into sporopollenin (see their hypothesis regarding sporopollenin as a polycarotenoid, Section A-4.2.4).

Sporopollenin deposition on growing spores or pollen grains have been comprehensively studied by many workers, and appear to be consistent among vascular plant species of different kinds (ferns, angiosperms or gymnosperms).[8,34,35,44,65,68,69,74-79] It is claimed that sporopollenin precursors, as well as nutritious substances, follow special strands ("wicks", possibly viscin threads when present) to reach the tetrad or the microspores.[80,81] Their diameter reaches ca. 30-40nm. These strands fill the loculus, arranged in a weft, and traverse the spore wall, hence leaving channels through the exine where they exhibit a rod-shaped structure.[81]

Eventually, tectal elements are created on top of the tectum and intine inside the thickening exine.[7,14] The senescence of the tapetum, concomitant with the maturation of microspores coats them with tryphine (and pollenkitt sometimes).

By contrast, very little is known on the exine ontogeny in algae and fungi, when it exists. As aforementioned in Section A-2.2, identification of the resistant polymer that composes it with sporopollenin has been subject to controversy. In any case, no or little deposition seems to come from the outside: those macromolecules develops from within the maturing spores.[72]

Fungi have been studied a bit more in details (*Mucor mucedo* and *Rhizopus sexualis*).[62] It has been suggested that hyphae secreted precursors into the future spore before sporopollenin polymerisation started.

2.4 Isolation of exines

Isolating sporopollenin has long been a critical issue to workers that studied its nature and properties. Owing to the prominent inertness of this material and its resistance to chemical, physical and biological aggressions (see Section A-3.2), sporopollenin particles have been extracted by stripping off pollen grains or spores of their other components. Extracted exines are the skeletons (or rather the shells) left after removal of the particle "flesh" (sporoplasm). However, consistency in the method appears to be crucial for repeatability and reproducibility. Moreover, the extraction procedure must be considered when comparing results from different teams, since strong conditions may modify sporopollenin structure and purification may be more or less extensive.

2.4.1 Harsh extraction procedures

During the 1930s, Zetzsche *et al.*[53-56] reported the first method of preparation of morphologically intact pollen or spore wall devoid of any cytoplasmic components (fats, genetic material or proteins). They found that the contents could be expelled by treatment with organic solvents (mainly diethyl ether, acetone and ethanol) and boiling alkaline solution (typically sodium or potassium hydroxide). This yielded shells bearing the following characteristics:

- hollow and representing ca. 25% of the initial mass;
- retaining the original shape of the particle;
- devoid from nitrogen;
- consisting of at least two layers: intine and exine.

It appeared that the cellular part, as well as the external tryphine and/or pollenkitt, could be cleared out fairly easily. Several workers[82-86] consequently used modified versions of Zetzsche's extraction protocol, and it was noticed the proportion of sporoderm could drop down to 2% in a few species.

By contrast, intine elimination seemed to be a critical step of the procedure. Zetzsche *et al.*[53-56] discovered that the intine could be removed by various treatments over several days:

- reaction with cuprammonium hydroxide;
- acidic hydrolysis with 40% hydrochloric acid;

- acidic hydrolysis with hot 72% sulphuric acid;
- acidic hydrolysis with hot 85% phosphoric acid.

First, the treatment with cuprammonium hydroxide was only partly successful, and rapidly abandoned. Then, hydrochloric acid hydrolysis was not as effective as the other two acidolyses. More importantly, hydrochloric and sulphuric acids were found to introduce chlorine and sulphur respectively in the final product. According to Shaw *et al.*,[36] acidolysis in concentrated phosphoric acid was the best choice to obtain a cellulose-free sporopollenin since them found no phosphorus was introduced by this treatment. Shaw and Apperley[85] eventually demonstrated by solid-state ^{13}C-NMR that cellulose was still present in samples that had been treated with hot concentrated phosphoric acid over a couple of weeks. Only sulphuric acid was able to remove all traces of intine. In conclusion, a balance had to be found between clearing all cellulose and introducing impurities in exines. Therefore many workers used hydrolysis in concentrated phosphoric acid as a compromise.[12,13,36,72,84]

Yet Shaw and Yeadon[82,86] also noticed that exines from some species could not withstand the same treatments and cited a few examples that collapsed after treatment in boiling potassium hydroxide: *Fraxinus excelsior* L. (ash), *Populus nigra* L. (Lombardy poplar), *Lupinus* sp. L. (lupin) and *Platanus* sp. L. (plane).

In the meantime, Erdtman,[87] in the 1960s, had introduced acetolysis as a cleaning method for palynological sample preparation. A mixture of acetic anhydride and sulphuric acid was used to deprive pollen grains or spores from their inside while retaining the particle shape. This reaction was meant to simulate the process of fossilisation, in order to compare extinct and extant species. Acetolysis has been frequently used for structural elucidation and palynological investigations despite its limitations:[88]

- acetolysis affects the precursors of sporopollenin and can therefore be used only on completely mature pollen or spores;
- removal of intine may yield fragmentation of thin or discontinuous exines from certain species, or their collapsing thus being misleading about their diameter, sculpturing and shape;
- certain tectal elements or external attachments to apertures may be lost, if they are too loosely bonded to exine.

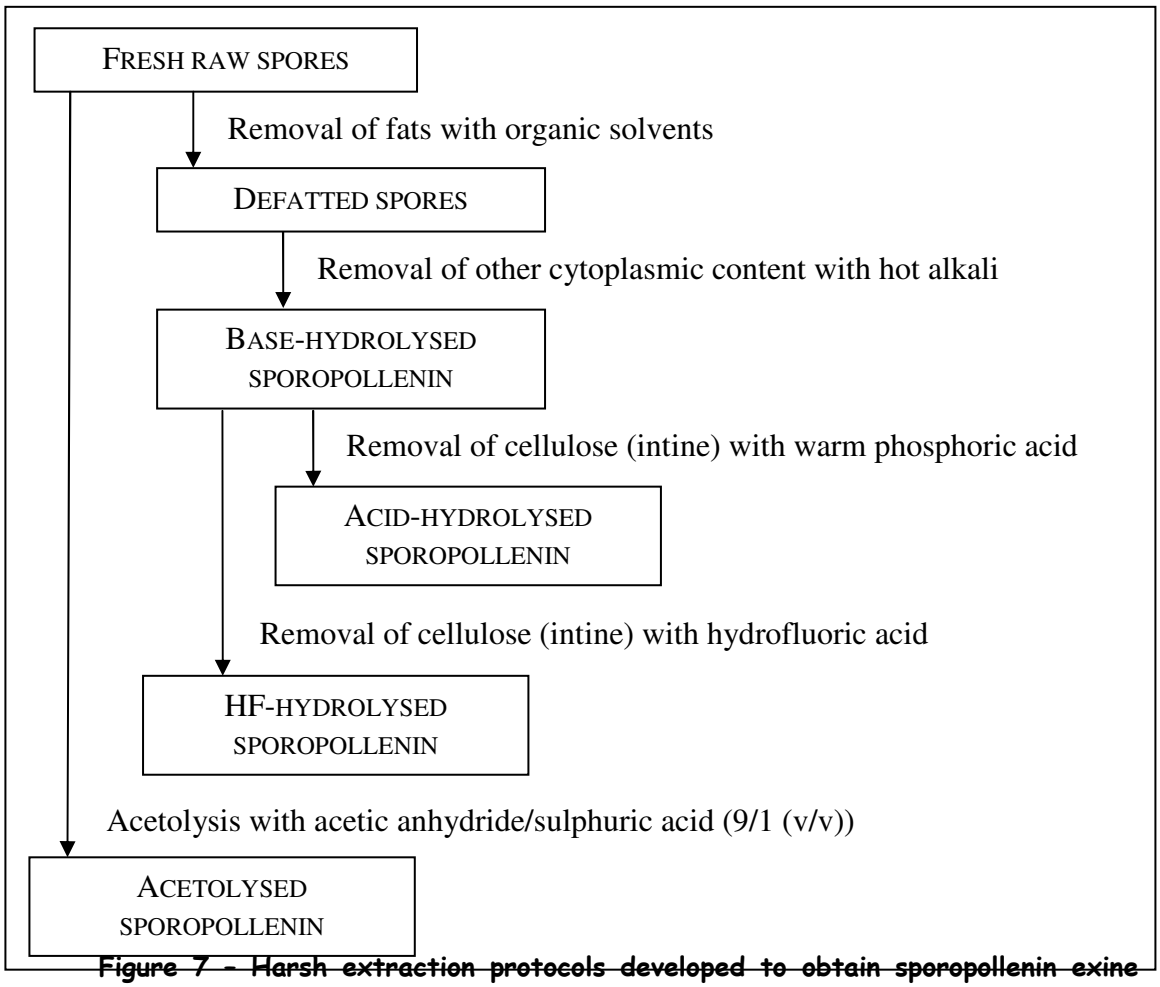

Figure 7 - Harsh extraction protocols developed to obtain sporopollenin exine shells by chemical means

Later on, in attempt to discover sporopollenin's chemical nature, some teams[36,89-91] insisted on the fact that acetolysis or acidolysis modified the composition of the material itself. It could dehydrate it, introduce acetyl or phosphate groups or, more importantly, cross-link the polymer. To avoid such parasite reactions, Domínguez *et al.*[89] developed a method involving anhydrous hydrofluoric acid in pyridine at 40°C, and claimed it isolated unaltered sporopollenin. The extracted exines did not fluoresce when stained with calcofluor which indicated the entire removal of polysaccharidic material. Also the efficiency of this technique was monitored by IR when compared to acetolysis. The spectra of untreated pollen grains and their sporopollenin showed complete similarities apart from the spectroscopical cellulose fringerprint. On the other hand, IR confirmed that acetolysis modified sporopollenin structure: the peaks at 1250-1100cm^{-1}, accounting for C-O stretching, were probably due to acetylation of hydroxyl groups.

In fact, exines have not only been used as a source of sporopollenin but also as microcapsules, as detailed in Section A-6.3. For such an application, extraction of pure unmodified sporopollenin was not the point. Therefore most steps were not considered, as long as most of the internal material could be removed. In order to obtain empty capsules suitable for pharmaceutical purposes, some patentees have treated pollen with 6M hydrochloric acid at 110°C for 24h.[92-94] They claimed the resulting material was deproteinised, and thus non-allergenic, but the capsules were not made of pure sporopollenin.

2.4.2 Mild extraction procedures

In contrast with those strong treatments, summarised in Figure 7, mild extraction conditions have also been investigated. Indeed, it has already been pointed out that most of these processes could affect sporopollenin structure.[89,90]

An effective method has been described to gently separate sporopollenin exine from sporoplasm: spores were suspended in aqueous 4-methylmorpholine-*N*-oxide and sucrose under alkaline conditions and heated at 70°C or 20°C for 1h. This resulted in the release of sporoplasm out of exine, which was then purified,[95-97] although it was originally tuned for isolation of intact sporoplasms (as opposed to spore walls).[98] Dissolution of sporopollenin was also reported when treatment lasted.[95]

In the case of saccate pollen, some workers[47,99-101] found that exine ruptured by hydration in distilled water. Since the remaining protoplast was left intact,[101] debris only contained exines. Ergo, simple autoclaving and solvent washings were used to purify them, and no harsh treatment was involved.[47,99,100] Similarly, physical breakage of the pollen grains by grinding, mechanical stirring and/or ultrasonication was commonly used by some teams.[48,90,102] Fragments were then decanted in a discontinuous glycerol gradient and filtered through a mesh cascade. This was used in particular before the enzymatic extraction detailed below[90,102] or to specifically collect the wings of saccate pollen.[90]

Finally, several workers[90,102-105] have incorporated enzymatic steps to isolate sporopollenin. For instance, removal of intine without use of a strong acid was made possible with cellulase. Also, a fully enzymatic protocol was developed by Wiermann *et al.*[48,102] on *Corylus avellana* L. (hazelnut) pollen. Once treated, particles were washed exhaustively with boiling methanol (and other solvents). The same workers[90] repeated this procedure on *Pinus mugo* Turra (mountain pine) pollen after it had been extracted

with successive solvents. In both cases, each enzymatic step removed an element foreign to sporopollenin at a time. The enzyme sequence was composed of protease, lipase, amylase, pectinase, cellulases and hemicellulase. This protocol was claimed to produce sporopollenin that retained the intact chemical morphology of the original pollen grain or spore.

3 Physical properties

The first physical characteristic of spores and pollen grains is their consistency of size, within one species, as well as their high monodispersity.[7,12] Sporopollenin particles are also remarkably resistant to physical, biological and chemical non-oxidative aggressions.[12,13,57] The refraction index of sporopollenin $(1.48)^3$ and its specific gravity (ca. 1.4) testify to the compact nature of the material itself.[106] This makes it largely insoluble in most of the common solvents.[107] Finally, exines substructure has been investigated to describe the subunits of sporopollenin.[108] In addition, the outer wall is tunnelled with an array of nano-sized channels, superimposed with the meshwork of sporopollenin.[80,109,110] Finally, due to some of its chemical constituents, sporopollenin was highly suspected to absorb UV light.[42,48,111,112]

3.1 Geometrical data

Spores and pollen grains have been said to be highly monodispersed, within one species.[7,12] Their consistency of size implies their being free-flowing powders and suggests interesting characteristics for microencapsulation within sporopollenin exines. This explains also the ability of *Lycopodium* spores to form even suspensions, especially smokes or clouds, and thus their use for pyrotechnics.[17]

Species	Vernacular name	Spore/pollen size (µm)
Lycopodium spec.	club moss	40
Lycopodium clavatum L.	club moss	25
Cannabis sativa L.	hemp	25
Lolium perenne L.	ryegrass	20
Ambrosia trifida L.	giant ragweed	15
Aspergillus niger Tiegh.	n/a	4

Table 3 – Species under investigation by Sporomex Ltd. and their spore/pollen size

In addition, Nature has provided the possibility of a wide variety of sizes to choose from in respect of the species source, from 1µm for *Myosotis* spec. pollen to 250µm for *Cucurbita* spec. pollen.[7] Some of the biological properties of the resulting particles directly depend upon their size. Hence their potential applications involve the choice of a suitable species. Therefore co-workers at Sporomex Ltd. are currently

developing studies on several species, so as to cover a broader size range (See Table 3).

It is of note that *Chlorella vulgaris* Beij. does not produce any spore, since it reproduces by asexual mitosis. Its cells have a size varying from 2-8µm.[40] Sporopollenin being contained in its cell walls, particles extracted from it have the same size range and completely lack monodispersity.

3.2 Resistances of sporopollenin

Faegri and Iversen[46] described sporopollenin as "one of the most extraordinary resistant materials known in the organic world". Brooks and Shaw[34] stated "sporopollenins are probably the most resistant organic materials of direct biological origin found in nature and in geological samples". This can be further reiterated by the survival of some intact exines in ancient sedimentary rocks, dating back from more than 500 million years old.[12,113] Whereas the cytoplasmic, genetic and polysaccharide components are systematically destroyed by diagenesis (fossilisation process), the resistant exine may remain unchanged and form part of the organic sediments (kerogen).[60,113]

This illustrates sporopollenin's (and exine's) relative resistance to high pressure, mechanical stress and biological decay.

3.2.1 Chemical resilience

The different methods developed to isolate sporopollenin from *L. clavatum* proved its exceptional stability and chemical inertness (see Section A-2.4). Indeed, it is highly resistant to a variety of hot strong acids (including phosphoric acid, sulphuric acid and hydrofluoric acid), alkalis (e.g. concentrated sodium or potassium hydroxides) and organic solvents (e.g. acetone, methanol or dichloromethane).[53-55,57,85] In keeping with this, the Erdtman's acetolysis [with 9/1 (v/v) acetic anhydride/sulphuric acid] was shown not to degrade sporopollenin,[87] but there may be chemical reactions that modify its structure like cross-linking and acetylation, as emphasised below in Section A-3.3. In contrast, hydrofluoric acid solution was reported not to modify the chemical composition of sporopollenin and hence be useful for intine removal.[89]

Also, in the past few years, the integrity of exine was checked after stirring 2h or 24h in DCM, ethanol, water, toluene, DMF or DMSO, at room temperature or 50°C.[12,13] SEM pictures revealed that particles isolated from *L. clavatum* L. (25µm) were not

soluble in these solvent and stayed undamaged. Sporopollenin exines from *Lycopodium* spec. (40µm particles) however were partly broken after 24h of stirring at room temperature or even 2h at 50°C.

Nonetheless, numerous chemicals were found capable of degrading sporopollenin, including oxidisers (e.g. nitric acid, potassium permanganate, ozone, chromic acid or nitrobenzene) or fused potash (see Section A-4.1.1), or of dissolving it, such as 2-aminoethanol (see Section A-3.3).[36] This was mostly explained by its high degree of unsaturation.[72]

3.2.2 Biological resilience

The survival of exine in the digestive tract is fully discussed in Section A-5.2.

As aforementioned, sporopollenin was found able to resist decay after millions of years.[12,37,60,113-115] The enzymatic extraction procedure developed by Wiermann *et al.*[90,102] has proved sporopollenin survived a wide range of enzymes (protease, amylase, lipase, cellulase and hemicellulase). This may explain why it does not easily submit to bacterial decomposition or to digestion. At a certain point, attack of sporopollenin by microorganisms was considered possible although complete biodegradability was still doubted.[35]

However, it is important in nature that sporopollenin be biologically degraded, for instance to enable germination to occur and to recycle the material after fecundation. Above all, "all natural substances have some (…) enzyme that will break it down, otherwise we would quite simply be submerged in these materials", as Faegri stated.[116] A number of bacteria were found able to degrade sporopollenin under certain conditions (e.g. pH or aerobic milieu).[65,66,116] Some plant enzymes can also hydrolyse exine, for example those produced by fungal rhizoids to feed on pollen. Furthermore, after pollination, intine secretes an enzyme cocktail (acid phosphatase, ribonuclease, esterase and amylase) to break up the exine.[66] In the same vein, a pollen esterase has been found in *Hordeum vulgare* L. (barley) pollen that hydrolyses sporopollenin, in order to form late pores.[117]

Incidentally, sporopollenin was also expected to be destroyed in the blood stream, as a foreign body. An unknown enzymatic sequence linked to the clotting cascade has also been discovered that degrades sporopollenin in the blood, both *in vivo* and *in vitro*.[118]

3.2.3 Physical and mechanical resiliences

It must be highlighted that, whereas sporopollenin material *per se* resists chemical, physical and biological aggressions, exines themselves may be damaged under similar conditions. Indeed, some plant species develop spores or pollen grain with very thin exines or exine elements only loosely linked together.[72,88] Removal of intine and/or sporoplasm may thus lead to exine fragmentation, collapsing or bursting. This was first noticed by Shaw and Yeadon[82,86] on several species whose exine could not be recovered after potassium hydroxide treatment: *Fraxinus excelsior* L. (ash), *Populus nigra* L. (Lombardy poplar), *Lupinus* sp. L. (lupin) and *Platanus* sp. L. (plane). Recent experiments with *Chlorella vulgaris* cells, *Ambrosia trifida* pollen or *Aspergillus niger* conidia corroborated these results: the amount of sporopollenin in the wall did not suffice to hold it intact under mechanical or thermal stress after extraction of the other components.

Moreover, many workers also mention disruption of pollen grains by stirring and/or subjection to ultrasounds.[47,48,90,102] The species chosen for such treatments were therefore of a more fragile nature.

3.2.4 Thermal resilience

Sporopollenin appears to undergo carbonisation and coalification with heat. Different changes occur depending on the temperature:[34]

- under 100°C: no change;
- 100-180°C: slow colour changes;
- 180-220°C: darkening and evolution of water, methane and carbon dioxide;
- over 220°C: quick darkening and release of more volatile chemicals (hydrogen sulphide, dihydrogen and light hydrocarbons).

A more detailed investigation by IR and elemental analysis showed that sporopollenin was dehydrated by heat (loss of hydroxyls with creation of carbon-carbon double bonds), and, above 400°C, aromaticity drastically increased.[37]

3.3 Behaviour towards solvents & solubility

Spores float on water and are barely wetted. A familiar school demonstration consists in spreading *Lycopodium* powder on the surface of water and employing it such that one's hand remains dry when immersed in it.[119] This can be first explained by the presence of fats (pollenkitt and/or tryphine) coating the spores. A second explanation comes from the chemical structure of sporopollenin (see Section A-4.3): it seems to gather very hydrophobic properties, most probably due to its hydrocarbon skeleton. On the other hand, empty exines only float for a while but seem to progressively absorb water inside so that they eventually sink. By contrast, both spores and sporopollenin exines readily soak up oils, organic solvents and especially ethanol, in which they very quickly produce a suspension due to their being highly monodispersed.

Moreover, sporopollenin from most sources is insoluble in common organic and inorganic solvents over the boiling range of such liquids.[12,13,120] It behaves as resin beads that can be filtered. Incidentally, its insolubility in dioxane enabled to distinguish it from lignin.[35] However, hot 2-aminoethanol, a common solvent for lignin, was found to "dissolve" exines from many species: various gymnosperms and angiosperms[120] and more recently, *Chlorella vulgaris* (slightly).[42] Exines from *Typha angustifolia* L. (lesser bulrush) pollen were claimed to be soluble in both in 2-aminoethanol[105] and in piperidine.[121]

Southworth[107] studied exhaustively the solubility of sporopollenin from *Ambrosia trifida* L. and found it was insoluble in hydrolytic acids or bases, in lipid solvents or detergents. She claimed it dissolved in fused potash and many oxidising agents; it seems however more likely that sporopollenin was rather irremediably degraded by these reagents (see Section A-3.2). On the other hand, actual dissolution (as opposed to complete destruction) of sexine was observed in 2-aminoethanol, 3-aminopropanol and 2,2',2"-nitrilotriethanol. Solubility of many species in hot 2-aminoethanol, previously investigated, was also reviewed in the same publication. Several species (pines, maize, ragweed or bulrush, for example) yielded sporopollenin particles at least partly soluble, with the sexine being much more soluble than the nexine. However *Lycopodium clavatum* exines, extracted with potassium hydroxide and phosphoric acid treatments, were classified as insoluble.[36]

One can rightly discuss the word "dissolution" for sporopollenin since the

solubilisation mechanism has not yet been perfectly understood. In the case of ethanolamine, the action of the solvent has been described as a partial degradation or a chemical combination of 2-aminoethanol in sporopollenin structure at high temperature.[105] The resulting functions (supposedly amide and hydroxyl) were said to augment sufficiently the interactions with the remaining solvent so as to dissolve the derivatised exine. Exine sporopollenin was however able to precipitate out and recompose by replacement of the solvent by water. This may explain the insolubility of some particles. For instance, after mild enzymatic extraction, sproropollenin from *T. angustifolia* L. was completely soluble (sexine and nexine) up to 4% (w/v) in hot 2-aminoethanol, whereas it was not after acidic treatment (with either acetolytic mixture or phosphoric acid). This was explained by the chemical modifications of sporopollenin: the anchoring functions said to react with 2-aminoethanol may have been phosphorylated or acetylated; ergo the solvent could no longer attach to acid-hydrolysed sporopollenin (AHS) or acetolysed sporopollenin (AcS) and dissolve it.

In the light of the updated knowledge on sporopollenin chemical composition and reactivity, it seems far more likely that acidic treatments affect it in another way. Indeed it is most probable that the anchoring groups in sporopollenin be carboxyls, amidated with 2-aminoethanol by heating (see discussion in Section B-5.2.3 for details on reaction of sporopollenin with amines). As acetylation would target hydroxyl groups, it would not change the reactivity of carboxyls, and phosphorylation (as detailed in Section B-5.1) would even activate carboxyls so that they should react more readily with 2-aminoethanol. As a consequence, the explanation propounded by Wiermann *et al.*[105] is dubious.

A more acceptable justification of AHS and AcS being insoluble (while enzyme-treated sporopollenin is soluble) lay in the most certain cross-linking of sporopollenin by acid treatments. Indeed, heating sporopollenin in phosphoric acid or acetolytic mixture might cause carbon-carbon bond formations by reaction of active methylenes *via* such as Michael-, Claisen- or Knoevenaggel-type reactions. The different units of cross-linked sporopollenin would not dissolve since they would no longer be able to separate from each other.

Whatever the exact mechanism is, and despite Southworth's conclusions,[107] the solubility of sporopollenin does not appear to depend on the species, but rather on the extraction procedure. Therefore, although sporopollenin from *L. clavatum* was classified as insoluble by Shaw,[36] a mild extraction could be expected to enable its dissolution in

2-aminoethanol.

Furthermore, molten 4-methylmorpholine *N*-oxide has also been shown to "dissolve" (*sic*) exines, as well as intines.[95] Loewus *et al.* observed that, at 72-75°C, this cyclic amine oxide ruptured the sporoderms from *Lilium longiflorum* Thunb. (Easter lily) around the apertures, released intact sporoplasms and dissolved the intines, leaving empty exines. Over 90°C, this treatment eventually liquefied the exines into a non-miscible phase. This was later used as an extraction method for structural analysis.[96]

Recently, Maack has claimed sporopollenin from *C. vulgaris* was soluble in DMSO, glycerol and aqueous media.[42,122,123] Applications to very dilute solutions (0.1% (w/w)) have been envisaged for skin cosmetics, especially anti-wrinkle, or for treatment of microbial diseases.[123] However, attempts to repeat these dissolution results have failed so far.[124]

3.4 Decorations

Amongst the sculpturings that feature in the sexine, two types of decorations are visible from the outside: over the tectum are the tectal elements and within the sexine the apertures. Pictures and diagrams displayed in Section A-1.2 illustrate some tectal elements and apertures present in the spores and pollen grains used in this study.

Tectal elements are little embossments scattered around the spore or pollen grain and dependant on the plant species.[2] For example, *L. clavatum* L. spores are reticulated on their distal face, *i.e.* the side that faced outwards the growing cluster (tetrad) is decorated with a honey-comb-like structure; *Lycopodium* spec. spores are psilate, *i.e.* smooth; and *A. trifida* pollen grains are echinate, *i.e.* they are covered by small spikes.

Apertures are zones of different thickness in the exine layers.[2] Different types can be distinguished: *laesurae* are scars of the grouped growth of spores, on their proximal face, *i.e.* the side facing inwards the growing cluster (tetrad); laesurae form *monolete* (single line) or *trilete* marks (Y-shaped) according to the shape of the tetrad; pores and colpi are the other main apertures, involved in the maturation of spores and pollen grains. For instance, *L. clavatum* L. and *Lycopodium* spec. bear trilete spores, and *A. trifida* tricolporate pollen grains[24] (*i.e.* with three apertures that are combinations of a pore and a colpus).

3.5 Ultrastructure and nanochannels

It is accepted that sporopollenin units form a spongy network ca. 70nm large in mesh.[108] Different precise models have been proposed for the ultrastructure of exine: an arrangement of interconnected granules,[99,100,125] a quasi-crystalloid molecular structure,[126] a colloidal crystal self-assembled organization,[78,127-131] or multi-helical units.[80,106,108,132]

Sporoderm, and *a fortiori* exine layer, "is not a barrier to penetration", as Pettitt wrote.[110] It is indeed traversed by microchannels,[110,133] as expected from the connecting strands described in Section A-2.3.[81] Sporopollenin meshwork was found to intertwine with the array of channels, whose diameter was first reported at about 40-70nm, probably after broadening by oxidative extraction methods.[109] A more recent work described those radial nanochannels as being approximately 25nm in diameter in mature pollen (but wider at a younger stage of spore development).[80]

This same study, based on a previous work[132] over five species, proposed a model of ultrastructure endorsing most of the previous discoveries. Sporopollenin was said to polymerise into radial rod-like subunits ("tufts"). In the microspore growth, they are evident as columellae, from which tectum, foot layer and endexine are yielded. Each exine subunit seems to be centred on a nanochannel. Around this hollow core would be a corona ("binder zone") composed of multi-helical sporopollenin subunits.[80] The overall diameter of those substructures is 70-100nm in young microspores, and reaches up to 200-250nm on mature exines.[134] Moreover, several studies[80,110] demonstrate that the channels not only cross the exine (both ectexine and endexine) but also the intine. It was shown as well that they enable particulate material to enter the sporoderm, although colloid metals permeate through exine even where no evident nanochannels were found. The consistence of the studies from species to species in vascular plants (amongst which *Lycopodium* spp.) tends to firmly back up this hypothesis.

3.6 Ultraviolet (UV) absorption properties

Protective properties of sporopollenin against UV-light is emphasised by the fact that spores carry away fragile genetic material. Furthermore, some workers have actually found sporopollenin solutions in aminoethanol absorbed UV.[42,122,135] Full UV spectra of sporopollenins from different origins (vascular plants) have been established by Southworth[136] on microtome sections of fixed spores: a maximum absorbance was found in the wavelength range 280-300µm, depending on species.

UV properties were first explained by similarities, often underlined by Shaw *et al.*,[85,137] of sporopollenin with polycarotene, such unsaturated system being UV-absorbent itself.[138] UV absorption was more commonly accounted for by some aromatic moieties found in sporopollenin chemical structure. For example, coumaric acid and its derivatives were found responsible for absorbing UV-B.[8,48,111,112,139]

Several authors therefore concluded sporopollenin was UV-screening or, at least, UV-absorbent.[8,42,111,122,138]

4 Structure characterisation studies

Various attempts have been made to elucidate chemical structure of sporopollenin from pollen grains and spores from several species. Since sporopollenin is extremely resistant and inert, many classical techniques could not be used. However, different chemical features have been established, although its definitive composition and the biochemical pathways involved in its synthesis are not yet clear. The different workers who attempted to better understand the chemical composition of sporopollenin raised a vast controversy. Discussion is not yet over and still faces the mysterious nature of sporopollenin.

Note: For comparison purpose, some teams have largely used a synthetic polymer obtained by oxidative polymerisation of β-carotene.[140] It has been integrated in the analytical process of sporopollenin and therefore appears below in several tables and paragraphs under the name 'poly-β-carotene' or simply 'polycarotene'.

4.1 Techniques and results

Due to the great resistance of sporopollenin and its lack of solubility in any solvent, conventional techniques of investigation were not readily available to determine its chemical composition. Degradation methods were first utilised, along with chemical derivatisations. Later on, biochemical procedures led to clearer ideas of sporopollenin biosynthesis pathways. Finally, spectroscopy enabled important progress.

4.1.1 Chemical degradation studies

Identification of the degradation products after ozonolysis, potash fusion, nitrobenzene oxidation, aluminium iodide attack or pyrolysis was performed by TLC, GC, HPLC and/or MS.

4.1.1.1 Combustion elemental analysis

All results of combustion elemental analyses were consistent over the time within one species and using the same sporopollenin extraction method.[53-56,82,86] A first general conclusion was that sporopollenin is nitrogen-free. Also, little variation was

found from species to species. The main variations (especially the quantity of oxygen) were associated with changes in biological process during evolution, vascular plant being found to contain more oxygen, although it may well be due to inconsistencies in the purification method, more particularly the removal of intine. Examples of results are gathered in Table 4. Generally speaking, elemental proportions have been reported in many species (angiosperms, gymnosperms and cryptogams) to fit the following ranges: %C 56-63%, %O 29-37% and %H 7-9%.

Species	Extr.	Proportions (% (w/w))				Ref.
		C	O	H	N	
Aspergillus niger	A	79.7	11.8	8.5	0	[37]
Corylus avellana	A	68.8	22.4	8.8	0	[56]
Lilium henryi	A	60.1	32	7.9	0	[14]
Lycopodium clavatum	A	65.3	26.1	8.6	0	[56]
		59.0	32.8	8.2	0	[82,86]
		65.2	26.1	8.7	0	[14]
Mucor mucedo	A	62.1	30.4	7.5	0	[14]
Pinus sylvestris	A	67.1	23.9	9.0	0	[56]
		59.2	32.2	8.6	0	[82,86]
		55.6	36.3	8.1	0	[14]
poly-β-carotene		63.9	28.4	7.7	0	[14]

Extr.: extraction methods

A: acetone treatment, potassium hydroxide hydrolysis and phosphoric acidolysis

Table 4 – Examples of elemental analyses of sporopollenin

Based on the carbon/hydrogen ratio [ca. 5/8 (mol/mol)], Zetzsche *et al.*[54] suggested the first hypothesis of sporopollenin composition: a polymer of terpenoid nature.

Recently, elemental analysis was used to prove the bonding system of carbons in sporopollenin was equally shared between CH and CH_2.[141] Solid-state ^{13}C NMR confirmed the low signal for CH_3 and quaternary carbons.

4.1.1.2 Kuhn-Roth oxidation

During their investigations, Zetzsche *et al.*[53-55] stirred sporopollenin from *L. clavatum* in chromic acid under reflux to carry out a Kuhn-Roth oxidation. Any acetic acid formed was then distilled off and its amount reflected the loading of methyl groups bonded to a carbon atom: ca. 1.2mmol.g^{-1}.

Note: This method would however not detect *gem*-dimethyl groups on the same

carbon.[36,142] The previous method can only be regarded as affording minimal values.

4.1.1.3 Ozonolysis

Amongst other chemolyses, ozonolysis was a very common way of decomposing sporopollenin. Resulting ozonides were decomposed by hydrogen peroxides under acidic conditions. Oxidation products were found, by GC, HPLC or GC-MS, to be a mixture of carboxylic acids. Their exact composition appeared to vary from species to species and from workers to workers, as indicated in Table 5. Incidentally, ozonolysis was found not to affect the intine, which sometimes remained intact when it was not extracted first (e.g. *L. clavatum* or *Pinus sylvestris*).[86]

Species	Extr.	Degradation products	Ref.
Lycopodium clavatum	A	simple dicarboxylic acids (malonic, succinic, glutaric and adipic acids)	54
Lycopodium clavatum	A	7-hydroxy-, 6,11-dioxo- and underivatised 1,16-hexadecanedioic acid and diacids (malonic – suberic acid)	82,86
Pinus sylvestris	A	1,16-hexadecanedioic acid and diacids (malonic – suberic acid)	
Lycopodium clavatum & *Lilium henryi*	A	mono- and dicarboxylic acids	73,113,137
Pinus pinaster	B	hexanedioic acid, fatty acids, paraffins	143
Betula alba	B	myristic acid, paraffins	
Ambrosia elatior	B	hexanedioic acid, stearic acid, paraffins	
Capsicum annuum	B	ω-dicarboxylic acids	

Extr.: extraction methods
A: acetone treatment, potassium hydroxide hydrolysis and phosphoric acidolysis
B: HF treatment, potassium hydroxide saponification, hydrochloric acidolysis

Table 5 – Ozonolysis of sporopollenin: degradation products

Ozonolysis is known to cleave double bonds and ether linkages, thus releasing the corresponding aldehydes and acids, under appropriate conditions. This was confirmed on sporopollenin by IR monitoring: reduction of C=C stretching (ca. 1650-1600cm^{-1}) and C-O stretching peaks (ca. 1150-1100cm^{-1}) parallel to an increase of C=O stretching bands (ca. 1700cm^{-1}).[143]

Shaw and Yeadon[82,86] reduced the acids resulting from ozonolysis so as to change oxygenated carbon to methylenes and obtained a mixture of fatty acids, dominated by palmitic acid. Brooks and Shaw[35,36,73,113,137] and their co-workers[15,144] showed similar oxidative products were obtained by ozonolysis of sporopollenins and polymers of several carotenoids.

4.1.1.4 Potash fusion and nitrobenzene oxidation

By degradation in fused potassium hydroxide, sporopollenins from *Lycopodium clavatum* L., *Pinus sylvestris* L. (Scots pine) and *Lilium henryi* Baker (Henry's lily) were shown to release phenolics compared by TLC (see Table 6).[36,82,86,137] Incidentally, potash fusion of *L. clavatum* exines also produced a fraction of *n*-alkanoic acids (pentanoic to undecanoic acids).[82] The earliest trials estimated the loading of aromatic building blocks to account for ca. 10-15% of the weight of the sporoderm.[82,86] On the other hand, the conclusion to further experiments by Shaw *et al.*[36,137] was that aromatic products originated from a carotenoid skeleton, produced as artefact by the forcing conditions.

Species	Extr.	Degradation method	Major degradation products	Ref.
Lycopodium clavatum, *Pinus sylvestris* and *Lilium henryi*	A	potash fusion	*p*-hydroxybenzoic acid (*m*-hydroxybenzoic acid) protocatechuic acid *n*-alkanoic acids	36,82,86,137
poly-β-carotene		potash fusion	*p*-hydroxybenzoic acid *n*-alkanoic acids	36,82,86,102,137
Corylus avellana	B	saponification	*p*-coumaric acid (*p*-ferulic acid)	102
		nitrobenzene oxidation	*p*-benzaldehyde *p*-coumaric acid	
		potash fusion	*p*-hydroxybenzoic acid	
Pinus mugo (wings)	B	saponification	*p*-coumaric acid (ferulic acid)	90
		nitrobenzene oxidation	*p*-benzaldehyde *p*-coumaric acid	
		potash fusion	*p*-hydroxybenzoic acid	

Extr.: extraction methods
A: acetone treatment, potassium hydroxide hydrolysis and phosphoric acidolysis
B: pollen disruption followed by enzymatic treatment

Table 6 – Degradation products obtained by potash fusion, nitrobenzene oxidation or saponification

Later on, another study was conducted on sporopollenin from *Corylus avellana* L. (hazelnut).[90,102] After enzymatic purification, saponification, potash fusion and oxidation in nitrobenzene yielded *p*-coumaric acid, *p*-hydroxybenzoic acid and *p*-benzaldehyde respectively, as the major aromatic degradation products. The conclusion drawn was that *p*-hydroxyphenyl structures were most probably building blocks of sporopollenin. Phenols were considered to account for at least 18-20% of the total dry

weight, and to be branched to the backbone by patterns close to suberin or cutin, but very different to lignin.[90] The same workers also investigated these degradations on polycarotene and found only little aromatic compounds in the resulting products.[102]

Yet the previous work by Shaw *et al.*[36,82,86,137] showed some phenolic degradation products were present even when sporopollenin had been isolated through a harsh protocol involving saponification. Thus, phenolic building blocks cannot be connected to sporopollenin backbone by labile bonds such as ester functions.[90,102,145]

4.1.1.5 Treatment with aluminium iodide

Aluminium iodide is a compound known to split ether linkages selectively. After non-structure-modifying extraction of sporopollenin from *Pinus mugo* Turra (mountain pine) pollen sacci, it was subjected to a treatment with aluminium iodide.[145] The main degradation product was found to be *p*-coumaric acid. This experiment corroborated other results showing *p*-coumaric acid may be a monomer of sporopollenin (see Sections A-4.1.1.4 and A-4.1.1.6). In addition, it showed that *p*-coumaric acid should be bonded to sporopollenin backbone by ether functions.

4.1.1.6 Pyrolysis

Species	Extr.	Degradation products	Ref.
Various (including *Lycopodium clavatum* and *Pinus sylvestris*)	A	ionene, naphthalene, anthracene and their derivatives	146
poly-β-carotene		ionene	
Pinus mugo	B	*p*-coumaric acid (terpenic hydrocarbons)	145
Pinus sylvestris	B	*p*-coumaric acid	147

Extr.: extraction methods
A: acetone treatment, potassium hydroxide hydrolysis and phosphoric acidolysis
B: pollen disruption followed by enzymatic treatment

Table 7 – Products of pyrolysis of sporopollenin

Combustion of different sporopollenins (including from *L. clavatum* and *Pinus sylvestris*) under inert atmosphere (pyrolysis), coupled with mass spectrometry and, sometimes GC, has consistently yielded aromatic compounds. The findings of the different workers were however different:

- Achari *et al.*[146] found ionene and similar hydrocarbon aromatic compounds;
- Wehling *et al.*[145] detected mainly *p*-coumaric acid attached to its acid group by ester linkage, and possibly by ether bond;

- by pyrolytic methylation electron impact MS, Mulder *et al.*[147] also found this compound in sporopollenin from *Pinus* sacci.

Incidentally, polycarotene pyrolysis yielded ionene only, corroborating previous demonstrations that carotenoids give aromatic compounds when heated.[146] Failure to obtain peaks above m/z = 295 exclude the presence of polyphenol as in lignin.[145]

A recent study was conducted on unextracted *Lycopodium cernuum* L. spores.[148] However, the authors tended to consider the results as arising from the sole sporopollenin. Thermochemolysis with tetramethylammonium hydroxide at 300°C released mainly saturated linear carboxylic acids (in the range C_8 to C_{22}), unsaturated linear acids (C_{16} and C_{18}), linear ω-diacids and benzoic acid derivatives. Subsequent pyrolysis (at 610°C) liberated yet other products: *p*-coumaric acid and ferulic acid, as well as their saturated counterparts, *n*-alkanoic acids and *n*-alkenes and alkanes. This investigation was supported by FTIR spectroscopy and confirmed that sporopollenin had aromatic moieties, including hydroxycinnamic acids, within an aliphatic framework built from lipids.

4.1.2 Derivatisations of sporopollenin

Apart from degradation studies, functional group identifications performed on sporopollenin also involved derivatisations as part of the structure elucidation.

4.1.2.1 Halogenation

Direct bromination of sporopollenin evidenced the presence of unsaturations. Bromine was loaded onto sporopollenin to a level of 50%; substitution could not be excluded although addition on unsaturations seemed more likely.[36,53] On the basis of bromine being attached exclusively by covalent addition to double bonds, a loading of 3mmol.g^{-1} of carbon-carbon double bonds can be estimated. This highlighted the high degree of unsaturation in sporopollenin.

Quantitative experiments later confirmed the direct uptake of bromine by sporopollenin.[12,13,149] Bromosporopollenin was hydrolysed in alkali and released bromide precipitated on silver nitrate. Gravimetric results then gave the loading of bromine (see Table 9). Iodine value, obtained by back-titration of Wij's solution (iodine chloride) after absorption to sporopollenin,[12,13] was not reliable for this purpose. Indeed, oxido-reductive properties (see Section B-4.4) of sporopollenin had been neglected at

that time since iodine is also consumed by reduction.

Other halogenations have been performed as well. Hydroxyl groups have been substituted by chlorine using phosphorus pentachloride or phosphorus oxychloride, and aromatic groups have been reacted by chloromethylation using zinc chloride, dimethoxymethane and thionyl chloride.[12]

4.1.2.2 Attachment to hydroxyls

Species	Extr.	Loading of hydroxyls ($mmol.g^{-1}$)	Ref.
Lycopodium clavatum	A	9.8	53
		4.3	150
		1.15	12
Pinus sylvestris		8.5	56
		6.3	150
Secale cereale		4.6	56
Lilium henryi		8.4	150
polycarotene		1.2	150

Extr.: extraction methods
A: acetone treatment, potassium hydroxide hydrolysis and phosphoric acidolysis

Table 8 – Quantification of hydroxyl groups in sporopollenins

In order to detect and quantify hydroxyl content, acetylation was performed on sporopollenin. The release of acetyl esters by saponification then enabled an estimate of the loading of hydroxyls.[12,53-56] Since the saponification method lacked of precision due to a reliance solely on acid base titrations, the release of acetyl attachments was determined by radiochemical techniques, after acetylation by ^{14}C-labelled acetic anhydride.[150] Results obtained for exines of different origins are gathered in Table 8.

Another technique was to add 9-fluorenylmethyl carbamate (Fmoc) groups onto sporopollenin hydroxyls. Further detachment with piperidine led to a UV-active adduct whose amount was assessed by UV absorbance (see Table 9).[12,13] Extreme variations were found and this probably related to the inconsistency in extraction since any remaining cellulose intine would give rise to erroneous results.

4.1.2.3 Reaction on carbonyls

The carbonyls present on sporopollenin were reacted with Brady's reagent (2,4-dinitrophenylhydrazine) to form the corresponding hydrazones. The resulting product was readily detected by IR as it exhibited characteristic peaks (C=N at $1616cm^{-1}$, NO_2 at 1512 & $1335cm^{-1}$).[12,13] Given that Brady's reagent has four nitrogen atoms and

sporopollenin none, the number of reactive sites was established by combustion elemental analysis (see Table 9). Further distinction between aldehydes and ketones was attempted using Fehling's solution; no precipitate being observed, it has been reported that no aldehyde were present.[12,13] However, results were in fact not conclusive since any precipitate of cuprous oxide could not be detected due to its probable adhesion to the solid sporopollenin.

Analytical technique	Result ($mmol.g^{-1}$)	Analysed functional group	Function loading ($mmol.g^{-1}$)
bromination & gravimetric analysis	Br^-: 5	unsaturations: >C=C<	2.5[12,13]
titration with sodium hydroxide	OH^- consumed: 1.3	acidic functions: carboxyls, lactones, phenols	1.3[12]
Brady's & elemental analysis	N: 2.4	carbonyls: >C=O	0.6[12,13]
attachment of Fmoc-Cl and UV analysis of released Fmoc-piperidine	Fmoc-piperidine: 0.4-1.4	hydroxyls: -OH	0.4-1.4[12,13]

Table 9 – Quantification of various functional groups in sporopollenin

4.1.2.4 Acidic functions

Some functional groups on the surface of sporopollenin are involved in acid-base equilibrium. In this case, exines can parallel acidity studies undertaken on activated carbons.[151] Sporopollenin's structrure is so complex that it may alter the strength of these acido-basic groups. Therefore, and similarly to activated carbons, distinct acidity constants (K_a) cannot be distinguished for each functional group in sporopollenin. Exines can thus be characterised by a continuous distribution of acidity constants. The concept of conventional functional groups can be used in the case of sporopollenin as it is to characterise the surfaces of activated carbons. These groups exhibited by sporopollenin are divided, according to their typical pK_a interval, into: carboxyl (pK_a=2.0-4.0), lactone (pK_a=4.0-7.0) and phenol (pK_a=7.0-10.0). A full investigation of acidity of activated carbons is carried out by successive use of sodium bicarbonate, sodium carbonate, sodium hydroxide and sodium methanolate to precisely evaluate the levels of carboxylic acids, lactones, phenols and enolisable ketones.[152] A similar trial has yet to be undertaken on sporopollenin.

To date, sporopollenin's acidity has been assessed by back-titration against dilute sodium hydroxide.[12] The results, displayed in Table 9, accounted for all functions

that could react with sodium hydroxide *i.e.* carboxylic acids, lactones and phenols.[152]

4.1.2.5 Attachment of thiols and amines to sporopollenin

Despite its inertness, sporopollenin was also used as a solid-phase reagent with the perspective of various derivatisations. In addition to the examples previously shown, anchoring functions were implemented to the polymer with the perspective of developing spacers or linkers for solid-phase organic synthesis and/or scavenging.

Bromosporopollenin was further derivatised by nucleophilic substitution. Thiolation was attempted on it by reaction with thiourea or sodium hydrogen sulphate.[13,153] Preliminary investigations were carried out to explore properties of thiosporopollenin in terms of nucleophilicity and oxido-reductive characteristics.[153]

The substitution of amines to sporopollenin is attractive since such functional groups can enable attachment of a wide variety of substances due to the efficient nucleophilicty of amines. Ammonia and primary amines were found to covalently attach to sporopollenin while secondary and tertiary amines formed labile bridges.[12,13] Furthermore, aromatic amines readily bound in large quantities.[12,154] Diamines could also easily be used to create spacers for further reaction, despite possibilities of cross-linking.[12,154] Succinic acid, for instance, yielded amide links with aminated sporopollenin. Attachment of amino acids was also successfully attempted.[13,149] Hypothesis of an amide linkage between ammonia or amino groups and sporopollenin was never supported by any strong evidence though.

4.1.2.6 Staining

The reactivity of different specific dyes on sporopollenin was explored in attempt to detect the presence of different substances and functional groups. An overview of some of them is summed up in Table 10. Most of the early workers tested sporopollenin for its cytochemical and histochemical properties, from Braconnot[17] to Zetzsche.[53-55] Staining properties of sporopollenin enabled to distinguish its different layers (endexine and ectexine)[2], to compare it with other resistant materials (e.g. lignin, cutin or cellulose) and to characterise some typical groups.

Histology of orbicules showed they were composed of lipids other than carotenoids, since they stained positively with Sudan III but negatively with antimony dichloride or concentrated hydrochloric or sulphuric acid.[14] This contradicted the hypothesis of Shaw *et al.*[137] that carotenoid precursors of sporopollenin might

accumulate in Ubisch bodies.

Stain	Specificity	Stained layer	Ref.
Alcian blue	pectin	endintine	[2]
auramine O	lipids	ectexine	[143]
Calcofluor white	cellulose & chitin	intine	[2]
fuchsine	aldehydes	ectexine	[2]
iodine water	starch	none	[17]
iodine in sulphuric acid	cellulose	intine	[53]
Nile blue A	anionic groups	exine	[35]
Nile azure B	anionic groups	exine	[35]
osmium tetroxide	unsaturated aliphatic carbon-carbon bonds	exine	[35]
periodic acid-Schiff base	cellulose & carbohydrates	intine	[2]
Sudan IV	cutin & suberin	none	[35]
toluidine blue	anionic groups	exine	[35]

Table 10 – Overview of different staining methods envisaged on sporopollenin

4.1.3 Tracer and biochemical studies

A first investigation on the biochemical pathways of sporopollenin synthesis was carried out in the 1960s in *Lilium henryi* Baker (Henry's lily).[73,137] The presence of carotenoids and their ester derivatives in anthers of the flowers was followed in time during the growth of the buds and correlated with the formation of sporopollenin. Anther carotenoids and their derivatives were collected in maturing buds and polymerised under oxidative conditions. Ozonolysis of the resulting polymer gave degradation products that were close to those obtained from sporopollenin. These results were paralleled by surveys between sporopollenin development and carotenoid production in other taxa: *Lilium longiflorum* Thunb. (Easter lily), *Ranunculus repens* L. (creeping buttercup) and *Geum coccineum* Sibth. & Sm. (scarlet avens). The concomitance of sporopollenin and carotenoids was recurrent in all vascular plant species studied.[144] It was also observed in spores of some fungi like *Mucor mucedo* Fr. By contrast, when carotenoids were absent from the fungal sporangium, spores did not produce any sporopollenin. This was the case in the fungus *Rhizopus sexualis* Callen for instance. These results were the main source of Brooks and Shaw's theory of sporopollenin as an oxidative polymer of carotenoids. Three illustrative examples of carotenoids are given in Table 11.

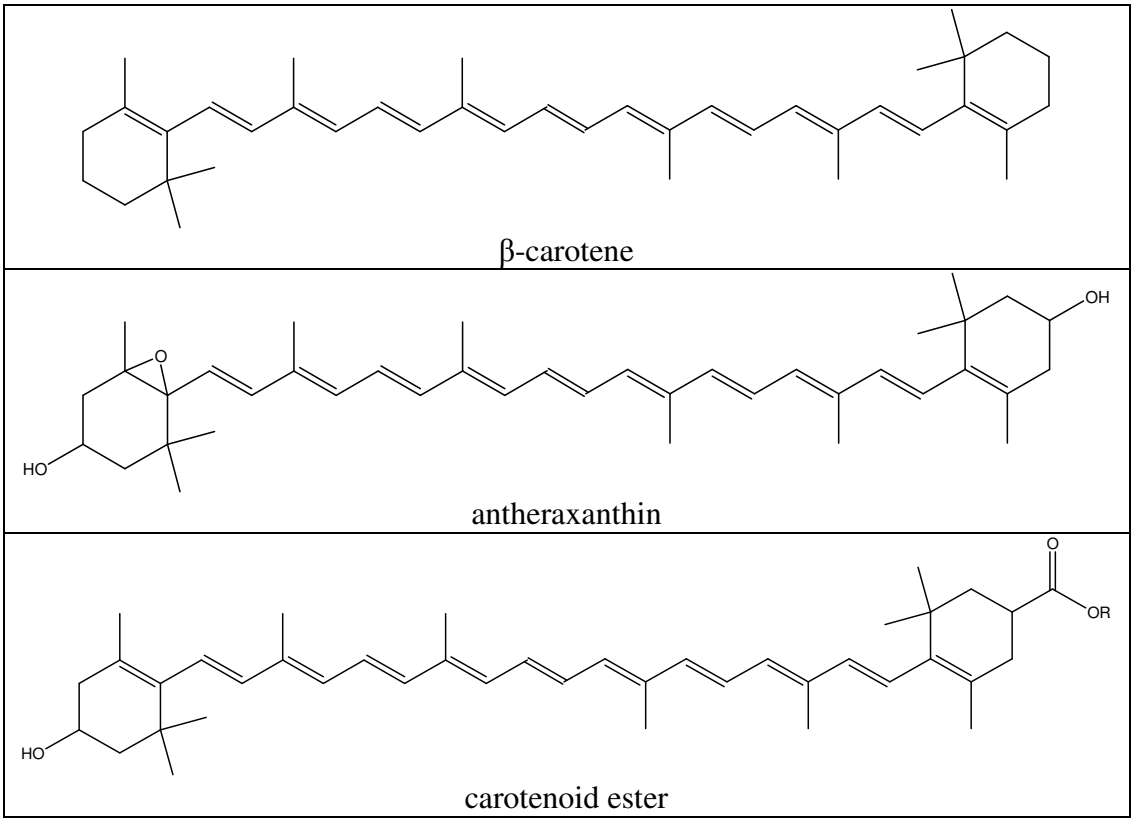

Table 11 – Examples of carotenoids

Furthermore, some radiochemically labelled precursors (see Table 12) fed to different plants were found to incorporate in sporopollenin, although in quite low levels.[34,35,83,113] High incorporation loadings were obtained with carotenoids or their precursors in fungi and *Cucurbita pepo* L., but no radiolabel was passed to sporopollenin in *Lilium henryi* Baker. This last problem was considered to be due to the stage of development of the flowers, and emphasised the unreliability of such *in vivo* experiments.

Arguing that the previous results obtained on sporopollenin from vascular plants were not unequivocal, Wiermann *et al.*[155] carried out an inhibition experiment. In the plant nutrient solution, they mixed norflurazon, a herbicide that blocked completely the biosynthesis of any carotenoid within the anthers of *Cucurbita pepo* L., and found that sporopollenin was still developing normally. Therefore, they concluded that sporopollenin was not synthesised from carotenoids. It was later argued that incorporation previously acknowledged by Brooks and Shaw actually came from tryphine and pollenkitt remnants.[47]

In attempt to discover part of the biosynthesis of sporopollenin, an improved method was developed by Wiermann *et al.*[104] in which anthers of *Tulipa gesneriana* L.

cv. "Apeldoorn" were incubated in solutions of ^{14}C-labelled precursors (see Table 12), from mid to late postmeiotic stages of development. Large amounts of glucose and acetate were lost as carbon dioxide during catabolism, but some entered the sporopollenin structure; tyrosine and mevalonate were almost not incorporated and washed away during sporopollenin extraction; palmitate and malonate seemed to enter the structure only in variable quantities.[47,104,156] Access of the labelled substances to the loculus was questioned.[104] To improve the application method, it was suggested that cross sections of the stamens should be incubated instead of the whole anthers. In contrast to the other tested products, and more importantly, phenylalanine appeared to be an important precursor of sporopollenin. Its aromatic ring was completely integrated in the structure, according to the tracer experiments performed with the amino acid marked in different positions (U-^{14}C, ring U-^{14}C and 1-^{14}C), and the whole phenylpropane unit was probably kept intact.[47,104,156] These experiments were backed up in *Cucurbita maxima* Duchesne to show the phenomenon had no phylogenetic restriction.[47,104]

Precursors	Species	Incorporation in sporopollenin	Ref.
^{14}C-acetate	*Mucor mucedo*	none	35,83
^{14}C-mevalonate		little	
^{14}C-palmitate		none	
^{14}C-β-carotene		little	
^{3}H-β-carotene		some	
^{3}H-β-carotene	*Neurospora crassa*	some	35
^{14}C-acetate	*Cucurbita pepo*	some	35,83
^{14}C-palmitate		some	
^{14}C-mevalonate	*Lilium henryi*	none	35,83
^{14}C-antheraxanthin		none	
^{14}C-phenylalanine	*Tulipa gesneriana* cv. "Apeldoorn" and *Cucurbita maxima*	high	104,156,157
^{14}C-tyrosine		very little	
^{14}C-glucose		some	
^{14}C-acetate		variable	
^{14}C-mevalonate		little	
^{14}C-malonate		quite high	
^{14}C-*p*-coumaric acid		variable	
^{14}C-acetate	*Cucurbita maxima*	little	158
^{14}C-malonate		little	
^{14}C-linoleic acid		little	
^{14}C-oleic acid		high	
^{14}C-stearic acid		little	

Table 12 – Summary of the tracer studies on sporopollenin

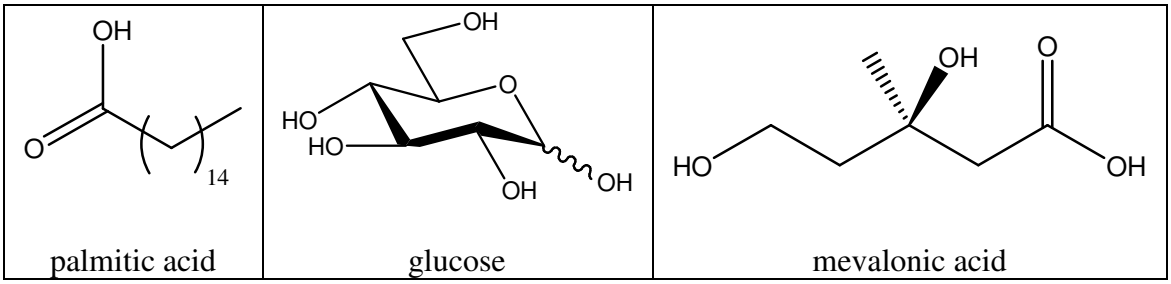

palmitic acid | glucose | mevalonic acid

Table 13 – Some aliphatic precursors used in tracer studies

Degradation studies of the ^{14}C-tagged sporopollenin were then carried out, after incubating anthers in ^{14}C-phenylalanine solution.[47,104,156] Enzymatic degradation with esterase showed no release of markers. On the other hand, ^{14}C-*p*-coumaric and ^{14}C-*p*-hydroxybenzoic acids (illustrated in Table 14) were formed by saponification and potash fusion, respectively, of sporopollenin from anthers incubated in labelled phenylalanine.

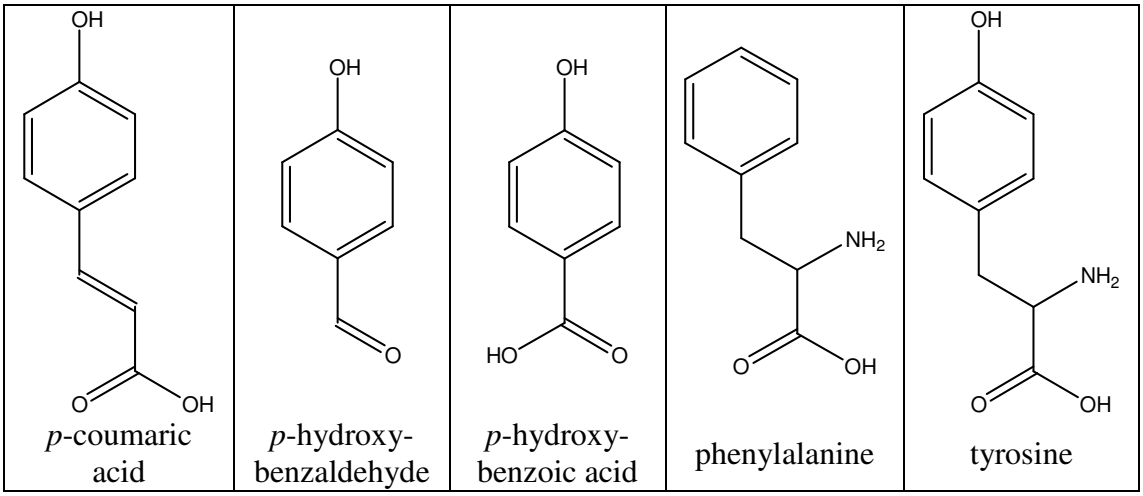

p-coumaric acid | *p*-hydroxy-benzaldehyde | *p*-hydroxy-benzoic acid | phenylalanine | tyrosine

Table 14 – Some phenylpropanoids and phenolics in tracer studies (precursors and degradation products)

Whereas the aromatic systems were quite well defined in sporopollenin, new aliphatic precursors had to be identified since carotenoids were found improbable. During an inhibition study performed in a green alga (*Scenedesmus acutus* Chodat), oleic acid was found to be incorporated into sporopollenin.[97] A significant tracer study was carried out by Wiermann *et al.*[158] on sporopollenin isolated from *Cucurbita maxima* Duchesne (see Table 12). The tracking of fatty acids was pursued from its first precursors: acetate and malonate were found to incorporate in sporopollenin; the first one especially was detected to various levels depending on inhibitors applied to competing metabolic pathways (such as sterol biosynthesis). Among fatty acids directly

applied as precursors, stearic acid and more importantly oleic acid were found to form part of sporopollenin, thus corroborating the previous findings.[97] Linoleic acid however was not confirmed in the polymeric structure.

4.1.4 Spectroscopic techniques

Spectroscopic techniques have long been used on sporopollenin degradation products. Mass spectrometry, coupled with chromatography, was extensively employed to characterise the residues from ozonolysis, pyrolysis, oxidations and other degradation processes. Other techniques such as infrared and X-ray have been used to study whole sporopollenin particles. NMR has been used for several years to study solutions of materials but it was not until the late 1980s that solid-state NMR gave interesting fine enough spectra for analytical purposes of sporopollenin. The results obtained using these techniques suggest that sporopollenins are composed mainly of long saturated aliphatic chains with varying amounts of aromatics, with significant variations due to divergent phylogenetic origins.

4.1.4.1 Infrared spectroscopy

Shaw and Yeadon[82,86] were the first to perform infrared spectroscopy of sporopollenins. After their work on exines of various origins (including *Pinus sylvestris* pollen and *Lycopodium clavatum* spores), they made several observations:

- They compared sporopollenin's spectrum with that of cork and reported that the band at 1740cm^{-1}, indicating esters in cork, was absent from sporopollenin's spectrum.
- After methylation with diazomethane, this same band was still lacking, so they concluded that carboxyls were absent. This was later contradicted and the presence of carboxyls was finally acknowledged in all sporopollenins by Shaw and his co-workers (see below).
- Peaks around 1500 and 1600cm^{-1} indicated the presence of aromatic rings, which was confirmed by the release of oxalic acid after ozonolysis (see Section A-4.1.1.3).
- Intensity of the band at 1510cm^{-1} increased after methylation, probably highlighting methylated phenols.
- The fact that spectra of exines from several plant species were similar showed

that sporopollenins from different origins are closely related.

More recent studies on sporopollenins from *Magnolia grandiflora* L. (bull bay),[135] *Hibiscus syriacus* L. (garden hibiscus),[135] *Tulipa gesneriana*,[159] *Cucurbita pepo*,[159] *Typha angustifolia*,[141,160] as well as many other plant species (ferns, mosses, gymnosperms and angiosperms)[143,161] corroborated the phylogenetic spectral similarities and thus, the common structures of sporopollenin from different origins.

General features of sporopollenins infrared spectra (detailed in Table 15) emphasised the importance of aliphatic chains in the macromolecule and the broadness of certain peaks, with possible overlapping of signals, indicated the environment diversity for those functional groups. Interpretations were given with more or less precision depending on the quality of the spectra, but the main bands were consistently showing hydroxyls, aliphatic carbons, carbonyls, unsaturations and ether groups. The main controversies that were raised by these various studies concerned the presence of carboxylic groups, the similitudes with polycarotene and the occurrence of aromatic moieties.

Wave number (cm^{-1})	**Peak form**	**Interpretations suggested**
3500-3400	strong, broad	hydroxyls (O-H ν)[82,86,135,141,143,159-161]
2930 & 2850	strong, sharp	methylenes (C-H ν)[82,86,141,143,159-161]
2700	shoulder	carboxyls (O-H ν)[143]
1750-1650	medium	carbonyls (C=O ν)[82,86,135,141,159-161]
1625	medium	amines (N-H δ)[141,160]
1600-1500	variable	aromatics[82,86,143,159,161] or olefins[143,159,161] (C=C ν)
1480-1440	sharp	aliphatic carbons (CH_2 δ)[141,143,160]
1200-1000	broad, variable	ethers (C-O ν)[82,86,135,143,159,161]
840	medium	aromatic (C-H oop ω)[141,160]
730	medium	aliphatic carbons (CH_2 ρ)[143]

ν: stretching; δ: scissoring; ρ: rocking; oop ω: out of plane wagging; ρ: rocking

Table 15 – Infrared interpretations

As aforementioned, Shaw and Yeadon[82,86] believed that carboxyl groups were absent from sporopollenin. However Shaw and his team later revised their conclusions.[34-36,73,113,137] The presence of carboxyls in sporopollenin is now widely recognised.[135,143,159,161]

Also infrared studies were carried out on sporopollenins isolated from different species in order to try and show resemblance between their spectra and that of polycarotene.[34-36,73,113,137] Given the resolution of their spectra, they considered that

sporopollenin and polycarotene had very similar IR spectra, which supported their theory of sporopollenin being a polycarotenoid (see Section A-4.2.4). With the development of Fourier transform technique though, higher degrees of resolution were offered. Wierman *et al.*[155,159-161] then showed that the spectra of sporopollenin were much more complex than that of poly-β-carotene. This contradicted the previous conclusions thus weakening Shaw's theory. In their respective interpretations of IR spectra, Schulze Osthoff and Wierman[90] emphasized the aromatic components of sporopollenin whereas Hayatsu *et al.*[162] insisted on the aliphatic moieties.

On the other hand, aromatic components of sporopollenin were extensively investigated (in *Pinus mugo* sacci), and some characteristic signals have been highlighted (see Table 16).[90]

Wave number (cm^{-1})	Peak form	Interpretations suggested
1625	sharp	aromatics
1600	sharp	aromatics
1500	sharp	aromatics
1430	medium	aromatics
830	sharp	*p*-hydroxylated aromatics

Table 16 – IR interpretations of aromatic bands by Schulze Osthoff & Wiermann[90]

Later on, the same team[159] showed that sporopollenin from *Tulipa* spec. had a more important aromatic nature than that of *Cucurbita pepo*, corroborating the idea that sporopollenins differ from species to species by their aromatic side chains. They also demonstrated that sporopollenin acquired its spectroscopic characteristics from the very beginning of its polymerisation. Only few changes appeared during maturation of exines, mainly broadening of signals (and thus overlapping of peaks) due to positioning of identical functional groups in various chemical environments.

Aromaticity of sporopollenin seemed uncontested until Domínguez *et al.*[143] denied the presence of aromatic functions on sporopollenin extracted from four different spermatophyte species by HF-hydrolysis. This was however inherent to their preparation method. It was indeed implemented with a special initial acidolysis with hydrochloric in 1,4-dioxane under reflux to eliminate lignin-like phenolic material, and then a saponification with potassium hydroxide in methanol under reflux to remove all aromatic compounds linked by ester bonds.

A series of infrared spectra was also recorded on sporopollenin isolated from

Typha angustifolia pollen by enzymatic extraction.[141,160] Consistent IR spectra, after sequential hydrolyses in acidic methanol, supported the hypothesis of uniformity of the polymer, while suggesting ether bonds cross-linked its skeleton.[141] Peracetylation of sporopollenin affected most of its hydroxyl groups to yield acetyl esters as confirmed by changes on the spectrum:[160]

- decrease of hydroxyl peak (3425cm^{-1});
- apparition of intense signals at 1738cm^{-1} (C=O ν), 1373cm^{-1} (CH_3 ρ), 1243cm^{-1} (C-O ν), 1020cm^{-1} (C-O δ);
- sharpening of peak at 1436cm^{-1} (CH_3 δ).

The FTIR spectra obtained in a recent study,[148] conducted on *Lycopodium cernuum* L. spores, and combined with thermochemolysis and pyrolysis (see Section A-4.1.1.6), were in agreement with the previous data, *i.e.* strong bands due to hydroxyl groups (3350cm^{-1}), aliphatic units (2800-3000cm^{-1}), carbonyl bonds (esters at 1740cm^{-1}, carboxylic acids at 1700cm^{-1} and ketones at 1680cm^{-1}) and ether (1050-1300cm^{-1}). A strong aromatic band at 1510cm^{-1} was also observed and its presence was attributed to the fact that *L. cernuum* generally grow under important UV exposition (tropical regions of South-East Asia, at high altitude) and developed a high level of UV-absorbing components, namely hydroxycinnamic acids.

4.1.4.2 X-ray photoelectron spectroscopy (XPS)

A precise elemental composition of sporopollenin was determined by X-ray photoelectron spectroscopy.[135] After acetolysis, exines purified from *Magnolia grandiflora* L. (bull bay) and *Hibiscus syriacus* L. (garden hibiscus) were found to be composed only of carbon, oxygen and hydrogen. No traces of silicon or metallic element were detected. More precisely, same peaks at 287eV on the C(1s) spectra of both exines suggested a common aliphatic backbone for the sporopollenins of these two angiosperms. Results also tended to show a wide variety of environments for these aliphatic carbons, which was supportive of the findings in IR.

The presence of carbon [285eV, C(1s)] and oxygen [532eV, O(1s)] was later[141] corroborated on sporopollenin obtained from *Typha angustifolia* by enzymatic extraction and acidic methanolysis. Contradictory results indicated the presence of nitrogen [399eV, N(1s)], but were attributed to contamination by enzymes during extraction process. Identification of different chemical bonds by XPS confirmed the

presence of groups such as aliphatic carbon chains, carbonyls, carboxyls and alkoxyls. The relative amounts of the different chemical groups were suggested as follows:

- proportions of carbon functions: 61% in C-C or C-H, 22% in C-O (esters, ethers, or alcohols), 14% in C=O or O-C-O (carbonyls, diols, etc.), 3% in carboxyls (esters or acids);
- proportions of oxygen functions: 88% in C-O and 10% in C=O.

4.1.4.3 Nuclear magnetic resonance (NMR)

Conventional NMR had long been unsuitable to study sporopollenin since it is not soluble in any medium. However, solid-state ^{13}C NMR was first used on sporopollenin-like polymers in 1983 obtained from a unicellular green alga, *Botryococcys braunii* Kütz. When initially applied to actual sporopollenins, the commencing technique only gave poorly resolved signals: 15-20ppm (weak, C-CH_3); 29-30ppm (high, broad, C-CH_2-C and other aliphatic C); ca. 60-70ppm (weak, C-O); ca. 120-130ppm (broad, olefinic and/or aromatic C).[84,85,91,96,141,160,161,163,164] In latter studies such assignments were confirmed on sporopollenins from many different species (including *L. clavatum* L., *Pinus* spec., *Ambrosia trifida* L. and *Typha angustifolia* L.) with a better resolution.[141,160,161]

In addition, a broad signal at ca. 170ppm has then been consistently found on all sporopollenins highlighting the presence of carboxyl groups. The extraction method (see Section A-2.4.1) had a direct impact on this signal; it was systematically reported as strong after acetolysis because the signal of acetylated hydroxyls was added to that of other carboxyls;[91,163,164] but otherwise, it was very weak after alkaline and acidic hydrolyses.[84,85,161] Wilmesmeier *et al.*[161] and Espelie *et al.*[96] managed to resolve this multiplet into 4 peaks, which they interpreted as follows: 145ppm (very weak, quaternary aromatic C); ca. 165ppm (ester); ca. 175ppm (acid); and ca. 200ppm (ketone). Espelie's extraction involving mild conditions (with 4-methylmorpholine *N*-oxide, see Section A-2.4.2),[96] an interpretation highlighting esters was not surprising. However, Wilmesmeier *et al.*[161] hydrolysed sporopollenin fully with potassium hydroxide and phosphoric acid. Therefore, the presence of esters would be seen as very unlikely unless steric hindrance was such that the functional groups could not be cleaved by the extraction treatments.

In some of the past studies, other interesting signals were mentioned: 40ppm (shoulder, **C**-CO)[141,160,165,166] and ca. 105ppm (medium or weak, O-C-O), denoting the

presence of ethers and/or hydroxyls.[165,166] After peracetylation of sporopollenin, two signals increased intensely: a sharp peak at 19-20ppm (methyl groups) and a strong broader one at 170ppm (carboxyls), both characteristic of acetyl groups.

Comparison of *Tulipa gesneriana* and *Cucurbita pepo* carried out by solid-state NMR led to the same conclusions as those deduced by IR spectroscopy (see Section A-4.1.4.1): phylogenetic differences mainly affect aliphatic/aromatic ratio within a particular sporopollenin, and spectral properties of the latter do not change much with maturation (apart from peaks overlapping due to complication of macromolecule and multiplication of different chemical environments for same functional groups).[159]

An extensive table of solid-state ^{13}C NMR signals is given in Appendix A.

More recently, successful dissolution, in deuterated 2-aminoethanol, of sporopollenin, enzymatically extracted from *Typha angustifolia* L. (lesser bulrush) and *Torreya californica* Torr. (California torreya) pollens, led to its solution NMR study.[103,121,167] These results have however to be interpreted carefully, in the light of the discussion regarding solubilisation of sporopollenin (see Section A-3.3): "dissolution" could possibly lead to a separation of each aminated unit of the whole polymer; solution NMR would therefore not give data on the intact structure but rather on its constituents.

Plant species	Crosspeaks δ_H/δ_H (ppm)	Interpretation
Torreya californica[103]	7.48/6.70 7.13/6.70	2,6-disubstituted 1,3-cresol
	7.79/6.72 7.59/6.72	2,6-disubstituted 1,3-cresol
	7.51/6.41	2,6-disubstituted phenol
Typha angustifolia[167]	7.41/6.63 7.07/6.63	2,6-disubstituted 1,3-cresol
	7.72/6.65 7.53/6.65	2,6-disubstituted 1,3-cresol
	7.45/6.35	2,6-disubstituted phenol
	7.64/6.18	2,6-disubstituted phenol
Typha angustifolia[121]	7.45/6.15	substituted phenol
	7.25/6.58	substituted phenol
	6.77/6.48	substituted phenol

Table 17 – Solution COSY NMR interpretation

Nevertheless, the solubility in aminoethanol was limited ($5g.L^{-1}$) and, at first, only ^1H NMR was studied. Spectral interpretation was restricted to the aromatic region (5.8-8.2ppm), due to solvents and references interferences. Such studies showed distinct

similarities between both species and COSY showed the existence of two types of aromatic systems: 2,6-disubstituted 1,3-cresols and 2,6-disubstituted phenols.

To overcome the solubility limit, so as to extend the study to ^{13}C NMR and HETCOR, sporopollenin was either peracetylated or silylated to form a much more concentrated solution in piperidine.[121] Much finer ^{1}H NMR spectra were obtained, enabling to define the shape of signals to be better defined and the coupling constants to be determined with precision. The results and interpretations are gathered in Table 18.

Signal				**Interpretation**	**Sp.**
δ (ppm)	**Sh.**	***J* (Hz)**	**Int.**		
7.45	doublet	13	1H	*trans*-disubtituted alkene	N, P & S
6.15	doublet	13	1H		
7.25	doublet	8	2H	*para*-methoxy phenol	
6.58	doublet	8	2H		
6.77	doublet	8	n/a	*para*-substituted phenol	
6.48	doublet	8	n/a		
4.5-5	broad	n/a	n/a	polyhydroxy aliphatic units	P
3.7	multiplet	n/a	n/a		N & S

δ: chemical shift *J*: coupling constant Sp.: sporopollenin(s) P: peracetyl sp.
Sh.: signal shape Int.: integration N: native sp. S: silyl sp.

Table 18 – Solution ^{1}H NMR interpretation by Ahlers *et al.*[121]

COSY NMR (2D $^{1}H,^{1}H$ correlation) confirmed the presence of olefinic systems and of two possible aromatic systems.[121] The lowest aromatic signals suggested an oxygen atom on the arene; as the signal at 6.58ppm did not change after silylation or peracetylation, the actual group was more likely to be an ether than a phenol, whereas since the signal at 6.48ppm was drastically reduced, it indicated a hydroxyl group. All of the aromatic units were interpreted as being potentially 4-methoxy or 4-hydroxy cinnamic acids. The polyhydroxy aliphatic constituents were confirmed by XPS investigations and HETCOR NMR (2D $^{1}H,^{13}C$ correlation).

4.1.4.4 Ultraviolet-visible (UV-Vis) spectroscopic study

As a complement to infrared and X-ray investigations, UV-Vis spectra of sporopollenin were also determined, after solubilisation in hot 2-aminoethanol.[135] The maximum peak at 289nm confirmed the presence of aromatic groups on side chains. Coupled with IR findings, this was interpreted as an aromatic ether (Ph-O-CH=CH-), linked to an aliphatic backbone by an ester bond. Differences observed between two angiosperm taxa (*Magnolia grandiflora* L. and *Hibiscus syriacus* L.) suggested side chains were peculiar to species, and similar IR fingerprints implied they did not consist

of a single compound.

4.2 Historical review of sporopollenin structure

4.2.1 Overview of the theories on sporopollenin structure

Date	Suggested structure	Authors and reference
1931	poly-terpenoid	Zetzsche & Vicari[54]
1964	co-polymer with a fatty-acid and a lignin-like fractions	Shaw & Yeadon[82,86]
1968	oxidative polymer of carotenoids and carotenoid-esters	Brooks & Shaw[36,73,137]
1980s	phenol-containing polymer	Wiermann *et al.*[90,102,145,156]
	aliphatic core	Guilford *et al.*[84] Espelie *et al.*[96]
mid-1990s	*possible coexistence of two types of sporopollenins*: aliphatic & phenolic	De Leeuw & Largeau[50] Van Bergen *et al.*[64]
	aliphatic polymer cross-linked by aromatic side-chains	Wiermann *et al.*[104,141,168,169] Kawase & Takahashi[135]
1999	aliphatic lipidic polymer	Domínguez *et al.*[143]
2000s	aliphatic lipidic core cross-linked by phenolic moieties	Van Bergen *et al.*[41]

Table 19 – Timeline of the hypothetical structures of sporopollenin

The different theories regarding chemical structures of sporopollenin, summarised in Table 19, are comprehensively depicted below. The earliest theory related sporopollenin to terpenoids (in the 1930s) and then more precisely to carotenoids (in the 1960s).[36,73,137] In between, it was shortly believed to have a lipidic and a lignin-like moieties.[82,86] The lipidic nature of sporopollenin was put forward again in the late 1980s, after solid-state NMR studies.[84,96] This emphasis on its aliphatic character contrasted however with the discoveries of oxygenated aromatic units in sporopollenin, from the early 1980s.[90,102,145,156] To explain those differences, some reviewers envisaged the possibility of two radically different kinds of sporopollenins: one mainly composed of phenolic constituents and the other mainly of aliphatic units. However, they also took in consideration the hypothesis of aromatic and aliphatic moieties to be linked in a

common mixed monomer.[50,64] Nevertheless, the aliphatic core was recognised as preponderant in sporopollenin by most researchers, including the discoverers of phenolic building blocks. A controversy was soon opened regarding its aromatic constituents. Wiermann's team,[104,168,169] Kawase and Takahashi[135] combined all results to elaborate the hypothesis of an aliphatic backbone cross-linked with aromatic side-chains, while Domínguez and co-workers[143] rejected aromatics as being foreign components.

In any case, current researchers, since the 1980s, agree that sporopollenin is not a unique chemical material, but a family of related polymers showing phylogenetic divergence.

4.2.2 Pioneering work

As early as the late 1920s, Zetzsche *et al.*[53-55] carried out the first significant work on isolated sporoderm in order to determine its chemical composition. By staining and degradation methods (with cuprammonium hydroxide or 80% phosphoric acid), they found intine was made of cellulose. Upon the results of carbon/hydrogen ratio (ca. 5/8 (mol/mol)), they suggested exine could be of terpenoids-type nature,[54] although without any further proof.

4.2.3 Sporopollenin as a co-polymer of lignin and fatty acids

Studies about sporopollenin were resumed in the 1960s, when palynology gained interest in the scientific community. First basing their conclusions on ozonolysis and infrared, Shaw and Yeadon[82,86] suggested a more precise composition of sporoderms, based on the study of *L. clavatum* spores and *P. sylvestris* pollen: 10-15% cellulose (in intine), 10% xylan (ill-defined layer) and 65-80% sporopollenin. They described sporopollenin as composed of a lignin-like fraction (15-30% of exine) masked by or sandwiched between lipid layers composed of unsaturated oxygenated hydrocarbon building blocks with 16 carbons or less.

Yet they acknowledged the negative results to lignin tests such as its lack of reaction with phloroglucinol, or its non-solubility in dioxane.[34,35] Later, the presence of lignin was again claimed in endexine, based on histochemical properties (staining with safranin o, cyanin and azure B); inertness to phloroglucinol was explained by a lack of

aldehyde groups.[170] The similar IR spectra they obtained showed that sporopollenins of different species had close structures and most probably shared common biosynthetic pathways.[82,86]

Shaw and Yeadon's work was later backed up by Potonié *et al.*,[171] who reinterpreted their findings and suggested new sporopollenin structural units including unsaturated cycles. This last description also explained the aromatisation of fossil sporopollenin and was compatible with the following structural hypothesis.

4.2.4 Sporopollenin as a polycarotenoid

In 1968, a long-lived but soon after controversial hypothesis was raised by Brooks and Shaw:[36,57,73,137] sporopollenin as an oxidative polymer of carotenoids and/or carotenoid esters. At that time, no apparent biological function had yet been assigned to the large amounts of carotenoids found in flower anthers. Brooks and Shaw mainly based their theory on biochemical relationships between the presence of sporopollenin and carotenoids in *Lilium henryi* and *Cucurbita pepo* anthers; they argued that flower carotenoids could provide the expected unsaturated conjugated system of a cross-linked polymer with carbon-methyl groups. They comforted their point by a series of comparisons between sporopollenins of diverse origins and artificial polymers of β-carotene or carotenoids collected from *L. henryi* anthers. Resistance to acetolysis, elemental analysis, infrared spectra and degradation studies (ozonolysis, pyrolysis and potash fusion) seemed to show some similarities but, despite very thorough analyses, all results were not completely unequivocal.[34,35] Interestingly, this theory finally gave an explanation to the presence of plant carotenoids.[72]

Further investigations were performed in attempt to support this theory. Concomitant presence or absence of sporopollenin and carotenoids[34,35,144] in different species (including algae, fungi, ferns, angiosperms and gymnosperms), systematic comparisons between sporopollenins of various origins and poly-β-carotene (by IR spectroscopy, combustion elemental analysis, pyrolysis, potash fusion and ozonolysis)[34,35,37,73,113,137,144,146] and radiolabelling experiments[83] in *Mucor mucedo*, *Neurospora crassa*, *Lilium henryi* and *Cucurbita pepo* strengthened it. Cytochemical studies tended to show sporopollenin contained aliphatic hydrocarbon chains, unsaturations, ketone and certainly conjugated systems. By the end of the 1970s, a hypothetical structure was eventually drawn.[34,35]

The hypothesis of sporopollenin being of carotenoid origin was severely

contradicted in the 1980s by further biosynthetic studies. A first contradictory work[155] demonstrated that an efficient inhibitor of carotenoid biosynthesis in the anthers did not affect the production of sporopollenin in *Cucurbita pepo* L. The peremptory conclusions of Shaw's team upon their findings were also criticised and moderated. For instance, incorporation of labelled precursors of carotenoids into sporopollenin was said to be relatively low.[102]

More importantly, while extracts from microbial organisms gave the best match with polycarotene, sporopollenin from vascular plants (ferns and spermatophytes) showed important dissimilarities to synthetic β-carotene polymer in term of spectroscopic data and degradation products.[102,155] Furthermore, the identity of the resistant polymer present in microorganisms with sporopollenin, in the acceptation of that found in ferns, angiosperms and gymnosperms (typically, extracted from *L. clavatum*), was found dubious (see Section A-2.2).[45,155]

Finally, the role of anther carotenoids was redefined.[47] They do not contribute to sporopollenins but to pollenkitt and tryphine, in which they are involved in protections against the light and/or oxidation.

4.2.5 Aromatic components of sporopollenin

Brooks and Shaw's theory did not offer a satisfactory explanation to the presence of phenolic components in sporopollenin.[47,90] According to Shaw and co-workers,[36,137,146] aromatic compounds found in degradation products of sporopollenin were artefacts produced under the harsh conditions of fused potash or pyrolysis. Yet they denied any real aromaticity in sporopollenin itself.

In the late 1980s, several workers[90,102,145] found that *p*-coumaric and derivatives were important degradation products of sporopollenin by potash fusion, nitrobenzene oxidation, aluminium iodide attack or pyrolysis. Their presence in the structure was backed up by a recent study[148] and confirmed by IR spectroscopy.[90,135,148] Tracer experiments were the most convincing.[104,156] Results demonstrated mevalonate and tyrosine were not taken up into sporopollenin, while *p*-coumaric acid, glucose, malonate and acetate were integrated in exine to a certain extent. Phenylalanine was however found an important precursor of sporopollenin biosynthesis. By using different marking positions, it was proved the aromatic ring, and most probably the whole phenylpropane unit, was kept intact in the final polymer. Since this motif, rendered by the aromatic amino acid, was degraded as phenolics, phenylpropanoid metabolism *via* phenylalanine

ammonia lyase enzyme was suggested as a metabolic pathway in sporopollenin biosynthesis.[47,104] In the early 2000s, solution NMR of solubilised sporopollenin (see Sections A-3.3 and A-4.1.4.3) confirmed the presence of phenols (potentially 4-hydroxy and 4-methoxy cinnamic acids) in sporopollenin.[121] It must be noted that these hypotheses and findings are however limited to angiosperms (namely *Tulipa* spec., *Cucurbita* spec. and *Typha* spec.).

4.2.6 Aliphatic backbone of sporopollenin

In 1988, FTIR spectra of sporopollenin were interpreted as highlighting the predominant aliphatic building blocks.[162] The same year, solid-state NMR of sporopollenin confirmed this highly aliphatic nature.[84,96] Despite their extensive studies of phenolics in sporopollenin, Wiermann *et al.*[47] acknowledged this discovery and concluded that sporopollenin was mainly composed of an aliphatic backbone to which aromatic side groups were attached, possibly phenols. Later, spectroscopic studies, led on two angiosperms in the mid-1990s, supported this hypothesis.[135]

Guilford *et al.*[84] insisted on the multiplicity of sporopollenins; according to them, it is not a unique substance but rather a series of related biopolymers, derived from largely saturated precursors (e.g. fatty acids). Sporopollenin should be considered a class of polymers and not a single homogeneous macromolecule.

Kawase and Takahashi[135] concluded that the aliphatic backbone of sporopollenin should be universal among different taxa (possibly all, but at least vascular plants), each species then producing its own aromatic (or conjugated) side chains, which cause the diversity in macroscopic morphology and properties. This point of view has now been supported by many researchers, especially Wiermann's team.[104,141,159,161,168,169]

The aromatic components of sporopollenin had been traced and explained in quite a satisfactory manner before any precursors or motifs of the aliphatic part had yet been suggested. Finally, solid-state NMR data as well as destructive methods (pyrolysis and oxidation by ruthenium oxide) led to a tentative structure for the backbone based on tetra-, hexa- and octacosanes. In 1996, Couderchet *et al.*[97] incidentally found, by tracer studies with a ^{14}C-tagged precursor, that oleic acid was incorporated into an algal resistant polymer, which they called sporopollenin.

Results of Domínguez *et al.*[143] on *P. pinaster* Aiton (maritime pine), *Ambrosia elatior* L. (annual ragweed) and *Capsicum annuum* L. (pepper) showed that sporopollenin was composed of an ether-linked core portion branched with abundance

of the motifs drawn in Table 20, together with other similar ones where the double bond position is changed along the carbon chain. They purified sporopollenin by acid-catalysed hydrolysis with aqueous hydrochloric acid in dioxane, in order to remove lignin-like aromatic portions, and by saponification with methanolic potash, so as to eliminate aromatic or fatty compounds linked by ester bonds. Therefore, no aromatic portion was found in sporopollenin. They concluded sporopollenin was a polymer of unsaturated fatty acids, and linoleic and linolenic acids were suggested as putative precursors.

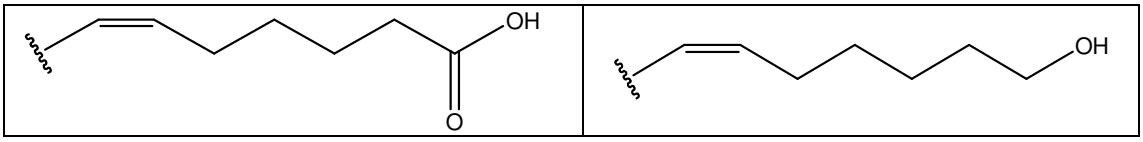

Table 20 – Molecular domains found abundantly in some sporopollenins according to Domínguez *et al.*[143]

After enzymatic extraction, spectroscopic data obtained by Wiermann *et al.*[141,160] on *Typha angustifolia* tended to show that carboxylic groups were minor in sporopollenin, contrary to hydroxyl functions. An ether-linked core was therefore conjectured as dominant in native polymer. Acetolysis and peracetylation were thought to induce a bias in the previous studies, and oxidative degradations by changing primary hydroxyls to carboxyls.

Later findings raised a controversy regarding the aromatic side-chains of sporopollenin.[143] On the one hand, all teams acknowledged the preponderance of the aliphatic backbone, as stated above. On the other hand, although the aromatic extensions seemed generally recognised (see Section A-4.2.5), their pertaining to the exact structure of sporopollenin was finally disclaimed by Domínguez *et al.*[143]

The use of different extraction and purification protocols seemed a satisfactory explanation to these results:

- when obtained under mild conditions (enzymatic process), sporopollenin exhibited phenolic moieties;
- after isolation under harsh conditions (hydrolysis with aqueous hydrochloric acid in 1,4-dioxane under reflux, saponification in methanolic potassium hydroxide and acidolysis in anhydrous hydrofluoric acid), no aromatic motifs were detected.

It came to conclusion that aromatic constituents of sporopollenin were connected to the aliphatic core by ester and ether bonds. Such a hypothesis was raised in the early 1990s by Mulder *et al.*[147] and finally confirmed by these findings.

4.2.7 Two types of sporopollenin?

Basing their hypotheses on the previous studies (see Sections A-4.2.5 and A-4.2.6), some reviewers of plant resistant biopolymers have suggested there existed two types of sporopollenins (at least),[50,51,64] as detailed in Table 21.

To explain these different chemical types of sporopollenin, several conjectures were raised, still to be verified: they could arise from the chromosomic content of the organism, the layer of the sporoderm considered or the ontology proper to each group of plants. Joined presence of both types in a single exine or even in the same layer was also suggested, but the lack of consistence in the extraction methods used in the literature made comparisons impossible.[51]

Variety	Chemical characteristics	Main source(s) of data
1	oxygenated aromatics units (especially *p*-coumaric and ferulic acids)	Wiermann *et al.*[90,102,104,145,156,168,169]
2	mostly aliphatic structure	Works with solid-state NMR[84,96] Domínguez *et al.*[143]

Table 21 – Two hypothetical varieties of sporopollenins

Nevertheless, the main theory, recognised by the previous reviewers,[41,51] remains that of a mixed co-polymer with an aliphatic core and aromatic extensions.

4.2.8 Algaenans and sporopollenins

The chemical composition of highly resistant biopolymers has also been studied in algal cysts. These macromolecules generally fulfil the usual requirements to be considered as sporopollenins: resistance to aggressive treatments (including acidic and alkaline hydrolysis, and acetolysis), UV fluorescence and IR fingerprint patterns comparable to those of sporopollenin from vascular plants. However, chemical investigations showed the long-believed "carotenoid hypothesis" was not in accordance, which was the main reason invoked by some authors to not classify them as sporopollenins.[59] Actually, their element ratios and their solid-state ^{13}C NMR spectra distinguished them from sporopollenins. They are now classified as *algaenans*.[41]

In a few microorganisms, the structural components of some of those natural macro-compounds and how they are assembled seem to have been considerably better understood:

- the algaean in zygospore cell walls of *Chlamydomonas monoica* was identified as a polymer of fatty acids and alcohols cross-linked by ether and ester bonds;[61]
- the two resistant macromolecules (termed PRBs) from *Botryococcus braunii* were described as a poly-isoprenoid and a long-chained fatty-acid polymer.[58-60]

Some authors developed the hypothesis that algaenans, found in algal cyst walls, evolved in sporopollenins in terrestrial plants.[41,51] Apart from the incorporation of phenolic moieties, which are absent from algaenans, sporopollenins have shorter alkyl chains (16-18 carbons, as opposed to 25 to 34) and are only cross-linked by ether bonds.

4.3 Hypothetical structure

As the present review (Section A-4) emphasises, the chemical structure of sporopollenins is still controversial. In summary, all of the features of sporopollenin structure that have been established with unambiguity are listed as follows:

- Sporopollenins are composed of only three elements, carbon, hydrogen and oxygen, with a C/H ratio of 5/8 (mol/mol) like terpenes; nitrogen and metals are absent.
- They are constituted of an aliphatic matrix, common to most species of vascular plants (ferns, gymnosperms and angiosperms); the carbon skeleton is cross-linked by various side-groups whose exact nature, position and number are directly species-dependant.
- Certain chemical functions are present on all sporopollenin types: carbon chains, conjugated unsaturated systems, hydroxyls, ethers and methyls; others are only confirmed in some species (like *L. clavatum*) carbonyls (ketones), carboxyls (acids, esters).
- Aromaticity of sporopollenin is strongly debated, although it seems reasonable to link the aromatic/aliphatic ratio to each species; for instance, phenyls and phenols are recognised features in sporopollenin from *L. clavatum*.

The presence of aromatic moieties is a controversial aspect of the composition, although most authors seem to accept the large aliphatic nature of sporopollenin with

some phenolic components (see Sections A-4.2.5 and A-4.2.6). Another stumbling block lies in the degree of saturation of sporopollenin. The similarities of sporopollenin with poly-β-carotene have been highlighted and a terpenic backbone suggested, while saturation seemed another favoured hypothesis (see Sections A-4.2.4 and A-4.2.6).

To date, the most satisfying hypothesis is that sporopollenin should be a co-polymer of cinnamic acids and fatty acid units, whose proportions vary from species to species, assembled from monomers present in the sporangium during spore/pollen development.[41] Following this hypothesis, a putative formula, displayed in Figure 8, has been proposed recently.

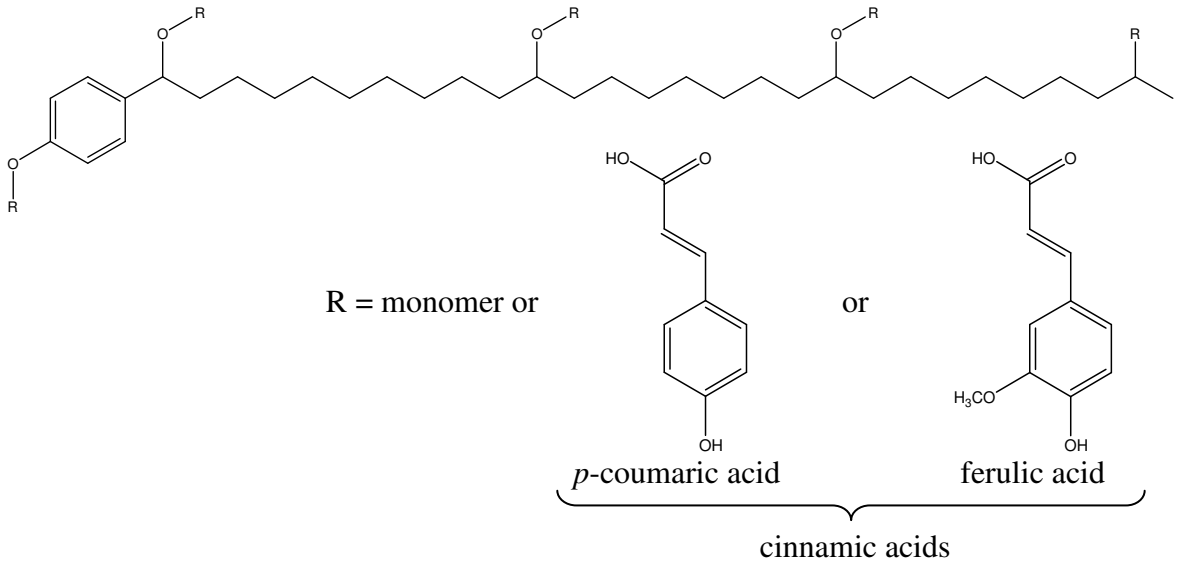

Figure 8 – Hypothetical simplified structure of a sporopollenin building block[41] – The substituents R can either be linked by ether bonds or, in case of the two cinnamic acids, also through ester bridges

This proposed structure meets many different features confirmed in sporopollenin, precisely the presence of long aliphatic chains, aromatic cross-linkers (mainly cinnamic acids), ether cross-linkages and a few ester functions. However, some important confirmed characteristics and observations have not been taken into account. Methyl and hydroxyl groups have been neglected and the proportion of oxygen has largely been underevaluated.

Also, another issue lies in the justification of the high level of bromine covently attached to sporopollenin by simple contact of liquid bromine. Bromine uptake has long been interpreted as a proof of the existence of conjugated olefinic systems. But no current theory found in the literature suggested such unsaturations. In fact, the structure proposed in Figure 8 would match the high bromine value of sporopollenin (ca.

5mmol.g^{-1}, see Section A-4.1.2.1) if attachment of bromine to aromatic rings was considered.

4.4 Putative role of sporopollenin

The role of sporopollenin has long been only hypothetical. Initially, Zetzsche *et al.*[53-55] thought it was an exoskeleton that simply protected spores from mechanical stress. Later, Shaw and his team,[36,57,72,73] through their theory of sporopollenin as a polycarotenoid (see Section A-4.2.4), developed that sporopollenin could also offer some protection against UV light and desiccation. The most recent reviewers[41,51] finally confirm and cumulate the previous suggestions: sporopollenin has a structural role of protection against chemical, mechanical, thermal and luminous damages. The aliphatic backbone of sporopollenin is described as a hydrophobic water barrier. Cinnamic acid moieties give to the material its UV-shielding propertied. Aliphatic hydrocarbon chains and ether-bondings of the building-blocks reinforce it against mechanical and chemical aggressions.

5 Biological properties

5.1 Toxicology

Spores and pollen grains can be found in many food sources such as mushrooms or honey. Additionally, bee pollens have been demonstrated to be good nutrients for athletes; they can provide energy, stamina and endurance.[172] Pollen is being actively marketed for alleviating certain health afflictions and as a beneficial dietary supplement. Pollen tablets are also used as desensitizing against allergy or as "natural food", especially by athletes. Also some firms propose *Chlorella vulgaris* as a nutraceutical.[42] Pollen or spores may or may not be beneficial, but anyway a reasonably valid observation is that they are not harmful to humans even when ingested in large amount.

before oral ingestion 30 min after ingestion 60 min after ingestion

Figure 9 – Degradation of sporopollenin in the blood stream – SEM[173]

Sporopollenin is a naturally occurring polymer found in spores and pollen grains. From the previous observation, it can thus rightly be considered harmless to health, all the more that all of the allergens (proteins) have been stripped out by the extraction protocol. This is shown by combustion elemental analysis: sporopollenin was found to be virtually nitrogen-free (see Section A-4.1.1.1). A study led by Maack[42] proved that sporopollenin from *Chlorella vulgaris* was harmless and could be rubbed on the skin with no irritation, swallowed without any danger (LD_{50} *rat* > 2000mg/kg) or even injected in the blood stream. Moreover, sporopollenin particles were found to cause an antigenic reaction and to bind to antibodies.[174] They should therefore be easily eliminated from body fluids or tissues by macrophages. Importantly, direct enzymatic catabolism was also observed in the blood[118] as detailed below. Hence, spores and pollen grains can be eliminated by human body, and their exine completely removed. Their degradation in blood was studied by Jorde and Linskens,[173] whose SEM pictures

are displayed in Figure 9.

As a consequence of its non-toxicity, sporopollenin can be envisaged for applications in fields like cosmetic, food or pharmaceutical industry. It can safely be rubbed on the skin, ingested, injected or inhaled. The applications envisaged could target body oils or ω-3 oils protection, and oral delivery of specialised food or drug, for example.

5.2 Migration into the blood stream following oral ingestion

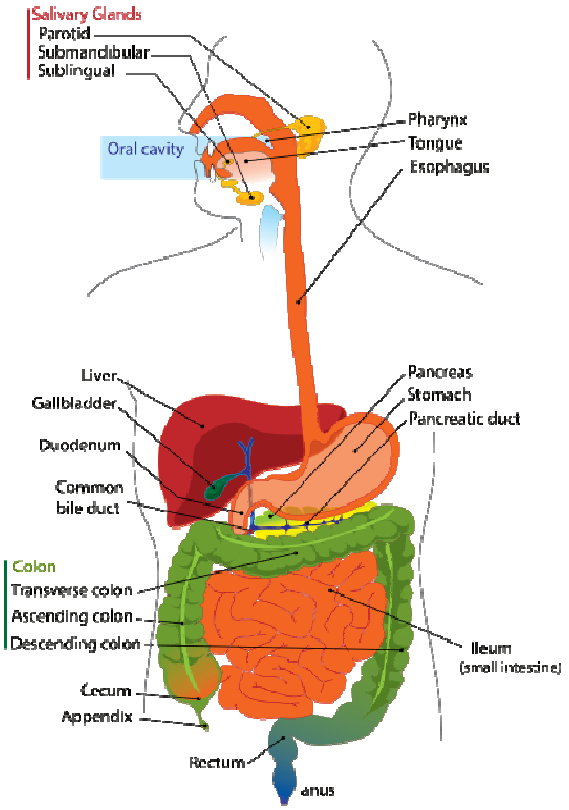

Main parts	Conditions[118] pH	enzymes
oral cavity (mouth)	neutral	amylase
oesophagus	neutral	none
stomach	1-2	pepsin
duodenum	5-6.5	proteases, lipases, amylases
jejunum	4.5-6.5	
ileum	6.5-8	
colon	neutral	none

Figure 10 – Schematic view of the GI tract[175]

With a 200m^2-wide surface, the gastro-intestinal (GI) epithelium represents the largest interface between the external environment and the body interior. It is designed to selectively let nutrient and small molecules pass from the GI tract lumen into the blood vessels, while it restrains the entry of pathogens, toxins and undigested macromolecules. However, some chemicals can cross this major barrier by two main uptake pathways: transcellular (through gut lining cells) and paracellular (between cells)

transports. The former has a constraining size limitation whereas the latter, although less active, may allow macromolecules and even particles to enter the blood stream.[165,166,176-178]

As early as 1844, Herbst observed oral absorption of undigested starch grains in the blood of a dog. Over the following half century, several of other researchers subsequently added evidence to this phenomenon, with starch granules, charcoal beads, sulphur crystals or foreign cells. In the 1960s, Volkheimer *et al.*[179-183] repeated similar experiments and verified that different microparticles can be found in many body fluids (blood, lymph, and even cerebrospinal fluid) following oral ingestion. The particular mechanism by which macromolecules enter the systemic circulation still remains unknown, although there have been many suggestions.

Volkheimer *et al.*[178-184] coined the term *persorption* to describe it. Persorption was later restricted to a peculiar mechanism: paracellular transport of micrometric solid colloids. Transcellular transports though were found more efficient mechanisms of penetration of solid particles in the micron-size range through the epithelial cell layer of the GI tract. Absorption was seen to occur through phagocytic specialised cells (called M-cells of Peyer's patches) present in the duodenum and jejunum epithelial cells.[166,176,177,185] More recent studies tend to prove that all epithelial cells (including enterocytes) may be sites of endocytosis of microparticles. This active transcellular transport has eventually been described as the main mechanism of particle absorption.[165,166,186-189]

Amongst the particles used by Volkheimer and its team[180] were *Lycopodium clavatum* spores. They were found in the blood stream of rats, following ingestion. Spores can thus pass through the gut wall to the body fluids without undergoing any digestion. Jorde and Linskens[173] also studied the absorption of *L. clavatum* spores, as well as *Secale cereale* pollen grains (rye) and their further degradation in the blood stream: most of it was catabolised after an hour.

It was therefore expected that sporopollenin particles should be able to survive all the GI tract conditions (different pHs and enzymes), traverse its wall and enter the blood stream, where it would be degraded.

5.2.1 Clinical trials

Some clinical experiments have been performed, along with co-workers,[118,124,190] on human volunteers to check the previous findings and extend them to empty sporopollenin capsules. Particle population was counted in blood samples after oral ingestion of S-type sporopollenin exines or initial spores (both being ca. 28μm). Uptake doses were formulated either as milk shakes, sweets or dispersions in yogurt.

It was verified that sporopollenin particles were indeed carried from the digestive system into the blood stream. It was also found that that transfer is relatively rapid a phenomenon in comparison to digestion: particles seem to enter the blood a few minutes after their ingestion and a maximum is reached after ca. 10min. After 1h, almost no particle was visible in the blood.

Clinical trial performed after ingestion of L-type sporopollenin exines (ca. 40μm) showed very little absorption, whilst uptake of sporopollenin exines extracted from *A. trifida* (ca. 15μm) led to a much more important penetration of particles into the blood stream. This seems to confirm Weiner's note in 1988 that the smaller the corpuscle, the stronger the penetration.[176]

5.2.2 Possible mechanism

In vitro experiments[118] showed that sporopollenin extracted from S-type *L. clavatum* spores was catabolised at 37°C in whole blood and plasma but not in serum. Therefore, the clotting cascade, whose components are still present in plasma but not in serum, was expected to be intimately involved in the enzymatic degradation of sporopollenin.

In whole blood (especially *in vivo*), macrophages must also eliminate whole particles in a short time in order to avoid thromboses or embolisms. As said before in Section A-5.1, it has been shown that sporopollenin was indeed antigenic.[174]

5.2.3 Applications

A hypothesis of size exclusion can rightly be raised for the phenomenon of gastro-intestinal absorption; and this has a big impact on applications of sporopollenin exines in cosmetic, food and drug delivery. Different particles could indeed be chosen for different purposes. For example, large exines (L-type *Lycopodium* spec., ca. 40μm)

that would not pass the gut barrier could be envisaged for topical applications, like sun and cosmetic creams: the encapsulated product would be released by rubbing exines on the skin. Medium-sized exines (S-type *L. clavatum* L., ca. 25µm) would be better designed for oral delivery of drugs and nutraceuticals, as they would cross the gut lining and the encapsulated product would be released in the blood stream then dispatched in the whole body. And small exines (*Aspergillus niger*, 3-5µm) would be ideal for respiratory delivery, as they would cross the nasal ways and reach the lungs alveoli easily,[26] to then join the blood *via* transmucosal transport; larger exines may also be deposited along the respiratory tract depending on their size and therefore give focussed delivery.

6 Sporopollenin in microencapsulation

Most commonly, encapsulation refers to a formulation technique used in pharmacology to enclose medicines into a relatively stable shell, allowing them to be taken orally or in suppositories, for instance. In its broadest acceptation, it simply means a physical way of entrapping a product into a capsule. In this study, encapsulation, or better *microencapsulation*, is used to name the physical mean of attaching chemical compounds into a coating of a few micrometers to a few millimetres in diameter. In this chapter, the usage of sporopollenin exines as microcapsules is reviewed.

6.1 Microencapsulation

Carrier systems used to formulate active principles (e.g. in pharmaceutics or in cosmetics) can be classified in three main categories (particles, emulsions and capsules) and three different size scales (nano-, micro- and macro-).[166,191]

Particle is a general term for an individual granular or colloidal element, either empty or porous used in physical chemistry to load a chemical. *Micro-* and *nanospheres* constitutes beads containing a continuous porous matrix loaded with the fill;[186,191] it is noteworthy that some workers confusingly named them "particles".[166,186,192] *Capsule* describes a hollow particle containing a core and acting as a temporary barrier. The use of capsules is called encapsulation. An emulsion can be utilised as an alternative to particles. Lipidic *vesicles,* such as liposomes, could be considered both as an emulsion and a capsule.[165,191]

The size of the *particles* may vary depending on the purpose of formulation. Macroparticles have long been used in pharmacology to produce orally medicines (e.g. caplets, coated tablets or pills, and gelatin capsules). Nanosized carriers are used to facilitate transcellular transport: they enhance transdermal, transmucosal and transintestinal deliveries, as well as entry of the drug within target cells.[12,192-194] On the other hand, microsized ones have a great potential as aids to cross dermal or intestinal barriers, but their scope reaches also the food industry.

This study part was focussed on *microencapsulation*, i.e. the use of capsules of the size of a micrometer to a few hundred micrometers.

6.1.1 Reasons for microencapsulation

The process of microencapsulation involves coating and/or entrapment of an ingredient within another material. The isolation of the core leads to a wide range of applications:[195]

- limitation of interactions between the fill and external components;
- taste, odour or colour masking (especially with pungent core);
- improvement in the handling properties of viscous liquids, sticky fluids, hydrophobic products, etc.;
- inhibition of evaporation of volatile fills;
- increase of shelf life or stabilisation of fragile compounds by protection from oxidation, for instance;
- protection against processing or external conditions.

Sometimes, the objective can be a controlled release of the encapsulant, *i.e.* a regulation of the rate at which the core leaves the microcapsule. This may depend, for example, on the temperature, the medium or the capsule porosity.[191]

The release of the core, if not controlled, can be induced by mechanical compressive force on the shell, dissolution in a liquid, change of medium conditions (temperature, pH), melting of the capsule, or breaking and opening due to a shearing force or enzymatic digestion of the particle.[195]

The main domains of application of exine microcapsules lie in drug delivery, in topical formulation of cosmetics and in protection of encapsulated specialised food.

6.1.1.1 Drug delivery

The interest in the delivery of highly potent macromolecules, such as nucleic acids, proteins or peptides, has recently been increasing.[191,192] It has then fuelled the recent technological therapeutic advances regarding administration methods, in order to improve the performance of these medicines. No delivery route is a panacea. They are even opposed by their main merit: parenteral administration is the most efficient for macromolecules, but non-invasive modes are largely preferred by patients. Their chief disadvantages are given in the following Table 22.

The non-invasive administration of macromolecular drugs faces numerous obstacles among which are: poor absorption, rapid metabolism, and biological and chemical instability; ergo they are commonly administered by injection, as this short-

circuits the major barriers: physical walls (impermeable skin layers and mucosal tissues), chemical and enzymatic degradations (digestion in the gastro-intestinal tract), and poor solubility in aqueous systems (hence low bioavailability).[191,192]

However, the discomfort caused to patients, ranging from pain or needle-phobia to real trauma for long-term treatments, along with the need for the wounds to heal, and the requirement of trained personnel and safe aseptic environment, has stimulated the implementation of alternative delivery routes.[191,192] Transdermal and transmucosal ways have been actively investigated, but the emphasis has been put on oral route, for its attractiveness to most patients. The aforementioned barriers have however to be countered.

Route of administration	Description	Main limitations
Parenteral[194,196-199]	by mean of injection	patient discomfort (pain, trauma…); small doses; toxic side effects; need for aseptic conditions
Sub-cutaneous	*in the deepest skin layer*	
Intramuscular	*in the muscle fibre*	
Intravenous	*in the vein lumen*	
Oral[191,192,194]	by mean of swallowing	difficulties in swallowing; gastro-intestinal barrier; gastric juices; toxic side effects
Transdermal[192]	by topical application on the skin	skin barrier; often local; possible need for a patch
Transmucosal[191,200]	by topical application on a mucosa	mucosal barrier; toxic side effects
Sublingual	*through the epithelium beneath the tongue*	
Buccal	*through the mouth mucosa*	
Rectal	*through the rectum mucosa*	(patient discomfort)
Pulmonary[191,194]	*through the lung mucosa*	(restricted to aerosols or gases)
Nasal[192]	*through the nose mucosa*	(restricted to aerosols or gases)

Table 22 – Main routes of drug delivery and their disadvantages

The skin provides an attractive and readily accessible site for drug delivery. Despite the absence of enzymatic barrier, the low penetration rate limits it considerably. Amongst other methods, microcapsules have been used for that purpose, for example liposomes, niosomes[201-203] or "microsponges".[192]

The great variety of mucosal tissues in the body can be targeted as potential sites for drug delivery like the tongue, the mouth, the rectum, the nose and the lungs.[192,204] Strictly speaking, transmucosal delivery does not encompass passage through the gastro-intestinal mucosa, which is separated under the name *oral route*. Hence, transmucosal route also bypasses the gastro-intestinal barrier, but another enzymatic

obstacle arises along with a low permeation rate again. To avoid metabolic destruction of macromolecules in the mucosa, enzyme inhibitors have been added to the drug formulation, and penetration enhancers are usually co-administered, once more. Lipidic microcapsules have again been of use to enter mucosal tissues.[200] And also have spray-dried hydrophobic particles of fatty acids, esters and salts been developed for respiratory administration of drugs.[192]

Oral route is, by far, the favourite and most convenient non-invasive delivery mode.[1,191,192,194] To overcome the critical obstacles of the acidic hydrolysis in the stomach, the enzymatic metabolism all along the way and the bacterial fermentation in the intestine, varied approaches have led to different techniques. They include the use of prodrugs to alter the drug physicochemical properties, enzyme inhibitors to limit the metabolic degradation and penetration enhancers to reduce the contact time between drug and gastric juices. Nevertheless, protection of the active macromolecules is the best strategy for it maintains its original activity and avoids toxic side-effects of enzyme inhibitors. Microencapsulation seems thus exactly indicated.

6.1.1.2 Food industry

Microcapsules are commonly used in industrial food nowadays.[195] Isolation of incompatible products can be exemplified with citric acid in teas, encapsulated because in bleaches tannins. Delayed release of acids can be used in cured meat. Handling improvement can be observed with some sticky hydrophobic flavours like menthol or limonene.

Protection of food ingredient is the main aim of microencapsulation though. Many artificial aromas, specialised oils, vitamins, minerals, sweeteners or colouring agents are especially sensitive to oxygen and beneficiate from entrapment in a shell.

In general, several effects are expected on one encapsulated ingredients. Two products are given below in examples. They use multi-purpose encapsulation against problems listed thereafter:

- β-carotene: water insolubility, dusting problems and air-oxidation sensitivity;
- aspartame: hygroscopicity, poor flowability, short sweetness perception and thermal instability.

6.1.1.3 Cosmetics

It is noteworthy that active products that cross the skin barrier are not considered

as cosmetics but as drugs. Such products are discussed in previous Section A-6.1.1.1. Cosmetics include all preparations (but soap) applied to the human body for beautifying, preserving or altering, cleansing, colouring, perfuming, conditioning or protecting the skin, hair, nails, eyes, lips, or teeth.[186]

Microencapsulation could beneficiate to skin-care preparations. These creams, unguents, lotions or pomades generally possess a fatty base. Some fatty acids are also used as active principles, like arachidonic acid against wrinkles.[205] In any case, they experience therefore the same degradation as described for specialised oils in the previous paragraph (See Section A-6.1.1.2) and UV-screening along with antioxidant preservation could be of great interest for them.

6.2 Existing carrier systems

Nowadays, a number of different nano- and micro-capsules have been developed. Most of them apply to drug delivery or cosmetic formulation. They can be classified in broad categories:

- Lipidic vesicles: nanoparticles composed of a surfactant membrane; of variable size (25nm-3µm);[192] they are mainly used for transmucosal and over all transdermal drug deliveries;[204]
  - ✦ Virosomes:[192,204,206] spherical, virus-like vesicles composed of a lipidic monolayer;
  - ✦ Liposomes:[191,204] spherical vesicles composed of a phospholipidic bilayer (or multilayer);
  - ✦ Cochleates:[192,204] cylindrical vesicles composed of a lipidic multilayer;
  - ✦ Niosomes:[204] spherical vesicles composed of non-ionic surfactants;
- Biological capsules:[204] obtained from living cells or viruses after inactivation; nano-sized; generally considered as “dirty”, since they may contain contaminants or toxins;
  - ✦ Live inactivated bacteria or viruses:[191,204] live cells used as hosts after neutralisation of their hazards; infamous for their lack of inner space and their potential reactivation;
  - ✦ Bacterial ghosts:[204] bacterial membranes stripped from their cytoplasm; safer, with a bigger void;
  - ✦ Erythrocytes:[191,204] live cells used as hosts; problem of blood contamination

and compatibility;

- ✦ Yeast cells;[207]

- Artificial microparticles: particles (1-100µm) obtained by different processes, with a fill dispersed in a matrix or encapsulated within a coating;
  - ✦ Spray-dried and milled particles:[195,198,200,208,209] particles obtained by spray-drying or milling of a mixture or emulsion of fill with a non-polymeric matrix;
  - ✦ Natural polymers:[191,204,206,209-215] polymeric membranes coated around cores, or fills inserted within polymeric beads;
  - ✦ Synthetic organic polymers:[166,191,216-218] particles obtained by polymerisation of a monomer in emulsion with the fill, or by insertion of cores within preformed polymers;
  - ✦ Synthetic mineral solids:[219,220] porous particles yielded by precipitation on a template destroyed after casting.

Class of materials	Examples of materials
Fats and fatty acids[198,200,209]	Waxes, oils, paraffin, oleic acid, lauric acid, palmitic acid, stearic acid
Fatty acid derivatives[198,200,209]	Magnesium stearate, phosphatidylcholines, phosphatidylglycerols
Carbohydrates[198,209]	Glucose, lactose, sucrose
Natural polypeptides[191,195,198,204,209,214,215]	Gelatine, polyglutamic acid, casein, gum Arabic, albumin, gluten
Natural polysaccharides[191,195,204,206,209-213]	Pectin, cellulose, chitin, chitosan, alginate, maltodextrin, starch
Artificial organic polymers[166,191,204,208,216-218]	Poly(lactic acid), poly(methylmethacrylate), poly(alkylcyanoacrylate), poly(methylidenemalonate), poly(lactide-co-glycolide)
Mineral solids[209,219,220]	Silica, calcium carbonate, calcium phosphate, clay

Table 23 – Main materials used for synthesis of mixed microparticles

The variety of products used to create artificial microparticles is illustrated in Table 23. Three approaches can be envisaged to make particles: dispersion of the fill in a matrix, coating of the material around the core or insertion of the latter in the preformed capsule.

All these particles and capsules show common drawbacks. First, most of them can only encapsulate products of a limited size. Thus, they carry macromolecules (e.g.

proteins or nucleic acids) with difficulty, with the exception of some polymeric shells.[216] For example, poly(lactide-co-glycolide) microspheres have been designed for the controlled release of an oligonucleotide.

In general, microparticles or microcapsules are obtained with poor size homogeneity, especially by spray-drying or milling techniques. Therefore, templates have been used to shape the final particles. Some of these biomimetics have been cast from spores, owing to the high monodispersity of the latter: pollen[219] from *Brassica* spec. L. (family of cabbages, rape, turnips and mustards), *Taraxacum* spec. Cass. (dandelions), *Trifolium* spec. L. (clovers) and *Papaver* spec. L. (poppies), and microsporidians from silkworms.[210]

6.3 Sporopollenin exine shells as micro-capsules

Processes of isolation of sporoderm that have been developed (see Section A-2.4) involve that acids, bases, solvents or enzymes enter spores or pollen grains. It constitutes circumstantial evidence that the sporopollenin wall can be traversed by chemical and even macromolecules. In addition, investigations of sporopollenin substructure, quickly reviewed in Section A-3.5, clearly stated the presence of nano-sized channels tunnelling through all layers of exine as well as through intine. Moreover, a tracer study show colloids can traverse the exine across areas lacking obvious passages.[80] Exines can thus be considered as empty permeable closed capsules. So chemicals, especially liquids, can rightly be suspected to diffuse inside either passively or by a forced method.

An extensive study was carried out on bisaccate pollen grains from *Pinus* spp. (pines) regarding the permeation of latex, dextran and Evans blue (an anionic dye) through the external wall.[221] Sexine (the external, sculptured layers of exine) was found to be highly permeable to macromolecules with a Stokes' radius up to 100nm. On the contrary, this work claimed nexine (the internal, non-sculptured layers of exine) was completely impermeable to molecules with Stokes' radius above 4nm and anions, but seemed more permeable for smaller products.

Microencapsulation was then envisaged in emptied spore and pollen exines. A few examples have been patented for the purpose of drug delivery.[92-94] Exine shells show for oral application one of their mightiest potential. Indeed, sporopollenin capsule

have been shown to readily cross the gastro-intestinal mucosa without undergoing any digestion or acidic damage by the gastric juices (see Section A-5). Should a drug be tightly attached to it by physical entrapment, it could enter the blood stream, on the condition that a suitable formulation is set up. Transport of sporopollenin through muscosae was envisaged.[118,124,222] For example, most pollen can indeed reach nasal tissues, as hay fever proves it. As another example, fine conidia from *Aspergillus* spec. are well known to reach the pulmonary alveoli.[26]

Some inventors even envisaged the use of exine microcapsules by transdermal route.[92,93] However no scientific work has shown any example of large particles crossing the skin layer. Exine capsules were thus investigated only from the perspective of protection of the encapsulated drug before topical application in cosmetics, or simply to formulate a powdery drug as opposed to a cream or a liquid.[195] UV-screening and antioxidant properties of sporopollenin were studied in the following Part B in order to apply it, for instance, to active principles of a fatty nature (e.g. prostaglandins used against psoriasis[205]).

A whole investigation is currently in progress at Sporomex Ltd. in order to apply sporopollenin capsules to oral drug delivery, topical preparation and food protection.[118,124,222]

B. Results and discussion

1 Extraction of sporopollenin

Prior to any work on encapsulation, chemical derivatisation or physical characterisation, an extraction protocol had to be implemented to form either empty sporopollenin exines or empty composite capsules (with intine and exine). Extraction of sporopollenin particles had two objectives. The first aim was to obtain empty and undamaged capsules, whether made of pure sporopollenin exines or composed of cellulose intines within sporopollenin exines. The second one was to produce an almost pure sporopollenin polymer for chemical reactions.

The different isolation procedures used in the present study have been adapted from the literature,[12,13,36,53-57,85,87] although some specific methods reviewed in Section A-2.4 were omitted. Enzymatic extraction for instance was regarded as too long (over 100 days) and cytoplasm removal with *N*-methylmorpholine as too "dirty" (nitrogenous debris left). Steps considered include simple refluxes in mineral bases and acids, or in organic solvents, as well as acetolysis.

In order to enable a potential encapsulation, the inner content (*sporoplasm*) had to be removed from spores or pollen grains. During the treatments and washings, it was also aimed to eliminate completely any nitrogen, which would indeed be related to allergens (mainly proteins). This was monitored by combustion elemental analysis. A 'full extraction' was initially designed using *L. clavatum* L. spores and shorter versions and lateral approaches were then explored. They yielded particles with different specificities, having more or less cellulose, and more or less nitrogen, for instance. Extraction procedures were then adapted to different species.

In the present study, when sporopollenin was used for chemical derivatisation, a thorough extraction had to be carried out for the polymer to be left "neat". Usage of pure sporopollenin, for chemical derivatisation, after full extraction (named AHS, see B-1.1) was only performed with particles from S-type spores from *Lycopodium clavatum* L. (or more rarely with L-type spores from *Lycopodium* spec.).

1.1 'Full procedure'

The first extraction process was adapted from previous works by Kettley[12] and Boasman,[13] which were both based on the literature (Zetzsche's early work[53,54] and protocols customed by Shaw *et al.*[14,85]). This method is detailed in Section C-2.1.1 and the corresponding elemental analysis results are gathered in Table 65 (p. 213) and Table 66 (p. 213). This protocol concerned initially *Lycopodium* spp. only (both S-type and L-type). However, it became a standard from which other processes were adapted to different species (see Section B-1.5).

1.1.1 Protocol implementation

Spores were firstly stirred in acetone under reflux. This initial step was a way of clearing spores from their lipidic content (tryphine, pollenkitt, cell membranes, etc.). These defatted spores (DFS) were recovered by filtration.

Following the predating studies aforementioned,[12,13] DFS was then treated in 6% aqueous potassium hydroxide for 12h under reflux, with refreshing of the base after 6h. This reagent hydrolysed the proteins, nucleic acids or other nitrogenous product possibly present in or around the cells. By-products were eliminated by reflux in ethanol for 2h. Base-hydrolysed sporopollenin (BHS) was recovered by filtration and its combustion elemental analysis (see Table 65, p. 213) showed less than 0.5% nitrogen (w/w), 0% being reached only with some inconsistencies.

However, a more extensive investigation, coupled with parallel studies of collaborators in the same laboratory,[124] showed that reflux in aqueous sodium hydroxide was a better option since it yielded base-hydrolysed microcapsules which were free from nitrogen, even without previous treatment with organic solvents.

In order to ensure the best removal of nitrogenous material, spores were treated under reflux. Additionally, in accordance with former studies,[12,13] base was renewed after half of the reaction time; the reaction mixture was then simply filtered and the particles re-suspended in fresh aqueous base. Although this was believed to improve the elimination of nitrogenous material, it did not appear critical, and the typical results of combustion elemental analyses (displayed in Table 65, p. 213) were the same after a single treatment or a hydrolysis involving base refreshing. Also a parallel investigation showed that increasing the base concentration and/or the reaction time directly related to the loss of nitrogen in more important proportions. This result was used in the present

study to implement a 'one-pot' extraction procedure, detailed in Section B-1.3.

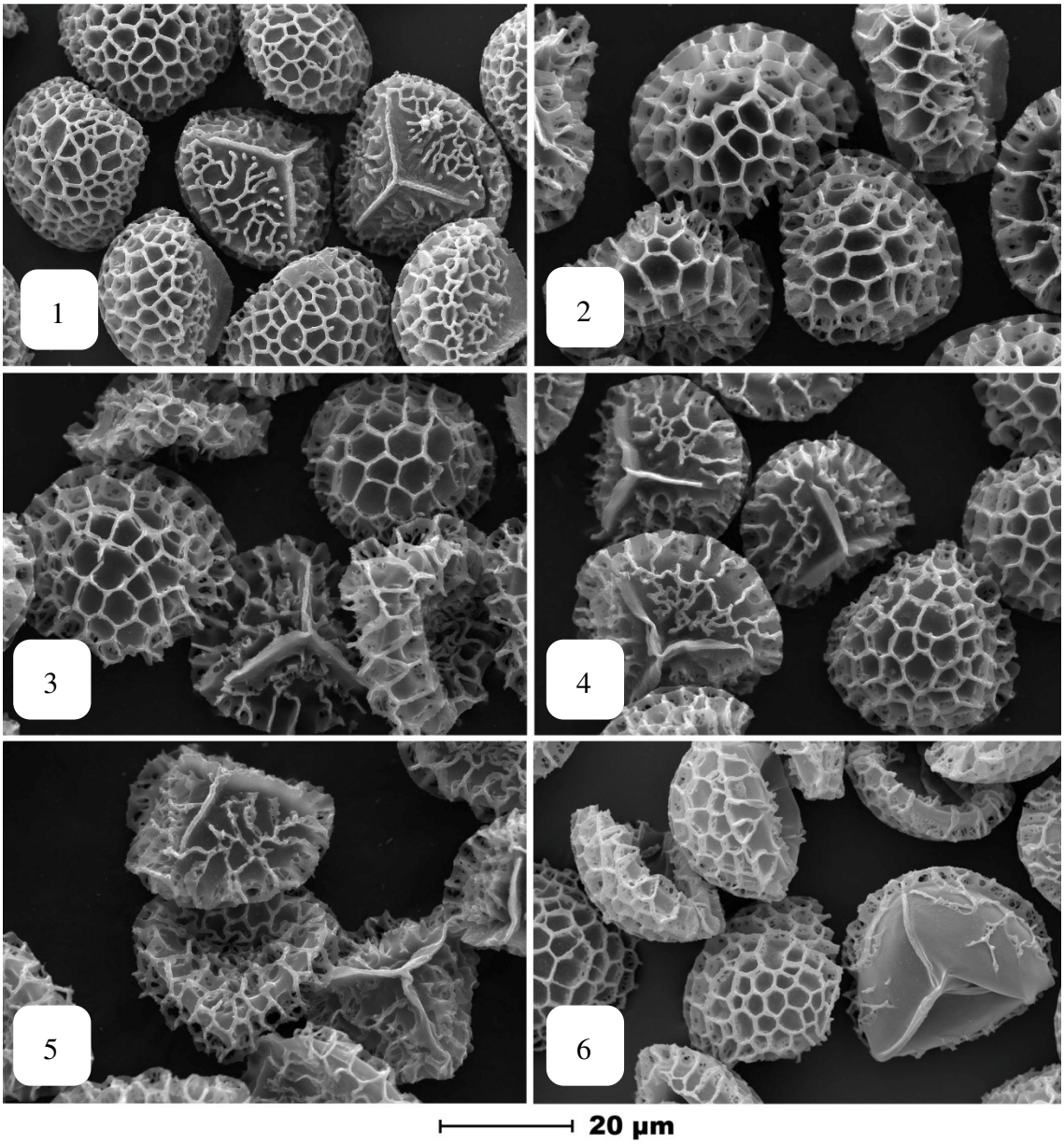

Figure 11 – S-type *L. clavatum* spores and particles extracted thereof – SEM pictures: parent spores (1); DFS (2); BHS (3); AHS (4); 'one-pot' BHS (5); and acetolysed sporopollenin (6)

Note: Some microcapsules are crushed by the hypervacuum applied within the SEM.

To remove the polysaccharides present in BHS, especially those forming the intine layer (cellulose and, to a much lesser extent, pectin, glucan, mannan, etc.). The strength of the acid to use was debated in the literature (see Section A-2.4). For this study, a compromise had to be accepted balancing efficiency and constraining conditions.

Hydrofluoric acid,[89] for instance, was regarded as too tedious and dangerous hence not considered for this study. Neat sulphuric acid[85] was to be avoided for three reasons: it would impair some applications, since it is not generally accepted in pharmacy and food industry;[223] it introduced a large proportion of sulphur in sporopollenin;[36] and in early trial studies was found to darken the exines and therefore probably damage them. On the opposite, phosphoric acid is classified as a safe food additive[223] and its use would not prevent any internal use. It was therefore utilized in this study to eliminate the intine, despite its probable incomplete action[85] and possibility of introducing some phosphorus into the sporopollenin. As a consequence, BHS was further treated with concentrated phosphoric acid under reflux for a week. Particles collected by filtration were then dehydrated in DCM with TFA. Acid-hydrolysed sporopollenin (AHS) was finally dried at 60°C or under vacuum. By combustion elemental analysis, AHS was also found free from nitrogen (see Table 66, p. 213).

1.1.2 Resulting microcapsules

For both S-type and L-type *Lycopodium* spec. spore, two kinds of microcapsules were made available by this extraction procedure: BHS and AHS. SEM pictures of such particles, displayed in Figure 11 and Figure 13, show that they were intact after extraction.

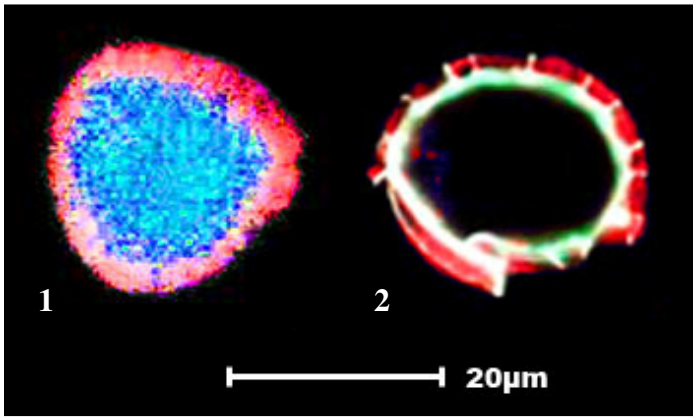

Figure 12 – Initial spore and empty capsule – LSCM pictures: S-type *Lycopodium clavatum* L. spore (1); corresponding empty exine (AHS) (2).

BHS, whether obtained from hydrolysis in potassium or sodium hydroxide, formed a composite of cellulose intine and sporopollenin exine. It constituted empty shells, which could therefore be used for microencapsulation, as verified by confocal microscopy (see Figure 14). However, BHS could not always be obtained consistently

nitrogen-free (see Table 65, p. 213), thus impairing some potential applications in pharmaceutical, food or cosmetic domains.

AHS, which was purely made of sporopollenin exines, also constituted an empty microcapsule, as verified by confocal microscopy (see Figure 12 and Figure 14) and by LM on microtome sections (see Figure 18 and Figure 19). Interestingly, thanks to the consistent absence of nitrogenous material (detectable by combustion elemental analysis – see Table 66, p. 213), no applicative restrications should be feared. In addition, AHS contains virtually no polysaccharides and can be considered as pure sporopollenin. Therefore it was also utilised for chemical derivatisation.

1.2 'Hemi-procedure'

In a longer term, it was envisaged that the extraction of spore and pollen exines might be undertaken on an industrial scale. Therefore attempts were made to use a more environmentally-friendly protocol, avoiding organic solvents, and being shorter and more energy-efficient. This method is detailed in Section C-2.1.2 and elemental analysis results given in Table 67 (p. 214) and Table 68 (p. 215).

The first step, with acetone, was bypassed since the basic hydrolysis should also eliminate the lipidic content by saponification. Ergo the alkaline refluxes in either sodium or potassium hydroxide hydrolysed both nitrogenous material (e.g. proteins, nucleic acids) and fats (e.g. cytoplasm membranes, tryphine, pollenkitt). After washing with water and boiling ethanol, a 'one-pot BHS' was obtained; this product is discussed in details in the next Section B-1.3.

As in the full procedure, the cellulose of the intine was decomposed by an acidic hydrolysis step with phosphoric acid. After washing with water and ethanol, avoiding any other solvent, an almost cellulose-free 'two-pot AHS' was obtained whose elemental analysis results proved it was free from nitrogen.

1.3 'One-pot' alkaline procedures

A more extensive study showed that caustic soda was a better alkali than potash, to use for extraction of S-type particles from *L. clavatum*. It was checked that hydrolysis of both S-type and L-type DFS in 6% aqueous sodium hydroxide under reflux for 12h (conditions similar to those implemented with potassium hydroxide, in the aforementioned 'full treatment') yielded a nitrogen-free 'one-pot' BHS, as checked by

combustion elemental analysis (see Table 67, p. 214). Also, SEM observations, displayed in Figure 11 and Figure 13, showed that these particles were intact after reflux in 6% (resp. 12%) sodium hydroxide for twice 6h (resp. once 6h) or after reflux in 10% potassium hydroxide for 12h.

It was verified by LSCM that intine was not an impedance to encapsulation of Evans blue, which was successfully loaded in 'one-pot' BHS (see Figure 27). In contrast, oils were not easily loaded passively, as this was constistently verified (see Section B-3.2.1).

To sum up, a simple and competitive one-pot extraction was implemented. This method is detailed in Section C-2.1.2.1 and elemental analysis results are gathered in Table 67. It consisted in a single 12h reflux in 10% potassium hydroxide or 6h reflux in 6% sodium hydroxide, followed by aqueous and ethanolic washings. These procedures yielded empty nitrogen-free particles, formed by sporopollenin exine strengthened with cellulose intine, enabling encapsulation.

1.4 Procedures involving acetolysis

As a case of comparison, acetolysis with sulphuric acid/acetic anhydride 1/9 (v/v), originally designed by Erdtman,[87] was explored to extract exine microcapsules. This method is detailed in Section C-2.1.3 and elemental analysis results are gathered in Table 69 (p. 215). Acetolysed S-type sporopollenin was composed of intact particles as checked by SEM (see Figure 11). However, extraction with Erdtman acetolysis alone did not yield nitrogen-free sporopollenin and introduced sulphur into the exines, as checked by combustion elemental analysis. Ergo, it was not further used to extract particles from *Lycopodium* spec. However, it proved useful to isolate capsules from *Ambrosia trifida* pollen, since it was damaged by either basic hydrolysis or treatment with phosphoric acid, as shown in Section B-1.5.

Nevertheless, pioneering studies led by co-workers[190,222] envisaged the use of acetolysis in conjunction with an alkaline hydrolysis step, either before or after. In these independent studies, elemental analysis of the resulting base-hydrolysed acetolysed sporopollenin or acetolysed BHS seemed to show no nitrogen. Other investigations by co-workers[190,222] are currently under progress on this method in order to limit the introduction of sulphur by either reduction of the acid proportion or its replacement by hydrochloric acid or acetic acid.

1.5 Milder conditions for extracting exines

It is interesting to note that often the literature[34,46] describes sporopollenin as the most robust naturally occurring organic polymer but it is clear from the following observations and results outlined in the present Section that not all sporopollenins from different plants have the same stability, which strongly indicates differences in the structure of sporopollenins from different plants. Such variations may be due to different extent of cross-linking, for example.

However, some bibliographical sources[82,86] state that not all spores can withstand equal treatment with the same resistance. Specific extraction steps and optimal conditions of temperature, concentration and reaction time to obtain nitrogen-free, undamaged, hollow particles could thus be expected to depend on the pollen or spore species.

Different procedures were explored to try and extract undamaged sporopollenin exines from frail spores and pollen. In particular, extraction parameters were modified to meet the characteristics of each capsule to be extracted. Damaging conditions observed during the development of extraction protocols are described thereafter. In addition, adapted procedures are detailed for each species studied here (L-type *Lycopodium* spec., *A. trifida*, *A. niger* and *C. vulgaris*).

It is of note that further investigations are currently under progress to try and determine standard operating procedures of extraction designed for each type of spores that would yield undamaged microcapsules which are firstly more consistant in term of absence of nitrogen,[124,190] and/or secondly that would be lighter in colour (for some applications where appearance is important).[190]

1.5.1 Fragility of L-type *Lycopodium* spec.

A particular note regarding L-type *Lycopodium* spec. spores is worth mentioning although they were globally extracted under the same conditions as S-type *L. clavatum* spores.

These L-type spores did not seem to react to organic solvents and alkaline conditions differently from S-type spores. It was shown that both S-type and L-type spores resisted degradation by concentrated alkali [concentration tested up to 20% (w/w)], under a large range of temperature (20-100°C) and after up to 24h of reaction. Under the conditions used to extract S-type BHS, *i.e.* reflux in acetone for 4h followed

by reflux in 6% aqueous potassium hydroxide for twice 6h (see Section B-1.1), L-type spores did not show any crack by SEM (see Figure 13).

By contrast, L-type spores were more sensitive to acidic conditions. Indeed, after 7 days of treatment in concentrated phosphoric acid under reflux (which is the treatment used for S-type *L. clavatum* spores), some cracks were observed by SEM (see Figure 13). This fragility seemed inconsistent though, since, in some cases, exines were extracted undamaged.

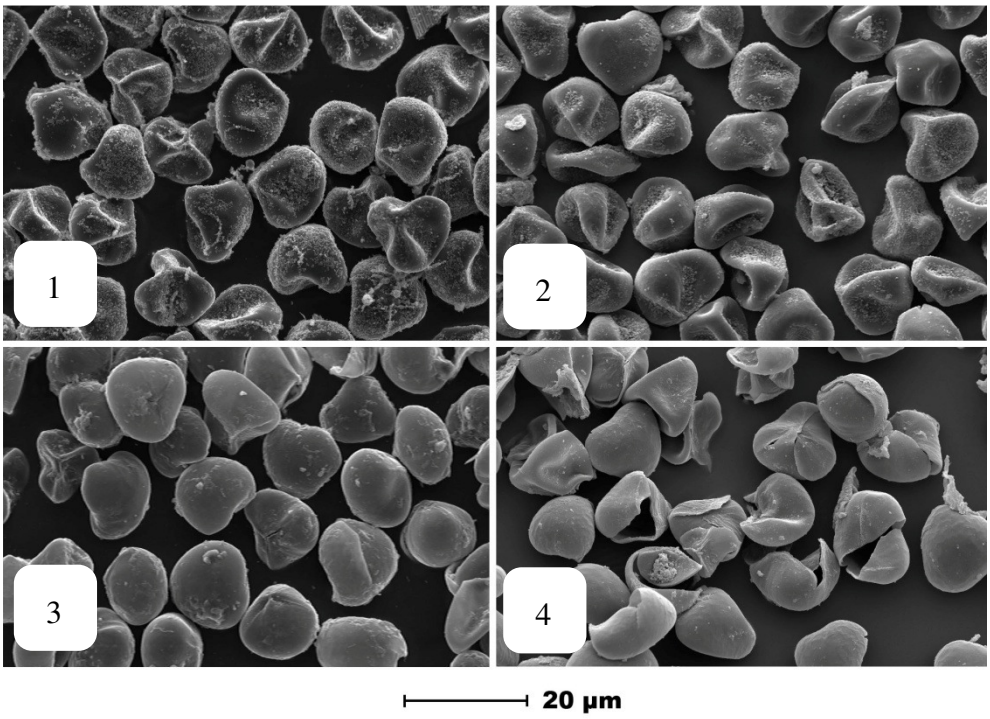

Figure 13 – L-type *L. clavatum* spores and particles extracted thereof – SEM pictures: parent spores (1); 'one-pot' BHS (2); intact AHS (controlled conditions) (3); and cracked AHS (stronger conditions) (4)

However, when L-type spores were successfully extracted using the 'full procedure' described in Section B-1.1, resulting empty L-type AHS microcapsules were more likely to burst open under mechanical stress. For example, mechanical or magnetic stirring or pressure created cracks similar to those observed in Figure 13. Such particles especially did not bear compression filling (see Sections B-3.2.2 and C-4.1.1.2).

With the collaboration of co-workers,[124,190] a milder extraction procedure was implemented. Precisely, L-type *Lycopodium* spec. spores were extracted under strictly controlled conditions of temperature: acetone treatment was performed at 60°C, alkaline hydrolysis at 80°C and phosphoric acid treatment at 60°C. As aforementioned, the last, acidic step was also found to be the most critical with regard to the integrity of the

microcapsules. Its reaction time was thus limited to 5 days instead of 7.

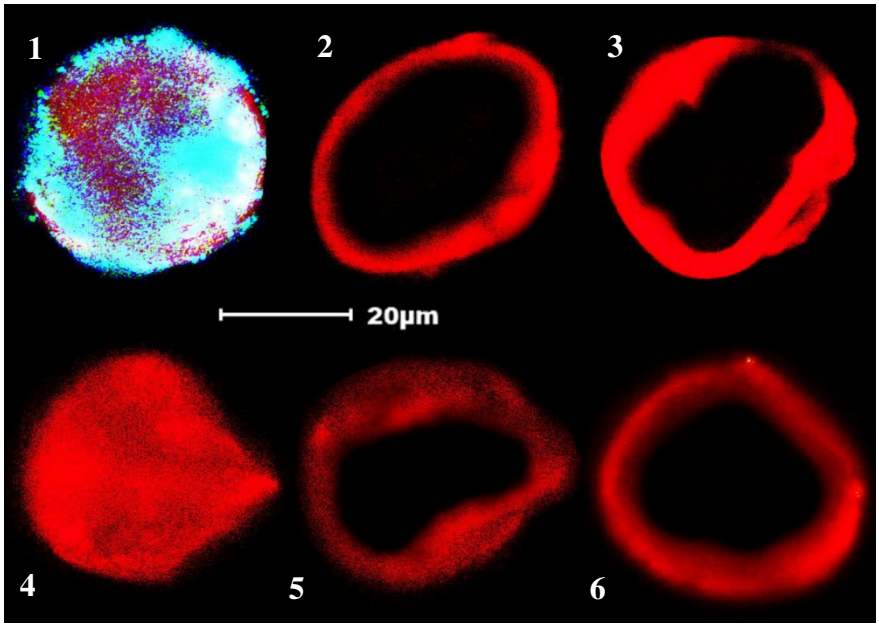

Figure 14 – L-type *L. clavatum* spores and particles extracted thereof – LSCM pictures: parent spores (1); 'one-pot BHS' (2); 'two-pot AHS' (3); DFS (4); BHS (5); and AHS (6)

Note: Both AHSs shown here (3 & 6) were extracted under controlled conditions (temperature and contact time).

1.5.2 Extraction of microcapsules from *Ambrosia trifida*

Extraction of *A. trifida* pollen was explored using three different methods.

1.5.2.1 'Full procedure' of extraction

In a first approach, the 'full procedure' described for S-type spores in Section B-1.1 was applied with similar conditions to *A. trifida* pollen. Precise procedures are described in Section C-2.2.1 and elemental analysis results given in Table 70 (p. 217).

After reflux of the raw pollen in acetone for 4h, DFS was isolated either by filtration or centrifugation. When DFS was treated with aqueous alkali, no particles could be recovered if the conditions were too strong. Precisely, when 3-6% potassium (or sodium) hydroxide was used under reflux for 1h or more, the resulting BHS seemed too fine to be decanted by centrifugation or to be filtered, even on a porosity-grade-5 filter, and thus it was not isolated.

However, a much milder alkaline hydrolysis was set up using 0.2% (w/v) sodium hydroxide at 80°C for 1h. BHS could then be isolated by centrifugation and treated with phosphoric acid under reflux for 1h. The final AHS particles were found still to contain nitrogen [0.78% (w/w)]. Presence of nitrogen was most probably due to the alkaline step being too mild. Therefore stronger conditions were explored. After reflux of DFS in 1% (w/v) sodium hydroxide for 1h, the resulting BHS was not easily filtered from strictly aqueous media. However, after addition of ethanol, particles could be recovered and treated with phosphoric acid under reflux for 1h. Despite the stronger alkaline concentration, AHS particles also contained nitrogen although in lesser proportion [0.52% (w/w)].

Treatment of BHS with concentrated phosphoric acid under reflux was not tried for more than 1h. Removal of cellulose was thus considered only very partial. It was verified by LM of microtome sections (see Figure 20) that AHS particles recovered were intact and empty. In the future, if extraction of *A. trifida* pollen appears to be useful, it could be envisaged to extend this acidic treatment in order to try and lower both nitrogen and cellulose contents, since the influence of acidic treatment on the integrity of resulting exines had not been monitored.

1.5.2.2 Extraction involving acetolysis

The second method used involved acetolysis, a procedure initially developed by Erdtman.[87] The protocol is detailed in Section C-2.2.2. Pollen was first centrifuged in glacial acetic acid, then heated at reflux with a mixture 9/1 acetic anhydride/sulphuric acid (v/v) for 1min and finally washed with acetic acid.

This yielded particles that could easily be isolated by filtration or centrifugation, hence being most probably intact. This was checked by microtome sections coupled with LM (see Figure 20), technique which also showed that they were empty capsules. The extracted particles were found not to be nitrogen-free though, given the combustion elemental analysis shown in Table 71 in Section C-2.2.2 (p. 217), and, although this was not verified, sulphur was very likely to have been introduced (similarly to what happened in acetolysed *Lycopodium* spp.; see Table 69, p. 215). The final material was believed to be a mixture of sporopollenin, protein impurities and cellulose.

1.5.2.3 Extraction using hydrochloric acid

Lastly, a brief protocol was found in patents registered by Tawashi and Amer[92-

[94] and applied directly to *A. trifida* pollen. The precise protocol is detailed in Section C-2.2.3. In a sealed tube, raw powder was suspended in 6M hydrochloric acid at 110°C for 24h. Resulting hydrolysed particles were easily filtered on a porosity-grade-4 sinter. Their integrity was verified by SEM (see Figure 15) and they were found to be nitrogen-free by combustion elemental analysis (see Table 72, p. 218). This proved that *A. trifida* pollen can resist strong hot acidic conditions.

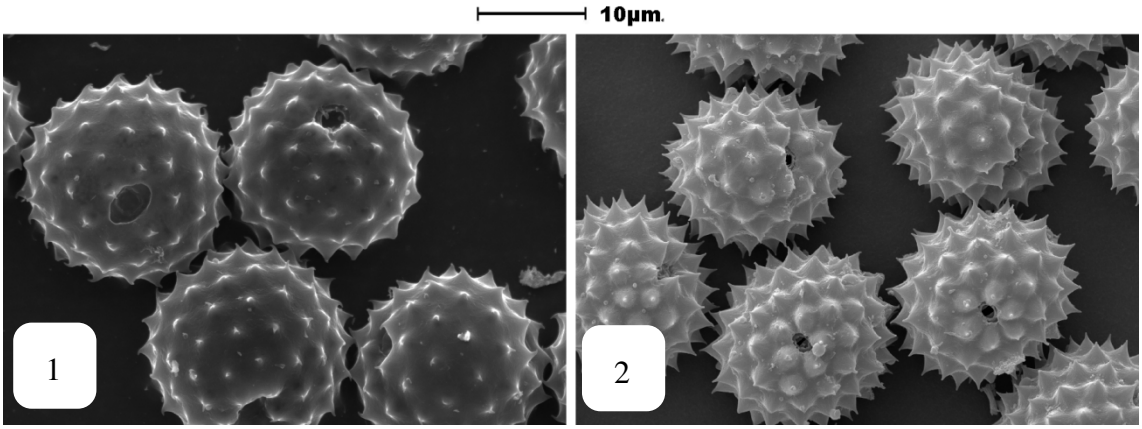

Figure 15 – *A. trifida* pollen (1) and particles extracted thereof using hydrochloric acid (2) – SEM pictures

1.5.3 Extraction of microcapsules from *Aspergillus niger*

As detailed in Section A-1.2.3, the composition of *Aspergillus niger* conidial walls is still controversial although a polysaccharidic complex of chitin and glucan has now been identified with certitude.[27,33] Spores were thus likely to resist acids only poorly, despite the possible presence of sporopollenin as suggested by Shaw *et al.*[34-37]

For this study, *A. niger* conidia were obtained as a gift from Tate & Lyle PLC (Selby, UK). In fact, the actual spores were not given as an isolated dry powder. On the contrary, the entire culture medium was provided, which contained the actual fungi hyphae, granular support (gound maize cob or cotton seeds), nutrients (soy flour) and other possible solid contaminants (cotton fibre), all being suspended in an aqueous brew.[27] Therefore, they had to be isolated as well as extracted. Due to their minute size (4.1-5.0µm in diameter[28,33]), filtration could not be envisaged. Solid was thus concentrated in the brew either by decantation after several weeks in the culture tub or by centrifugation of the suspension, and water was finally removed by freeze-drying.

However, the resulting solid was a mixture of spores and contaminants which

needed further treatments. Therefore, in order to simplify the process, the extraction protocol was not implemented on the dry powder but directly on the culture brew. As most contaminants to be eliminated were made of cellulose-type fibres (ground maize cob, cotton fibre, etc.), an acidic hydrolysis was first explored. Concentrated phosphoric acid was diluted in the brew [1/1 (v/v)] that contained the spores and the mixture stirred under reflux for 6h. No particles could be recovered by centrifugation after such a treatment (detailed in Section C-2.3.1) and were considered to have been destroyed by the acid, as expected.

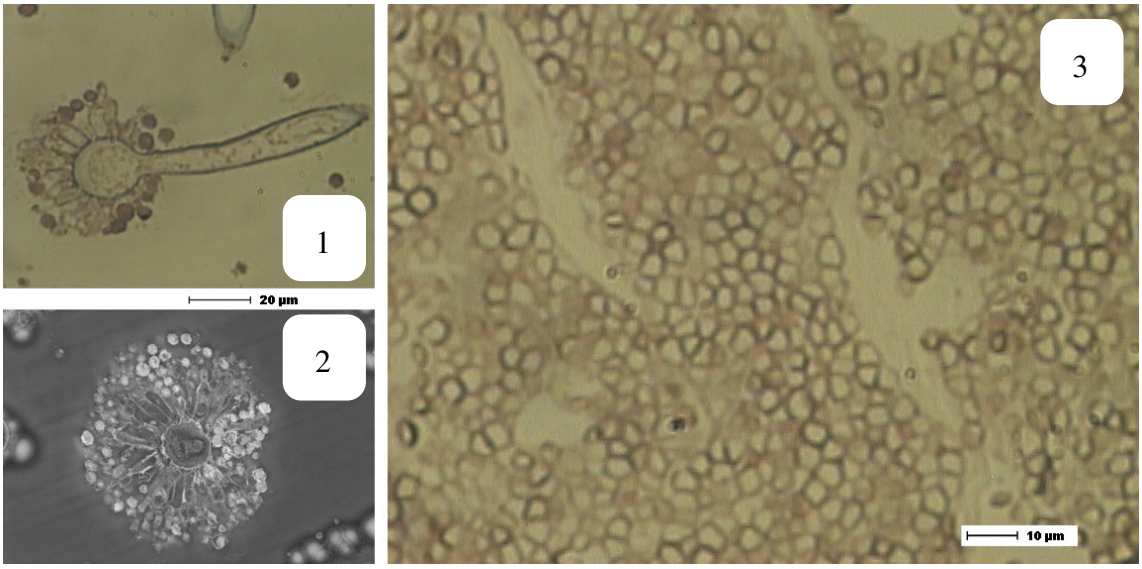

Figure 16 – Microtome sections of *Aspergillus niger* – whole hyphae on the left showing the sprouting conidial heads: LM image (1) and SEM picture (2) – base-hydrolysed spores on the right (3)

Spores being damaged by reflux in acids, as experienced initially, a basic hydrolysis was attempted in order to eliminate the fibrous contaminants and the sporoplasm. Therefore, *A. niger* conidia were subjected to a reflux in caustic potash followed by series of washings, as described in Section C-2.3.2. Potassium hydroxide pellets were dissolved into the brew where *Aspergillus* was grown, up to a concentration of 10% (w/v). The resulting alkaline mixture was then stirred under reflux for 4h and a solid was successfully recovered by centrifugation, and successively washed in various organic solvents and dried. This treatment yielded empty capsules as observed by SEM of microtome sections (see Figure 16). Nitrogen content was not monitored on this sample, but a recent study of the extraction of *Aspergillus niger* spores showed that nitrogen content dropped from 2.32% in original dried unextracted solid to 1.81% in the

base-hydrolysed spores (using 6% potassium hydroxide under reflux overnight). In the hypothesis that conidial walls are mainly composed of a chitin-glucan complex,[27,33] the removal of nitrogen might involve more elaborated treatments such as diazotisation.

1.5.4 Extraction of microcapsules from *Chlorella vulgaris*

According to the literature,[42] *C. vulgaris* cysts contain sporopollenin and could resist caustic treatments. Therefore, extraction trials were attempted to isolate this sporopollenin. The same steps were investigated as in the 'full treatment' described for *L. clavatum* spores, in Sections B-1.1 and C-2.1.1: acetone reflux, base hydrolysis and acid hydrolysis.

After acetone treatment, as described in Section C-2.4.1, particles were easily recovered by filtration and yielded a free-flowing powder upon drying. The resulting particles were then treated with 6% (w/v) aqueous potassium hydroxide under reflux followed by washing (see Section C-2.4.1). This formed tightly packed aggregates but the emptiness of the capsules yielded could not be easily evaluated due to their small size. However, it was found in this study not to resist acidic treatment. The alga was treated with phosphoric acid, as described in Section C-2.4.2. Particles coagulated and formed a paste that could not be satisfactorarily drained by filtration or centrifugation and hardened into brittle glass-like lumps upon drying.

Adding to its lack of monodispersity and poor resistance to strong conditions, *C. vulgaris* was not further investigated and no usable capsules were obtained from its cells. Ergo, nitrogen content was not monitored on this sample.

2 Physical characteristics

2.1 Size and wall thickness of sporopollenin exines

The size and wall thickness of exines were determined to more completely characterise them from different sources (especially S-type and L-type *Lycopodium* spec. spores). Such information is important in contributing to the understanding of why there are differences in stability of such particles and to best enable potential applications to be found. For example, an exine with a thin but robust wall but which is large can offer a large volume for encapsulation with high loading and good protection.

Additionally, when the extinction coefficient of sporopollenin was evaluated (see Section B-4.2.3), the actual thickness of sporopollenin crossed by the light that passes through an exine shell appeared to be a key parameter. This adds to the importance of measuring these physical characterics.

2.1.1 Size

Size and monodispersity of *L. clavatum* L. and *Lycopodium* spec. spores, and their respectively extracted particles, as well as *C. vulgaris* Beij. cells, were monitored by light scattering.[224] Results are gathered in Table 24.

		Average size (µm)	**Median size (µm)**
***L. clavatum* L. (S-type)**	spores	30.14 (13.94)	29.31
	empty exines	24.89 (12.14)	24.13
***Lycopodium* spec. (L-type)**	spores	38.29 (18.38)	37.21
	empty exines	37.59 (22.22)	36.20
***C. vulgaris* Beij.**	full cells	50.24 (54.30) 1,194.23 (506.16)	39.81 1,096.48

Standard deviation is given in brackets where available.

Table 24 – Data obtained by light scattering on *Lycopodium* spp. spores, on their empty exines, and on *C. vulgaris* cells

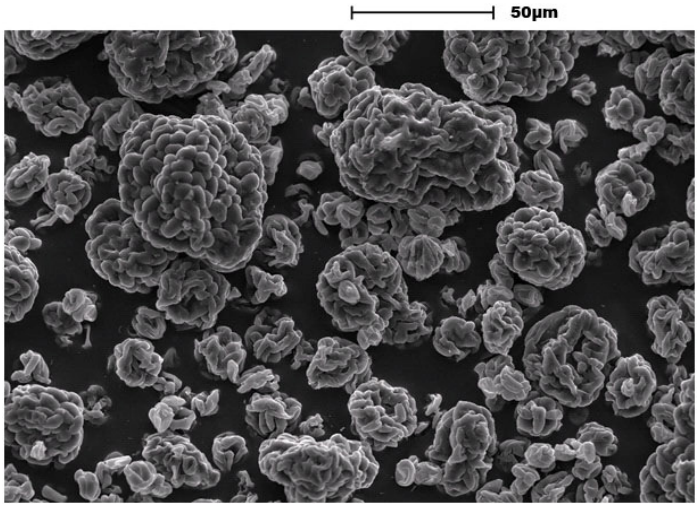

Figure 17 – Aggregated *Chlorella vulgaris* Beij. cells – SEM picture

For *C. vulgaris*, the particle population repartition in function of size showed two different broad peaks. This clearly showed that the cells of this green alga did not form a monodisperse powder; this was explained by their coalescence into aggregates shown in Figure 17. In contrast, *Lycopodium* ssp. spores and their extracted exine (see Figure 11 and Figure 13) showed a high monodispersity. It is noteworthy that extraction slightly reduced the overall diameter of the particles indicating that some cytoplasm and/or coating cement may have been removed; however, this is open to speculation since the measurement error is high, as the standard deviation shows. It is doubtful that light scattering is a good method for such irregular particles as spores and exines. It is indeed generally used for particles which are more even than exines like carbon black, polystyrene beads or silica.[225,226]

A more precise measure of spore diameter has been done by a co-worker[190] with direct measurements on print-outs of SEM pictures. His study shows that an average diameter of S-type *L. clavatum* AHS particles was found to be 27µm (standard deviation 5µm).

2.1.2 Wall thickness

Empty particle wall thicknesses were established directed by light microscopy observations of microtome sections (see Section C-3.2). Many of the embedded particles had collapsed due to incomplete loading of the monomer before the resin was polymerised for sample preparation. The wall thickness measurements were made on whole filled spores.

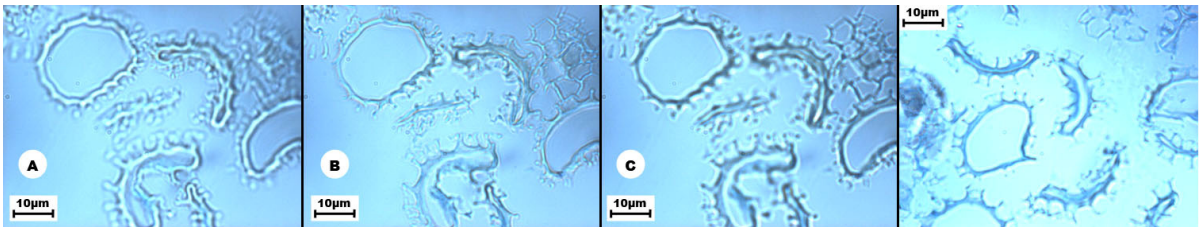

Figure 18 – AHS from S-type *L. clavatum* L. – LM images (microtome sections): including three different focuses (A, B, C)

First, a difficulty was faced during the measurements as the stain used (toluidine blue) did not dye the spore walls properly. As a consequence, a second problem occurred: the microscope focus was ambiguous, thus giving too high an error in the values. These problems had thus to be addressed before pursuing the measurements.

Therefore, a first experiment was performed on S-type exines. Different thickness values were recorded from three focuses on a same microscopical image, given in Figure 18. After several measures, gathered in Table 25, an average thickness and a standard deviation were obtained for each focus (A, B, C).

	Replicates	Average wall thickness (µm)
A	12	1.87 (0.79)
B	8	1.40 (0.51)
C	12	1.95 (0.84)

Standard deviation is given in brackets.

Table 25 – AHS from *Lycopodium clavatum* L. S-type - Measurements of wall thickness on three focuses (A, B & C)

Images A & C were considered to be out of focus. Therefore, the same focus as used for B was kept for all the other pictures. Only pictures in focus were taken into account in the final measurements. Due to the large number of crushed particles that were not considered, only few pictures were taken for each type of particles. However, ca. 10-15 records were determined on each image, thus reducing the standard error. Results of wall thickness for all three species are gathered in Table 26.

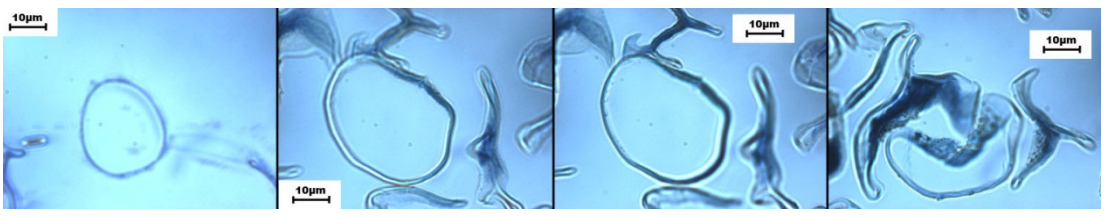

Figure 19 – L-type *Lycopodium* spec. AHS – LM images (microtome sections)

Particles	LM images	Replicates	Average wall thickness (µm)
S-type AHS *L. clavatum* L.	Figure 18	29	1.20 (0.34)
L-type AHS *Lycopodium* spec.	Figure 19	28	1.53 (0.23)
15µm AHS *A. trifida* L.	Figure 20	61	1.57 (0.31)

Standard deviation is given in brackets.

Table 26 – AHS from three species - Measurements of wall thickness

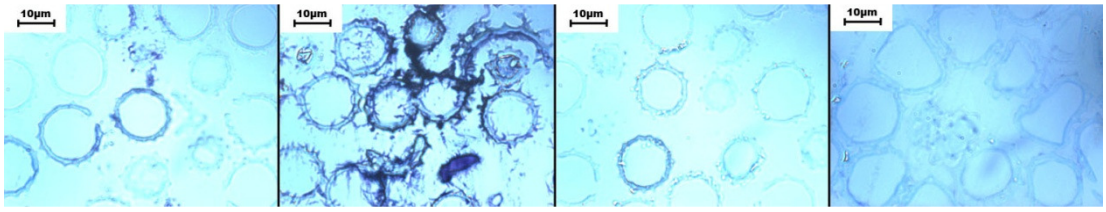

Figure 20 – 15µm *A. trifida* L. AHS – LM images (microtome sections)

2.2 Resistance to pressure

The maximal pressure S-type *Lycopodium clavatum* L. spores could resist was evaluated by compression under increasing weight (see Section C-3.1). Loose powder was compacted into a 13mm-diametered tablet in a press commonly used to prepare potassium bromide discs for IR spectroscopy. Bearable weight was considered maximum when spores broke open, releasing their sporoplasm: this was marked by a sudden fall of pressure. Impact of the weight on empty exines was evaluated by SEM: above a limit, particles appeared cracked. Results are gathered in Table 27.

Particles	Maximum bearable weight (tonnes)	Breaking threshold (Pa)
S-type *L. clavatum* spores	5	369,500,000
S-type AHS	10	739,000,000

Table 27 – Maximum bearable weight over a 13mm-diametered tablet and corresponding breaking pressure limit

Spores burst open with more facility due to the inner content: their wall rapidly became tensed under 5 tonnes; hence it ruptured within seconds. By contrast, in empty exines, sporopollenin could exhibit its elasticity to bear higher pressure for a longer time. AHS particles were not immediately broken by application of 10 tonnes over the tablet. But, since 10 tonnes were the limit of the die used for measurement, no higher

pressure could be tested. However, after maintaining 10 tonnes for 30s or more, some cracks could be seen in empty particles by SEM. This enabled a section view of exine wall to be observed, as in Figure 21.

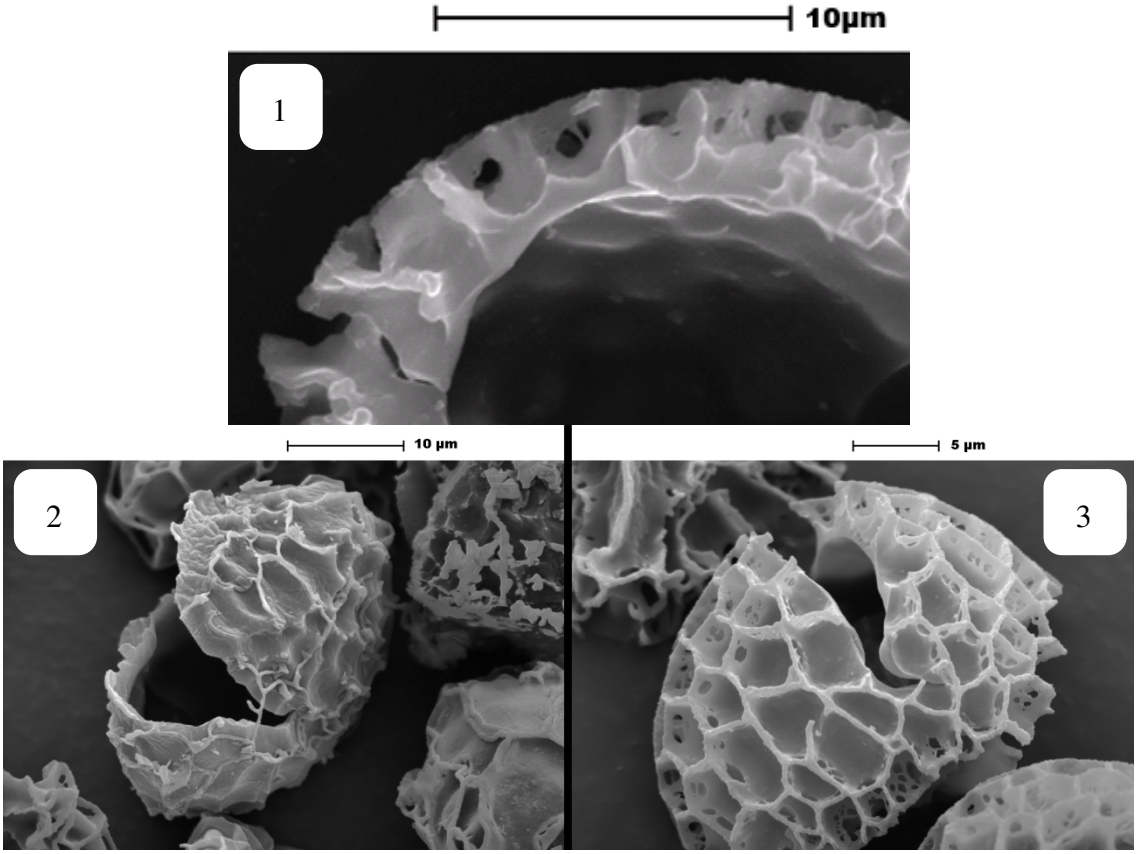

Figure 21 – SEM picture of S-type AHS: section of the wall of a cracked exine (1); and cracked exines after a 2min compression under 10 tonnes (2 & 3).

2.3 Density

Particle type	Particle type	Density ($g.cm^{-3}$)
S-type	spores	0.374 (0.006)
	BHS	0.214 (0.010)
	AHS	0.152 (0.013)
L-type	spores	0.644
	BHS	0.426
	AHS	0.149

Standard deviation is given in brackets where available.

Table 28 – Density values of loose *Lycopodium* spp. spores and their empty shells

Measurements of densities were first recorded in this study by weighing directly

a known volume of loose powder of either raw spores or empty particles of *Lycopodium* spp. (see Section C-3.3.1) and results of these determinations are gathered in Table 28. The use of *Lycopodium* spores in pyrotechnics as a flammable smoke[17] is evidence of the lightness of this powder. As expected hollow sporoderms were even lighter, due to their air content that replaced the natural cytoplasm.

An experiment showed that S-type *Lycopodium clavatum* spores float on water and sink in light oils within hours.[226] By this comparative means, the density of a spore *per se* was estimated approximately as being between 0.7g.cm^{-3} (density of the oil used) and 1g.cm^{-3} (density of water). To better evaluate this value, raw spores were compressed to expel as much air as possible from the final tablet, without cracking the exine and leaching the cytoplasm out (pressure less than 369,500,000Pa) (see Section B-2.2). Results are displayed in Table 29.

Weight (g)	Diameter (mm)	Thickness (mm)	Pressure (t)	Tablet density (g.cm^{-3})
0.498	13.593	5.251	1	0.653 (0.014)
0.515	13.435	5.407	2	0.672
0.481	13.480	4.920	3	0.692 (0.104)

Standard deviation is given in brackets where available.

Table 29 – Density of S-type *L. clavatum* spore tablets

In the hypothesis of spores being hard non-compressible spheres, the best compaction factor for randomly distributed perfect monodispersed particles is 0.66. The density of a single hard spore (ρ_{spore}, g.cm^{-3}) would then be: $\rho_{spore} = \frac{\rho_{tab}}{0.66}$, with ρ_{tab} (g.cm^{-3}) the density of the tablet. It was however very likely that under compression, the spores were significantly deformed. Their flattening probably left minor quantities of air in the final tablet. Therefore, it was believed that the density of a tablet mirrored the one of a single spore, with only slight underestimation. Real density of one isolated S-type *L. clavatum* spore thus lay in between: (values in g.cm^{-3})

- under 1 tonne: $0.653 < \rho_{spore} < 0.989$;
- under 2 tonnes: $0.672 < \rho_{spore} < 1.018$;
- under 3 tonnes: $0.692 < \rho_{spore} < 1.048$.

The density of spores is finally barely below 1, which fits the expectations. The pressure used for compression did not appear critical, although air seemed to have been more efficiently expelled by higher pressure.

Density of the sporopollenin material itself was estimated by weighing tablets of

empty exines (AHS). The powder was crushed under 10 tonnes the same way as above (see Section C-3.3.2). Particles were expected to collapse and most air to be removed from the resulting cylindrical pellet, whose size and weight gave the approximate density as being ca. 1g.cm^{-3} for both S- and L-type *L. clavatum* AHS (no replicate).

A more reliable measurement of the density of sporopollenin polymer was eventually determined by pycnometry (see Section C-3.3.3). Values were determined for AHS extracted from S-type *L. clavatum*. However, pycnometry was extended to BHS (*i.e.* composite particles containing cellulose as well) and to raw spores (in which case the material included cytoplasm and cellulose). Results are gathered in Table 30.

Particle type	**Density (g.cm^{-3})**	**Standard deviation (g.cm^{-3})**	**Replicates**	**Standard error (g.cm^{-3})**
spores	1.168		1	
BHS	1.330	0.024	2	0.210
AHS	1.084	0.297	2	0.017

Table 30 – Density values obtained by pycnometry on S-type particles extracted from *L. clavatum* L.

3 Physical encapsulation in sporopollenin exines

3.1 Purpose

In Section A-6.1, attention was drawn to the multiple applications of microencapsulation and its large development in food, cosmetic and pharmaceutical industries. Existing microcapsules used for drug delivery or protection of the encapsulated product are catalogued in Section A-6.2. Most of them are artificially created by various techniques such as spray-drying, milling or vacuum-tumbling. Such methods prove to be rather costly in materials and energy and generally yield particles lacking high monodispersity. Often synthetic products have to be designed for specific purposes, which leads to long and expensive procedures to get the artificial microcapsule legal approved for human use. Natural compounds have the advantage of being sustainable, biocompatible and biodegradable, but could be allergenic or suffer law restriction, as gelatine, for instance, and other substances isolated from animals – mainly after sanitary problems. Also they usually offer poor protection. Microcapsules obtained from living organisms (bacteria, yeast cells, etc.) are considered dirty as it is difficult to strip them off of all their contaminants, toxins or allergens; in addition, they do not have a very large inner cavity *i.e.* a poor loading capacity. Moreover, macromolecules (proteins, oligonucleotides or polysaccharides) can be loaded in only very few microcapsules available on the current market.

As underlined in Section A-6.3, sporopollenin exine particles extracted from various plant spores and pollens (especially *Lycopodium* spp. spores) can be loaded with various products and they could be used as effective microcapsules. The interests of sporopollenin as microcapsules are numerous.

Being obtained from plants, sporopollenin is renewable, biocompatible (see Section A-5.1) and biodegradable, and does not exhibit the drawbacks of products from animal origin. Extraction protocols described in Section B-1 have now been developed to remove all allergens from the resulting empty shells; the absence of nitrogen is the cornerstone to verify such a property. Also, pollen and spores are available on a large scale; for example, estimates suggest that the spruce forests of central and southern

Sweden produce 750,000 tonnes of pollen every year,[34] and a field of maize around 175 kg per hectare in a year.[227] Cultivated crops could therefore be used commercially as a cheap source of pollen. *Lycopodium clavatum* L. spores are already available for sale in ton quantities for quite a modest sum of money, as shown in Section A-1.2.1. Also, companies such as Graminex LLC (Saginaw, US) and Phabia AB (Ängelholm, Sweden) produce tonne quantities of pollen (especially from cereals) from which they extract the cytoplasm by cryogenic means for the nutraceutical market. In conclusion, there is already a plentiful supply of raw pollen and spore materials which could be expanded upon enormously to produce microcapsules by inexpensive non-toxic means and using regents used in the food industry.

In addition, sporopollenin exine shells isolated from a single plant species are extremely monodispersed,[7,12] very resistant to chemical, physical or biological aggressions,[12,34,46,113] and offer a large internal cavity which is readily loadable. Furthermore, it was observed that exine microparticles were taken up through the GI tract lining into the blood stream (see Section A-5.2).

By collating all those observations, it became evident that empty sporopollenin exines were excellent candidates for microencapsulation with a large variety of potential industrial applications. Therefore physical encapsulation of various substances in exine shells was extensively studied in order to implement optimal filling methods adapted to each targeted product, to entrap a variety of substances as wide as possible (including polar and non-polar substances, as well as macromolecules), and also to be able to reach the highest loading levels. Finally novel properties of the sporopollenin polymer itself were investigated as they justify even more the application of exine capsules to the food industry in particular.

3.2 Encapsulation of neat liquids

As aforementioned, empty extracted spores or pollen grains could have a mighty potential for encapsulation. Encapsulation of various products was therefore studied in order to implement filling procedures. In a first time, this was investigated with neat liquids. Indeed, sporopollenin was described in Section A-3.5 as a porous shell traversed by nano-channels. As a result, liquids were expected to enter exine capsules by simple contact, driven inside by capillarity or by vacuum.

3.2.1 Passive filling

3.2.1.1 Microtome sections

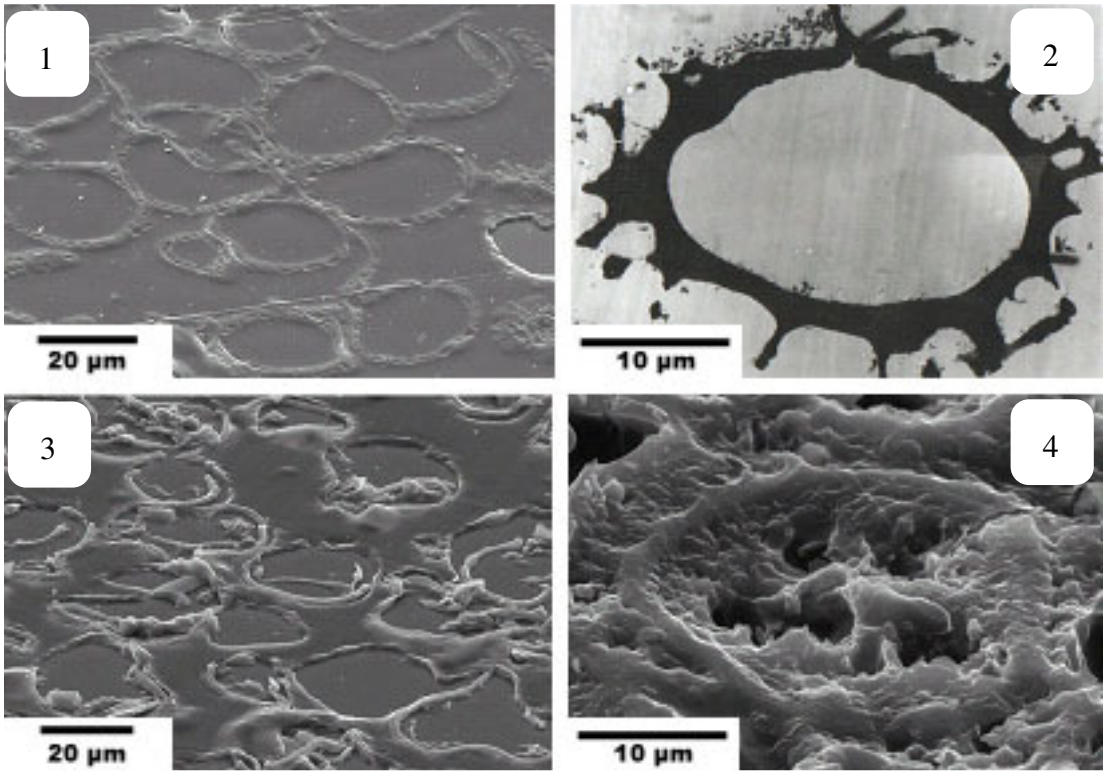

Figure 22 – Microtome sections of inclusions of S-type exines from *L. clavatum* embedded in acrylic resin: SEM (1) & TEM (2) pictures of empty exines; SEM pictures of initial spores (3) and encapsulated calcium chloride (4).

The first discovery of passive loading of a liquid into extracted sporopollenin exines occurred by chance when attempts were made to verify the emptiness of the microcapsules by microtome sections. A physical cut of the capsules was performed supposedly to inspect the inside. The protocol followed the method decribed in Section C-1.4.3. Exines were first embedded in acrylic resin and then sliced. By TEM or SEM observations of the resulting microtome sections, various encapsulation phenomena were observed. When empty particles were cut, the hollow of their inside was never observed. As the matter surface was as smooth around the particles as inside, it was concluded that the resin passively penetrated the capsules before the cut. Also SEM images of microtome sections of resin-filled exines clearly showed the continuity of the microtome knife scores as they passed with continuity from outside to the encapsulated material inside the exines (see top right image in Figure 22). Even if emptiness *per se* was not proven, encapsulation was thus demonstrated. Images of microtome sections

were also taken with initial spores, as well as with encapsulated calcium chloride. Examples obtained with S-type particles from *L. clavatum* are displayed in Figure 22.

3.2.1.2 Encapsulation of limonene

Light microscopy observations over the time were also a simple way used to monitor the passive encapsulation process. Exines were passively filled with limonene (following the protocol described in Section C-4.1.1.1) and the contact of the terpene with the sporopollenin was immediately observed by LM. Limonene is an essential oil commonly used (under the trade name Histoclear®) in palynology to make LM pictures of pollen grains and spores appear translucent, while air-filled exines are black and opaque. Air bubbles were easily seen as dark circles, as shown on Figure 23. During the loading process, the bubbles escaped the capsule which appeared lighter and lighter until it finally became translucent and pale brown. It is noteworthy that limonene being very fluid, its passive loading took less than 30s.

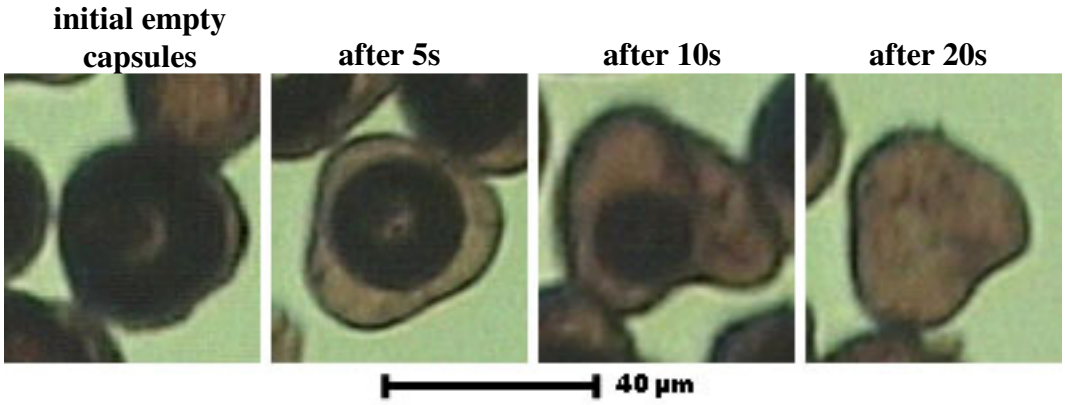

Figure 23 – L-type sporopollenin exines slowly filled with limonene passively – LM pictures: black = air bubble; light brown = exine

3.2.1.3 Encapsulation of oils

Fats are more or less sensitive to air and light; ω-3 fatty acids for instance are very fragile. With time, they go rancid, *i.e.* they get darker, thicker and aquire a strong pungent unpleasant smell and taste. Shelf life of various lipids used in food industry can be increase by addition of antioxidants to them. Encapsulation is a very useful alternative, as discussed in Section A-6.1.1. Therefore exines loaded with oils have a large potential of application, all the more that sporopollenin proved to be UV-protective and antioxidant, as developed in Section B-4.

Thus passive encapsulation was also carried out with different oils. Following

the protocol detailed in Section C-4.1.1.1, S-type and L-type AHS were loaded with cod liver oil, sunflower oil, soybean oil, rapeseed oil, echium oil, *Lyc-O-Mato*® (lycopene-dyed soybean oil), (+)-limonene (*Histoclear*®) and eicosapentenoic acid by simple mixture of the extracted empty exines with the fats. Successful encapsulations were verified by LSCM and the images observed were similar to those displayed in Figure 24. With oil loading level been $1cm^3.g^{-1}$, a free-flowing powder was obtained after the mixture was left standing for 1h, in each case. However, the sample kept a damp aspect for a longer time when more oil was used, and a paste was obtained when oil loading exceeded ca. $2.5cm^3.g^{-1}$. In order to overcome this limit, other filling methods had thus to be implemented; these procedures are further discussed in Section B-3.2.2.

3.2.1.4 Encapsulation of waxes and solid fats

Solid lipids, such as cocoa butter, beeswax or carnauba wax, were also passively encapsulated in S-type and L-type sporopollenin following a similar procedure to that described in the previous Section B-3.2.1.3. However, they had to be melted first and were thus maintained at higher temperature throughout the passive loading process as detailed in Section C-4.1.2.1.

Lipid (melting point if above RT)	**Main chemical components**
beeswax (64-66°C)	myricyl palmitate, myricyl cerotate, myricyl hypogaete, ceryl hydroxypalmitate, free cerotic acid, heptacosane, hentricontane[228]
carnauba wax (78-85°C)	polyesters of long hydroxy acids, their esters with octocosanols to tetratricontanols[228]
cocoa butter (35-38°C)	triglycerides: stearate (34%), oleate (34%), palmitate (25%), α-linolenic acid (2%)[229]
cod liver oil	triglycerides: oleate, gadoleate, palmitate[1]
echium oil	triglycerides: α-linolenate, stearidonate, linoleate, oleate, palmitate, γ-linolenate, stearate[230]
rapeseed oil	triglycerides: oleate (58%), linoleate (22%), α-linolenate (9%), palmitate (6%)[231]
soybean oil	triglycerides: linoleate (56%), oleate (21%), stearate & palmitate(16%), α-linolenate (7%)[231]
sunflower oil	triglycerides: linoleate (48-74%), oleate (14-40%), palmitate (4-9%), stearate (1-7%)[232]

Table 31 – Composition of some natural fats

Cocoa butter was loaded at 40-50°C, beeswax at 70-80°C and carnauba wax at 90-100°C. Actual melting points of solid fats are gathered in Table 31, along with the main chemicals that compose natural oils.

3.2.1.5 Encapsulated neat liquids

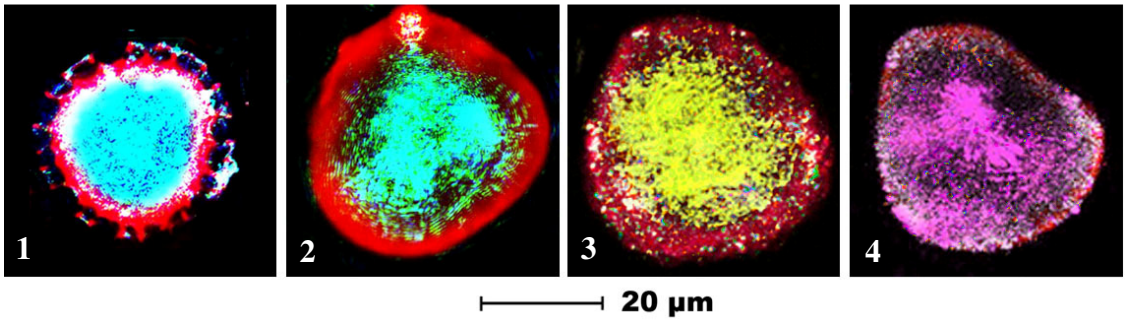

Figure 24 – Encapsulation of oils – LSCM pictures: fish oil (cyan) in S-type AHS from *L. clavatum* (red) (1), fish oil (cyan) (2), yellow-dyed sunflower oil (yellow) (3) and lycopene-dyed soybean oil (pink) (4) all three in L-type AHS from *Lycopodium* spec. (red).

Mixtures of oils with different fat-soluble dyes were used in order to rapidly observe the loading by LM (no picture was actually recorded). Precisely, sunflower oil and limonene were mixed with solvent O blue, red or yellow; and soybean oil was stained with lycopene (in commercial *Lyc-O-Mato*®). After this initial verification, encapsulation of the different oils was monitored by LSCM, technique which requires a longer mounting process. Examples of pictures obtained are gathered in Figure 24.

Figure 25 – L-type *Lycopodium* spec. spores passively filled with isopropanol

In addition, small alcohols (methanol, ethanol, propanol, isopropanol, *n*-butanol and isobutanol) were also encapsulated in sporopollenin exines (see Section C-4.1.1). Loose sporopollenin powder was found to form even dispersion in them (as it does in oils) and encapsulation phenomenon was more rapid than with oils. Alcohols were not observed by LSCM since they do not fluoresce under laser excitation. However, alcohol-loaded exines appeared translucent by LM, as can be seen in Figure 25, as opposed to black and opaque when dry (air-filled).

3.2.2 Other methods of filling

Passive filling process relied on capillarity to draw the liquid inside the porous exine microcapsules. Therefore the maximum level was limited by a thermodynamic equilibrium. In order to try and enhance the loading level, other encapsulation methods were investigated.

A first alternative was proposed which used compressed empty exines instead of loose powder. Air was drawn out of the microcapsules by crushing them in a press commonly used to make potassium bromide discs for FTIR spectroscopy, as detailed in Sections C-4.1.1.2 and C-4.1.2.2. The liquid to be encapsulated was then poured over the resulting tablet, or alternatively the latter was dropped in it. Exine pellets were found to fill up like sponges and to soak up the liquid within minutes.

However, to form the tablet, sporopollenin elasticity was at stake. Indeed, loose powder was crushed into a 13mm-diametered cylinder under 10 tonnes for at least 2min. As discussed in Section B-2.2, such a high pressure maintained over more than 30s caused some exines to crack. This limited the used of compression filling since fissured microcapsules could not be of use to protect the loaded product.

Type (origin)	Extraction	Loading process (1h)	Loading ($cm^3.g^{-1}$)
S-type capsules (from *L. clavatum* L.)	BHS	passive	2.0
		vacuum	2.5
	AHS	passive	2.5
		vacuum	3.5
L-type capsules (from *Lycopodium* spec.)	BHS	passive	2.5
		vacuum	3.0
	AHS	passive	3.0
		vacuum	4.0

Table 32 – Approximative maximal loading of cod liver oil in different types of capsules extracted from *Lycopodium* spp.

As a consequence, a second alternative was developed to minimise any damage done to the capsules. Following the protocol detailed in Sections C-4.1.1.3 and C-4.1.2.3, an intimate mixture of loose exine powder with the liquid to be encapsulated was subjected to a vacuum. This drew air out of the capsules so that the oil present outside was forced into them. This was especially useful to drive the capillarity balance to completion. It appeared that less product was left outside by this procedure, since a

free-flowing powder was still obtained when the oil loading level in S-type AHS reached up to ca. $3cm^3.g^{-1}$.

A maximal loading of cod liver oil in S-type and L-type BHS and AHS was determined in testing how powdery the final sample was to the eye. Since AHS did not contain cellulose intine, it was lighter than BHS (see Section B-2.3) and thus it was expected to house a larger volume of fill per unit of mass. This was confirmed by the results, shown in Table 32. Samples were prepared with increasing loadings and maximal value was recorded when oil was found visible on the outside, *i.e.* when the final sample was starting to look more like a paste than a powder.

For applicative purposes, this loading limit had to be considered since highly loaded samples were sticky and less free-flowing. A number of industrial installations (e.g. pipes) do not withstand slurries or liquid, and thus lipids in a free-flowing powdery state would be most useful. However, in using sporopollenin for this aim, the loading limit would not have to be exceeded. Otherwise, a few solutions (which are given hereafter as indications of potential future studies) could be envisaged in order to obtain a dry formulation of the product. A coating could be added over the particles to separate them, using materials such as gum Arabic, starch or wax. The charge balance on the exine surface could also be modified, so that the particles repelled each other. Finally, *L. clavatum,* being used as a dusting powder, sporopollenin exines could be used to dilute loaded particles and by capillary suction (*i.e.* passive filling), empty exines would soak up excess of unloaded oil.

3.2.3 Viscosity of the loaded product

The viscosity of vegetable oils (and other fats) was thought to be an impediment to their encapsulation in sporopollenin microcapsules. Lipids were thus initially loaded under vacuum as warm emulsions oil/ethanol [ca. 9/1 oil/ethanol (v/v) at 40°C] (see Section C-4.1.1). Temperature made the mixture more fluid and ethanol was supposed to enhance encapsulation process by possible surfactant properties. During the following vacuum filling, alcohol was eventually evaporated and oil only remained inside the exines.

However, heat could be detrimental to fats especially fragile ones (e.g. echium oil goes rancid more quickly at 50°C). In addition, due to its lipidic characteristics, sporopollenin was readily suspended in oil without help from any aiding agent such as ethanol. Finally, any kinetic issue raised by viscosity did not appear critical, as a

vacuum being applied for 1h was found sufficient to obtain a free-flowing powder (with an oil level inferior to the limit indicated in Table 32). As a conclusion, oils were eventually encapsulated neat and at room temperature. Only solid fats were heated as discussed previously in Section B-3.2.1.4.

Also, the influence of lipid viscosity on encapsulation process was investigated. Precisely, a comparison was drawn between (+)-limonene, a very fluid essential oil, sunflower oil, a more viscous vegetable oil, and cocoa butter, a solid fat which was very viscous in its molten state at 40°C (temperature of loading). All three fats were passively loaded in L-type AHS to a level of $1cm^3.g^{-1}$ (protocol detailed in Section C-4.1.1.1). The approximate time after which a free-flowing aspect of the final powder was observed was then recored, and results are gathered in Table 33.

Fat passively encapsulated in L-type exines	**Time of encapsulation*** (min)
limonene	2-5
sunflower oil	30-45
molten cocoa butter	ca. 60

* determined as the time after which the final powder appeared free-flowing

Table 33 – Time of encapsulation of three fats of different viscosity

Limonene was encapsulated within minutes while sunflower oil had to stand for more than 30min in contact with exines to be fully loaded. Cocoa butter was even longer to fill. Identical experiments were performed using respectively compression and vacuum loadings, following protocols described respectively in Sections C-4.1.1.2 and C-4.1.1.3. Results showed a similar trend, but time differences were not as significant, since the three lipids were loaded within 10min.

It led to the conclusion that the more fluid a fat, the easier it is to be encapsulated, being it passively, under vacuum or by compression mean. This phenomenon was confirmed with very liquid oils (ethyl eicosapentenoate and echium oil) and thick fats (beeswax and carnauba wax), the formers being far more readily absorbed into the capsules by capillarity than the latter, which were partly wasted on the outside of the exine shells.

As mentioned previously, ideally encapsulation of molten waxes had to be carried out at high temperature throughout the process. Whereas passive and compressive fillings of warm waxes were easy, vacuum loading was always performed at room temperature so that the fat was solidifying outside and across the nano-channels.

3.3 Encapsulation of solids and solutions

As aforementioned, encapsulating liquids (mostly oils) was relatively straightforward as it basically consisted in a mixture of the liquid with the exines while a drive force was applied to draw it inside. However, in order to load a solid that could not be melted, a fluid had to be added as a medium to drive the solute into the microcapsules.

3.3.1 Encapsulation of dyes

3.3.1.1 Loading processes

Initially, encapsulation of solids was illustrated using a series of dyes, namely methyl orange, malachite green, Evans blue and Nile red. The stains to be encapsulated were initially dissolved in a suitable solvent. Choice of the solvent was central to control the loading process and the final level of encapsulated solid as discussed below. Dyes were dissolved either in water or in ethanol, depending on their solubility (see Table 34). Saturated aqueous methyl orange solution was obtained at room temperature with a low concentration (ca. 0.5g.cm^{-3}). Malachite green and Evans blue were dissolved either in water or in ethanol (up to 3g.cm^{-3}), and Nile red was solubilised only in ethanol (up to 3g.cm^{-3}), but in no case saturation was reached.

Dye	Solubility	
	in ethanol	in water
methyl orange	insoluble	soluble in hot water
malachite green	very soluble	very soluble
Evans blue	soluble	soluble
Nile red	very soluble	insoluble

Table 34 – Solubility of the dyes encapsulated in exines[233]

The resulting solution was then encapsulated following one of the same protocols as implemented for neat liquids, namely passive, compression or vacuum encapsulation method (see Sections B-3.2 and C-4.1.1). Filling performances followed the same pattern as observed with oils in the previous Section B-3.2. This is summarised in Table 35.

Passive filling efficiency, in term of capacity and speed, was found low; compression and vacuum techniques improved and accelerated the loading. As noted in Section B-3.2.2, compression of sporopollenin was found detrimental to the capsules as

cracks were observed by SEM in some of them (see Figure 21). Exines encapsulated ethanolic media more rapidly than aqueous solutions. This was most probably due to the lipidic nature of sporopollenin, which had less affinity with water. Due to the slow loading water, empty exines had a tendency to float on it.

Solution	Encapsulation method	Maximum capacity ($cm^3.g^{-1}$)	Approximative time of filling* (min)
Malachite green in water	Passive	2.5	10-15
	Compression	3.5	2-3
	Vacuum	3.5	2-3
Nile red in ethanol	Passive	2.5	5
	Compression	3.5	1-2
	Vacuum	3.5	1-2

* determined as the time after which the final powder appeared free-flowing (with a $1cm^3.g^{-1}$ loading)

Table 35 – Encapsulation of aqueous and ethanolic solutions in S-type AHS – Performances in term of volume capacity and time of loading

Finally, once the stain solution was entrapped in the microcapsules, the solvent was removed. Ethanol was drying in an oven at 60°C or evaporated under vacuum (if vacuum loading had been applied). Water was removed either under vacuum over phosphorus pentoxide or, more quickly, by freeze-drying.

The whole procedure of encapsulation of solids is fully given in Section C-4.1.3, including dissolution, filling of the microcapsules and drying of the solvent.

3.3.1.2 Encapsulated dyes: results

Surprisingly, presence of dyes inside exines capsules was not clearly visible by LM. When sporopollenin was loaded with methyl orange, malachite green, Nile red or Evans blue, the expected coloured glow was very dim, and sometimes not even observed (see Figure 26). However, LM could not reveal if the observed product (when visible) was actually inside or simply left on the outer surface.

Incidentally, it is noteworthy that an independant study showed results that tended to prove actual encapsulation.[234] When a magnetic iron salt was precipitated inside sporopollenin exines, the whole powder was attracted to a magnet, proving the salt could not be outside the capsules. As similar loading techniques were used in that work as in the present study, real encapsulation of the dyes could be expected.

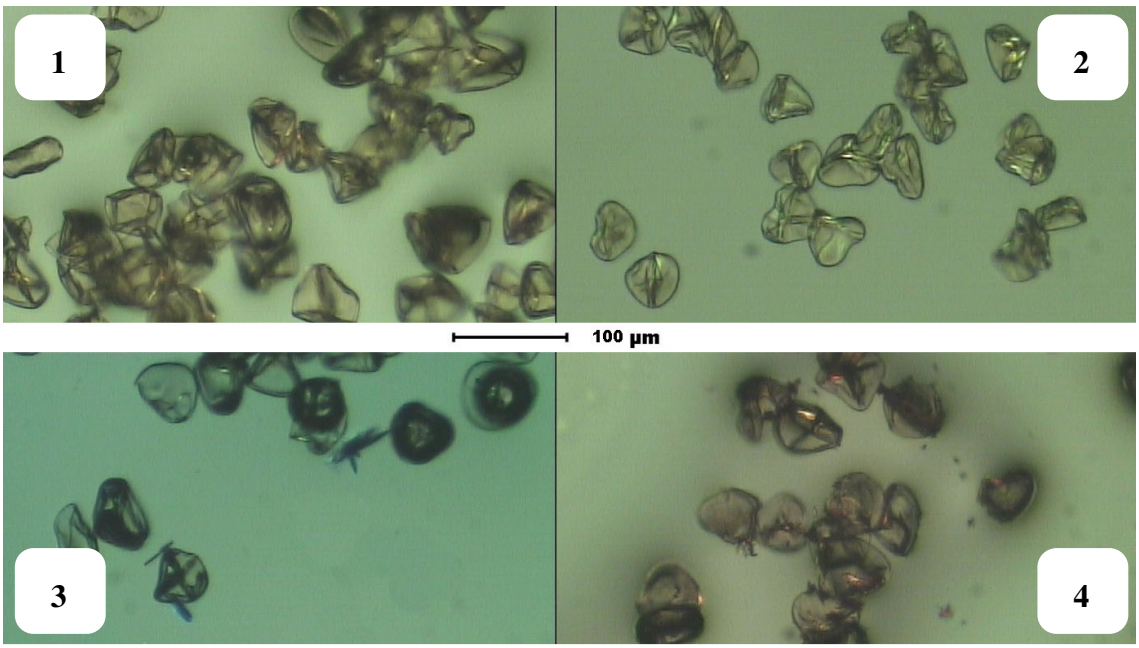

Figure 26 – L-type sporopollenin exines filled with dyes – LM pictures; light brown = exine; AHS filled with methyl orange (1), with malachite green (2), with Evans blue (3) and with Nile red (4).

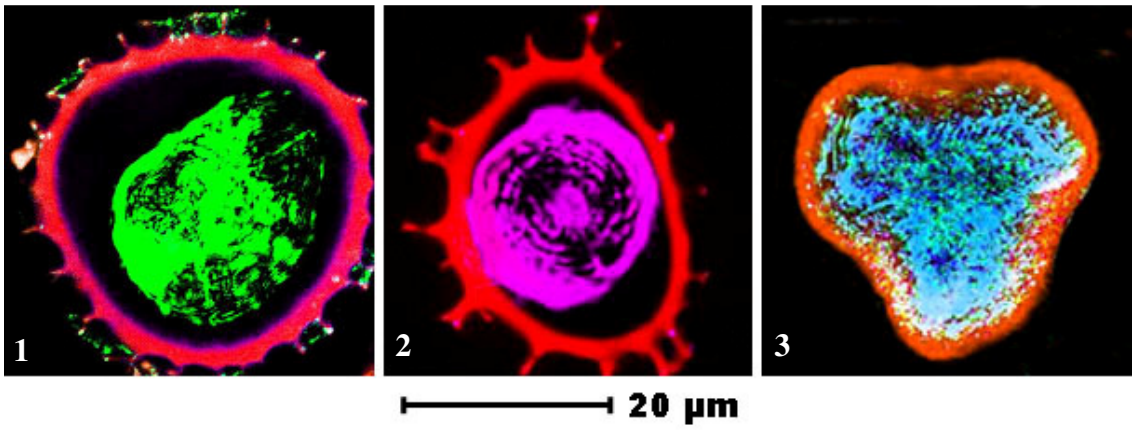

Figure 27 – Encapsulation of stains – LSCM pictures: malachite green (in green) (1), Nile red (in pink) (2) and Evans blue (in cyan) (3) encapsulated in S-type exine from *L. clavatum* (in red)

Eventually, the use of confocal microscopy added convincing confirmation of materials being successfully encapsulated. Indeed, laser scanning confocal microscopy (LSCM) records view of the inside of the observed item, their being cells or spores. Different sections could be seen without any actual slicing. At first, various stains were encapsulated and LSCM pictures shown in Figure 27 confirmed that they were inside the exines.

3.3.2 Encapsulation of proteins

3.3.2.1 Encapsulation methods

As mentioned in Section A-6.1.1.1, many macromolecules (especially proteins, are becoming of interest in the drug market and their encapsulation has attracted a large interest. Therefore microencapsulation of various proteins was attempted in sporopollenin exines.

A list and some images of the encapsulated proteins are given in Section B-3.3.2.2, but the general protocols of encapsulation were the similar for all of them and followed that implemented with dyes in Section B-3.3.1.1 and described in Section C-4.1.3. The targeted protein was initially dissolved in a suitable solvent. The solution generally had a water base but a drop of ethanol was often added as a surfactant to help and obtain a more even suspension. Empty AHS and BHS were indeed found to float on water as aforementioned. However, ethanol has to be used with care since it could denature the protein to encapsulate.

The resulting solution was encapsulated in AHS or BHS passively, by compression or under vacuum. The protein was eventually precipitated inside the microcapsule by removal of the solvent. Water and ethanol were evaporated under vacuum over phosphorus pentoxide but never at high temperature since this would have denatured the protein. Therefore freeze-drying was much more efficient.

3.3.2.2 Encapsulated proteins: LSCM observations

Following the method decribed above, various proteins were encapsulated in S-type and L-type AHS and BHS. First trials were performed with cheap readily available ones like ovalbumin, α-amylase and β-D-galactosidase. All three were loaded as aqueous solutions and the final loaded microcapsules were dried under vacuum over phosphorus pentoxide. Once encapsulation was verified by LSCM (see Figure 28), it was extended to proteins with potential applicative perspectives: antibiotics like bacitracin, hormones like insulin, somatropin (*Humatrope*®) and other growth hormones (1,097Da and 3,340Da), an anti-AIDS drug like enfuvirtide (*Fuzeon*®), and integrin beta-1 antibody. Their actual encapsulation was systematically verified by LSCM (see Figure 28 and Figure 31).

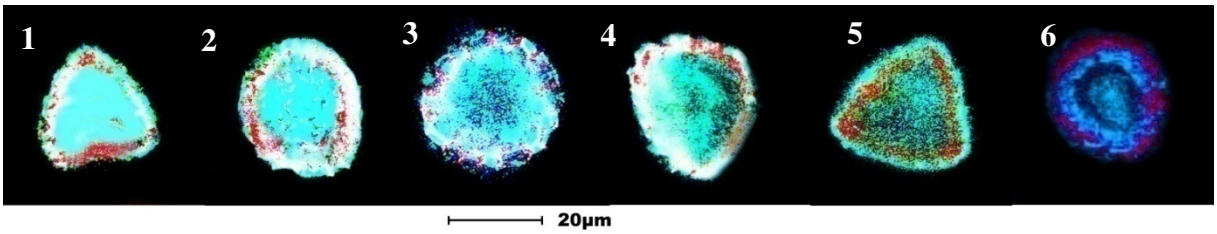

Figure 28 – Encapsulation of some proteins – LSCM pictures: α-amylase (1), β-lactase (2), growth hormone (1,097Da) (3), growth hormone (3,340Da) (4), enfuvirtide (5), alkaline phosphatase (6) (all cyan or blue) in S-type AHS from *L. clavatum* (red and/or white)

3.3.2.3 Nano-channels in sporopollenin and protein size

A priori, the size of the proteins that can successfully be encapsulated, given by their Stokes' radius, is limited by the diameter of the nano-channels that traverse the exine shell. As discussed in Section A-3.5, the size of the nanotubes is still controversial but could range from 25nm to 70nm. An exclusion phenomenon was thus expected.

The size of a protein (its Stokes' radius) is correlated to its molecular weight. For example, a formula is commonly used[235,236] to link the Stokes' radius R_S of a globular protein of density v to its molecular mass M and its sedimentation coefficient S in a solvent of viscosity η and of density ρ; this is given by the following equation (N_A being Avogadro's number):

$$R_S = \frac{M \times (1 - v \times \rho)}{6\pi \times \eta \times S \times N_A}$$

Encapsulated protein	Molecular mass (kDa)
artificial growth hormone (from Ipsen)	1.097
Bacitracin	1.423
artificial growth hormone (from Ipsen)	3.340
enfuvirtide (*Fuzeon*®)	5.065
insulin	6
somatropin (*Humatrope*®)	22.125
ovalbumin	45
α-amylase	54
integrin beta-1 antibody	150
β-D-galactosidase (β-lactase)	464

Table 36 – Molecular weights of the different protein encapsulated in exines

The size exclusion is therefore equivalent to a mass exclusion and there theoretically exist a maximum size of macromolecules that can be encapsulated. Exclusion phenomenon was thus assessed by trying to load bigger and bigger proteins.

Consequently, a wide range of protein molecular weights was studied. Table 36 summarises the scope of protein size investigated, from ca. 1kDa up to 464kDa.

According to the literature,[237] β-D-galactosidase, the biggest protein encapsulated in the present study, is a tetramer with a hydrodynamic radius of 8nm. Even with the smallest hypothesis of 25nm-sized nano-channels, it is therefore not surprising that such a protein easily entered exines.

3.3.2.4 Choosing loading levels and efficiency

Maximal loading was limited by the protein solubility. Indeed, solution volume itself being restricted to around $3cm^3.g^{-1}$ (see Table 35), the highest loading could only be obtained by increasing the concentration to its maximum, *i.e.* by using a saturated solution.

This led to search for a better solvent than water, in order to increase the solubility, endorsed by the lack of affinity AHS and BHS had for aqueous media and by an easier evaporation of volatile solvents as opposed to water during the drying process. Pure ethanol seemed an obvious choice, since it is easier to evaportate, compatible with food and drugs (in term of toxicity) and has good surfactant properties. In actual applications though, ethanol should be used with care since it could cause some proteins to be denatured. However, this study aimed only at demonstrated that encapsulation of protein was possible. Therefore it was not verified that the encapsulated macromolecules were in their natural state and, most proteins were commonly dissolved in a mixture 4/1 water/ethanol (v/v). Solvent was removed by evaporation under vacuum and further freeze-drying.

Another technique was developed to increase the loading level of artificial growth hormones and of enfuvirtide. Use of DMSO as a solvent was expected to increase the solubility of the proteins and thus their final loading. Following the protocol described in Section C-4.1.3.1, each protein was dissolved in DMSO to a much higher concentration than in water, in ethanol or in WE41 and encapsulated by vacuum method. Once the solution was inside the sporopollenin microcapsules, the protein was precipitated out by addition of a very large excess of diethyl ether, in which they are not soluble. DMSO was removed by further ethereal washings and ether was finally evaporated under vacuum. However, ether could have formed a gum in association with DMSO and stayed trapped in sporopollenin spongy structure. This possibility was not verified though.

Ideally, solubility of the protein to encapsulate should have been studied, but a precise value would involve large quantities and prove costly. Therefore, an approximate maximum concentration was obtained when each protein was encapsulated. The ratio of sporopollenin and protein was decided to match the loading level targeted in the final sample. According to the protocol detailed in 4.1.3, the solid was first dissolved in a suitable solvent. The quantity of liquid was kept minimal to improve the encapsulation performance and the concentration value was measured. These values are summarised in Table 38 and Table 74.

The amount of material to be loaded was based on the usual dosage of drugs under investigation. In the perspective of a potential oral delivery application, 0.5 to 1.0g sporopollenin doses were planned. Therefore, exines (0.5-1.0g) were loaded with normal doses of formulated medicine when available (*Humatrope*® and *Fuzeon*®), or to posology levels of pure drugs (synthetic growth hormones). The medical doses currently used are given in Table 37.

Protein (formulation)	**Protein structure & details**	**Therapeutic dose (mg)**	**Nitrogen content (atoms/molecule)**
somatropin (*Humatrope*®)	human growth hormone 191 residues 22,125Da	1-10mg	257
"light" GH	artificial growth hormone 1,097Da	50-300mg	n/d
"heavy" GH	artificial growth hormone 3,340Da	10-50mg	n/d
enfuvirtide (*Fuzeon*®)	anti-HIV drug 36 residues $C_{202}H_{298}N_{50}O_{64}$ 5,065Da	90-100mg	50

n/d: not determined

Table 37 – Current medical dosage of various protein drugs used for injections

Complete dissolution was assessed by visual observation. With the concentration obtained, a maximum theoretical loading was deduced, considering that $3cm^3$ of solution were loaded before removal of the solvent, and with the hypothesis that all of the solute was left inside (see Table 38). Weight difference, measured with very accurate balances on very dry samples, was a first method to evaluate loadings after encapsulation of saturated solutions and drying. Another possibility was to determine the values by combustion elemental analysis, given that the protein was the only nitrogenous compound in the final mixture. This was, of course, not possible for

unknown compounds, like the two synthetic growth hormones in this case. However, those results were not as reliable, probably because of a lack of sample homogeneity.

Protein	Solvent used	Concentration ($g.L^{-1}$)	Theoretical maximum loading level ($mg.g^{-1}$)	Determined loading level ($mg.g^{-1}$) & efficiency of loading (%)
α-amylase (54kDa)	water	41	123	362† (294)
β-lactase (464kDa)	water	52	156	210† (135)
somatropin (22,125Da)	WE41	13	390	7.8† (2)
				3.1* (1)
GH (1,097Da)	water	14	42	40† (95)
	WE41	29	87	60† (69)
	DMSO	82	246	n/d
GH (3,340Da)	water	19	57	8† (14)
	WE41	102	306	8† (3)
				40† (13)
	DMSO	130	390	n/d
enfuvirtide (5,065Da)	water	54	162	269* (166)
	WE41	90	270	339* (126)
	WE41	130	390	421† (108)
	DMSO	94	282	720† (255)

WE41: 4/1 water/ethanol (v/v); n/d: not determined; † determined by weight difference; * determined by combustion elemental analysis (%N)

Table 38 – Loadings of various proteins in S-type AHS – Results obtained after encapsulation by vacuum filling

Moreover, a problem of encapsulation was raised by LSCM observations. Indeed relatively large excesses of proteins, especially artificial growth hormones, were sometimes found precipitated outside exine capsules. Therefore, evaluation of the loading could not be considered so accurate. In some cases, excess hormone was then re-dissolved and re-encapsulated under vacuum; this showed some improvement by LSCM as well as by visual obervation. This was much visible for the "light" growth hormone, since the targeted loadings of 60-300$mg.g^{-1}$ were probably excessive; this led to the use of too much solvent and the hormone precipitated outside during freeze-drying. Enfuvirtide was also deposited outside the capsules as view by the white powder on the surface, hence the actual loading being found above the expected limit (see Table 38). The high value measured after encapsulation with DMSO was probably also due to residual ether left forming a gum with the anti-viral protein.

Encapsulation of the various proteins in Table 38 (and potentially others) demonstated they can be loaded at levels that could lead to their practical use in the clinic. Indeed, proteins (and other macromolecular drugs) cannot withstand gastric or intestinal conditions as they get digested. Ergo they are only available for parenteral administration. Encapsulation in exines could be a first step towards their oral delivery since sporopollenin microcapsules are stable to gastric fluid and readily enter the blood stream thus acting as a protective vector. However, it has been shown in Section B-3.2.1 that aqueous media passively fill the exines. Therefore gastric juices are expected to enter sporopollenin microcapsules as other acidic aqueous media would. Therefore, encapsulated drugs which release in stomach or are decomposed by the entry of gastric fluid into the exines cannot be delivered orally without prior extra protection within the vector. Two similar strategies are currently under investigation.[124] The first method, *co-encapsulation*, consists in encapsulating the targeted drug within a lipidic vesicle (such as a liposome) before loading in exine. *Coating* uses the opposite approach: exines are first filled with the drug and then covered with a protective substance (wax, fat, starch…).

Drugs such as growth hormones, insulin and somatropin are only administered to date by injection; hence there could be significant advantages to be gained if such medications could be taken orally (much easier to take, less painful, etc.) (see Section A-6.1.1.1). By encapsulation of ethanolic-aqueous solutions of the proteins, most of the therapeutic dosages could be reached using amounts of sporopollenin (2g or less) that were considered reasonable to form one swallowable pill. In extreme cases, DMSO could even be used to further increase the dose, especially for drugs that are really none water-soluble – this would illustrate a case of risk benefit balance.

3.3.2.5 Encapsulation and release of alkaline phosphatase

Alkaline phosphatase (ALP) is a hydrolase enzyme (EC 3.1.3.1) produced by human beings in the liver, the bones and the placenta and sourced for scientific purposes in *E. coli* or porcine stomach mucosa.[6] It catalyses the removal of phosphate groups in the 5- and 3-positions of nucleotides, as well as in various other types of molecules such as proteins or alkaloids. It works under slightly alkaline conditions (as opposed to acid phosphatase). The formula weight of laboratory ALP was 57kDa.

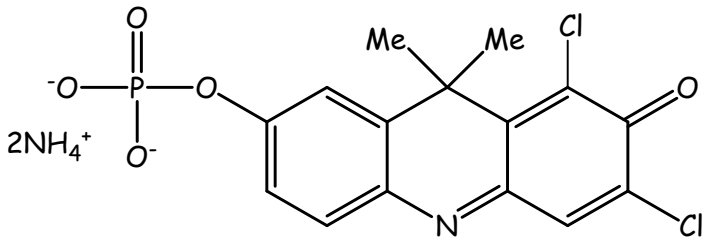

Figure 29 – Formula of DDAO-phosphate

The activity of ALP was assayed by a standard procedure[238] before and after it had been encapsulated in S-type *L. clavatum* AHS. Loading of the enzyme was performed by centrifugation, as described in Section C-4.3.2. By high-speed spinning, exine capsules were subjected to an acceleration gradient: air being lighter, it was expelled from inside and replaced by the liquid. Encapsulation efficiency was controlled by LSCM (see Figure 28). The activity of ALP once released would show, by comparison with initial ALP activity, that encapsulation does not denature the enzyme.

Experiment	Temperature (°C)	Absorption per min ($\times 10^{-2}$ min^{-1})	Activity (mU)
baseline	22	0.00	0.00
free enzyme		1.25	0.48
leached enzyme (1st flush)		0.73	0.28
leached enzyme (2st flush)		0.16	0.06
baseline	37	0.00	0.00
free enzyme		1.67	0.64
leached enzyme (1st flush)		1.30	0.50
leached enzyme (2st flush)		0.20	0.08
leached enzyme (3rd flush)		0.14	0.05
leached enzyme (4th flush)		0.00	0.00

Table 39 – ALP activity before and after encapsulation

ALP activity was measured regarding its catalysis of the dephosphorylation of 9*H*-(1,3-dichloro-9,9-dimethylacridin-2-one-7-yl)phosphate, diammonium salt (DDAO-phosphate) as a substrate in alkaline-buffered conditions (see Figure 29). UV absorbance of the enzyme/DDAO-phosphate mixture was followed in time at 650nm. DDAO, the product of dephosphorylation of DDAO-phosphate, has a molar extinction

coefficient at this wavelength of ε=26,000$dm^3.cm^{-1}.mol^{-1}$. Exact procedure and activity calculations are detailed in Section C-4.3.

The first trials were performed at room temperature. Results are gathered in Table 39. It was first checked that the baseline showed actually no activity, as expected. Activity of free ALP was measured in triplicate at RT: results were repeatable and it was checked that introducing enzyme or substrate first did not influence the result determination. ALP was then encapsulated by centrifugal mean and its activity was evaluated upon release in PBS. It was not completely lost, but a lower value than initial activity was found (0.28mU as opposed to 0.48mU). This could be explained by some denaturation or by incomplete release. A second flush proved some active enzyme was further leached out, showing ALP tended to stick to the exines or in the filter. Nevertheless, the sum of both activities obtained after first and second flushes (0.34mU) did not reach the level of free enzyme. That meant either that some enzyme was denatured (thus inactive) or that some was retained inside the capsule, or both.

Since the temperature was not optimal for the enzyme, a second round of experiments was carried out at body temperature. Experiments were also implemented with further flushes until no activity could be detected, *i.e.* until no enzyme was detached from sporopollenin. Finally, after 3 flushes (the 4^{th} one being nil), the sum of all activities of leached ALP (0.63mU) almost equalled the initial activity of free enzyme (0.64mU).

As a conclusion, ALP visibly stuck to sporopollenin, and this can be expected for any protein. Indeed, side chains of the enzyme residues were exposed to sporopollenin polar groups (carboxylic acids, hydroxyls, etc.) and formed then H bonds or salt bridges. This led to an adherence, sporopollenin playing the role of tertiary structure. That may explain the loss of some activity after only one flush. Weak H bond were easily broken. Moreover, PBS has quite an acidic pH (7.4) compared with the optimal pH of ALP (9-10). That is probably why after several washings, even the stronger ionic linkages did not last. This showed that a protein is not denatured by encapsulation in sporopollenin exine capsules.

3.3.3 Encapsulation of nucleic acids

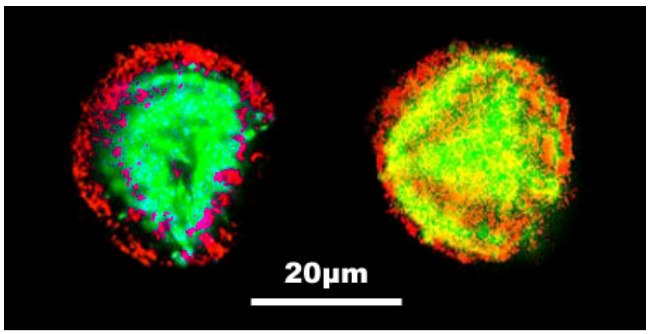

Figure 30 – Encapsulated nucleic acids – LSCM pictures: fluorescein-tagged oligonucleotides (yellow-green) in S-type AHS from *L. clavatum* (red)

Encapsulation of nucleic acid was first attempted in S-type AHS from *L. clavatum* with DNA extract from calf thymus (ethanolic solution) following the vacuum process (see Section C-4.1.3). However loaded material could not be evidenced by LSCM since nucleic acids *per se* do not fluoresce. This issue was overcome by using two fluorescein-tagged synthetic oligonucleotides (a 6,393Da 19-mer and a 4,141Da 12-mer) provided by Prof. T. Brown (University of Southampton). Both of them were clearly detected (see Figure 30) and characterised by the typical fluorescein glow that slowly faded under the confocal lasers. This result was the object of a publication.[193] Also encapsulation of a thymidine derivative, TSAO-T, was obtained using the protocol detailed in Section C-4.1.3 (see Figure 31).

Nucleic acid-based therapeutics, like antisense ribonucleic acid, RNA inhibition, gene therapy, nucleoside analogues, ribosymes and aptamers, has currently a large impact on the market place.[239] Encapsulation of related medicines in exines could, in turn, lead to state-of-the-art oral drugs.

3.3.4 Encapsulation of various other products

Encapsulation of dyes, proteins and nucleic acids was found successful. Consequently, filling of exines (passively, by compression or under vacuum) was extended to a wide variety of products, following the protocols given in Section C-4.1.3. It was achieved with the products listed thereafter and examples of LSCM pictures obtained are displayed in Figure 31:

- carbohydrates and related compounds like gum Arabic, starch (1,000-20,000kDa) and ascorbic acid;

- amino acids: glycine, β-alanine, α-histidine, tyrosine, α-phenylalanine and tryptophan;
- oligopeptides and derivatives: PL30-FITC (a 984Da oligopeptide) and NU:UB 363-FITC (a 1178Da anthraquinone derivative of an oligopeptide);
- other organic compounds: ibuprofen and fish vaccines (of unknown structure).

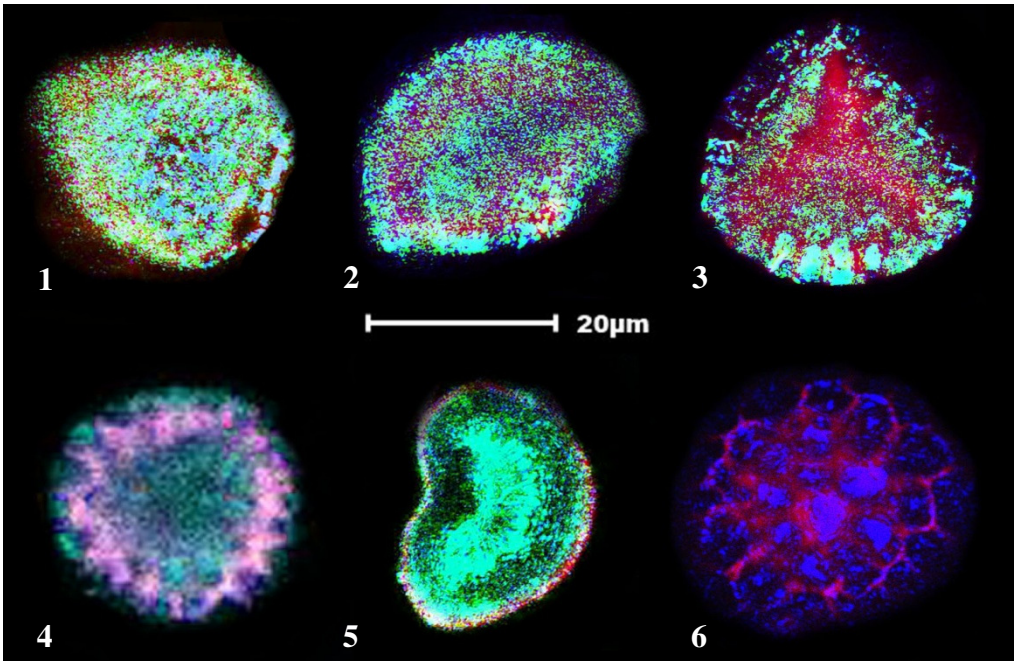

Figure 31 – Encapsulation of various products – LSCM pictures: integrin beta-1 antibody (1); TSAO-T (2); NU:UB363-FITC (3); starch (4); ascorbic acid (5); and tryptophan (6), (all cyan or blue) in S-type AHS from *L. clavatum* (red and/or pink)

In conclusion, the scope of substances that were loaded in exines gathers liquids and solids, as detailed before, being lipophilic and hydrophilic. This was a remarkable result since the lipidic nature of sporopollenin was suggesting it to be a barrier to hydrophilic compounds. This underlines sporopollenin's exceptional properties in terms of polarity.

A first hypothesis to explain such results is that nano-channels that traverse the exine are of two kinds with regard to polarity. This could be rendered by a segregation of the functional groups in sporopollenin polymer. In this case, the non-polar tubules would exhibit carbon chains on their interior while the polar ones would be carpeted with oxygenated functions.

The other possible explanation relies on works related to the ultrastructure of exine. Sporoderm ontogeny is now recognised[240,241] to include a step of deposition of polymerising sporopollenin onto a *glycocalyx*, glycoproteic network coating the spore

cell. In mature spores, this hydrophilic polymer is thus embedded in sporopollenin. Therefore, this could be the source of the dual behaviour of exines concerning polarity and their versatility with regard to encapsulation.

3.3.5 Critical evaluation of the loading methods

As emphasised above, each encapsulation method (see Section C-4.1.1) was implemented to overcome the limits or problems of the precedents. Passive filling worked by capillarity until a thermodynamic balance was reached (see Table 32 and Table 35). Despite the relative elasticity of sporopollenin, compression protocol, developed to improve the previous one, was the most detrimental towards the particles. Vacuum filling seemed optimal, although it required a long application time (ca. 1h) and thus a control of the conditions (e.g. temperature of fragile proteins). Centrifugal loading was only illustrated in the present study with the encapsulation of alkaline phosphatase in small samples (see Sections B-3.3.2.5 and C-4.3.2).

Also, intrinsic characteristics of the product to encapsulate were the other limiting factor. Fragility of the compounds had to be considered as the filling conditions could prove detrimental. For instance, oils and other fats got oxidised when left for too long in aerobic conditions (as further discussed in Section B-4.1.1). Similarly, fragilities of some proteins were given by the commercial retailers. For example, alkaline phosphatase was unstable at room temperature; hence loading of proteins had to be performed ideally at low temperature. Use of a cold room, for instance, enabled to encapsulate fragile enzymes and hormones at -10°C by either vacuum or centrifugal method (see Section C-4.1.3).

Solvent had also to be chosen carefully as certain conditions damaged some proteins. For example, ovalbumin was denatured by ethanol. Solubility was not to be neglected though. As a consequence, a balance between high saturation concentration and compatible solvent had to be reached. High concentration (often saturation) was targeted in order to insert as much solid as possible despite a solvent volume limited by the capsule capacity (around $3cm^3.g^{-1}$).

Waxes and cocoa butter that were loaded in melted state (see Sections B-3.2.1.4 and C-4.1.2) had to be kept hot or warm all along the filling process, ideally. These conditions were not respected during vacuum loading, so the lipids solidified partly

outside the particles before complete entry. Additionally, some quantities of ethanol, found to improve suspension and loading of aqueous solutions, were initially used in conjugation with oils: an emulsion was formed at 40-50°C prior to filling; it was later found to degrade fragile oils and not to improve the loading of non-polar products, hence abandoned (see Section B-3.2.3).

3.4 Conclusion

Various encapsulation techniques have been implemented in order to demonstrate the use sporopollenin exines as microcapsules. Successful encapsulation has been demonstrated on a large range of products being organic, inorganic, macromolecular, polar or lipophilic. Liquids and solutions were most probably loaded through the nano-channels present in exine structure. It has been shown that they were large enough (25nm diameter) to allow entry of big macromolecules. In order to explain the fact that both polar and apolar products could enter the exines, it was hypothesised that the channels could be of two types with regard to polarity, or alternatively they could have an amphiphilic behaviour given by the presence of a glycocalyx embedded within sporopollenin.

This versatility of sporopollenin provides a wide scope of applications. In particular, oral drug delivery seemed especially adapted to macromolecules such as proteins, polysaccharides or oligonucleotides. Importantly, it has been shown that proteins can be released from within exines in their native active form. Thus sporopollenin seems not to impair drug activity during encapsulation.

The large cavity also provides high loading possibilities. This could be especially useful for applications in cosmetics or food industry. Oils, very common products in those two branches, have been encapsulated with success. They should benefit from novel properties of sporopollenin that have been discovered during the present study. These new characteristics, detailed in the next Section B-4, are UV-shielding capacities, antioxidant properties and taste-masking abilities.

4 Newly-discovered properties of sporopollenin microcapsules

As reproductive particles, plant spores and pollen grains ensure the scattering of genetic material in safe conditions for future reproduction. Their fragile DNA strands and other inner content must thus be protected against external aggressions, especially in the case of wind-borne pollens. Therefore pollen wall would be expected to shield UV or to limit its effects, and to prevent aerial oxidation, both potential causes of genetic mutations. This hypothesis, formulated from the observations of Nature, was partly confirmed by the literature[42,138] (see Section A-3.6). The tentative chemical description of sporopollenin as a highly unsaturated carotenoid-like polymer also tended to demonstrate the role of exine as a UV screen.[85,137] Finally, some UV-absorbing compounds, especially *p*-coumaric acid, have been found in sporopollenin.[8,111,242]

The protective effect of sporopollenin might not only be due to its UV-screening properties: it could also be an efficient oxygen barrier, or an antioxidant agent. Indeed, Maack suggested that it had radical scavenging properties.[42,122,123] Independantly, a parallel was drawn between sporopollenin aromatic moieties, especially phenolic components (see Section A-4.2.5), and commercial antioxidants like tocopherol, BHA or BHT; comparison of sporopollenin with polycarotene also reinforced the pattern of clues that it might be antioxidant.

Sporopollenin-encapsulated products would be largely applied to oral ingestion (either of food or pharmaceuticals). Therefore, it was interesting to assess their flavour. As capsules, exines were especially expected to mask the taste of the inner product.

In this section, it will be described how unsaturated oils were used to evaluate the impact of encapsulation in AHS and BHS on their degradation by exposure to light (see Section B-4.2) and to air (see Section B-4.3). In addition Section B-4.5 also shows the taste-masking ability of the capsules using pungent oils.

4.1 Towards the importance of protecting lipids

Specialised oils are of great interest for food industry but they suffer from a distinctive taste and high instability when exposed to air or light.[243] Fats, such as oils, are very sensitive to external aggression, especially aerial oxidation, which is reinforced by light. Unsaturated fats (e.g. ω-3, ω-6 or ω-9 fatty acids) are particularly more sensitive since oxygen reacts more readily on their double bonds. It forms oxygenated functions on olefinic chains, epoxides or peroxides in the first instance, then alcohols, aldehydes, acids and ketones. Additionally, oxygen free radicals are generated by UV-induced photochemical reactions. Those highly reactive compounds damage lipids even more rapidly.

4.1.1 Rancidity

After standing for a while in a non-protected environment (e.g. exposed to UV light and oxygen), fats turn rancid; this can give them a dull colour, a pungent odour and a sour, strongly unpleasant taste (fishy, "painty", cardboard-like or warm-over flavours).[243,244] Oils generally become sticky, viscous and a bright yellowish. Rancid fats are not palatable. This phenomenon is due to reaction of fatty acids, especially unsaturated ones, and other fats with activated oxygen species and radicals.[245] That is why UV light increases decomposition rate. Commonly, peroxidation takes place on carbon chains by auto-oxidation, photo-oxygenation or enzymatic ways and yields hydroperoxides in the first instance, as well as epoxides and peroxide bridges. In absence of protection, further reactions tend to propagate the radicals and other sites are oxidised. Newly created oxygenated functions are unstable and subsequently change to hydroxyls, ethers, carbonyls and carboxyls.

Rancidity is therefore directly linked to the oil oxidation state. Non-oxidised oils are not rancid; that is why commercial oils are purified from oxidised by-products and generally mixed with antioxidants. In industry, the state of oxidation of an oil is assessed by its peroxide value (PV), its anisidine value (AV) and its total oxidation (Totox) value.[231,246-249] The acceptable limits vary from a company to another, and also according to the process steps. For example, pharmaceutical specialised oils (e.g. ω-3 oils) are generally accepted with lower values than cooking oils, and value limits

increase from the extraction to the packing or bottling, since the oil is oxidised when handled with. Generally, an oil is considered clean when: PV < 5-10meq/kg, its AV < 10-20 and Totox < 10-30.[205,250] In this study, all of the fresh oils used were considered to have acceptable PV, AV and Totox value, although some values could have been considered quite high by most of the producing companies (above the limits aforementioned).

4.1.2 Common commercial antioxidants

To prevent or reduce the rate of rancidification, most commercial oils are refined to remove degraded by-products and generally mixed with added anti-oxidants such as gallic acid, selenium, retinol, β-carotene, ascorbic acid, tocopherol, butylated hydroxyanisole or butylated hydroxytoluene (BHT).[205,251-254] Those preservatives however have limitations, for instance, some have been proved harmful and some exhibit unwanted side effects; for instance, BHT is banned from food industry in many countries[223] and tocopherol can act as a prooxidant under certain conditions.

Another way of protecting oils is to coat them with an airtight and/or opaque capsule. Cod liver oil or EPA, for example, are often sold in gelatine macro-capsules for this purpose. Moreover, micro-encapsulation, in sporopollenin exines in particular, could be envisaged as a good barrier to avoid contact between oil and oxygen, as well as a light screen.

As seen previously, sporopollenin has some similarities with polycarotene and contains some phenolic parts. Coincidentally, many common antioxidants (see those quoted above) fall into two categories: carotenoids (e.g. β-carotene and retinol) and phenols (e.g. gallic acid, ascorbic acid, tocopherol, butylated hydroxytoluene, butylated hydroxyanisole and butylated hydroxyquinone). Potential antioxidant properties were therefore hypothesised and this supported the use of exines as protective microcapsules for oils.

4.2 Protection of lipids from UV radiations

4.2.1 Effects of UV irradiation

Ultraviolet radiation has a wide range of effects on living organisms. For example, it belongs to the sight range of some lizards, fish or insects.[255] However, UV

radiation is highly energetic and causes damages to cell materials, like DNA lesions, inhibition of photosynthesis or inhibition of some enzymes.[256,257] Spores are especially vulnerable to UV light since they are mobile and carry away fragile genetic material.

Therefore, organisms have evolved a wide variety of UV-protecting processes, some of which must take place in spores (or simply in sporoderms):[138]

- avoidance, by living in the dark;
- repair of mutated DNA, or *de novo* synthesis of proteins and lipids;
- protection, by quenching reactive oxygen species, or by screening.

Different natural organic compounds offer a good UV-screening protection and/or act as good radical quenchers. They all are highly unsaturated (long chain molecules alternating double and single bonds or aromatic compounds): scytonemin, mycosporine-like amino acids, melanin, terpenoids, flavonoids, carotenoids, etc.[8,138,258] Many of these compounds are found in spores, and especially sporoderms: tryphine[47] contains large quantities of flavonoids and terpenoids and sporopollenin contains mycosporine-like amino acids and was compared to carotenoids.

4.2.2 UV-screening properties of sporopollenin

As emphasised in Section A-3.6, sporopollenin seems to have good UV shielding properties. Several research teams independently showed that it could contain UV-active moieties such as aromatic components.[8,42,111,122,138] Ergo exines were suggested to be suitable for micro-encapsulation of specialised oils, such as ω-3 or ω-6 oils, in order to protect them from UV-light degradation.

4.2.2.1 Preliminary evidence of protection against UV radiation

The suspected UV shielding properties of sporopollenin was evaluated on pure oils of different origins. Sunflower and soybean oils were both commercial food products; according to their packaging, they were poor in unsaturated fatty acids, which are more sensitive to oxidisation, and naturally rich in vitamin E, which is known to be an antioxidant (see Section B-4.1.2). Therefore, they were *a priori* more stable. Cod liver oil was also rich in vitamins A, D and E, which acted as antioxidants (see Section B-4.1.2). However, its richness in ω-3 fatty acids made it more sensitive to rancidity. According to the producers,[205] who provided them directly, plain rapeseed and echium

oils were also rich in unsaturated fatty acids, especially echium oil, which made them more susceptible to rancidification. Additionally, natural presence of vitamins was not emphasised by providers and was considered to be minimalistic in term of protection provided. Being more UV-sensitive, both of them represented materials which could give results over a relatively short period of time and, being unambiguously devoid of any additive, they could provide the opportunity to evaluate the properties of sporopollenin as sole preservative.

Influence of sporopollenin on rancidity was evaluated by use of peroxide value (see method given in Section C-4.2.2.1), the simplest assay routinely used in industry among those given in Section B-4.1.1. PV was measured before and after exposure of the oils to high intensity UV-light (see Section C-4.2.1), to evaluate the extent of oil degradation caused by radiation. A parallel set of experiments was implemented using oils that had been encapsulated in AHS with the methods discussed in Section B-3.2.1.3. PVs of encapsulated oil were determined using the same method that was employed with neat oil (see Section C-4.2.2.1), assuming that, during the agitation in chloroform necessary for the titration, the oil would be washed out of the exines.

PVs of encapsulated oils before and after UV exposure were expected to show less difference on the basis that sporopollenin acted as a UV-protector. The results, gathered in Table 40, show that exines gave some UV protection to encapsulated oils. It was first assumed that the preservation was due to a shielding effect of the exines. Investigation of the screening properties of sporopollenin will be discussed in Section B-4.2.3, which concludes that other protective mechanisms are also at stake, as further detailed in Section B-4.3.

Additionally, a commercial antioxidant, BHT, was used, in industrial concentration (wt. 1%), to determine by comparison the efficiency of sporopollenin microcapsules as a UV protection. It appeared that exines were as protective as BHT, with slight variations depending on which oil was concerned precisely, as shown in the results displayed in Table 40.

Oil	State of protection	Exposure to UV (h)	Peroxide value (meq.kg^{-1})
sunflower (commercial)	A	0	37.6 (8.4)
		2	31.2
		4	56.9 (3.3)
	B	0	39.7 (0.5)
		2	30.8
		4	49.6 (2.8)
	C	2	25.0 (1.9)
	D	0	47.1 (6.6)
		4	50.7 (5.4)
soybean (commercial)	A	0	10.2
		2	20.6
	B	2	10.5
	C	2	11.6
rapeseed (from producer)	A	0	5.2 (0.28)
		0.5	14.7
		1	18.2
		1.5	18.7 (2.1)
		2	33.7 (3.8)
	B	2	16.6
	C	0	7.8
		2	5.2
echium oil	A	0	7.5 (1.2)
		1	140.3 (48.4)
	B	2	57.5
	C	0.5	15.9 (2.7)
		1	13.2 (4.0)
cod liver (commercial)	A	0	5.4
		1	31.2
		2	136.6
	B	2	31.5
	C	2	58.9

Standard deviation is given in brackets where available.
State of protection:
A: neat oil; B: mixture 1/99 BHT/oil (w/w); C: oil encapsulated in S-type AHS [3/1 (w/w)]; D: oil encapsulated in L-type AHS [3/1 (w/w)]

Table 40 – UV irradiation of oils – protection by encapsulation in sporopollenin

4.2.2.2 Development of a method for the evaluation of UV protection of sporopollenin on oils

From preliminary results, sunflower, soybean and rapeseed oils were not found suitable for such an assessment. Their PVs were too high, even when fresh, and did not vary much when exposed to UV light. In contrast, echium and cod liver oils had a very low PV when freshly obtained and decomposed quickly when exposed to UV light; hence from a practical perspective provide excellent candidates for the study. Cod liver oil, being relatively cheap and readily available from a variety of commercial sources with reliable consistency, was thus chosen as the most suitable candidate.

Peroxide value is applicable to all normal fats and oils and its determination was regarded as a suitable method to evaluate fat rancidity given its simplicity and its consistency with a fixed procedure. However, its measure is highly empirical, and the slightest variation in the test procedure (e.g. in temperature or time) may result in variation of results.[246,247]

Therefore, the presence of sporopollenin in the titrated medium was suspected to have a direct influence in the PV titration. This hypothesis was supported by the fact that sporopollenin, being a highly unsaturated polymer, readily absorbs iodine, as already mentioned in Section A-4.1.2.1, hence biasing the PV titration by withdrawing the titrated product from the solution. For that reason, the method was modified by extracting the oil from sporopollenin by chloroform washing and separating the washings by either centrifugation or vacuum filtration. Thus the modified method was used on all subsequent determinations of PV. Therefore, the UV protection of sporopollenin was re-evaluated using cod liver oil and extracting oil from sporopollenin capsules before PV determination, according to the modified procedure detailed in Section C-4.2.2.2.

4.2.2.3 Effects of sporopollenin encapsulation on cod liver oil

The same principle of comparison was adopted as for the preliminary study (Section B-4.2.2.1) but using the modified protocol developed above in Section B-4.2.2.2 and detailed in Section C-4.2.2.2. Before PV titration, all fat samples (with or without exines) were mixed with chloroform and then filtered. First, PV of neat filtered cod liver oil was measured before and after it had been subjected to UV irradiation.

Secondly, cod liver oil was encapsulated in different types of sporopollenin exines (S-type or L-type, AHS or BHS) to a ratio oil/sporopollenin 2/1 (w/w), UV-irradiated and filtered. The PVs of each sample, gathered in Table 41, were compared to those of filtered oil before UV-exposure.

Samples	UV exposure time (h)	PV (meq.kg^{-1})
cod liver oil	0	14.9 (1.8)
	2	131.1 (0.6)
cod liver oil in S-type BHS*	0	9.3 (4.2)
	2	10.7
cod liver oil in S-type AHS*	0	5.4 (0.1)
	2	9.6
cod liver oil in L-type BHS (acidic form)*	0	13.8 (0.6)
	2	47.3
cod liver oil in L-type BHS (basic form)*	0	14.3 (0.4)
	2	10.8
cod liver oil in L-type AHS*	0	9.4 (0.1)
	2	9.4

Standard deviation is given in brackets where available.
* The ratio oil/sporopollenin was 2/1 (w/w)

Table 41 – Assessment of the damage to cod liver oil due to UV light

The PV of pure oil was found ten times higher after exposure to UV light. When cod liver oil was encapsulated in sporopollenin capsules, PV was stabilised. Ergo a UV-screening factor was hypothesised for both S-type and L-type sporopollenin. BHS was found a better protector than AHS. This could be explained by the presence of the cellulose layer entrapping degradation products or by chemical deterioration of the protective functional groups, brought about by the phosphoric acid extraction step in converting BHS to AHS (see Section B-1.1).

Some limited data also showed that higher loadings of oil made sporopollenin less protective. This could be due to residual oil left outside the capsules and thus biasing the measurement. Weakened protection upon increase of the oil loading was recently confirmed.[190]

Oils can resist oxidation for a certain period called oxidation induction time (OIT) during which their PV is stable and almost constant. After the OIT has been reached, oils' rancidity increases very rapidly. A preliminary time study was conducted by measuring PV regularly in parallel on samples of pure and of encapsulated oil. PV of neat oil augmented more rapidly therefore proving that the OIT of exine-loaded oil was

much longer (although not measured). More data regarding OIT values were obtained by using Rancimat apparatus, as explained in Section B-4.3.3.

The results found in the present study and displayed in Table 41 went along the lines of the previous investigations regarding UV absorption properties of sporopollenin (see short review in Section A-3.6). The fact that sporopollenin protected against UV was confirmed but the two following observations showed that UV screening was not the only reason. Interestingly, it was observed (see Table 41) that simple encapsulation of oil in sporopollenin particles reduced its PV from 14.9meq.kg^{-1} down to, for instance, 5.4meq.kg^{-1} when S-type AHS was used. Additionally, the acido-basic state of sporopollenin seemed to influence the protection it offered to oils (see Table 41): acidic L-type BHS was less protective, whereas basic BHS had a cleaning effect on oil, leaving it with a lower PV despite UV irradiation.

These observations could not be explained by simple UV-shielding properties. Therefore, the quantification of the amount of light shielded by a sporopollenin exine was necessary to at least assess if such shielding was a significant factor in protecting an encapsulated oil against UV and visible light. Such quantification was achieved by determining the extinction coefficient of sporopollenins from different plant sources as described in the following Section B-4.2.3.

4.2.3 Determination of sporopollenin absorption coefficient (ε)

The measurement of absorbance versus wavelength and its conversion to extinction coefficient is simple for molecular solutes, but is more complex for the case of micron-sized insoluble objects such as the spore particles used in this work. A key aim of the measurement was to quantify the fraction of light transmitted by a single wall of the exine shell and hence quantify the amount of light screened by a sporopollenin microscapsule to assess its importance in protecting a substance encased in its inner cavity.

At given a wavelength and temperature, the extinction (or absorption) coefficient ε of a solid particle (spore or exine) relates to the absorbance $A_{particle}$ of a single particle and to the sporopollenin thickness x by Beer-Lambert law as such:

$$A_{particle} = \varepsilon \times x$$

In term of transmittance $T_{particle}$ of a single particle, this is rendered by:

$$T_{particle} = 10^{-\varepsilon x}$$

The absorption coefficient of sporopollenin is thus directly related to its screening abilities and enabled to tell whether the polymer was merely a physical shield or whether the shielding was implied by more complicated mechanisms.

4.2.3.1 Mathematical principle and method

Technical details regarding this procedure are given in Section C-3.4.

To evaluate the extinction coefficient of sporopollenin, exines were sandwiched between two quartz plates to form a monolayer. The distance *d* between the quartz plates was determined using a microscope focus method and was found to be slightly smaller than the outer diameter of undistorted AHS shells. Light transmittance T_m of the monolayer within the quartz cell and blank transmittance T_{blank} of the empty quartz plates were determined by UV spectrophotometry in glycerol against air, on wavelength range 190-900nm. Absorbance *A* of the particle monolayer alone was deduced as:

$$A = -\log_{10}\left(\frac{T_m}{T_{blank}}\right) \qquad (1)$$

The sample, consisting of a partial monolayer of exines, contained an area fraction A_f covered with particles of transmittance $T_{particle}$ and absorbance $A_{particle}$, and an empty area fraction (1-A_f) of transmittance T_{blank} and absorption A_{blank}. In this situation, the measured transmittance T_m was given by:

$$T_m = \left(1 - A_f\right) \times T_{blank} + A_f \times T_{particle} \qquad (2)$$

The area fraction A_f of the quartz plates occupied by particles was evaluated by computer on snap shots of LM images of the monolayer.

Considering the distance *d* between the quartz plates (monolayer thickness) gave:

$$A = -\log_{10}\left[\left(1 - A_f\right) \times T_{blank} + A_f \times 10^{-\varepsilon d}\right] \qquad (3)$$

Hence:

$$\varepsilon = -\frac{1}{d}\log_{10}\left(\frac{10^{-A}}{A_f} + \frac{A_f - 1}{A_f} \times T_{blank}\right) \qquad (4)$$

Equation (3) enabled the estimation of *A*, equal to the absorption of a single particle thickness averaged over the area of the particle, and equation (4) the corresponding absorption coefficient ε.

Deriving the true extinction coefficient ε of sporopollenin then required evaluation of the exact distance *x* travelled by light through the actual substance of the

AHS. For particles consisting (in their undistorted state) of spherical shells with inner radius r and with uniform thickness t, the value of x is a function of the equatorial distance a from the centre of the particle according to:

$$\begin{aligned} x &= 2\left(\sqrt{(r+t)^2 - a^2} - \sqrt{r^2 - a^2}\right) && \text{for } 0 < a < r \\ x &= 2\left(\sqrt{(r+t)^2 - a^2}\right) && \text{for } r < a < r + t \\ x &= 0 && \text{for } r + t < a \end{aligned} \qquad (5)$$

The projected area average of x is given by:

$$\overline{x} = \frac{4}{3}\left(\frac{(r+t)^3 - r^3}{(r+t)^3}\right) \qquad (6)$$

Equation (5) has limiting values of $4t/3$ as r tends to zero (*i.e.* solid sphere) and $4t$ in the limit that $t << r$. For the same shell particles squashed flat, the particles would have a circular projected shape of almost uniform thickness equal to $2t$. Thickness and size values were collected in Section B-2.1 for each of the particles used here (*A. trifida* AHS, S-type *L. clavatum* AHS and L-type *Lycopodium* AHS).

Light transmitted through one particle was therefore considered to have crossed twice the thickness x of an exine wall. This translated to the measure absorbance as:

$$A = -\log_{10}\left[\left(1 - A_f\right) \times T_{blank} + A_f \times 10^{-\varepsilon x}\right]$$

Ergo, epsilon was:

$$\varepsilon = -\frac{1}{x}\log_{10}\left(\frac{10^{-A}}{A_f} + \frac{A_f - 1}{A_f} \times T_{blank}\right)$$

4.2.3.2 Results

Three types of particles were investigated, all being AHS, extracted from S-type *Lycopodium clavatum* L. spores, from L-type *Lycopodium* spec. spores and from *Ambrosia trifida* L. pollen. Incidentally, a monolayer was easier to obtain on quartz plates with S-type *L. clavatum* than with other particles. *A. trifida* pollen had to be suspended in ethanol first and the suspension spread over the plates, the monolayer forming by subsequent drying. This deposition technique was used each time a monolayer was not obtained with satisfaction using the dry method.

For each spore type, series of monolayers were prepared covering a range of area fractions. In each case, experimental results of absorption in function of area fraction showed a good agreement with equation (3), with averaged wavelength and a value of A set to 0.881. This confirmed the validity of equation (4) and the consistency of the data set.

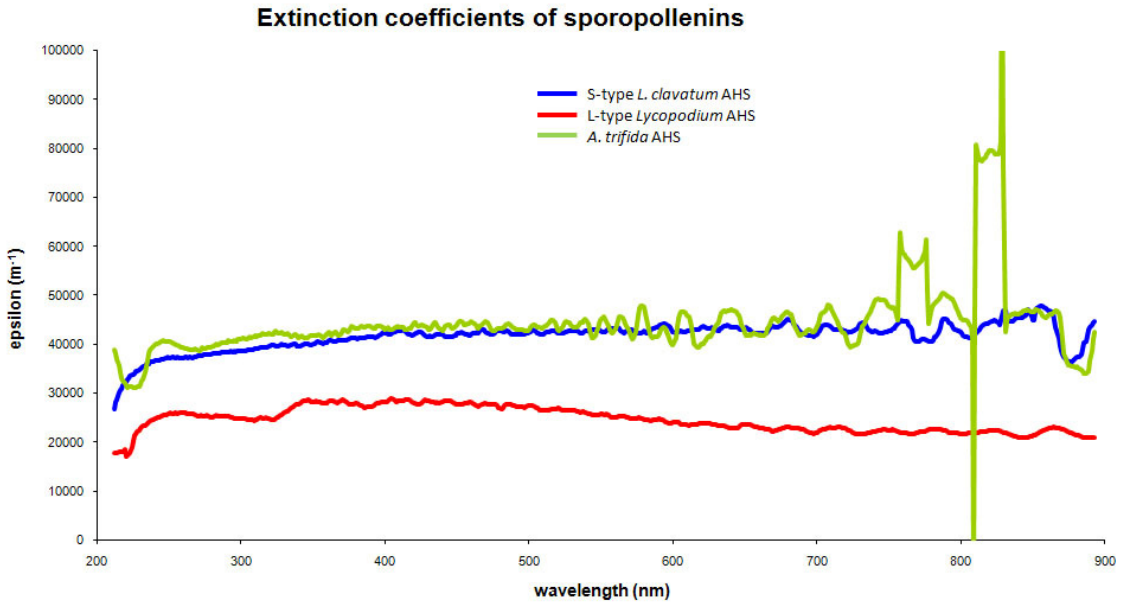

Figure 32 – Absorption coefficients of three sporopollenins in function of wavelength

Absorption A of each type of particle was plotted versus wavelength. The experimental uncertainties of A_m and A_f combined to reach the order of 30% in A. Hence the overall conclusion was that absorbance was almost independent of wavelength and very similar for the three spore types. The only comparable spectra were obtained for suspensions of sporopollenin particles extracted from unicellular algae.[259] Absorbance values were found to depend strongly on the alga type but the wavelength was very similar; the absorbance simply decreased progressively with increasing wavelength from 280nm to 700nm.

	wavelength		
	λ=400	**λ=600**	**λ=800**
S-type *L. clavatum* AHS	40,067	38,565	41,207
L-type *Lycopodium* AHS	30,848	24,687	21,520
A. trifida AHS	36,095	36,095	39,906

Table 42 – Extinction coefficients (ε, m^{-1}) of three sporopollenins at three chosen wavelengths (λ)

A simple estimate of extinction coefficient values was to consider the particles as completely crushed between the quartz plates. Under such a hypothesis, particles were approximated by cylinder of same diameter and height equal to the gap d between the plates. A preliminary estimate was then plotted versus wavelength, for each type of sporopollenin (see Figure 32). Following the results for absorbance, it appeared the extinction coefficients were almost constant all along the UV-visible range, although it

dropped slightly at higher wavelengths for L-type *Lycopodium* AHS and some inconsistencies were recorded for *A. trifida* AHS in red-range of visible light. Example values are given at three selected wavelengths in Table 42. Large *Lycopodium* AHS was found slightly less UV-absorbent.

	***A. trifida* AHS**	**S-type *L. clavatum* AHS**	**L-type *Lycopodium* AHS**
Outer radius (μm)	7.5	12.4	18.8
Wall thickness (μm)	1.6	1.2	1.5
Minimum $\bar{x}$ (μm)	3.2 [2*t*]	2.4 [2*t*]	3.0 [2*t*]
Maximum ε (m^{-1})	2.8×10^5	3.7×10^5	2.9×10^5
Maximum $\bar{x}$ (μm)	5.26 [3.35*t*]	3.29 [2.74*t*]	4.25 [2.78*t*]
Minimum ε (m^{-1})	1.7×10^5	2.1×10^5	2.0×10^5

Note: an absorbance value of A=0.88 (averaged over wavelengths 190-900nm) was used

Table 43 – Estimates of the limiting values of the wavength-averaged extinction coefficients for sporopollenin exine capsules.

Nevertheless, in order to derive the absolute value of ε, the average optical path length $\bar{x}$, corresponding to the measurement of A, which is an average over all the area occupied by particles, had to be estimated. The shell thickness t of exines was considered relatively small compared with the overall radius of the particles, and so $\bar{x}$ was expected to lie between 2t (corresponding to fully squashed particles) and slightly less than 4t (corresponding to undistorted spheres). Maximum $\bar{x}$ was calculated with equation (6). Table 43 lists the estimated values of $\bar{x}$ for the different spore types and the corresponding ε.

Typical value of absorption coefficient was $2\text{-}3\times10^5 m^{-1}$ for the three sporopollenins investigated. A relevant comparison can be made with carbon black particles as used in inks. The spectrum of carbon black particle suspensions is very similar to that of the algal-derived sporopollenins described by Xiong *et al.*,[259] the absorbance progressively and smoothly decreases with wavelength from 190 to 900nm. The extinction coefficient is $1.6\times10^6 m^{-1}$ at 450nm, approximatively 10 times higher than for sporopollenin. It was speculated that the absolute magnitudes of the extinction

coefficients may reflect the relative amounts of large, delocalised aromatic species with sp^2 hybridised carbon atoms and the sp^3 carbon content.

Considering a sporopollenin wall thickness t=1.5µm and an extinction coefficient $\varepsilon=2\times10^5 m^{-1}$, the transmittance a single sporopollenin wall is: T=0.50. This translates by a reduction of 50% in light intensity, whereas the same thickness of the previously cited carbon black would absorb 99.7% of light.[225] UV-screening properties of exines on encapsulated oils are therefore confirmed but not important enough to justify a protection as good as that evidenced in Section B-4.2.2. This underpinned a more important protective phenomenon: it was then hypothesised that sporopollenin had antioxidant properties. More precise studies are detailed in Sections B-4.3 and B-4.4.

4.2.3.3 Proposed improvements to the determination of extinction coefficient

The foregoing study in Section B-4.2.3.2 was further investigated by a co-worker.[225] Microscopic absorbance imaging was used to obtain spatially resolved absorbance "maps" of the particles at a single fixed wavelength of 450nm. This method, originally developed to characterise "Lab-on-a-chip" microchannel devices,[225] erroneously concluded AHS were not empty. This has recently been linked to problems of refraction in the particles.[225] Indeed, in suspensions in water or glycerol, exines were observed as opaque round spots by LM. Therefore, a more appropriate solvent was sought. Histoclear® (principally limonene) is marketed as product to assit microscopy visualisation of such as cells by making them more transluscent. Interestingly, when applied to spores and exines, a similar clearing effect was observed due to its refractive index ($n_{limonene}$=1.47[260]) being relatively close to that of sporopollenin ($n_{sporopollenin}$=1.48[3]).

As a consequence, distance x of light path was underestimated in the work detailed in Section B-4.2.3.2; hence the extinction coefficient values should be lower than the ones found, which would sharpen even more the conclusion that UV absorption is only a minor phenomenon in the protection of encapsulated lipids. In order to obtain a more accurate ε value, new experiments must therefore be implemented with a suitable solvent. An appropriate choice might be toluene as its refractive index is $n_{toluene}$=1.4961 at 632.8 nm at room temperature.[261]

4.3 Protection of lipids from aerial oxidation

The precedent experiments showed that UV-screening was not the major protecting effect of sporopollenin. Indeed, it was noticed that a simple contact of exines with oil sufficed to reduce its PV or at least to increase its shelf life. This property could interestingly be used to refine oils in industrial processes.

4.3.1 Refining oils with sporopollenin

Prior to their packaging, industrial oils are currently treated by different chemical processes involving sodium hydroxide or sodium nitrite as well as specific activated clays, in order to reduce their PV under accepted limits.[205] Sporopollenin's cleansing abilities could offer an interesting alternative to such refining treatments. Indeed, it would be a green and cheap procedure, sporopollenin being a readily available and inexpensive, recyclable, biodegradable and renewable resource. Therefore, its properties towards oil rancidity were evaluated with regard to reduction of PV of degraded oils as opposed to active protection to UV light (as in Section B-4.2).

Following the protocol given in Section C-4.2.3, cod liver oil was mixed with sporopollenin, to different ratios, rapidly stirred and filtered. PV of the oil was measured before and after that contact with exines in order to evaluate the impact of sporopollenin of oil rancidity. This was first performed on a cod liver oil that had been damaged by UV irradiation (see Section C-4.2.1) and had thus a PV of 35.7meq.kg^{-1}. The results are expressed graphically in Appendix C. The batches of sporopollenin used were all extracted from *Lycopodium* ssp. (either S-type or L-type) to give AHS or BHS. Exines used had been treated by a dilute acidic or basic solution prior to experiment so that their acidic functions (carboxyls and phenols mainly, as mentioned in Section A-4.1.2.4) were either protonated by hydrochloric acid (noted AHS-H$^+$ and BHS-H$^+$), or as salts, being potassium salts after potash treatment (noted AHS-K$^+$ and BHS-K$^+$) or as sodium salts after caustic soda treatment (noted AHS-Na$^+$ and BHS-Na$^+$).

According to the data shown in Appendix C, mixture of most batches of sporopollenin with the oil appeared to decrease its PV, with the noticeable exception of protonated L-type BHS. However, the acido-basic state of sporopollenin appeared to have little influence on oil. The differences observed were mostly due to data inconsistency and important errors between similar batches (e.g. sodium salt of L-type AHS reduced PV to 19.5meq.kg^{-1} in one experiment, but increased it to 39.8meq.kg^{-1} in

the other). In the future, repetitions of the study on more batches might confirm the hypothesis that the ionic form of sporopollenin has almost no impact on oil rancidity.

The experiments were reiterated using fresh cod liver oil, which had a PV of 14.3meq.kg^{-1}. Results are provided in a graph displayed in Appendix D. Data showed the cleansing properties of sporopollenin more impressively; indeed, in some cases, simple contact of fresh oil with sporopollenin seemed to reduce the PV, although the oil had not been initially damaged by UV irradiation. PVs were especially reduced when BHS was used, while AHS showed less (or no) refining capacities on fresh oil.

Method reproducibility was also monitored. PVs of cod liver oil were recorded in duplicates after it had been mixed with four different batches of BHS [(w/w) 10%] and subsequently filtered, according to the protocol given in Section C-4.2.3. Results obtained in duplicates on a same batch of sporopollenin were found within the same range, as shown in Appendix E and Table 44. However, a larger inconsistency (although still considered reasonable) was found between two batches of S-type BHS-K^+ (batches 1 and 2), while PVs of oil mixed two batches of L-type BHS-K^+ (batches 3 and 4) were reproducible.

	batch 1	**batch 2**	**batch 3**	**batch 4**
Average PV (meq.kg^{-1})	12.4	9.0	10.0	9.6
Standard deviation (duplicates)	0.3	0.9	0.9	0.1
Standard deviation (same type of BHS)	2.0		0.6	

Table 44 – Reproducibility monitoring in evaluation of sporopollenin's cleaning properties – PVs of oils treated with four different batches of BHS

It appeared that some batches of sporopollenin, when mixed in sufficient amount with oil (fresh or UV-damaged), refined it by lowering its PV. The best results were found to occur with S-type and L-type BHS as sodium or potassium salts, and to be repeatable and quite reproducible. Different refining rates were obtained depending on the quantity of sporopollenin used. Fresh cod liver oil had its PV halved from 18meq/kg to 9meq/kg when mixed with 7-14% sporopollenin (w/w); PV reached 0-1meq/kg when the ratio was over 50% (w/w). Further experiments emphasised that interesting purifying effects were already obtained with less than 10% sporopollenin (w/w), but PV decreased all the more since capsules were used in larger quantity.

In addition, similar results were obtained with rapeseed oil (58meq/kg reduced

to 40-46meq/kg) and echium oil (18meq/kg to 9-15meq/kg) with 10-20% sporopollenin (w/w), backing up the previous findings.

Incidentally, crude ryegrass (*Lolium perenne* L.) pollen also had an efficient cleansing effect, increasing with the proportion used (see Figure 33): from 19meq/kg for fresh cod liver oil, PV was reduced to 17, 12, 7, 8 and 8meq/kg with respectively 5%, 10%, 20%, 50% and 76% sporopollenin (w/w). However, this phenomenon was most probably due to antioxidant components found in the non-extracted sporoplasm. Indeed, antioxidant properties of bee pollen and extracts have been documented.[262,263]

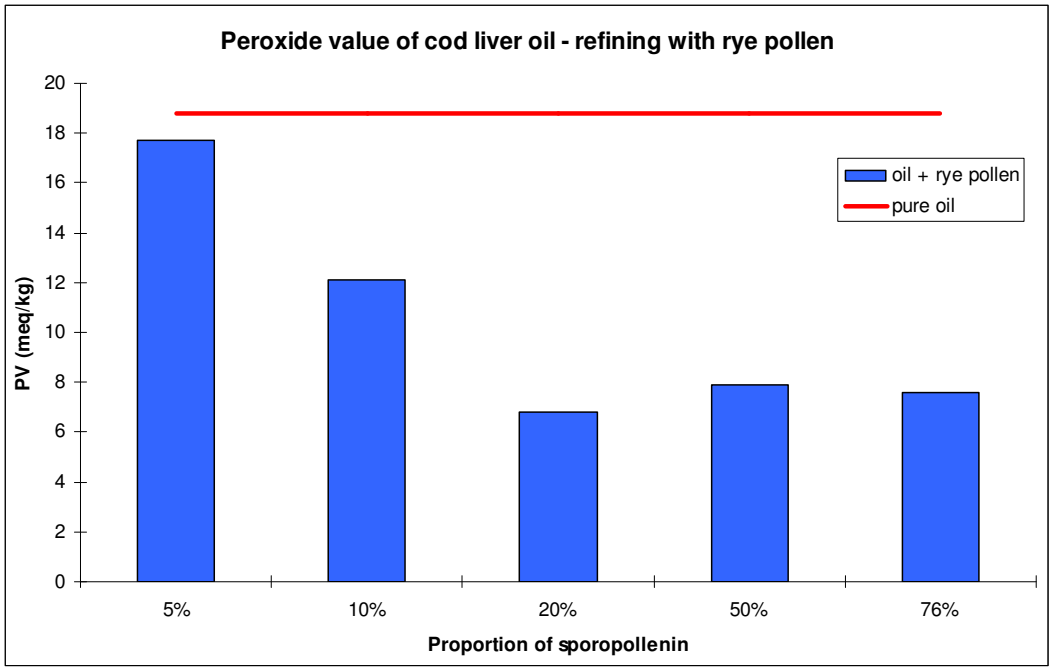

Figure 33 – Assessment of the refining effect of rye pollen on cod liver oil

It must be emphasised that these results involved only a short but intimate contact between sporopollenin and oil (stirring for 1min before filtration). As a consequence, it seems that sporopollenin possesses a refining property, and encapsulated products were protected despite insufficient partial UV-screening capacities. It was then deduced that interesting antioxidant properties could be expected.

4.3.2 Antioxidants and sporopollenin

The ambiguous chemical nature of sporopollenin has at least shown some unequivocal features. The literature reviewed in Section A-4 concluded on the presence of conjugated unsaturated systems, once considered as potential carotenoids[137] and, indeed, probably exhibiting carotenoid-like properties, and the presence of phenolic moieties. Since carotenoids and phenols are two categories of commercial antioxidants

(Section B-4.1.2), evidence put forward for their presence in the structure of sporopollenin is in accordance with it exhibiting antioxidant properties.

4.3.3 Determination of induction times of oils encapsulated in sporopollenin exines

Previous sections deal with the protection of oil encapsulated in exines due to screening of light and antioxidant properties endowed by sporopollenin. However, since plant pollens are dissipated by either insects or wind, it could be readiliy envisaged that sporopollenin exines might offer some protection against air oxidation. It was therefore decided to explore the use of a Rancimat® apparatus which is commercial instrument designed to to automatically detect to presence of volatile products obtained when an oil becomes rancid. The measurements were taken following the protocol described in Section C-4.2.4. The instrument determined the oxidative induction time (OIT) of several types of pure oil, *i.e.* the time after which the oils start producing volatile oxidation by-products. OIT is thus an evaluation of oil shelf life before rancidity. These results (shown in Appendix F and Table 45) were compared with OIT of the same oils that had been encapsulated in sporopollenin, to estimate how efficient a barrier sporopollenin was to oxygen. In addition, comparison with OIT of oils that were simply in contact with exine capsules gave a direct indication of antioxidant activity of sporopollenin.

Rancimat® apparatus is usually designed for liquid or melted fats. Therefore, a modified method had to be implemented to enable a powder sample to replace a liquid such that the air stream could flow freely in contact with as many particles as possible. This was achieved by suspending the oil-filled exines with as much dispersion as possible in glass wool. Air was then passed through the glass wool which was placed in the normal reaction chamber of the Rancimat®. A more detailed protocol is described in Section C-4.2.4. Experiments were performed on the following samples:

- neat echium oil;
- oil mixed with *Aspergillus niger* conidia or with their extracted capsules;
- oil mixed with microcapsules extracted from *Lycopodium* spp. (S- and L-types of BHS and AHS);
- oil encapsulated under vacuum in microcapsules extracted from *Lycopodium* spp. (S- and L-types of BHS and AHS);

- and oil mixed with commercial antioxidants, namely vitamin C or BHT.

Most trials were stopped after 84h. This limit was chosen after preliminary studies with neat echium, sunflower, rapeseed, soybean and cod liver oils which were all found rancid after that period of time. A sample was considered stable to air when OIT was higher than 84h. All OIT values obtained are displayed in Appendix F and Table 45.

Echium oil sample			
additive	**proportions (oil/additive) (w/w)**	**encapsulated?**	**OIT (h)**
none	n/a	n/a	35 (9)
vitamin C	5/0.1	n/a	>84
BHT	5/0.1	n/a	>84
S-type AHS	0.5/1	encapsulated	>84
S-type AHS	2/1	encapsulated	>84
S-type AHS	5/1	mixed	>84
S-type AHS	5/0.3	mixed	69 (2)
S-type AHS	5/0.1	mixed	38 (0)
L-type AHS	0.5/1	encapsulated	>84
L-type AHS	5/0.1	mixed	50 (1)
extracted *A. niger*	0.5/1	encapsulated	12 (1)
extracted *A. niger*	0.5/1	encapsulated	92
extracted *A. niger*	0.7/1	encapsulated	109
extracted *A. niger*	1/1	encapsulated	97
A. niger conidia	0.5/1	encapsulated	26
A. niger conidia	0.7/1	encapsulated	11
A. niger conidia	1/1	encapsulated	34

Standard deviation is given in brackets where available.

Table 45 – Oxidation inductive times of various echium oil preparations

Free echium oil turned rancid after ca. 35h when unprotected by any additive. On the basis of the observed OIT values only, raw *Aspergillus niger* conidia seemed to accelerate rancidification. On the contrary, extracted *A. niger* conidia extended oil stability. A slight inconsistency was however observed with one sample (shorter OIT), but still unexplained. OIT was prolonged as well when echium oil was simply mixed with *Lycopodium* spp. Also, a larger number of AHS appeared to be beneficial in protecting the mixed oil samples. When the oil was encapsulated in S- and L-types of AHS, the OIT was always over 84h, indicating an improved amount of protection. Based on this study, oil encapsulated in AHS compared favourably with commercial antioxidants, vitamin C and BHT.

Nevertheless, a finer comparison needed to be drawn. For this purpose, detailed Rancimat® results, plotted in Appendices G and H, were used. The Rancimat® machine blows a stream of air through a fat sample and volatile by-products of oxidation (formic acid, acetic acid, formaldehyde...) are then collected from the outcoming draft and dissolved in water. The conductivity of this solution increases proportionally to the concentration of by-products released by the fat and the quantity is directly commensurate to its state of rancidity. The conductivity measurements were then computerised in order to establish OIT values.

Conductivity measurement given in Appendix H showed the superiority of protection offered by vitamin C or BHT over AHS simply mixed to oil in the same proportion as commercial antioxidants would be: conductivity (ergo rancidity of oil) was quickly stabilised by classic preservatives. However, encapsulation turned out to keep conductivity *i.e.* oil rancidity lower (3-7µS.cm^{-1} as opposed to 18µS.cm^{-1} after 84h). As a conclusion sporopollenin can be much more powerful a preservative if used as a capsule, but proved to have potent protective effects even by simple contact. This supports the previous results (see Sections B-4.3.1 and B-4.3.2) showing the antioxidant properties of sporopollenin since this effect is not soly due to the oil being encapsulated.

4.3.4 Oil shelf life and mechanistic explanation

The results described in Section B-4.3.3 showed sporopollenin to act protectively against aerial oxidation and support the hypothesis of sporopollenin being an antioxidant. Therefore, it would seem possible that exines could be used to replace commercial antioxidants and form a natural, renewable, non-toxic and cheap preservative for industrial oils. In the results obtained to date, it would seem that encapsulated oil was the best protected, but even oil exterior to sporopollenin capsules appears to be protected to an extent. Recent results[190] have shown that a small quantity of spore capsules in a bottle of cod liver oil extended its shelf-life, with regard to its PV, which was kept lower than that of free oil for several weeks, thus endorsing the preliminary find in this study that oils simply mixed or in contact with sporopollenin can be protected. Lastly, there is the fascinating possibility that the exine particle might have the property to refine oils.

In attempt to explain these phenomena, it was decided to search for functional groups in sporopollenin that could act as oxido-reductive agents. Preliminary used PV determinations and the Tollens' test.

4.4 Preliminary investigation of oxido-reductive properties of sporopollenin

4.4.1 Interaction of sporopollenin with PV test

The normally used for method for peroxide value determination (as detailed in Section C-4.2.2.1) was modified in order to evaluate the influence of empty exine alone. The newly implemented protocol is fully described in Section C-4.2.2.3. It involved that same initial steps as the classic method: the sample to be tested (sporopollenin, without an oil) was shaken with potassium iodide in an emulsion of chloroform and acetic acid, the mixture was then set aside in the dark for 5min and finally quenched with an excess of water. The modification consisted in the addition of iodine to the resulting sample after quenching and immediately before titration. The quantity of iodine solution was such that it induced a blank volume $V_0 = 4cm^3$ of titrating solution necessary to reduce it to iodide. As a consequence, if a reducing compound was present in the sample, some original iodine would be reduced to iodide and the final titrating volume would be inferior to blank volume. On the contrary, if an oxidising product was present in the sample, iodide would be oxidised to iodine (like it occurs in a normal PV test, see Section C-4.2.2.1) and an increase in titrating volume would be observed. By difference with the blank volume V_0, the experiment is able to assess the oxido-reductive capacities of an additive, namely a batch of spore capsules in the present study.

S-type spores capsules		L-type spores capsules	
BHS	**AHS**	**BHS**	**AHS**
4.2 (0.2)	5.2 (0.1)	3.1 (0.4)	4.5 (0.4)
4.0 (0.1)	4.4	3.6	
3.7	4.2		

When trial was performed in duplicate, standard deviation is given in brackets.

Table 46 – Volume (cm^3) of titrating solution used on different batches extracted from *Lycopodium* spp.

A series of trials were carried out with S-type and L-type AHS and BHS respectively. As mentioned in Section C-4.2.2.3, the same mass (0.5g) of capsules was introduced in each sample, followed by chloroform, acetic acid, potassium iodide, and finally iodine (after quenching). The experiment was repeated with different batches of

sporopollenin to assess the consistency of each type of sporopollenin and the importance of the extraction process *per se*. The washing of sporopollenin, for example, may be problematic as it determines the quantity of alkaline left in BHS. For instance, sodium hydroxide, possibly present after the washings, is a common cleaning agent for oils to decrease their PV. Titrating volumes are gathered in Table 46.

Titrating volume above $4cm^3$ indicated a production of iodine in the medium, by oxidation of iodide ions. All batches of AHS, both S-type and L-type, were thus found oxidising. On the contrary, a titrating volume below $4cm^3$ was an indication of consumption of iodine from the mixture, which is the case for L-type BHS. A simple explanation would be that sporopollenin in such batches has reductive properties and converted iodine to iodide.

However, it is known that sporopollenin absorbs iodine by simple contact at room temperature, as it does with bromine, as summarised in Section A-4.1.2.1. Therefore previous results must be regarded carefully: in all cases, iodine adds onto unsaturations; and oxido-reductive effects would generate or consume some as well.

In conclusion, presence of sporopollenin in the titrated mixture has a direct influence on PV method, which reinforces the need to remove the exines before undertaking a PV titration. An obvious pattern was outlined: more important oxidising effects were observed on AHS than BHS. However, further experiments are needed to settle a definitive interpretation regarding the disappearance of iodine from the medium. In case of a very important addition to olefinic systems, even a reduction of the titrating volume below $4cm^3$ could mean oxidising properties for sporopollenin as opposed to reductive ones. Measuring iodine actually attached to sporopollenin would resolve any ambiguity.

4.4.2 Redox functions of sporopollenin

As seen previously, sporopollenin exhibited antioxidant properties. Amongst the chemical groups present on sporopollenin, those known to exhibit such properties could be of two types. The presence of carbonyls in sporopollenin raises the hypothesis of a redox system involving aldehydes. The other functions that could participate to oxido-reductive couples are phenols or hydroquinones. The latter explanation was not assessed here, although recent evidence has been obtained which strongly supports a phenol-like involvement.[190]

Aldehyde loading was assessed on different batches of sporopollenin with the

classical Tollens' test[244] (see Section C-5.1.4). Sporopollenin exines (S- and L-types of BHS and AHS) were mixed with Tollens' reagent. Silver metal was reduced by their aldehyde functions (see Figure 34) and then precipitated in sporopollenin's highly cross-linked structure.

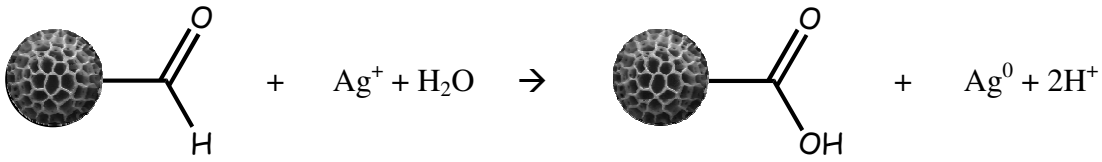

Figure 34 – Chemical reaction during Tollens' test

The silver content was dissolved in aqua regia and evaluated by ICP-OES. Different silver loadings were measured depending on the batch of sporopollenin. Results are gathered in Table 47. Importantly, the finding of metallic silver is indicative of sporopollenin possessing reducing functional groups characteristic of aldehydes but the quantity did not follow the pattern seen in the PV tests in Section B-4.4.1. Tollens' test revealed that L-type BHS and S-type AHS have almost the same level of reducing functions while their influences on PV were opposite (the former decreased the PV titrating volume while the latter increased it). Similarly, S-type BHS, which had little influence on PV, has a very poor loading of aldehydes on the basis of silver precipitated.

Sporopollenin type	Titrating volume in modified PV test* (cm^3)	Silver loading (ppm)	Aldehyde loading ($\mu mol.g^{-1}$)
S-type BHS	4.0	90.98	0.843
S-type one-step BHS	n/d	431.98	4.004
S-type AHS	4.8	821.54	7.616
L-type BHS	3.3	863.75	8.007
L-type AHS	4.5	412.72	3.826

* determined using the protocol given in Section C-4.2.2.3, see also Table 46;
n/d: not determined.

Table 47 – Tollens' test results on sporopollenin

Considering aldehydes as the sole reason for sporopollenin's antioxidant properties, a comparative exercise was carried out to determine the quantity of sporopollenin that would equate to commercial antioxidants used in normal industrial doses. In food-oil producing industries, common preservatives are mixed with oils in small proportions: less than 1% (w/w) and mostly 10-100ppm (see Section B-4.1). Thus, identical molar ratios commercial antioxidant/oil (mol/w) and sporopollenin's

aldehyde/oil (mol/w) could be reached at a certain oil loading level. This loading limit ($g.g^{-1}$) was calculated in function of the type of antioxidant as: $loading_{oil/sp.} = \frac{x_{AO/sp.}}{x_{AO/oil}} \times MW_{AO}$, with $x_{AO/sp.}$ ($mol.g^{-1}$) being the loading of antioxidant (aldehyde) in sporopollenin, $x_{AO/oil}$ ($g.g^{-1}$) the level of antioxidant commonly added to commercial oils, and MW_{AO} ($g.mol^{-1}$) the molar weight of the commercial antioxidant to compare with. Results of such a comparison, with 0.1% as a set antioxidant amount ($x_{AO/oil}$), are gathered in Table 48.

A wide range of oil loadings was found to suit usual levels of antioxidants. Interestingly, up to $4g.g^{-1}$ seemed a reasonable amount. As a consequence, the generally accepted maximal loading (ca. $3g.g^{-1}$) would perfectly match with an efficient antioxidant activity. Moreover, micro-encapsulation in sporopollenin exines was found closely compatible with any secondary protection such as tocopherol or BHT dissolved in oil.

Commercial antioxidants MW ($g.mol^{-1}$)	**BHT** ***220***	**BHA** ***180***	**β-carotene** ***536***	**ascorbic acid** ***176***	**tocopherol** ***431***
S-type BHS	185	152	452	148	363
S-type one-pot BHS	881	721	2,146	705	1,726
S-type AHS	1,676	1,370	4,082	1,340	3,282
L-type BHS	1,762	1,441	4,292	1,409	3,451
L-type AHS	842	689	2,051	673	1,649

Table 48 – Oil loadings in sporopollenin ($mg.g^{-1}$), for aldehyde ratio to equal the usual loading of commercial antioxidants [0.1% (w/w)]

Two conclusions can be drawn from these observations. Firstly, the modified PV test discussed in Section B-4.4.1 and detailed in Section C-4.2.2.3, exhibits some ambiguities and cannot be used quantitatively in a satisfactory manner. Secondly, it is doubtful that aldehydes, as revealed by the Tollens' test, are the only oxido-reductive functional groups involved in the antioxidant properties of sporopollenin.

The Tollens' test was an interesting primary experiment to assess the oxido-reductive properties of sporopollenin. However, colloidal silver might be lost in the process, thus underestimating the reducing potential of the polymer. It can therefore only be indicative of a reductive trend. Further recognised methods should confirm the phenomenon and better quantify the level of reducing functions. For example, it is proposed that established assays with DPPH (2,2-diphenyl-1-picryl-hydrazyl) and

ABTS (2,2′-azinobis(3-ethylbenzothiazoline-6-sulfonic acid) diammonium salt) could be used to determine the radical scavenging activity[264] and therefore view the antioxidant properties of sporopollenin by alternative reaction mechanisms.

The presence of aldehydes in sporopollenin has been confirmed by the Tollens' test. Nevertheless, the search for a reducing functional group in sporopollenin's structure is being pursued and it had recently been found by electrochemical experiments that a phenolic-type function is at least one factor playing a role in sporopollenin's antioxidant properties.[190]

4.5 Taste-masking ability

Most of the specialised oils are obtained from naturally and often pungent flavoured sources such as fish.[265,266] Thus they often present a strong, lasting and unpleasant taste. Since these oils contain a high level of unsaturated fatty acids or esters, such as ω-3 and ω-6 oils, they are beneficial to health and highly recommended by dieteticians. Food industry tends to use them more and more despite their pungent fishy taste.[243,265,267] This requires masking their taste using different techniques. Various flavourings and other products are added to them in order to make them palatable.[265,268-271] Also, a solution is to encapsulate the unpleasant component in a palatable shell. Very often, the capsule has a neutral taste, as it is the case with spray-dried whey protein-starch mixture,[272] or nanoparticles of chitosan.[273]

During evaluation of biological properties, it was noticed by a volunteer that sporopollenin exine capsules had a neutral, not unpleasant taste. Cod liver oil encapsulated in AHS or BHS was also found was found less tasty. Confident in this discovery, a taste study was implemented to test the flavour-masking abilities of sporopollenin capsules (AHS).

4.5.1 Sample preparation

Five different oil-loaded AHS samples were formulated using the vacuum-filling method described in Sections B-3.2.2 and C-4.1.1.3. Four of them contained encapsulated cod liver oil (a pungent oil) with increasing quantity: fish oil/AHS 0.5/1, 1/1, 2/1 and 4/1 (w/w); and the last one was filled with sunflower oil, a far more palatable oil: oil/AHS 2/1 (w/w). In order to evaluate the flavour of sporopollenin itself, a blank was also prepared by simply mixing AHS and water at room temperature to

constitute a paste of similar colour and consistency as the other samples. The samples were labelled at random. The procedure is detailed in Section C-4.2.5.

4.5.2 Flavour test

Twenty volunteers tasted a small aliquot of each sample in a random order. They were told that it could contain water, sunflower oil, cod liver oil, olive oil or cocoa butter, the last two ones being dummy choices. According to their sensation, the volunteers had firstly to determine what product was mixed with sporopollenin. Secondly, they scored the taste strength of each sample on a scale 1, for the mildest or the most palatable, to 5, for the strongest or the most pungent.

4.5.3 Statistical methods

The data for taste strength consisted of counts of observations so this data was analysed by Poisson regression. Overdispersion was examined using methods developed elsewhere.[274,275] The data for oil recognition consisted of binary observations (*i.e.*, taste and strength correctly identified or not). This data followed a Binomial distribution. Overdispersion was investigated using the approach of Williams.[276] Taste strength/oil recognition group was considered as a factor at six levels (blank, fish oil strengths 0.5/1, 1:/1, 2/1, 4/1, and sunflower oil). The blank was taken as the reference group against which all comparisons were made. Results from both approaches are presented as odds ratio (ORs) with 95% confidence intervals (CIs). There were no *a priori* reasons to expect differences for either age or sex, so results were not adjusted for these two variables. A nominal level of 5% statistical significance was assumed (two-tailed). The GLIM4 statistical computer package[277] was used to analyse the data.

4.5.4 Statistical results

The relationship between flavour strength and taste sample is presented in Table 49. There was no evidence of overdispersion in the Poisson regression model[274,275] so this component of variation was not considered further. There was a significant difference between 2/1 and 4/1 fish oil/sporopollenin with volunteers in either sample being significantly more likely to score these two compounds higher when compared to the blank. There was no evidence of dose-response within the fish oil compounds. This data was also analysed under a binomial model (r/n, with r being the actual score given;

n being the maximum achievable score of 5). Samples with 2/1 and 4/1 fish oil/sporopollenin were significantly more likely than the blank to have higher scores (OR=4.2, 95% CI=2.3-6.5; OR=3.3, 95% CI=1.8-5.9 respectively). The odds ratios for the other taste groups were similar to those from the Poisson regression, and in the same order of size.

Taste sample	Total score	Odds ratio	95% CI
blank	36	1.0	
fish oil (0.5/1)	44	1.2	0.8-1.9
fish oil (1/1)	40	1.1	0.7-1.7
fish oil (2/1)	**70**	**1.9**	**1.3-2.9**
fish oil (4/1)	**65**	**1.8**	**1.2-2.7**
sunflower oil	38	1.1	0.7-1.7

Table 49 – Relationship between taste strength and taste sample

Notes:

- Example interpretation: volunteers were 1.8 times as likely to score the 4/1 fish oil/sporopollenin sample high compared to the blank.
- Bold type indicates significantly different from the blank;
- Calculations subject to rounding errors.

The relationship between flavour masking and taste sample is presented in Table 50. There was no evidence of overdispersion in the Binomial regression model[276] so this component of variation was not considered further. There was a significant difference between 1/2 and 1/4 fish oil/sporopollenin and the blank. These two tastes were significantly more likely to be identified correctly compared to the reference sample. There was no evidence of dose-response within the fish oil compounds. Volunteers were one-third less likely to identify sunflower oil when compared to the blank.

Taste sample	*n* (positive)	Odds ratio	95% CI
blank	10	1.0	
fish oil (0.5/1)	8	0.7	0.2-2.3
fish oil (1/1)	7	0.5	0.2-1.9
fish oil (2/1)	**17**	**5.7**	**1.3-25.9**
fish oil (4/1)	**16**	**4.0**	**1.0-16.3**
sunflower oil	4	0.3	0.06-1.0

Table 50 – Relationship between flavour masking and oil recognition

Notes:

- Example interpretation: volunteers were four times as likely to identify correctly the 4/1 fish oil/sporopollenin sample compared to the blank.
- Bold type indicates significantly different from the blank;
- Calculations subject to rounding errors.

4.5.5 Interpretation

At first, it seemed that there was an important placebo effect: 50% of the volunteers could not recognize correctly the blank, which scored 36% as flavour strength. This confirmed that sporopollenin was quite neutral to taste. The most loaded two samples however were found easily to contain fish oil and seem to taste quite intensely (70% and 65%). This could be explained by some residual traces of fish oil on the outside of the sporopollenin capsules, which were immediately detected as such by tasters. On the other hand, it is interesting to find that sporopollenin loaded up to 1/1 (w/w) with fish oil had its results hidden by the placebo effect: fish oil taste was even less facile to discover and almost ranked the same flavour strength (44% and 40%). Finally, sunflower oil was absolutely not detectable, as only 20% of the tasters recognized it, and moreover its score was as low as that of the placebo (38%).

4.5.6 Conclusion

Although most volunteers agreed that sporopollenin is very mild, they were not able to taste fish oil encapsulated in it when its loading was kept under 1/1 (w/w). Nevertheless, they were able to find a fishy flavour in highly loaded sporopollenin, probably because of the presence of oil out of the exine particles. A double encapsulation (e.g. with wax) might be a good correction to hide the residual taste, as well as the addition of a nice flavour (e.g. limonene). In any case, non pungent oil, like sunflower oil, cannot be detected at all.

Sporopollenin seems to keep the flavour of its encapsulated oil quite mild and hardly recognizable. However the encapsulation process is at stake and therefore any outer residues on the surface of sporopollenin exine particles reveal the presence of any pungent material in the mixture.

Sporopollenin is thus believed to retain oil in its inner cavity. As such, taste pads cannot detect or recognize the encapsulated material. The intrinsic flavour of

sporopollenin is found bearable and very mild. This only taste is sensed by the volunteers when no encapsulated material leaks out from the particles, which can make pungent food much more palatable.

All the novel properties discovered in sporopollenin seem to come together to the overall conclusion that application of spore exine particles to food industry would be largely beneficial. Indeed, sporopollenin capsules obtained from natural sustainable sources could be use for two purposes. It could first protect fragile oils from light and, more importantly, from aerial oxidation. Finally, it could formulate pungent fats into palatable preparations. For example, it would perfectly suit preparations of ω-3 oils from fish origin.

5 Chemical derivatisation of sporopollenin exines

Most of the commercially available resins now on the market have synthetic polystyrene beads as their matrices.[278-281] Therefore, they possess many flaws: they lack monodispersity, they are sensitive to heat, mechanical strain and chemical attack, they have to swell in solvents to be efficacious, and they can be rather costly. By contrast, sporopollenin particles can be obtained cheaply (see Table 1, in Section A-1.2.1) and in large quantities;[34,227] as detailed in Section A-3.2, they resist relatively high temperature, very important physical stresses (like high shear stirring or ultra-sonication) and their matrix is inert to most aggressive chemical substances (including strong acids and bases, and most organic solvents).[12,34,46,113] Additionally, sporopollenin is readily available under a granular form and does not need milling or grinding.[7,12] Exine particles (from a single plant origin) display very high monodispersity which facilitates filtration processes and leads to homogeneous reactivity during functionalisation.

It has therefore the potential to be a suitable substitute to artificial resins, provided that it can be successfully derivatised with the same functional groups. Various functionalisation of sporopollenin are presented in this Section, which include attachment of ammonia, amines, halogens, azides and thiol groups. They were all prepared with AHS extracted from S-type *L. clavatum* L. spores (or more rarely L-type *Lycopodium* spec. spores), using successively the different functional groups present in sporopollenin and summarised in Section A-4.3.

FTIR spectroscopy was used, amongst other analytical techniques, to characterise the various derivatised sporopollenins. Therefore, an FTIR spectrum, displayed in Appendix I-1, of underivatised AHS from S-type *L. clavatum* L. was obtained for comparative purpose.

5.1 Phosphorus in sporopollenin structure

Sporopollenin was isolated from *Lycopodium clavatum* L. spores by successive heatings in acetone, potassium hydroxide and phosphoric acid, according to the 'full protocol' described in Section B-1.1. The resulting material was described by the

literature reviewed in Section A-4 as a polymer containing only carbon, hydrogen and oxygen, and to some extent, it is now considered to be nitrogen-free. Yet, several authors[87] acknowledged modifications in the structure of sporopollenin following Erdtman's acetolysis,[85] sulphuric or phosphoric acid treatment.[60] In this study, phosphorus was very likely to be present due to the last treatment although some workers found only little phosphorus in *L. clavatum* spores after the same treatment.[222]

The presence of phosphorus, other than residual mineral phosphate, had already been acknowledged in sporopollenin[282] although no explanation for its occurrence was advanced. It was confirmed in AHS by solid-state ^{31}P NMR. A single but broad signal appeared on the spectrum at a chemical shift $\delta = 4.2$ppm. This indicated a single type of phosphorylated species, most probably phosphate groups. However, the broadness of the peak showed that these phosphates were in various environmental configurations, most likely coupled on hydroxyls and/or on carboxyls (see Figure 35). The band was shifted to $\delta = 5$ppm and decreased in intensity when AHS had been treated overnight with 6% (w/v) sodium hydroxide under reflux. By contrast, no peak was found with BHS.

FTIR study did not contradict the hypothesis of phosphorus being link to sporopollenin structure. Indeed, the peak at 1728cm^{-1} could show an ester or an anhydride group.[283] The formation of phosphoric esters on hydroxyls or phosphoric carboxylic mixed anhydrides was likely and would possibly increase the reactivity with nucleophiles. However a direct proof for P-O bond was difficult to obtain from infrared spectroscopy. P=O stretch vibration gives a signal around 1315-1180cm^{-1}, in the same region where C-O and C-N stretching bands also appear.[284] A slight shoulder peak at 1050cm^{-1} might show the O-H bending of the P-O-H group. This shoulder peak disappeared after further reaction of AHS.

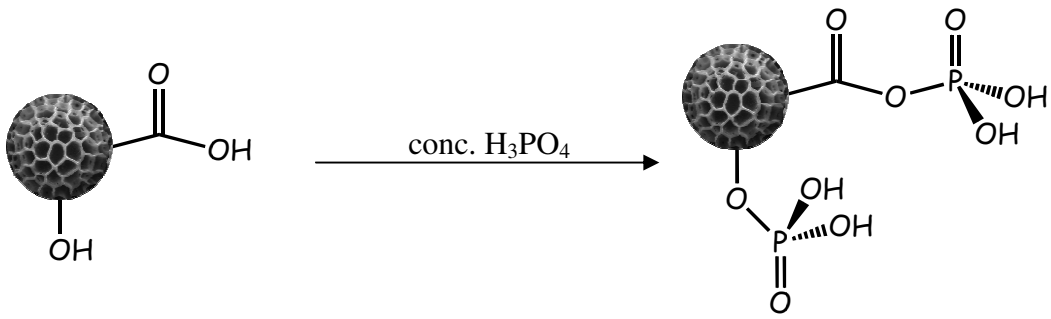

Figure 35 – Phosphorylation of sporopollenin hydroxyls and carboxyls by phosphoric acid treatment

A loading of 1.03 wt. % (0.33mmol.g^{-1}) of phosphorus was determined for a typical batch of S-type AHS by hydrolysing the assumed esters and mixed anhydrides, and measuring the concentration of phosphorus in the filtrate *via* ICP-OES.

Concentrated phosphoric acid is hygroscopic,[261] *i.e.* it is a dehydrating agent.[285] Therefore, in spite of the low level of phosphorus on AHS, phosphoric acid treatment could have had an important activating effect on carboxylic acids. Indeed, mixed phosphoric and carboxylic anhydrides could certainly be formed thus making carboxylic groups easy to dehydrate. A reaction of a mixed anhydride with another carboxylic group would then form an anhydride (see Figure 36): the overall level of phosphorus would not be high, but dehydrated carboxyls would be very reactive.

Figure 36 – Possible dehydration of carboxylic groups of sporopollenin

Reagents expected to interact with sporopollenin carboxyls had their reactivity explained by this hypothesis of activation of AHS. For instance, a simple comparison of reactivity of BHS (without phosphoric acid treatment) and AHS (obtained from BHS by phosphoric acid treatment) highlights the role of the phosphoric acid treatment (see next Section B-5.2).

Moreover, it is reported that phosphoric acid can dehydrate alcohols into alkenes.[285] It can therefore also be expected to dehydrate sporopollenin, thus eliminating some hydroxyl groups to form more double bonds. Consequently, the possible presence of a conjugated olefinic system, as mentioned in Section A-4.1.2.1, might arise from the acidic treatment while native sporopollenin as it is in untreated parent spores could have a more saturated aliphatic sytem. Also AHS was expected to be more unsaturated than sporopollenin material yielded by milder extraction treatments, such as enzymatic processes (see Section A-2.4.2).

5.2 Reaction with ammonia and amines

5.2.1 Purpose

Sporopollenin was used in the past as a support for solid-phase synthesis[286] and as a resin for column chromatography.[284,286] These applications involved derivatising some chemical functions of sporopollenin. Primary amines, for instance, have been shown to attach covalently to exines.[53-55,57] Carboxyl groups, that have been found in the structure of sporopollenin,[287] as shown in Section A-4, were hypothesised as being the anchoring groups. However the exact type of bond was not yet fully characterized. In this study, this type of chemistry was explored with ammonia, in the first instance, and then with different types of amines as well.

The main purpose for developing ammonia or amine-derivatised sporopollenins was to use them as a new type of resins bearing available amino groups. As emphasised in the introduction of Section B-5, commercial resins suffer many drawbacks. In general, they cannot withstand harsh physical or chemical conditions. Most polymeric beads need to swell before being active and lack of monodispersity. Moreover, they can prove quite expensive. On the opposite, sporopollenin exine particles gather resistance, monodispersity and cheapness. Therefore, aminated exines could be applied as supports for solid-phase organic synthesis, as ion-exchange resins, as chromatographic static phases or as scavenging resins. In addition, reaction of sporopollenin particles with ammonia or amines could alter their physical, chemical or biological properties; for instance their polarity, their surfactant characteristics, or their biological absorption.

5.2.2 Reaction with ammonia

Sporopollenin (AHS) (**1**) was stirred in concentrated aqueous ammonia following the procedure detailed in Section C-5.2. After recovery by filtration and thorough washing with water, the resulting ammonia-treated sporopollenin (ATS) (**2**) was dried. Nitrogen was detected by combustion elemental analysis (see Table 79). Results are displayed in Table 51. Final nitrogen levels were of the same order as that found in commercial resins.[278,281]

The different reaction parameters directly influenced the final nitrogen loading in ATS (**2**) as shown in Table 51 and detailed comments and interpretations of the results are given in the following two paragraphs.

Reaction time (h)	Temperature (°C)	Catalyst	Nitrogen loading ($mmol.g^{-1}$)
12	22	None	0.41
24			0.45
72			0.51
96			0.70 (0.09)
12	120	None	0.63 (0.09)
96			0.84 (0.31)
12	120	NH_4Cl	1.37 (0.68)

Standard deviation is given in brackets when available.

Table 51 – Nitrogen loadings on AHS after reaction on concentrated ammonia

The final loading did not seem proportional to the time of reaction. Indeed, stirring the reaction mixture over three days only improved the loading by 10% when compared to one-day reaction. However, after four days, attachment of ammonia was driven to a higher level.

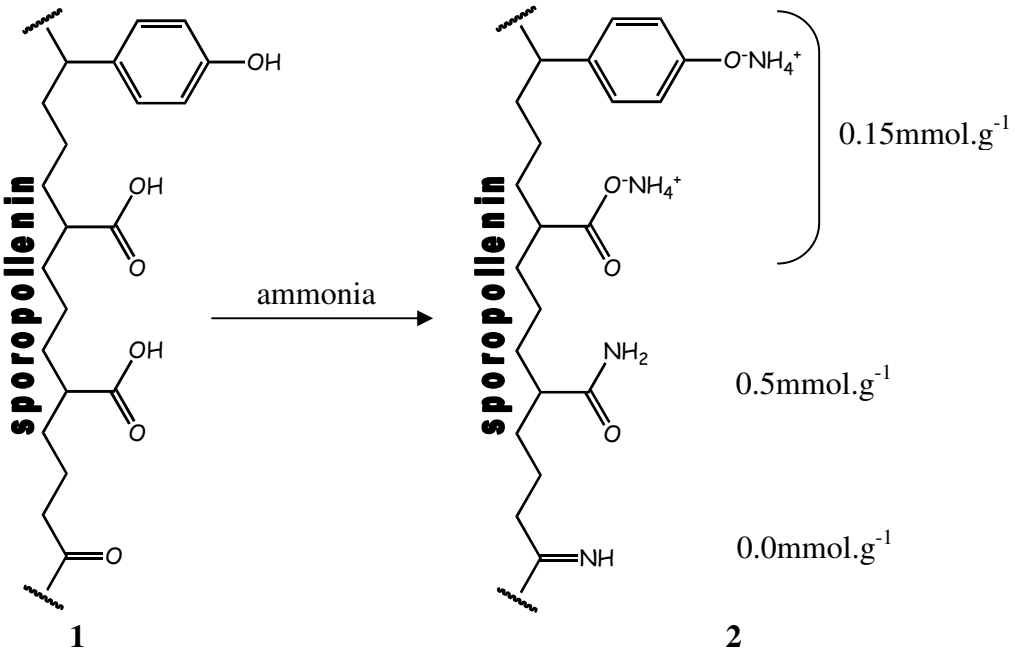

Figure 37 – Reaction of concentrated ammonia with sporopollenin – Hypothesis highlighting the functional groups concerned by potential changes and typical loadings of nitrogenous functions (cf. next Sections)

Adding ammonium chloride as a catalyst showed an interesting increase, although moderate, of the nitrogen loading. Use of this salt also added the possibility to label ATS with ^{15}N by using marked ammonium ions; this was used for solid-state ^{15}N NMR (see Section B-5.2.2.5.2). Even better improvements were obtained by performing the reaction in a thick-walled sealed container and heating the resulting mixture up to

120°C. When AHS was stirred overnight at high temperature in a sealed vessel with a small amount of ammonium chloride in concentrated ammonia, the level of nitrogen reached ca. 1.4mmol.g^{-1}. Those results should be considered with care though, as a part of the actual variation in the values was probably due to differences between the batches of sporopollenin used, knowing that different sources were used and that the 'full' extraction protocol showed some inconsistencies (see Section B-1.1).

5.2.2.1 Resistance to acidic conditions

By stirring ATS (**2**) in dilute hydrochloric acid at room temperature, the level of nitrogen decreased only slightly to ca. 0.5mmol.g^{-1}. This experiment showed nitrogen was attached to sporopollenin by different kinds of linkages. On the one hand, a small part (ca. 0.15mmol.g^{-1}) was cleaved by aqueous acidic treatment. This type of bond was very likely to be as an ammonium salt formed on sporopollenin acidic functions like carboxylic acids and phenols. It could also be an acid-labile covalent bond, like an imine yielded on carbonyls; however since imines are likely to be easily hydrolysed it was thought such functionalities would be unlikely. On the other hand, most of the nitrogen (ca. 0.5mmol.g^{-1}) was linked by some covalent bonds which resisted acidic conditions. Functional groups envisaged here were amides derivated from carboxyls and, less probably, stabilised imines formed on conjugated ketones (more unstable than amides). Hypotheses are summarised in Figure 37.

5.2.2.2 Basicity of ammonia-treated sporopollenin

Moreover, stirring product **2** in dilute hydrochloric acid at room temperature did not form any detectable chloride salt. This was checked by treatment of acidified ATS with dilute sodium hydroxide and detection of chloride ion by addition of silver nitrate (see procedure in Section C-5.1.2).

This indicated that the newly created nitrogenous functions on ATS (**2**) were not strongly basic. It also showed that no Schiff's bases resisted the acidic treatment: reaction with ammonia did not form any imine stabilised by conjugation in sporopollenin. Figure 37 sums up these findings.

5.2.2.3 Reduction

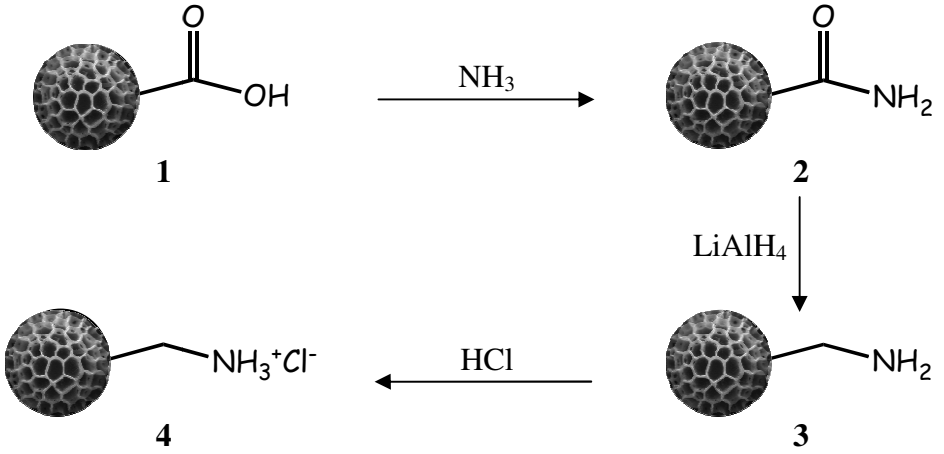

Figure 38 – Hypothesis of amide formation by reaction of ammonia with AHS – Potential functional groups involved in subsequent reduction

In order to better characterise the newly created functions, ATS (**2**) was reduced with lithium aluminium hydride following the procedure detailed in Section C-5.5. Contrary to the starting ATS (**2**), the resulting product **3** formed chloride salts **4** when stirred with hydrochloric acid at room temperature, proving its basic character. Gravimetric assay (chloride: 0.6mmol.g^{-1}) of this salt by precipitation on silver nitrate approximately matched nitrogen loading as measured by combustion elemental analysis (nitrogen: 0.55mmol.g^{-1}). Virtually all of the nitrogenous functions were thus reduced into basic groups. Therefore, it was most probable that they were all of the same nature. Based on the previous argument, only the hypothesis of an original amide on ATS would fit. The resulting reduced functional groups were then expected to be primary amines. The results are illustrated in Figure 38.

5.2.2.4 Dehydration

No ambiguity would be left to identify of the nitrogenous functions of ATS (**2**) as amides if, after dehydration, nitriles groups could be detected in the product **5**. Therefore, several conditions of dehydration were tried. Three experiments were implemented; ATS was reacted with phosphoryl chloride, with phosphorus pentachloride and with ethyldichlorophosphate in presence of 1,8-diaza-bicyclo[5.4.0]undec-7-ene (DBU), following procedures described in Section C-5.6. Expected reaction is illustrated in Figure 39.

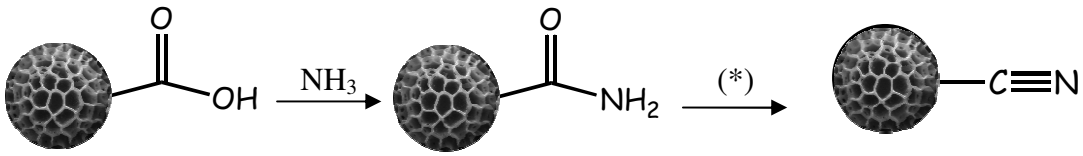

1 **2**

(*) $POCl_3$ **5a**
or PCl_5 **5b**
or $EtOPOCl_2$ +DBU **5c**

Figure 39 – Hypothesis of amide formation by reaction of ammonia with AHS – Potential functional groups involved in subsequent dehydration

Following any of those methods, no nitrile group could be detected by FTIR in polymer **5**. Indeed, the signal was expected as a weak band at 2200-2250cm^{-1} where atmospheric carbon dioxide masked it.[288-290] In the first two methods, chlorine was found in the final polymer: after hydrolysis of **5a** or **5b** in sodium hydroxide, a precipitate appeared in the filtrate upon addition of silver nitrate (method of detection described in Section C-5.1.3); presence of chloro groups was confirmed by FTIR (weak C-Cl bond signal at ~800cm^{-1}).[288-290] This halogenation was further investigated, as detailed in Section B-5.7.3.1, and explained by probable substitution of hydroxyl groups and activation of carboxylic functions. The last protocol left a large quantity of DBU sticking to ATS, as checked by combustion elemental analysis of **5c**. Further washings with water, ethanol and DCM could not remove it entirely.

Dehydration currently came out inconclusive. However, trials on larger scales with common dehydrating agents could be reiterated and the expected nitrile group could be detected by solid-state ^{13}C NMR, its peak appearing around 120ppm.[290] This signal being potentially masked by alkene and/or aromatic resonances, even better results could be expected by dehydrating ^{15}N-labelled ammonia-treated sporopollenin: expected nitrile in the resulting sporopollenin would give a signal at around 200-230ppm (with *N*-acetyl leucine as a 0ppm reference).[291]

5.2.2.5 Spectroscopic data of ammonia-treated sporopollenin

The previous observations and hypotheses pertaining to the sequential formation of a primary amide followed by a primary amine were backed up by spectroscopic investigations. Initial AHS (**1**), ammonia-treated sporopollenin (**2**) and the reduced product **3** were compared by FTIR spectroscopy (spectra displayed in Appendices I-1, 2 and 3 respectively) and solid-state ^{15}N NMR successively.

5.2.2.5.1 FTIR spectroscopy

Initial AHS (**1**) and ATS (**2**) had similar FTIR spectra (cf. Appendices I-1 and 2). The main difference was in the range 1700-1600cm^{-1}. Peak characteristic of carbonyl stretching shifted from 1705cm^{-1} in sporopollenin **1** to 1643cm^{-1} in **2**; that highlighted the conversion of carboxylic acids (or anhydrides) to amides (amide I band).[288-290] Amide II band, assigned to N-H deformation and C-N stretching, was also visible in the spectrum of **2** at 1602cm^{-1}, although its wavenumber was lower than expected.

On the opposite, the reduction of ATS (**2**) into product **3** strongly modified the FTIR spectrum (cf. Appendices I-2 and 3). The broad peak around 3500-3400cm^{-1} in the spectrum of **2**, assigned to O-H and N-H stretchings,[288-290] was reshaped in spectrum of **3** to three smaller bands: at 3550-3400cm^{-1} and 3450-3320cm^{-1} highlighting respectively asymmetric and symmetric N-H stretching in non-bonded primary amines, and at 3300-3000cm^{-1} showing N-H stretchings hydrogen-bonded primary amines.[288-290] All signals in the range 1700-1600cm^{-1},[288-290] characteristic of carbonyl stretchings weakened drastically, highlighting the consequences of reduction by lithium aluminium hydride. A shift of the peak around 1130 cm^{-1} to 1070 cm^{-1}, accounting for C-N stretching vibration,[288-290] was interpreted as an increase in bond length; that could indicate a conversion of an amide to a primary amine; indeed, amides exhibit 1.5 bonds due to electron delocalisation between oxygen, carbon and nitrogen atoms, ergo their C-N bonds are shorter than that of amines, which are single bonds.

In conclusion, Fourier transform-infrared spectroscopic data distinctly supported the hypothesis that reaction of ammonia with sporopollenin yielded primary amides, which turned to primary amines after reduction of the polymer.

5.2.2.5.2 Solid-state NMR

As aforementioned, introduction of ^{15}N in ammonia-treated sporopollenin was made possible by using a ^{15}N-labelled ammonium chloride as a catalyst. The resulting sporopollenin **2** (batch 9, 10, 11 or 12; see Table 78 and Table 79, pp. 236 & 237) could then be analysed by solid-state ^{15}N NMR. Due to the low loading of isotope, background noise was relatively high but the spectrum (displayed in Appendix J-4) distinctly showed two broad signals. It is of note that the peak at 0ppm is that of unreacted ammonium salts, which have a shift similar to that of the internal reference (*N*-acetyl leucine), whereas the peak at ca. 15ppm accounted for ammonium salts forming in **2**.[291-294] The band at 73ppm was interpreted as a covalent bond resonance.

Imines were not considered since they would not resonate at such a low frequency but would give a peak at 300-400ppm.[292,293,295] The signal could however correspond to an amide or an amine.

Reduction of **2** (batch 11; see Table 78 and Table 79, pp. 236 & 237) to give **3** (batch 5; see Table 96 and Table 97, p. 247) decreased the loading of nitrogen. Therefore the amount of ^{15}N in the reduced product **3** was low. This gave a relatively broad and weak peak in the resulting spectrum of **3** (displayed in Appendix J-4), with significant background noise.

In conclusion, solid-state ^{15}N NMR, whilst not offering strong enough confirmation on its own, was at least supportive of the covalent attachment of the primary amide **2** and its conversion into the primary amine **3**, which formed a salt **4**.

Additionally, solid-state ^{13}C NMR spectra (displayed in Appendices J-1 and 3) of AHS (**1**), ATS (**2**) and reduced ATS (**3**) were compared, once normalised against the peak at 128ppm, interpreted as aromatic and olefinic resonance.[288,296] All three spectra showed very similar contours. Treatment with ammonia did not significantly change the signals. That was expected in the hypothesis of amide bonds forming, as their peak would be approximately at the same shift (173ppm) as that of initial carboxyl groups.[288,296] On the other hand, when ATS (**2**) was reduced to product **3**, the band assigned to C=O in carboxyl derivatives (173ppm)[288,296] decreased, as expected. The peak at 73ppm had its intensity largely augmented. This was interpreted as the formation of C-N bonds,[288,296] linking the newly formed primary amines. The unexpected disappearance of the "methyl" peak at 14ppm has however not been explained.

In conclusion, solid-state ^{13}C NMR also supported the theory of amides forming in sporopollenin by reaction of ammonia with carboxylic groups, and their subsequent reduction to primary amines.

5.2.3 Reaction with amines

As observed with ammonia, amines were found to bind to AHS (**1**). A wide variety of amines has been attached to sporopollenin in the past recent years (aliphatic and aromatic, primary, secondary and tertiary, mono- and diamines)[12,13,154,297] but the exact nature of the bond formed was never determined. The proposed functions formed are the same as those initially advanced to explain the formation of ATS (**2**), *i.e.* amines could form ammonium salts, imines and/or amides with sporopollenin.

In the present work, reaction of sporopollenin with various amines was reiterated in order to characterise the nature of the functional bond formed.

5.2.3.1 Primary, secondary and tertiary amines

Reactions of various amines with AHS (**1**) had their conditions optimised by other workers.[12,13] In this study, aliphatic amines were reacted with sporopollenin **1** in order to compare their reactivity in relation to nucleophilicity and steric hindrance. Therefore amines chosen were 1-*n*-butylamine, 1-*n*-dodecylamine, diethylamine, triethylamine, allylamine and propargylamine. Sporopollenin **1** was stirred for 24h in a solution of amine in toluene under reflux according to the procedure described in Sections C-5.3.1, C-5.3.2 and C-5.3.4.

Resistance of the resulting adducts to acid was then assessed by a series of analyses at room and at elevated temperatures. The products **6** were first analysed by combustion elemental analysis (see Table 80 and Table 87) to determine the loading level L_1 of amine. Each product was then stirred in dilute aqueous hydrochloric acid to remove ammonium ions and the loading L_2, obtained by combustion elemental analysis (see Table 81), evaluated the stability of the nitrogenous functions to acidic conditions.

From the results gathered in Table 52, it appears that the loadings were fairly similar to those obtained by treatment with ammonia, *i.e.* in the same range as commercial resins (see Table 51). In addition, loadings L_1 showed that primary amines were much more reactive towards sporopollenin than secondary amines, presumably due to the higher steric hindrance incurred with secondary amines. As expected tertiary amines gave the lowest attachment since they would result solely in quaternary salt formation.

Attached reagent	Product	Loading L_1* (mmol.g^{-1})	Loading L_2* (mmol.g^{-1})	Nitrogen left†
1-*n*-butylamine	**6a**	0.90	0.54	60%
diethylamine	**6b**	0.52	0.27	52%
triethylamine	**6c**	0.26	0.00	0%
allylamine	**6d**	1.11	0.80	72%
propargylamine	**6e**	1.14	0.91	80%
n-dodecylamine	**6f**	1.15	N/d	N/a
aniline (in toluene)	**7a**	1.41	1.13	80%
aniline (pure)	**7b**	2.02	1.68	83%

* determined by combustion elemental analysis; † quotient of L_2 over L_1

Table 52 – Loadings of different amines reacted with AHS

The subsequent acidic treatment removed at least part of the nitrogen attached to AHS. This proportion was believed to represent the ammonium salts that the amines formed with the acidic functions of sporopollenin, while the nitrogen left corresponded to covalent bondings. The proportion of amines covalently bonded to sporopollenin depended on the type of amine attached. In the products **6a**, **6d** and **6e**, respectively 60% of *n*-butylamine, 72% of allylamine and 80% of propargylamine were linked covalently as opposed to ionically (see Table 52). This ratio dropped to 52% in the attachment of diethylamine, in product **6b**. As expected in the case of a tertiary amine, all of the triethylamine was attached to the sporopollenin **6c** *via* ionic bridges since the nitrogen was readily released by treatment with dilute hydrochloric acid. Also, the loading L_1 would indicate that the level of available acidic groups on sporopollenin able to form such salts was 0.26mmol.g^{-1}.

The expected trend was corroborated and a general law could be proposed: primary amines formed mainly covalent bonds (over two third of the attachment); attachments of secondary amines were equally shared between covalent and ionic linkages; and tertiary amines were only bound by salt bridges.

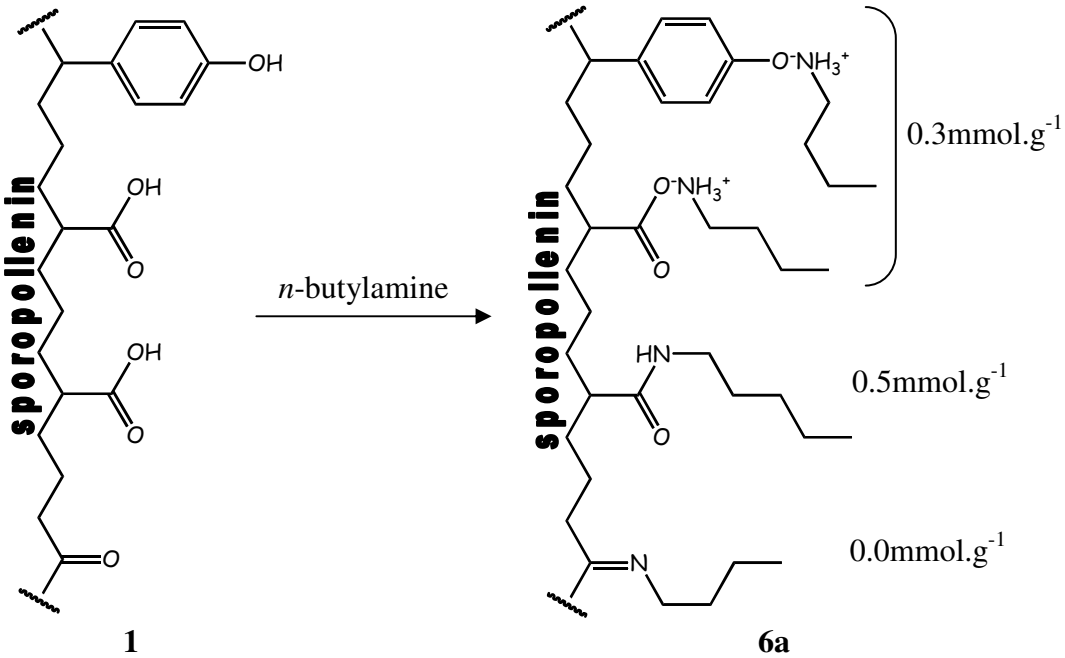

Figure 40 – Reaction of butylamine with sporopollenin – Hypothesis highlighting the functional groups concerned by potential changes and typical loadings of nitrogenous functions

This relates to the fact that triethylamine is commonly used as a base in reactions such as acylations, for instance, because of its poor nucleophilicity. And consequently,

tertiary bases, such as triethylamine or pyridine, can be used as catalysts in reactions of sporopollenin, for instance in the building of the spacer arm in Section B-5.2.4.1.

The treatment with dilute hydrochloric acid was also an attempt to form hydrochloride salts on the newly-formed nitrogenous functions. Gravimetric analysis of chloride attachment, following the method described in Section C-5.1.2, would quantify basic nitrogenous functions available on the sporopollenin. No chloride was detected. Hence these amine-treated sporopollenins failed to form hydrochloride salts. This suggested that a very weakly basic functional group had been formed. Such functions could therefore not be amines or stabilised imines. Since carboxylic groups (or their anhydride and ester derivatives) have been identified in initial AHS (**1**), the anchoring groups attaching those primary (and, to a lesser extent, secondary) amines could be amides, as it had already been hypothesised in ammonia-treated sporopollenin (see Section B-5.2.2). Figure 40 illustrates the hypothetical functional groups involved in reaction of butylamine with AHS to form **6a** and summarises the loading levels estimated from the analyses described here.

It was observed that allylamine and propargylamine linked to sporopollenins **6d** and **6e** with higher levels of both salts and covalent functions. However, those results need to be confirmed by further repetition in order to determine whether the increase is real or simply within experimental error. In case of an actually better loading, it could be explained by steric effects. Indeed, the increasing rigidity of propargylamine over allylamine over butylamine could ease their contact with sporopollenin functional groups within the intricate structure of the polymer. Interestingly, sporopollenin derivatised with covalently bonded unsaturated amines exhibited a new type of anchoring groups on sporopollenin. Double and triple carbon-carbon bonds are particularly suited to further "click-chemistry" with azides for instance.[298] Such derivatised sporopollenin particles could also be used as particulate additives in polymeric matrices to induce potentially novel properties (robustness or lightness for example).

5.2.3.2 Aliphatic and aromatic amines

An extensive study of the attachment of aromatic amines to AHS showed that a higher loading level of aniline (and derivatives) could bind to sporopollenin.[154] The attachment of aniline was reiterated here following the procedure detailed in Section C-5.3.3; sporopollenin **1** was treated either with neat aniline or with aniline in solution

in toluene to form the product **7**. The early findings mentioned above were corroborated by similar results, as displayed in Table 52, and it was also confirmed that a higher loading could be obtained by avoiding dilution and using pure aniline. The purpose of the present study was to offer a valid theory to explain the higher loading of aromatic amines.

Therefore, stability of the product **7** to dilute hydrochloric acid was tested at room temperature. It reduced the initial loading of aniline, as shown in Table 52, which highlighted that anilinium salts (ca. 0.3mmol.g^{-1}) had been formed. Interestingly, the resulting level of aromatic amines was still above that of aliphatic ones after a similar acidic treatment. However, after stirring the adduct **7** in acid at higher temperature (50°C), the loading of nitrogen decreased down to that obtained with aliphatic amines (ca. 0.6mmol.g^{-1}). It showed that two covalent functional groups were present in product **7**. It was ventured that the most stable function (the one resisting hot acid) was of the same type in aniline-treated sporopollenin **7** and butylamine-treated sporopollenin **6**, *i.e.* that they were amides.

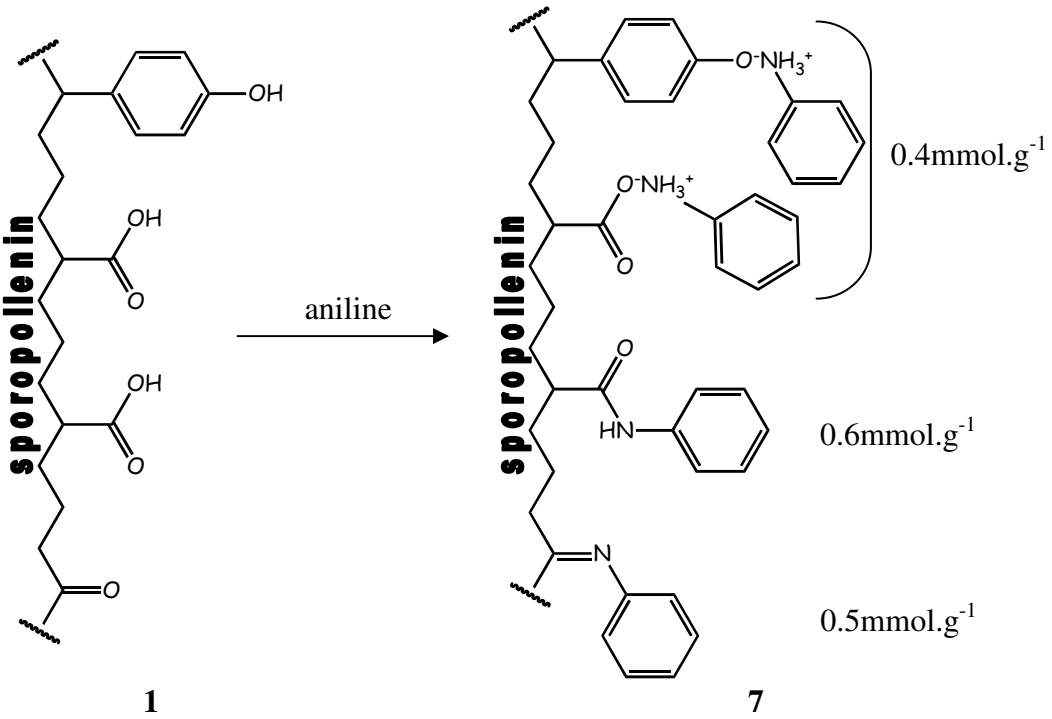

Figure 41 – Reaction of aniline with sporopollenin – Hypothesis highlighting the functional groups concerned by potential changes and typical loadings of nitrogenous functions

This went along the lines of the previous hypothesis developed in Section B-5.2.3.1. Amides (stable at room and mildly elevated temperature) most probably

formed in sporopollenin by treatment with either primary amines or aniline, to a loading level equivalent to that of carboxylic functions in AHS (**1**) (ca. 0.6mmol.g^{-1}). Some aniline was also linked to AHS by imine groups (labile at higher temperature), due to their stabilisation by the conjugated aromatic ring (ca. 0.5mmol.g^{-1}). And also anilinium salts were formed on the overall (ca. 0.3mmol.g^{-1}). Those results are illustrated and summed up in Figure 41.

5.2.3.3 Spectroscopic data of amine treated sporopollenin

The observations and hypotheses made, up to this point in the Section B-5.2.3, were backed up by spectroscopic investigations. FTIR spectra of butylamine- and aniline-treated sporopollenins **6a** and **7a** are displayed in Appendices I-4 and 5 respectively. Solid-state ^{15}N and ^{13}C NMR spectra of dodecylamine- and allylamine-treated sporopollenins **6f** and **6d** are given in Appendices J-5 and 6.

5.2.3.3.1 FTIR spectroscopy

The reaction of *n*-butylamine with AHS (**1**) to form **6a** resulted in an increased intensity for five characteristic peaks. Asymmetric and symmetric stretch vibrations of C-H bonds in aliphatic groups were most probably responsible for the signals at 2926cm^{-1} and 2852cm^{-1}.[288-290] Bands at 1640cm^{-1} and 1600cm^{-1} respectively showed amide I (C=O stretching) and amide II (C-N stretching and O-C-N deformation) vibrations. Finally, the small peak at 1444cm^{-1} could be due to the symmetric deformation of methylene groups or the asymmetric deformation of methyl groups. Those findings supported the hypothesis of an amide bond forming between sporopollenin carboxyls and the primary aliphatic amine.

Several changes also occurred on FTIR spectrum after reaction of sporopollenin **1** with aniline to form **7a**. The peak at 1700cm^{-1}, characteristic of carbonyl stretching in carboxylic acids, decreased while amide I and amide II signals respectively at 1640cm^{-1} and 1600cm^{-1} augmented.[288-290] Superimposition of signals caused by C-C stretch vibrations in the aromatic ring of the attached aniline could also explain the strength of the peak at 1600cm^{-1} as well as that of the peak at 1494cm^{-1}. Two peaks at 746cm^{-1} and 684cm^{-1} were common to both free aniline and derivatised sporopollenin, proving the covalent bonding between aniline and AHS. Such signals were due to C-H out of plane deformation in the monosubstituted aromatic ring. It is of note that the spectrum could

possibly exhibit vibrations due to N-C stretching in imines, but a signal of variable intensity would then be masked in the range 1700-1500cm^{-1} depending on its degree of conjugation.[288-290] Ergo, FTIR spectroscopy could not confirm that reaction of aniline with sporopollenin formed imines in product **7a**, although imines were most certainly present according to the findings shown in the previous Section B-5.2.3.2.

5.2.3.3.2 Solid-state NMR

An amine-treated sporopollenin was subjected to solid-state ^{15}N NMR. Precisely, that was performed on AHS after reaction with ^{15}N-labelled dodecylamine to form the product **6f** (see Table 52). The spectrum (shown in Appendix J-4) had less background noise than that obtained with ATS (**2**) (see Section B-5.2.2.5.2), but the main two peaks were found around the same position (ca. 20ppm and ca. 75ppm). The peak at 20ppm was assigned to an ammonium salt and that at 75pm to a covalent functional group, although NMR alone could not confirm it to be an amide.[291-294]

Spectroscopic profiles of dodecylamine-derivatised and allylamine-derivatised sporopollenins (**6f** and **6d**, respectively) were also obtained by solid-state ^{13}C NMR and compared to that of initial AHS (**1**), after normalisation of the spectra (shown in Appendix J-5) against peak at 128ppm (representing aromatic and conjugated olefinic systems).[288,296] The major changes caused by reaction of dodecylamine were the increase in methyl signal (peak at 14ppm) and that of other aliphatic carbons (peak at 30ppm and shoulder at ca. 20ppm). Reaction of allylamine also increased the signals of aliphatic carbons at 30ppm and 39ppm. By contrast, as expected, it did not change the peak of methyls at 14ppm but a strong band appeared at 105ppm that represented non-conjugated alkenes. After reaction of either of the two amines, band at 73ppm also augmented slightly, showing C-N resonance, superimposed on previous C-O signals.

Solid-state ^{1}H NMR however proved less convincing in demonstrating the nature of the bonding functionality. First, only mobile moieties of sporopollenin showed peaks, and only in wet conditions (in D_2O). Therefore, the spectrum of the initial AHS (**1**) (shown in Appendix J-2) exhibited only three broad peaks, accounting for aliphatic chains: methyl protons at 1.7ppm, protons of other saturated carbons at 1.8ppm, and protons of alkenes or close to hydroxyls at 4.2ppm.[288,296] However, the spectrum of dodecylamine-treated sporopollenin (**6f**) showed only two signals, much sharper and stronger than in AHS (**1**), due to the high mobility of the attached chain. Methyl protons of the newly-bound dodecylamine exhibited a peak at 2.0ppm while the band at 3.8ppm

probably represented the other aliphatic protons of the lipid chain. This proved that the dodecylamine was attached to sporopollenin in the product **6f**.

5.2.4 Further reactions on amino sporopollenin

Resin catalogues display several examples of amino polymers.[278,281] Derivatisation of sporopollenin with an available amino group would offer an alternative to artificial beads. Some examples taken from the literature demonstrate the potential application of such derivatisations of sporopollenin.[284,286] Reaction with ammonia or amines was used to make AHS particles suitable for various applications including solid-supported organic synthesis and ion scavenging. Sporopollenin displaying amines, such as that obtained after reduction of ATS **2** into product **3**, could form an amino derivatised solid support for organic synthesis, of polypeptides for instance.

5.2.4.1 Building a linker arm

In order to use sporopollenin particles as a solid support, implementing a spacer would most certainly prove necessary to avoid poor reactivity due to steric hindrance. For this purpose, diamines could prove useful. Their reactivity with sporopollenin is now well documented[12,154,297] and using a semi-protected diamine can easily build a linker arm avoiding any cross-linking: the free amine is considered to form an amide link with carboxyls displayed by sporopollenin and the protected amine is then left available after suitable decapping treatment.

On the other hand, choosing a short diamine had some advantages: it could be used pure thanks to its liquid state at room temperature or reflux temperature, and cross-linking may be minimised due to the shortness of the chain. In this work, ethylenediamine was therefore reacted with AHS (**1**) following the protocol described in Section C-5.4.1, in order to attach primary amines on the polymer and to yield **8**. Loading of ethylenediamine in product **8**, as measured by combustion elemental analysis (see Table 88), was 1.93mmol.g^{-1} (s.d. 0.15). Therefore the same level of free primary amine was expected to be available in the derivatised sporopollenin **8**. That actual value was assessed by chloride gravimetric analysis (see Table 88), as explained in Section C-5.1.2, and showed to be 1.30mmol.g^{-1} (s.d. 0.17) basic functions in the sporopollenin **8** that formed chloride salts. That level was considered to be the loading of available primary amines displayed by the ethylenediamine bound to sporopollenin.

Thus it was assumed that one of the amino groups of ethylene diamine was attached to the sporopollenin by forming an amide linkage leaving the remaining amine free and able to form a chloride salt. In addition, a sodium analysis, following treatment of the sporopollenin **8** with sodium hydroxide (see Table 88), as detailed in Section C-5.1.1, showed that the quantity of acidic functions in sporopollenin dropped from 1.20mmol.g^{-1} in initial AHS **1** to 0.15mmol.g^{-1} in **8** after attaching the diamine. This result was in agreement with the formation of amides from the carboxyl groups (ca. 1 mmol.g^{-1}) while phenols were left unchanged (ca. 0.2mmol.g^{-1}).

That base was then used to construct a spacer similar to that developed on artificial resins.[299] The eventual purpose was to make the derivatised particles suitable for such as solid-supported synthesis of oligonucleotides. Based on the evidence provided in this study for amide formation by reaction of ethylenediamine with sporopollenin, the whole procedure is illustrated in Figure 42. The first addition to aminated sporopollenin **8** was that of a diacid, by way of reacting succinic anhydride under reflux in anhydrous toluene according to the procedure described in Section C-5.4.2 to yield **9**. The loading of nitrogen did not decrease significantly in **9** (see Table 89) which supported the fact that the ethylenediamine attached was preserved and the amount almost unchanged (1.54mmol.g^{-1}, s.d. 0.04). Chloride gravimetric analysis of that released from **9** (see Table 89) showed that fewer basic functional groups were available (0.50mmol.g^{-1}, s.d. 0.01) *i.e.* that more than 60% of the free amines had reacted to give **9**. A sodium analysis (see method in Section C-5.1.1) confirmed that much more acidic functions were available in sporopollenin **9** (see Table 89), although the level recorded (2.29mmol.g^{-1}) seemed surprisingly high. Considering that 60% of the initial free amines had reacted, their succinylation produced 0.78mmol.g^{-1} of carboxylic acid functions. However, the sodium assay detected all acidic functions, *i.e.* the succinylated amines, the initial phenols and apparently other functional groups. An explanation could be that succinic anhydride reacted with sporopollenin hydroxyls to form ester linkages and thus the resulting particles exhibited more carboxyls. In the past,[12] attachment of acetyl groups up to a level of 1.15mmol.g^{-1} was reached by treatment of sporopollenin hydroxyls with acetic anhydride; on the basis that the same amount of hydroxyls would be successfully succinylated in the present case, and the overall quantity of acidic functions detected by sodium test would be ca. 2.1mmol.g^{-1}, which could explain the actual result.

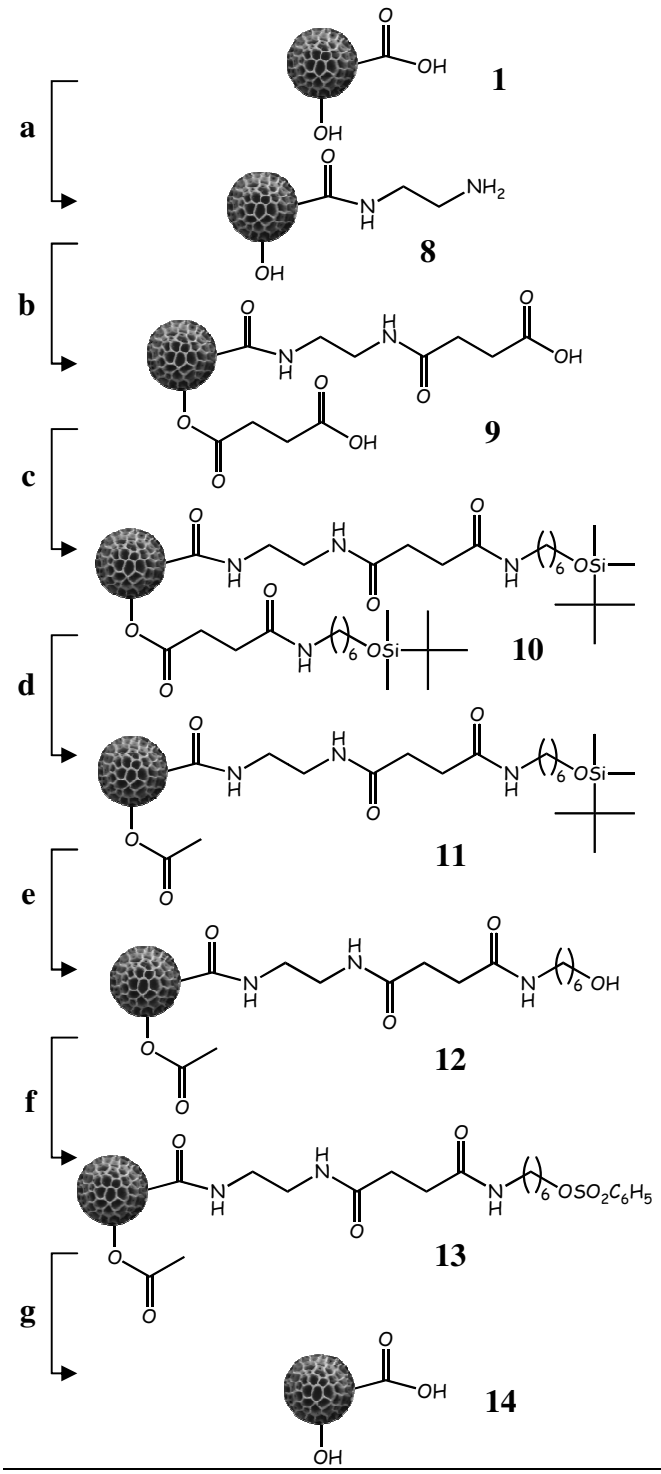

loadings (mmol.g^{-1})			
N*	Na^+ †	Cl^- ‡	Si or S¶
0.00	1.20	0.06	-
3.85 (0.31)	0.00	1.30 (0.17)	-
3.07 (0.07)	2.29	0.54 (0.05)	-
3.20 (0.30)	0.14	0.00	-
3.09 (0.15)	0.00	0.00	-
3.17 (0.17)	0.00	0.00	Si: 1.87
2.99 (0.10)	-	-	-
2.41	-	-	S: 1.05

Standard deviation is given in brackets where available.
* determined by combustion elemental analysis; † determined by sodium test (using sodium hydroxide); ‡ determined by chloride gravimetric analysis after treatment with hydrochloric acid; ¶ determined by ICP-OES

Figure 42 – Construction of a spacer on AHS – Expected reaction and analytical data – See notes on next page regarding reaction conditions

Notes: **a**: ethylenediamine in toluene, reflux, 24h; **b**: succinic anhydride in toluene, under nitrogen, reflux, overnight; **c**: 1-amino-6-(*tert*-butyl[dimethylsilyl]oxy)hexane in toluene, reflux, overnight; **d**: acetyl chloride in DCM, pyridine, room temperature, 2.5h; **e**: tetrabutylammonium fluoride in THF, room temperature, 42h; **f**: phenylsulphonyl chloride in DCM, pyridine, room temperature, 2.5h; **g**: sodium hydroxide, reflux, 2 days.

The last implementation of the spacer consisted of attaching aminohexanol on product **9**. Thus amide bonds were able to form at the end of each carboxyl in order to make the hydroxyl groups available in the final product **12**. However, in order to quantify the loading of hydroxyls displayed by the resulting aminohexanol-derivatised sporopollenin, the free hydroxyl groups of the reagent were initially capped by *tert*-butyl(dimethyl)silylation. This yielded the intermediate **10**. The reaction procedure is detailed in Section C-5.4.3. The amount of silyl attachment was measured by ICP-OES analysis of silicon after deprotection (see data in Figure 42). Sodium analysis of the resulting material **10** (see Table 90) showed that all of the carboxylic acids reacted on protected aminohexanol, leaving only phenols as available acidic groups (0.14mmol.g^{-1}). Amines left free in **9** were no longer detected by chloride gravimetry in **10**, possibly because of the steric hindrance induced by the silylated groups.

As shown on Figure 42, succinylation occurred both on free amines newly attached and on hydroxyl groups already naturally present in sporopollenin. In order to build a uniform linker arm based only on the former (ethylenediamine anchorings), the latter (succinylated hydroxyls) were transesterified by acetylation, following the procedure described in Section C-5.4.4. As expected, this did not change the negative results of sodium and chloride analyses (see Table 91). Ergo sporopollenin **11** had its newly created linker hydroxyls silylated while the ones originally present on AHS were protected by acetyls. It enabled orthogonal deprotection that would then leave hydroxyls only at the end of the spacer. *tert*-Butyl(dimethyl)silyl group was then specifically removed (see Section C-5.4.5) to create the final target resin **12**. No acidic or basic functions were detected in **12** by sodium or chloride analysis. Following the analytical process aforementioned, the released silicon was quantitatively collected and analysed by ICP-OES to determine the loading of hydroxyls now available in the target product **12** was 1.87mmol.g^{-1}.

Study of nitrogen loading in the course of building the spacer was not so

informative owing to the interference of AHS hydroxyls being succinylated in the process and to the introduction of heavier atoms (silicon). Logically, succinylation of **8** to **9** made nitrogen loading slightly decrease because of the addition of non-nitrogenous material to sporopollenin. Formation of **10** introduced nitrogen to sporopollenin but the increase in the actual measurement was minute, probably because the whole sporopollenin **10** had been made heavier by the silicon atoms. Acetylation then removed nitrogenous substituents hence combustion elemental analysis of sporopollenin **11** showed less nitrogen. Since deprotection made product **12** lighter without removing any nitrogenous functions, nitrogen proportion increased. The target resin **12** was considered to exhibit only one nitrogenous substituent; in this case, the arm possessed three nitrogen atoms, thus combustion elemental analysis was another way to determine the amount of spacer created, which was found to be 1.06mmol.g^{-1} (s.d. 0.06). This did not match the amount found by silicon ICP-OES but was in better agreement with the level of ethylenediamine attached and measured to be 1.30mmol.g^{-1} in **8**. To solve any ambiguity, a last analysis was therefore set up.

Sporopollenin **12** was derivatised with a sulphur-containing nucleophile to form **13**, following the protocol detailed in Section C-5.4.6. Alkaline hydrolysis released the substituents which were then analysed by sulphur ICP-OES. The loading of sulphur linked to hydroxyls in **13**, and subsequently removed, was found to be 1.05mmol.g^{-1}. This was in full agreement with nitrogen combustion elemental analyses in products **12** and, to a lesser extant, **8**. The loading of hydroxyls in the interesting resin **12** was finally considered to be ca. 1mmol.g^{-1}. Removal of the newly created linker arm was also attempted following the procedure described in Section C-5.4.7. No sulphur was found by combustion elemental analysis in the hydrolysed sporopollenin **14** which proved that all sulphur had been quantified by ICP-OES. However, some nitrogen was still present in **14** probably because the hydrolysis of the ethylenediamine was not complete.

In conclusion, sporopollenin could successfully be derivatised by a linker arm that finally displayed hydroxyl groups to a level of ca. 1mmol.g^{-1}. Those functions were then available for solid-phase organic synthesis of oligonucleotides, for example. A little improvement could be made by acetylating the initial AHS before any further attachment in order to avoid any secondary reaction.

5.2.4.2 Quaternization of sporopollenin

Sporopollenin particles possessing available amino groups have the possibility to

act as ion-exchange resins.[286] Indeed, in its initial state, after extraction from raw spores, AHS exhibited anionic functions, mainly carboxyls, lactones and phenols (see Section A-4.1.2.4); it constituted therefore a cation-exchange resin. On the other hand, an amino sporopollenin, after treatment with ammonia and reduction, contained cationic groups, namely primary amines (see Section B-5.2.2).

Quaternization of those amines should be envisaged in the future, by using a methylating agent such a methyl iodide, to form ammonium iodide groups. It would yield a positively charged polymer, as opposed to the anionisable initial sporopollenin, and would form an anion-exchange resin. Also, and interestingly, negatively charged alkaline AHS and positively charged quaternized aminosporopollenin would exhibit different surfactant properties worth further investigation, for instance to stabilise or disrupt oil/water emulsions.

5.2.4.3 Other perceived applications of amino-sporopollenin

Attaching diamines on sporopollenin could yield a solid reagent displaying terminal amines. This could be used to mimic existing products for other usages. Two examples are given below and can be interesting potential future developments of the attachment of amines to sporopollenin.

Firstly, an aminosporopollenin could be designed with a structure similar to that of liquid amines. This could be examplified by the attachment of *N*,*N*-diethyl-ethylenediamine through its primary amino group; the resulting product would display tertiary amines and such a product could potentially replace usual triethylamine in its use as a basic catalyst for ester or amide formation. The interest of such a mimic lies in the easiness of purification of heterogeneous catalysts by simple filtration as opposed to solvent extractions and/or chromatography for liquid ones.

Aminosporopollenin could also replace artificial aminated resins in other applications. By attachment of 4-aminopyridine, sporopollenin could then absorb tribromide ions (as pyridinium salts) and become a potent brominating reagent. Being solid, such product would offer safer protocols to brominate aromatic compounds, especially given bromine's toxicity and the complicated health and safety procedures industry has to undergo to use it.

5.2.5 Conclusion on anchor functionality

When sporopollenin is treated by ammonia or primary aliphatic amines, some salts were formed, as their lability in acidic conditions proved. However a large proportion of covalent bonds were also created. This was confirmed by solid-state ^{15}N NMR. Investigation of the basicity of the newly-created covalent functional groups proved they could be neither amines nor imines. By logical deduction, amide formation was hypothesised. Reduction of those covalent nitrogenous groups yielded basic functions, considered to be amines, which were in agreement with the hypothesis. That theory was supported by further FTIR and solid-state NMR studies. In the absence of dehydrating agents, most carboxylic acids react with ammonia or primary aliphatic amines to yield ammonium carboxylates but almost no amide. It is very important to observe that AHS easily yield covalent bonds probably due to a state of initial activation following the phosphoric acid treatment (see Section B-5.1).

Reaction of aniline with sporopollenin was also found to yield salt bridges and covalent bonds. Acidic treatments showed the presence of anilinium salts and two types of covalently-linked functions. They were interpreted as imines forming on carbonyls and amides on carboxylic groups. These multiple anchoring functionalities led to higher loadings of aromatic amines when compared to aliphatic ones.

5.3 Halogenation

5.3.1 Purpose

Halogens are well-known leaving groups in organic chemistry. Such functional groups have been largely used in polymeric resins designed for solid-phase organic synthesis; a typical example being Merrifield resin.[287,300] Most generally based on a polystyrene matrix, commercial resins suffer from poor resistance to chemical and physical aggressions;[12] hence usual applications of halogenated resins would benefit from a more robust support, such as sporopollenin exine particles, as they would be able to withstand stronger mechanical stress, higher temperature and harsher chemical conditions. Merrifield resin for instance could be mimicked with chloromethylated sporopollenin as this was done in 1980.[301]

Therefore, halogens could prove very useful in order to exploit the chemistry of sporopollenin. Halogens are indeed available for further functional interchanges by

nucleophilic substitutions, mainly. Elimination is, in this case, more of a problem than a required reaction. A particular interest in derivativatising sporopollenin with halogens was to use such derivatives as precursors of sporopollenin azides and thiols as detailed in Sections B-5.4 and B-5.5 respectively.

The scope of introduction of halogens in an organic compound is quite broad. Past studies have shown that several types of halogenations could be performed in sporopollenin: bromination,[12,13,54] chloromethylation[12] and chlorination.[12]

5.3.2 Bromination

Early work by Zetzsche *et al.*[54] showed sporopollenin readily absorbs bromine up to wt. 50%. This was confirmed in recent studies.[12,13] Bromination was repeated here by stirring AHS, after full extraction from *Lycopodium* spec. spores, with a solution of dibromine in chloroform at room temperature (see Section C-5.7.1).

	Sporopollenin	**Initial sporopollenin**	**Brominated sporopollenin**	**Bromine loading ($mmol.g^{-1}$)**
Mass (g)	S-type AHS	5.0 (0.0)	6.8 (0.2)	4.5 (0.5)
Elemental analysis*		%C 56.69 %H 8.32 %O 34.99	%C 32.28 %H 2.89 %O 19.84 %Br 44.99	5.64 (0.6)
Gravimetry		-	-	4.23 (0.3)
Mass (g)	L-type AHS	5.0 (0.0)	6.9 (0.3)	4.8 (0.7)
Elemental analysis*		%C 63.16 %H 7.79 %O 29.05	%C 36.28 %H 3.46 %O 16.96 %Br 42.70	5.34
Gravimetry		-	-	5.13

Standard deviation is given in brackets after the results where available.
* %O in initial sporopollenin was deduced by subtraction considering only C, H and O were present; %O in bromosporopollenin was calculated proportionally to %C with regard to initial sporopollenin and %Br deduced by subtraction considering only C, H, O and Br were present.

Table 53 – Loadings of bromine in sporopollenin *15* after bromination

As expected and according to the data in Table 53 and in Table 103, weight difference showed attachment of a heavy product to sporopollenin **15** and elemental analysis showed a large decrease in the weight ratio of carbon. This new attachment was confirmed to be bromine by gravimetric assay (see Section C-5.1.3): it was detached

from sporopollenin by base hydrolysis, the resulting bromide precipitated on silver nitrate and the final precipitate weighed to give the loading of bromine in bromosporopollenin (**15**).

The determinations of the amounts of added bromine by weight difference lacked precision because of potential loss of material (although minor) during reaction transfers and especially filtration steps. Hence, it was considered to give a lower evaluation. Calculations of bromine loading by elemental analysis involved the approximation of oxygen amount by proportionality to initial sporopollenin (see Section C-5.7.1). Ergo it was regarded as a simple indication of bromination level. Finally, gravimetry was thought to be the best assessment of bromine loading, although more replicates should confirm its reliability.

Both L-type and S-type of sporopollenin seemed to give quite similar loadings of bromine (ca. 4-5mmol.g^{-1}, see Table 53). This was in agreement with previous data[12,13] obtained in blind trials, in which good batch repeatability was observed with no distinction of spore type.

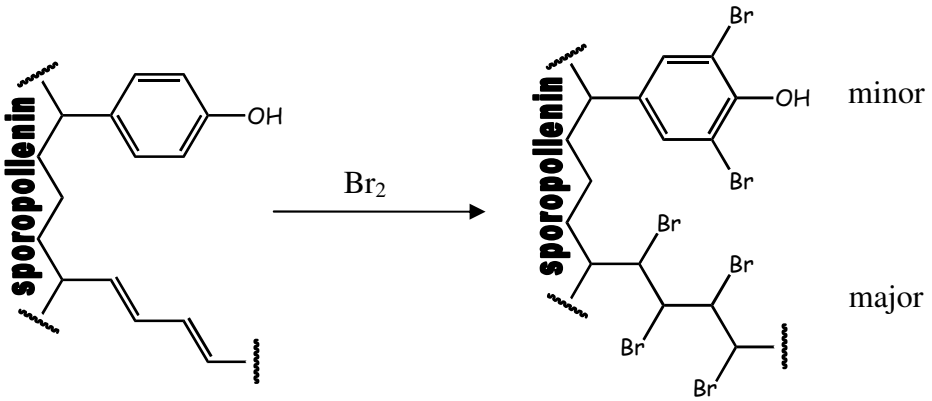

Figure 43 – Bromination of sporopollenin – Hypothesis highlighting the functional groups concerned by potential changes

Comparison of the FTIR spectra of initial AHS (**1**) and bromosporopollenin (**15**) (displayed in Appendix I-6) showed mainly two slight modifications. First, in the zone 1000-1500cm^{-1}, fingerprints were smoothed:

- a small peak at 1490cm^{-1} (interpreted as either the asymmetric deformation of methyl or methylene groups or ring vibrations from the aromatics)[283] disappeared, possibly indicating changes in unsaturation;
- a weak peak at 964cm^{-1} (interpreted as the out-of-plane C-H bending band for an alkene in *trans* position)[290] disappeared, supporting the hypothesis of an addition

on double bonds.

Secondly, appearance of a weak broad peak at 550cm^{-1}, interpreted as the stretching of a C-Br bond,[290] thus corroborated the bromination having taken place.

In conclusion, direct bromination of AHS was considered to occur mainly by electrophilic addition on carbon-carbon double bonds. However, it was difficult to observe whether secondary reactions such as electrophilic aromatic substitutions may have taken place, especially on phenolic moieties. For instance, FTIR spectra of aliphatic and aromatic bromo derivatives cannot easily be distinguished. FTIR study was therefore supportive of the theory of sporopollenin being brominated on unsaturations, as shown in Figure 43.

In conclusion, considering side reactions as negligible, bromine level was regarded as an indication of the degree of unsaturations in sporopollenin (as already highlighted in Section A-4.1.2.1). Initially, aliphatic systems only were considered and on this basis, there seemed to be 2-2.5mmol.g^{-1} of carbon-carbon double bonds in AHS, *i.e.* 4-5mmol.g^{-1} (0.05-0.06g.g^{-1}) of carbon atoms involved in alkenes. In agreement with such an interpretation of the results, 10% of sporopollenin's carbon atoms were thought to be involved in olefinic systems. Given this conclusion, it seems noteworthy to remind that part of the alkenes present in AHS might actually arise from dehydration of hydroxyl groups by treatment in hot concentrated *ortho*-phosphoric acid (see Section B-5.1). This may also explain that the present results of bromination are not in agreement with sporopollenin structures suggested in the literature (see Section A-4.3). Nevertheless, the presence of hydroxycinnamic acids seems recognised in the literature, as mentioned in Section A-4.2.5. Additionally, recent studies on antioxidant properties of sporopollenin confirmed that phenol-type components may constitute a non-negligible fraction of sporopollenin structure.[190] Therefore, it seems more likely that bromine actually added onto both aliphatic and aromatic unsaturations.

5.3.3 Chloromethylation

As mentioned in Section B-5.3.1, one of the best-known halogenated commercial resins is probably a Merrifield resin, which is a chloromethyl polystyrene.[287,300] It was thus an interesting example to mimic with sporopollenin. Chloromethylation of the aromatic components of AHS has been envisaged in previous studies.[12,301] Chloromethylation was repeated here by stirring AHS (**1**) in

dimethoxymethane in the presence of thionyl chloride and zinc chloride (see Section C-5.7.2) to yield the products **16a** (from S-type exines) and **16b** (from L-type exines).

Loading levels of chlorine in chloromethyl sporopollenin (**16**) were assessed by gravimetry, according to the procedure described in Section C-5.1.3. The results, gathered in Table 104, show that the experimental error was relatively high in some cases. Chlorine loading in S-type chloromethyl sporopollenin (**16a**) (0.97mmol.g^{-1}; s.d. 0.71) was found different from that in L-type one (**16b**) (0.34mmol.g^{-1}, s.d. 0.01), although within error. Data obtained on S-type chloromethyl sporopollenin (**16**) was not regarded as very reliable and more chloride gravimetric analyses should prove useful to back up such results.

Attachment of the chloromethyl substituent to AHS (**1**) to form the products **16a** and **16b** was confirmed by FTIR spectroscopy (cf. spectrum in Appendix I-7). A marked increase in the C-H stretch peak (ca. 2950cm^{-1})[288-290] was explained by the addition of methylene groups. Two distinct signals in the 1100-1050cm^{-1} range, characteristic of chloromethyl sporopollenin (**16**), might possibly be due to methylene rocking in the presence of halogen. Due to modest loadings, the fingerprint region was not well defined and stretch vibration of C-Cl bond was only visible in the spectra obtained with L-type exines **16b**, whereas it must have been hidden by other peaks in S-type **16a**.

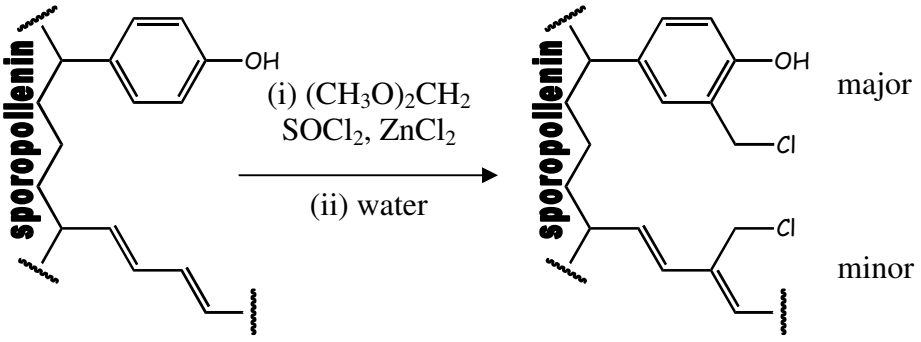

Figure 44 – Chloromethylation of sporopollenin – Hypothesis highlighting the functional groups concerned by potential changes

As a matter of fact, treatment of sporopollenin **1** with thionyl chloride under anhydrous conditions should also have readily activated carboxyl groups to yield acyl chloride, but these were most likely to have been completely hydrolysed by exhaustive water washings. Chloromethylation was believed to have taken place on sporopollenin aromatic moieties mainly; secondary chloromethylation of alkenes could be envisaged

although being probably only very minor. Aromatic components of sporopollenin have been shown to probably be mostly of phenolic nature (see Section A-4.2.5). Ergo chloromethylation most likely occurred on phenols. Those hypotheses are illustrated in Figure 44.

By comparison, from results found when building the spacer arm in Section B-5.2.4.1, it was suggested that the level of phenols in sporopollenin was ca. 0.2mmol.g^{-1}. To monitor this value, acidity of AHS was measured by back-titration with hydrochloric acid, after stirring exines respectively in 2M sodium hydroxide and 2M sodium bicarbonate.[302] Sporopollenin was found to consume 1.3mmol.g^{-1} of the former and 0.7mmol.g^{-1} of the latter, but the experiment was never reproduced. Back-titration from sodium hydroxide evaluated the overall loading of acidic functions in the polymer (considered to be phenols, lactones and carboxylic acids[151]; see Section A-4.1.2.4), while only carboxylic acid groups were concerned by the treatment in sodium bicarbonate.[152] Lactones were considered absent from sporopollenin, as they should have been saponified during the alkaline step of extraction, although this could be discussed. Therefore loading of carboxylic acid was found to be 1.3mmol.g^{-1} and that of phenols calculated by subtraction to be 0.6mmol.g^{-1}, which is higher than hypothesised before.

In conclusion, chloromethylation of sporopollenin appears to have taken place on phenols. Indeed, there seems to be a quantity of phenols large enough to accommodate the chloromethyl groups quantified. However, phenolic content of the sporopollenin extracted from *L. clavatum* needs to be ascertained to confirm such a hypothesis.

5.3.3.1 Chloromethylation of aniline-treated sporopollenin

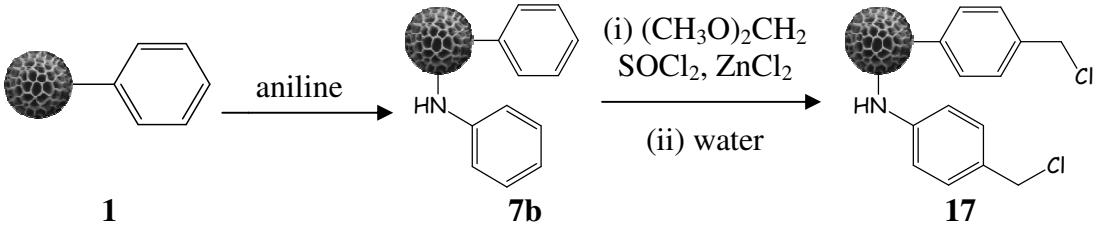

1 **7b** **17**

Figure 45 – Successive reactions: attachment of aniline to sporopollenin (cf. details regarding functional groups involved in Figure 41), then chloromethylation of the resulting product – Hypothesis highlighting the functional groups concerned by potential changes

Derivatisation of sporopollenin **1** with aniline has been detailed above in Section B-5.2.3.2. Direct refluxing of AHS (**1**) in neat aniline gave the product **7b**, which exhibited more aromatic rings potentially susceptible to chloromethylation. Derivatised sporopollenin **7b** had a level of aniline determined by combustion elemental analysis at ca. 2mmol.g^{-1} (see Table 52). It was chloromethylated under the same reaction conditions used before with native sporopollenin **1** (see Section C-5.7.2) and expected reactions are also illustrated in Figure 45.

According to the Table 104, the resulting loading of chlorine in **17**, obtained by chloromethylation of aniline-treated sporopollenin **7b**, only reached 0.7mmol.g^{-1} as determined by gravimetric analysis (see Section C-5.1.3). By contrast, original AHS (**1**) was chloromethylated into **16** up to a higher loading (0.9mmol.g^{-1}). The lower susceptibility of aniline-treated sporopollenin **7b** to chloromethylation over underivatised sporopollenin **1** could indicate that the phenyl ring of aniline was not sufficiently reactive under the conditions applied and that the attached aniline was perhaps inhibiting access to available chloromethylation sites on sporopollenin itself, by steric hindrance for instance. In conclusion, prior treatment of sporopollenin with aniline did not seem interesting to increase the loading of chloromethyl groups.

5.3.4 Chlorination of sporopollenin

Sporopollenin type	Chlorosporopollenin	
	Chlorinating agent	Chlorine loading* (mmol.g^{-1})
S-type AHS	PCl_5	0.93 (0.50)
	$SOCl_2$	0.60
L-type AHS	PCl_5	0.83 (0.62)
	$SOCl_2$	0.44

Standard deviation is given in brackets after the results when available.
* determined by gravimetric analysis

Table 54 – Loadings of bromine in sporopollenin after bromination

Sporopollenin's chemical structure exhibits an important level of hydroxyls (ca. 1mmol.g^{-1}; see Section A-4.1.2.2). Nucleophilic substitution of those functions by good leaving groups, such as halogens, could make AHS a powerful resin for solid-support reaction. Chlorination of sporopollenin has already been attempted in the past.[12] It proved sporopollenin's hydroxyls could be successfully substituted for chlorine. This

was reproduced here using two different reagents. Treatment of AHS (**1**) was carried out either with phosphorus pentachloride in anhydrous dichloromethane in the presence of potassium carbonate, or with thionyl chloride in dry diethyl ether. This yielded the chloro sporopollenins **18** and **19** respectively. Both procedures are detailed in Section C-5.7.3.

Loading levels of chlorine in chlorosporopollenins **18** and **19** were assessed by gravimetry, according to the procedure described in Section C-5.1.3, and data are displayed in Table 105. According to the results gathered in Table 54, treatment with phosphorus pentachloride seemed to give better loadings. However, reaction with thionyl chloride was performed only once, for comparative purposes and analytical error was quite high. Therefore statistical repetitions would be needed to validate the results. S-type exines were found slightly prompter than their L-type counterparts to attaching chlorine, probably because of structural divergence.

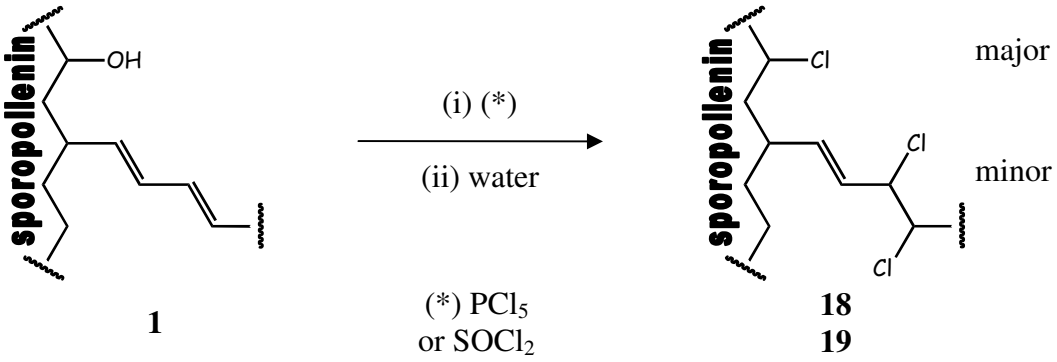

Figure 46 – Chlorination of sporopollenin with phosphorus pentachloride – Hypothesis highlighting the functional groups concerned by potential changes

Modifications that occurred on sporopollenin by chlorination were investigated by FTIR spectroscopy (cf. spectra in Appendices I-9 and 10). Important decreases in the O-H stretch peak (ca. 3500cm^{-1})[288-290] and, to a lesser extent, in the C=C stretch signal (ca. 1650-1600cm^{-1}) indicated that chlorine had successfully displaced hydroxyls and possibly been added across double bonds. A band at ca. 1050cm^{-1} could be assigned to P-O stretching,[288-290] explained by the presence of phosphorylated groups presumably incorporated into sporopollenin's structure by phosphorus pentachloride. Due to modest loadings, the fingerprint region was not well defined and stretch vibration of C-Cl bond was hidden by other peaks.

As it was hypothesised with thionyl chloride previously in Section B-5.3.3, it is most likely that phosphorus pentachloride activated carboxylic groups to form acyl

chloride that were eventually hydrolysed by exhaustive water washing. The main effect of phosphorus pentachloride treatment is considered to be the nucleophilic substitution of hydroxyl groups, both aliphatic and aromatic (phenol), for chlorine. Chlorine addition on carbon-carbon double bonds could also have taken place but was probably only minor. Those hypotheses are illustrated in Figure 46.

According to previous investigations,[12,13] hydroxyl loading was estimated to be 1.15mmol.g^{-1}, by acetylation with acetic anhydride, and between 0.4-1.4mmol.g^{-1}, by Fmoc analysis. As a conclusion, treatment with phosphorus pentachloride, and to a lesser extent with thionyl chloride, seemed to have yielded almost complete chlorine substitution of hydroxyl groups.

5.3.5 Substitution reactions of halogenated sporopollenins

Halogenated sporopollenin was expected to be a good substrate for further reactions. Indeed, halogens are well-known good leaving groups that can easily undergo nucleophilic substitutions. Two examples of functional group transformations were illustrated in the present study: azidation and thiolation of all three previously obtained halogenated sporopollenins (bromo-, chloromethyl- and chloro-sporopollenins).

5.3.5.1 Azidation

Azide ions are good nucleophiles.[303] They had already been used to substitute bromine in bromosporopollenin in a previous study.[13] This investigation provided, after reduction of azido-sporopollenin, an alternative route to obtain aminosporopollenin. Reduction was not necessary though to yield an interesting compound. Indeed, azido groups are important anchoring function for click-chemistry (cycloadditions).[298] Therefore, azido-sporopollenin could also be applied straightforwardly.

Azidation of brominated and chlorinated sporopollenins, prepared in the above Sections B-5.3.2 and B-5.3.4, was further explored. A complete FTIR spectroscopic study was also undertaken on azido-sporopollenins. This work is described below in Section B-5.4.

5.3.5.2 Thiolation

The second example of nucleophilic substitution consisted of the interconversion

of halogenated groups by thiols. Thiols are widely used as anchoring functions on commercial resins, applied to solid-phase organic synthesis for instance.[281] Thiolation of bromosporopollenin has already been proved successful in the past.[153]

A study of thiolation was extended here to all three halogenated sporopollenins prepared in above Sections B-5.3.2, B-5.3.3 and B-5.3.4. A thorough investigation of thiolation of bromosporopollenin was also undertaken, with various thiolating agents, analytical assays and further reactions on the resulting thiols. This study is described in the following Section B-5.5.

5.3.6 Conclusions

Halogenation of sporopollenin is an important way of exploiting its different functional groups to make it a novel type of derivatised resin. Unsaturation was targeted by bromination, aromatic rings by chloromethylation and hydroxyls by nucleophilic substitution by chlorine. Such reactions yielded potentially high loadings of anchoring functions for further interchange by nucleophiles. Due to the high degree of unsaturation of sporopollenin, bromination gave the highest results in term of halogen level. With subsequent nucleophilic substitution, bromosporopollenin seemed then especially well-suited for scavenging applications given the very good loading. Other halogenated resins could be used as solid supports. Analytical results of gravimetric methods should be repeated though, to support existing data and, should a level of chlorine in sporopollenin be confirmed at around 1mmol.g^{-1}, it would rival commercial resins.[278,281]

Derivatisation of sporopollenin with azides, in particular, offers two routes of applications: solid-support click-chemistry or amino resins. Thiolation of sporopollenin, as detailed in the following Section B-5.5, showed a great potential for applications of the resulting thiolated resin as a scavenger or as a solid support for organic synthesis.

In conclusion, halogenation proved to be the first step for making sporopollenin a potentially versatile solid reagent.

5.4 Azidation

5.4.1 Purpose

Click-chemistry is a chemical philosophy developed since 2001, mainly thanks

to Sharpless.[298] It involves an economic and, to some extent, ecological chemistry focused on joining small units, with minimal solvent use, least purification steps and high atom economy. Cycloadditions have been particularly favoured as they exhibit many of the targeted criteria. 1,3-Dipolar cycloadditions between an azide and an alkyne are the archetype of click-chemistry. This renewed the interest for azido groups.

A resin derivatised with azide functions could thus offer a novel polymer for solid-supported organic synthesis, for example. Azido-sporopollenin could also possibility be exploited as additives in co-polymers involving alkyne-type monomers [poly(acetylene)[304] and derivatives such as poly(paraphenylene vinylene) or poly(thienylene vinylene)[305]], in order to change their properties (e.g. density, resistance).

Also, azidation could be the first step of an alternative route to produce amino sporopollenin, as it has been done previously.[13] In such case, substitution of bromosporopollenin by azides was followed by reduction to yield primary amines.

After azidation of sporopollenin was exemplified in the past by substitution on bromosporollenin using sodium azide,[13] it was repeated in the present study and extended to chlorinated and chloromethylated sporopollenins. Each reaction was performed on halogenated sporopollenins with sodium azide in DMSO under reflux (see Section C-5.8).

5.4.2 Azidation of bromosporopollenin

The initial bromosporopollenin (**15**) was obtained following the method described in Section B-5.3.2 and the loading of bromine was determined by gravimetric analysis (see Section C-5.1.3) as being 4.35mmol.g^{-1}.

A large increase in weight ratios of carbon (39.73% to 64.15%) and nitrogen (0% to 7.39%) was observed by elemental analysis (see Table 102 and Table 107), respectively indicative of the loss of bromine and the attachment of azide. Alkaline hydrolysis of azido-sporopollenin **20** released no bromide as checked by addition of dilute silver nitrate solution, showing that all bromine had been removed (halogen assay by gravimetric analysis, see Section C-5.1.3). Combustion elemental analysis of the resulting azido-sporopollenin **20** (see Table 107) showed that the loading of nitrogen was 5.23mmol.g^{-1} and thus the level of azido groups 1.76mmol.g^{-1}. This was explained by the nucleophilic substitution of 40% of bromine for azide and elimination of the rest, side reaction facilitated by the fact that the resulting double bonds were probably

conjugated. These expected reactions are illustrated in Figure 47.

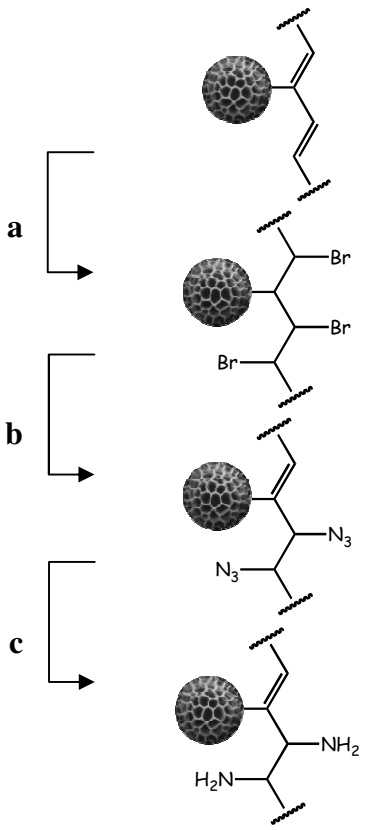

	loadings (mmol.g^{-1})		
	N *	Br †	Cl$^-$ ‡
1	0.00	-	0.00
15	0.00	4.35	-
20	5.23	0.00	-
21	1.54	-	0.00

* determined by combustion elemental analysis; † determined by bromide gravimetric analysis after hydrolysis in sodium hydroxide; ‡ determined by chloride gravimetric analysis after treatment with dilute hydrochloric acid

Figure 47 – Successive bromination, azidation and reduction of sporopollenin – Expected reactions and analytical data – See notes below regarding reaction conditions

Notes: **a**: bromine in chloroform, room temperature, overnight; **b**: sodium azide in DMSO, 60°C, 24h; **c**: lithium aluminium hydride in 1,4-dioxane, under nitrogen, reflux, 4 days.

FTIR study also confirmed successful azidation (cf. spectrum in Appendix I-11). The small broad peak at 550cm^{-1} relative to C-Br bond stretching[283] disappeared, while peaks indicative of azido groups[290] appeared: asymmetric stretching at 2094cm^{-1} and symmetric stretching at 1230cm^{-1}. It was excluded that this signal could be due to remaining residue of sodium azide in sporopollenin because of the very good solubility of sodium azide in water (417g.L^{-1} at 17°C[261]).

As mentioned above in Section B-5.4.1, product **20** could offer new scope to

click-chemistry with solid-support cycloadditions occurring on the anchoring azides. Nevertheless, azides could also be a step from amines, thus opening the usual applications of amino resins such as peptide synthesis (see Section B-5.2.1). In order to obtain primary amines from azido-sporopollenin **20**, reduction was effected by refluxing with lithium aluminium hydride in dioxane for 4 days (see Section C-5.5). Combustion elemental analysis (see Table 97) showed that the nitrogen content dropped to 2.15% *i.e.* 1.54mmol.g^{-1}, which was only slightly below to the loading of initial azides; ca. 12% the initial azides were lost. In addition, chloride gravimetric analysis (see Table 97) showed the level of basic functions that formed chloride salts was 1.43mmol.g^{-1} in the reduced azido-sporopollenin **21**. The basic functions were considered to be primary amines. Therefore, around 82% of the initial azides were reduced to yield available primary amines displayed by sporopollenin **21**. The rest might not have been reduced or could simply be hidden to formation of hydrochloride by steric hindrance. Expected reaction is illustrated in Figure 47.

The FTIR spectrum (displayed in Appendix I-12) of the reduced product **21** showed evidence of azides disappearing, as peaks at 2094cm^{-1} and 1230cm^{-1}, characteristic of azides,[290] were lost. In parallel, the broader peak around 3400cm^{-1} and the slightly visible band at 3200cm^{-1} could indicate amines. The disappearance of the carbonyl peak at 1700cm^{-1} was also observed, as expected. However, the weak signal of C-N-H deformation in an amine was not visible in the region 1650-1590cm^{-1} due to other bands overlapping.

5.4.3 Azidation of chlorinated and chloro-methylated sporopollenins

For comparative purpose, azidation was also attempted on S-type sporopollenins that had been previously derivatised so as to exhibit chloro groups (products **16**, **17**, **18** and **16**). Experimental conditions, detailed in Section C-5.8, were identical to that used with bromosporopollenin and the expected reactions were also nucleophilic substitutions of halogens by azides, as illustrated in Figure 48.

Chlorosporopollenins **18** and **19** were yielded by treatment with phosphorus pentachloride and thionyl chloride, respectively, as described in Section B-5.3.4. Chloromethyl sporopollenin **16** was obtained by the process investigated in Section B-5.3.3. In order to potentially increase the final loading of azides, a third starting

product was used: chloromethylated aniline-treated sporopollenin **17** whose synthesis had been described in Section B-5.3.3.1.

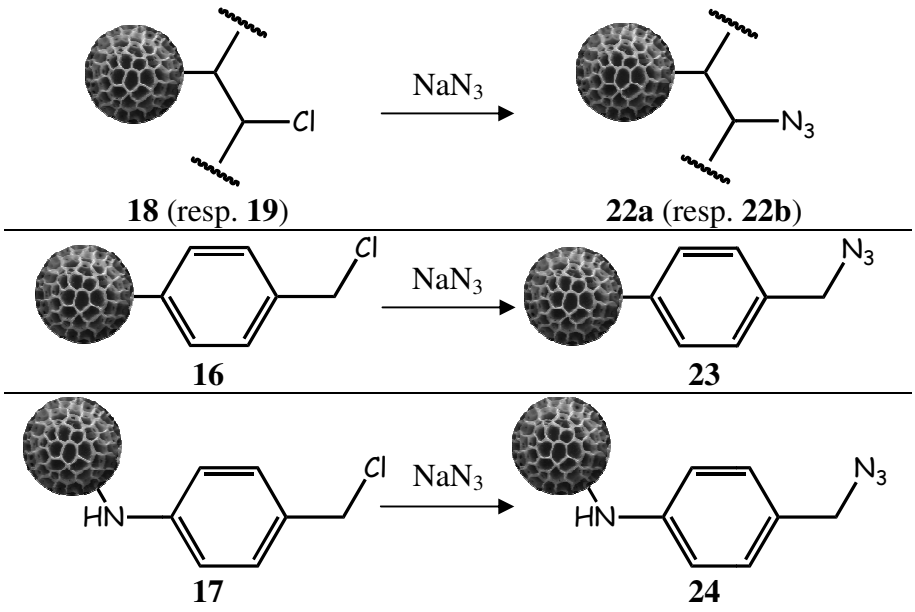

Figure 48 – Azidation of chlorinated and chloromethylated sporopollenins – Hypothesis highlighting the functional groups concerned by potential changes

Azide loadings were determined by combustion elemental analysis (see Table 107) and found to be relatively modest on chlorosporopollenin as shown in Table 55, by comparison with those obtained from bromosporopollenin (see Figure 47). Azidation did not occur on product **18** (obtained by treatment with phosphorus pentachloride); all initial chlorine was left intact and it was entirely recovered by reflux under alkaline conditions (see halogen assay in Section C-5.1.3). By reaction of sodium azide with compound **19** (obtained by treatment with thionyl chloride), 20% of initial chlorine was substituted by azides while 80% was left intact and quantified by halogen assay, according to the data shown in Table 55.

Better loadings were obtained from chloromethyl sporopollenins. In product **16**, 27% of chlorine was substituted by azides and the rest was quantitatively detected by halogen assay. By contrast, compound **17**, which did not seem so interesting initially, owing to its lower level of chlorine when compared in **16**, was finally a better substrate for azidation as 66% of its chlorine were substituted. Consequently, the resulting azidosporopollenin **24**, yielded by derivatisation of **17**, had the highest level of azide ($0.46 mmol.g^{-1}$) obtained in this study from chlorine-derivatised sporopollenins.

By comparison, 40% of bromine was substituted by azides in

bromosporopollenin (**15**), as highlighted in Section B-5.4.2, and this yielded a level of 1.76mmol.g^{-1} of azide groups. Steric hindrance could partly explain the results observed in azidation of the compounds **16**, **17**, **18** and **19**, bromine atoms being more likely to be available due to their large loading while chlorine atoms might have been hidden within structural folds of sporopollenin. In addition, chlorine is less good a leaving group than bromine. The fact that no bromine was left attached to azidosporopollenin **20** probably resulted from the conjugated positions of the brominated unsaturations in bromosporopollenin **15**: all of the bromine that was not substituted was completely removed by elimination. Similarly, substitution was easier in chloromethyl sporopollenins (**16** and **17**), since chlorine atoms were in benzylic positions.

Chlorinated sporopollenin			Azido sporopollenin			Ratio N_3 / Cl‡ (%)
Compound	Chloride loading* (mmol/g)	Nitrogen loading† (mmol/g)	Compound	Azide loading† (mmol/g)	Chloride loading* (mmol/g)	
18	0.93	0.00	**22a**	0.00	0.91	**0**
19	0.60	0.00	**22b**	0.12	0.48	**20**
16	0.90	0.00	**23**	0.24	0.70	**27**
17	0.70	1.07	**24**	0.46	N/d	**66**

* determined by chloride gravimetry; † based on combustion elemental analysis;
‡ quotient of azide loading in final product by chloride loading in initial sample

Table 55 – Loading of azide after azidation of different chlorinated sporopollenins

Due to the initial derivatisation with aniline, compound **17** must exhibit aromatic groups in different environments. Naturally occurring aromatic rings were most probably hidden as suggested before (see Section B-5.3.3.1), which explained the low loading of chlorine. Chloromethylation probably occurred mainly on newly displayed aniline groups, which must have been sufficiently exposed. This disposition made therefore these chlorine atoms highly susceptible to attack by azide, hence the high ratio of effective substitution.

FTIR spectra of azidosporopollenins (displayed in Appendices I-13 and 14) confirmed that azidation had occurred. Due to the low loadings, only weak signals were obtained. However, peaks at 2100cm^{-1} and at 1230cm^{-1} were unequivocal indications for the asymmetric and symmetric stretching of the azide group.[290]

5.5 Thiolation

5.5.1 Purpose

Catalogues of commercial resins offer a certain variety of thiolated linkers. Figure 49 gathers some representative examples, along with their sulphur loadings (as given by retailers). Polystyrene (PS) beads, for instance, have been derivatised with thiophenyl(2-chlorophenyl)methyl **A**,[281] thiophenyl(4-methoxyphenyl)methyl **B**,[278] *N*-(3-thiopropanoyl)aminomethyl **C**,[278] *N*-(3-thiopropanoyl)aminoethyl **D**,[281,306] thiomethyl **E**,[281] *N*-(2-thioethyl)aminomethyl **F**[280,307] and *N*-[2-(3- or 4-thiophenyl)-propanoylaminomethyl **G**,[278,281] and TentaGel™ and HypoGel™ resins with (3-thio-propanoyl)amino **H**.[308,309] Other supported thiols have been made up from commercial amino or chlorinated resins such as *N*-(2-thioacetyl)amino PS **I**,[308,309] *N*-[(4-thiophenyl)oxyacetyl]amino PS **J**[308,309] or (4-thiophenyl)oxymethyl PS **K**.[153]

Some of these thiolated polymers are applied to solid-phase organic synthesis.[281,310] For example, **A** and **B** are acid-labile resins used for preparation of thiols and symmetric disulphides respectively, by alkylation or acylation.[278,311] Polymers **C**, **D** and **H** are used in batch methodology, for SPOS, especially peptide synthesis and combinatorial chemistry,[312] the latter having been employed as a traceless linker in the synthesis of pyrimidines.[313,314] Support **E** has been used extensively to prepare polymer-supported silyl ethers for utilization in Mannich and aldol reactions;[315] it has also been employed in the traceless synthesis of pteridines.[307] Resin *para*-**7** was found to be a very good S_NAr-labile linker in the synthesis of aminopyridazines;[316] this polymer has also been used to prepare polymer-supported *N*-hydroxysuccinimide by reaction with *N*-hydroxymaleimide.[309] Supports **I**, **J** and **K** were tailored for solid-phase synthesis of peptides with C-terminal thioesters, which were then cleaved.[317] Cleavage of thioesters derived from this resin has been carried out with lithium borate, DIBAL, and sodium hydroxide to afford alcohols, aldehydes and carboxylic acids, respectively.

Thiol linkers that attach covalently, quantitatively and rapidly to electrophiles are also employed as scavengers. They can also form disulphide bridges to catch by-products under oxidative conditions. They generally prove handy for quick purifications in combinatorial synthesis products.

For instance, electrophiles such as α-bromoketones are scavenged by resin **F**,[281] and alkyl halides by both **F** and **G**.[318] Resin **F** also catches α-thiocarbonyls by oxidation

and condensation,[153] and resin *meta*-**G** is an effective scavenger in Williamson ether synthesis.[319]

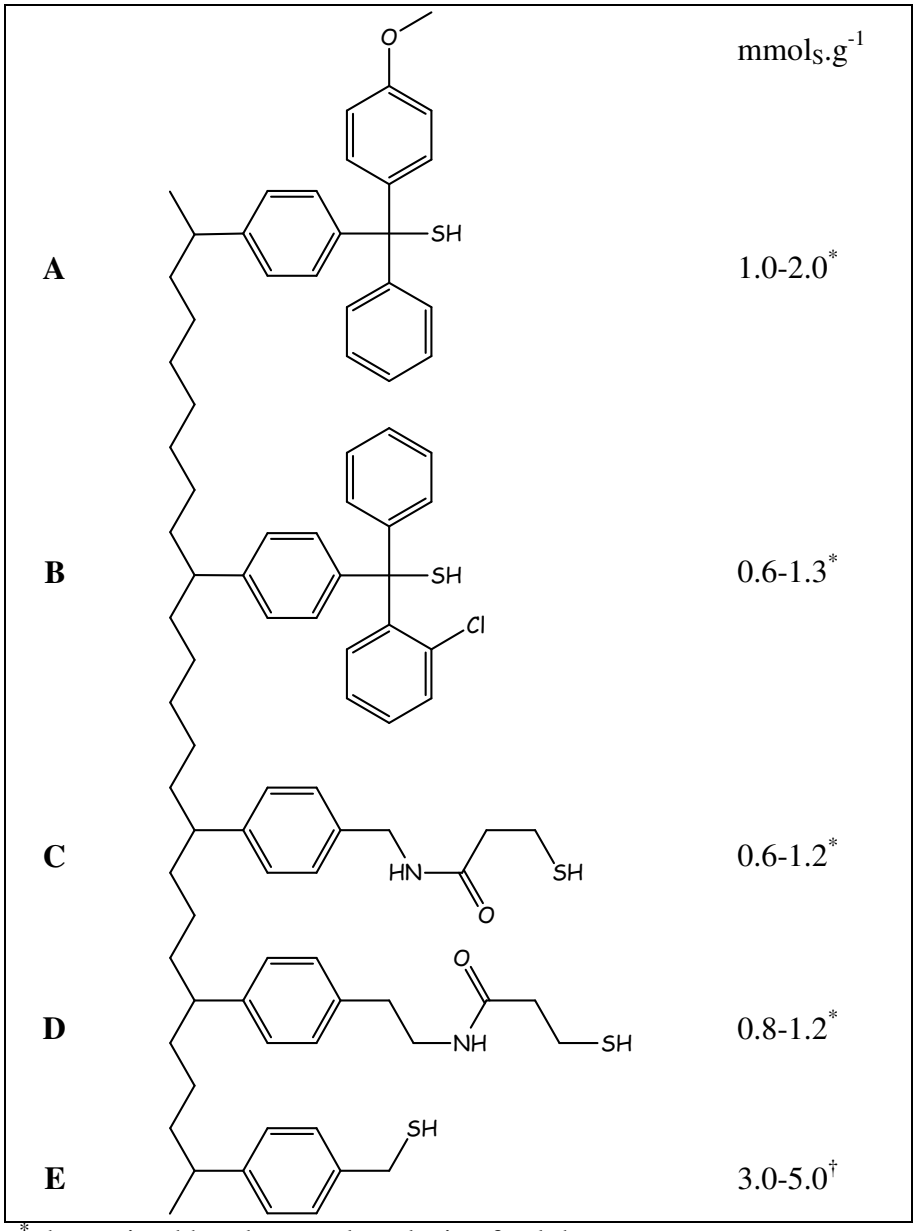

* determined by elemental analysis of sulphur

† determined by elemental analysis of chlorine, after derivatisation with 3,4-dichlorophenylisocyanate

Figure 49 – Catalogue of commercial thiolated resins (cont.)

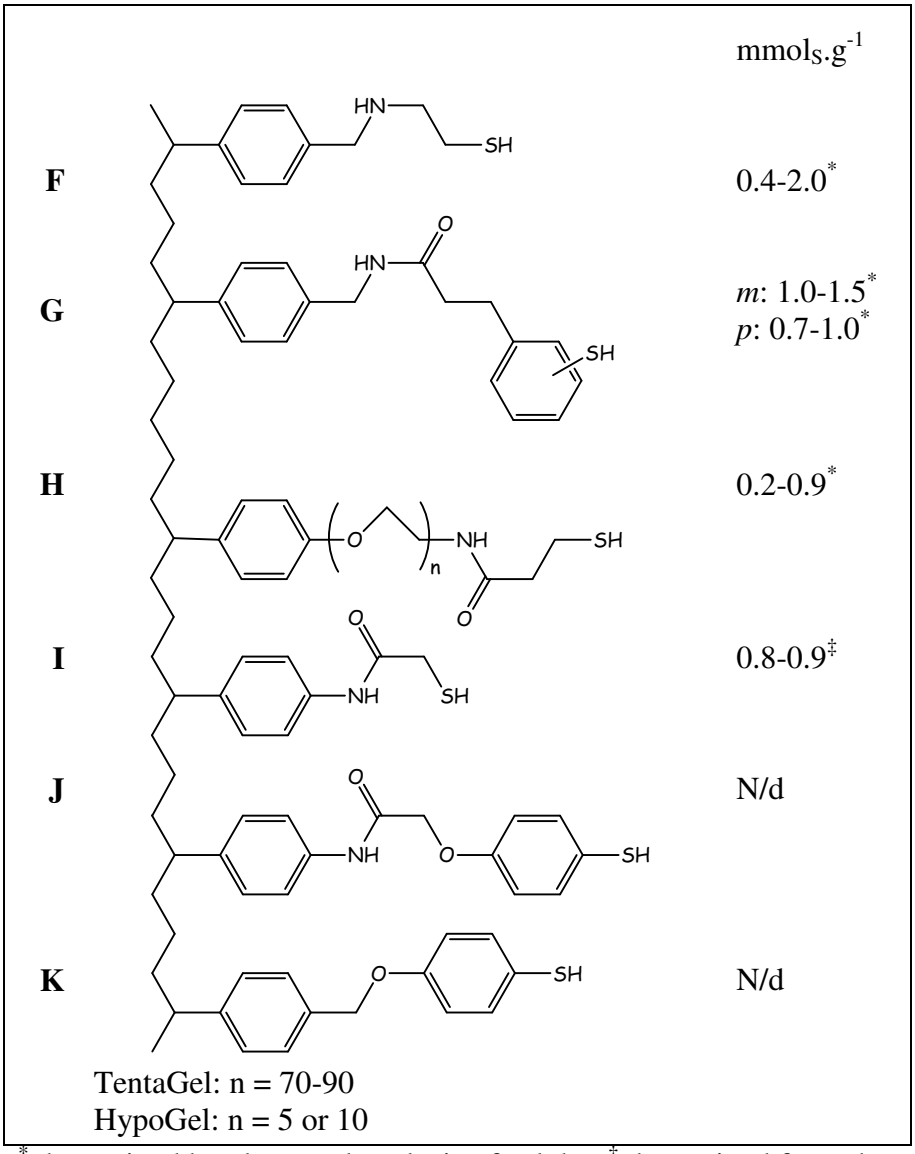

* determined by elemental analysis of sulphur ‡ determined from the amount of triphenylmethane produced by deprotection from trityl-protected thiols

Figure 49 – Catalogue of commercial thiolated resins[153,278,280,281,306-309]

As mentioned in the introduction of Section B-5, commercial resins suffer many flaws. Their matrix is generally damaged by high temperature, by high shear stirring or by strong acids, strong bases, and certain organic solvents. They often require swelling, their beads are quite heterodispersed, and they are rather expensive. Sporopollenin microparticles exhibit all the opposite qualities (cheapness, resistance, monodispersity). Therefore, exine would offer a novel support for thiolated resins on the condition that it is suitably derivatised.

Thiolation of sporopollenin was first exemplified in the past by substitution on bromosporollenin using thiourea or sodium hydrogen sulphide.[12] Properties of thiolated

sporopollenin thus obtained were then examined with regard to its nucleophilicity and its binding to free thiols.[153] In the present study, thiolation of sporopollenin was repeated, using various conditions. The work was broadened to the different halogenated sporopollenins presented in Section B-5.3. Also new thiolating agents were explored. In addition, the thiosporopollenins developed were investigated vis-à-vis reactions with nucleophiles, with free thiols and with heavy metals. This was the occasion to review some methods to determine the actual loading of sulphur and thiols of solids.

5.5.2 Thiolating agents

In former developments carried out on bromosporopollenin, bromine was substituted by thiols using sodium hydrogen sulphide or thiourea.[12,153] Resulting thiosporopollenin showed quite high loadings of sulphur (1-5mmol.g^{-1}), at least within ranges of values offered by commercial resins (see Figure 49). Ergo, these reactions were repeated, in a first instance, thus demonstrating reliability of the chemistry using sporopollenin. However some limitations, detailed below, had to be overcome; therefore, improvement of such chemistry was attempted with the implementation of new protocols, with other thiolating agents, namely thioacetic acid and sodium thiosulphate. Thiolation was also extended to other halogenated sporopollenins, which were developed in previous Sections B-5.3.3 and B-5.3.4, and it was also attempted on underivatised sporopollenin (AHS, **1**) in order to justify the need for halogenation steps.

5.5.2.1 Thiolation with sodium hydrogen sulphide

Sodium hydrogen sulphide is a common thiolating agent.[320] It displaces halide groups by nucleophilic substitution to yield a thiol directly and was therefore used to convert bromo-, chloro- and chloromethyl sporopollenins to thiolated sporopollenin. Following a procedure developed in the past[12,153] and detailed in Section C-5.9.1.1, such reaction was perfomed by stirring halogenated sporopollenins **15**, **16** and **18** in DMSO with sodium hydrogen sulphide under reflux overnight. DMSO was chosen as solvent because it encourages nucleophilic substitutions and its very high boiling point (189°C) increased the reaction kinetic. Expected reactions are illustrated in Figure 50.

It is first interesting to notice that underivatised sporopollenin **1** did not react significantly with the thiolating reagent (see Table 109, batch **0**), according to the results gathered in Table 56. Halogenation was thus required prior to thiolation of

sporopollenin.

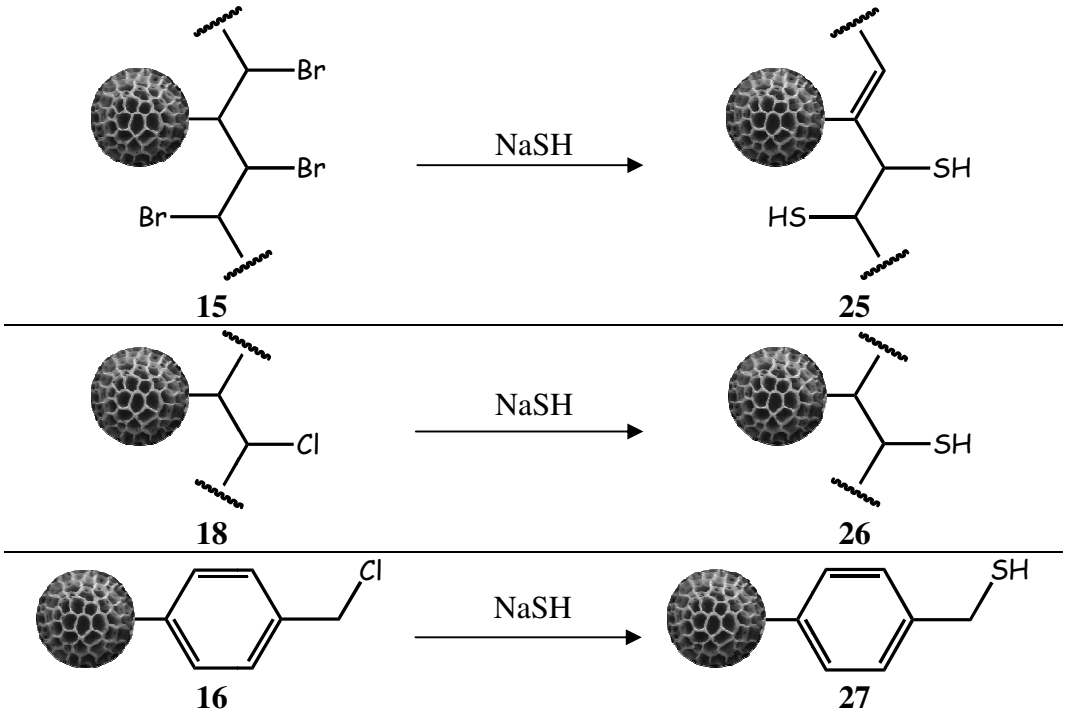

Figure 50 – Thiolation of bromo-, chloro- and chloromethyl sporopollenins with sodium hydrogen sulphide – Hypothesis highlighting the functional groups concerned by potential changes

Thiolation of bromosporopollenin **15** was performed at a constant ratio of sodium hydrogen sulphide to sporopollenin: 6 equivalent of sulphide were used, by comparison to the known loading of bromide on **15**. It was checked that all bromine was removed after thiolation: thiosporopollenin **25** was hydrolysed in sodium hydroxide and no precipitate was observed in the hydrolysate by addition of silver nitrate. The loading level of sulphur in the resulting thiosporopollenin was evaluated by combustion elemental analysis (see Table 109). It was concluded that ca. 60% of bromine atoms were substituted for thiols while the rest were eliminated to reform double bonds. Such side reactions were favoured by the conjugation of the system (see Table 56).

A study was conducted to determine the amount of sodium hydrogen sulphide required for optimum thiolation of chlorosporopollenin **18**. Elemental analyses were also performed to quantify the loading of sulphur in the resulting product **26** (see Table 109). In Table 56, it can be observed that the more concentrated the thiolating agent, the higher the loading. When 4 equivalents of sulphide were used, only 13% of chlorine groups were substituted for thiols. By contrast, when 16 to 45 equivalents of sulphide

were used, more sulphur was loaded in sporopollenin **26** than could be explained by simple substitution of chlorine for thiols (ratio S/halide >100%). This concentration effect was also noticed during thiolation of chloromethyl sporopollenin **16**: 6 equivalents of sulphide yielded 64% while 21 equivalents gave over 100% again.

Initial sporopollenin		Ratio NaSH/halide[¶] (mol.mol^{-1})	Thiolated product		
Sample	Halide loading[*] (mmol/g)		Sample	Sulphur loading[†] (mmol/g)	Ratio S / halide [‡] (%)
AHS **1**	0.00	-	**-**	0.01	-
15	4.39 (0.06)	6	**25**	2.78 (0.66)	60
18	1.00	4	**26**	0.13	13
	0.60	16		1.00	167
	0.44	23		1.04	236
	0.35	45		0.84	240
16	0.90	6	**27**	0.58	64
	0.80	21		2.44	164

Standard deviation is given in brackets after the results when available.
[*] determined by gravimetric analysis; [¶] equivalents of sodium hydrogen sulphide used vis-à-vis halide loading; [†] based on combustion elemental analysis; [‡] quotient of sulphur loading in final product by halide loading in initial sample

Table 56 – Loading of thiols after treatment of different halogenated sporopollenins by sodium hydrogen sulphide

A downside of sodium hydrogen sulphide is its capacity to polymerise. This explained the relatively high loadings of sulphur (ratio S/halide >100%). Indeed, each initial halide group might have given rise to a short oligosulphide chain in place of the expected free thiols, as illustrated in Figure 51. Ergo sulphur loadings determined by combustion elemental analysis was probably higher than that of actual thiols, due to the presence of oligosulphide chains.

Further optimisation of the use of sodium hydrogen sulphide is therefore needed. For instance, this problem of polymerisation could be tackled by reducing freshly obtained thiosporopollenin with 1,4-dithiothreitol (DTT).[321,322] As shown in Figure 51, DTT is expected to cleave the oligomeric chains and to give the desired thiols. Reductions had been performed in a past study[153] but their efficiency to cleave polysulphide chains was not properly assessed though; indeed the loading of sulphur had not been determined after reduction; however, the study showed that the level of thiols available for acylation did not change (ca. 20% of the sulphur reacted to attach nitrobenzoyl chloride). Further work is thus required to evaluate the interest of a reduction although it seems that it would not make more thiol functional groups

available.

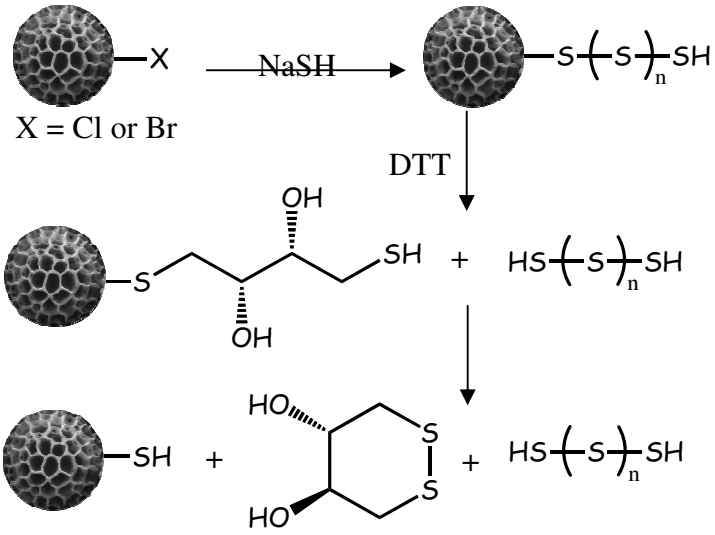

Figure 51 – Hypothetical polymerisation of sulphides during thiolation of halogenated sporopollenins with sodium hydrogen sulphide, and further potential reduction with DTT

5.5.2.2 Thiolation with thiourea

Thiourea has also been used in the past[12,153] to thiolate bromosporopollenin in two steps. Its mechanism involves nucleophilic substitution of halides to create an isothiouronium salt intermediate, which, in a second step, is hydrolysed under alkaline conditions.[320] Good yields (80-90%) have been observed in homogeneous chemistry.[323]

Bromosp. 15			**Thiosporopollenin 28**		
Bromine loading* ($mmol.g^{-1}$)	**Solvent**	**Temp.**	**Sulphur loading† ($mmol.g^{-1}$)**	**Nitrogen loading† ($mmol.g^{-1}$)**	**Ratio S / Br ‡ (%)**
4.39 (0.06)	DMSO	189°C	5.21 (1.10)	2.60 (0.75)	119
4.03	Methanol	22°C	0.74 (0.13)	0.86 (0.09)	18
4.35	Methanol	65°C	0.80	1.09	18

Standard deviation is given in brackets after the results when available.
* determined by gravimetric analysis after hydrolysis in sodium hydroxide;
† determined by combustion elemental analysis; ‡ quotient of sulphur loading in final product **28** by bromide loading in initial sample **15**

Table 57 – Results of the thiolation of bromosporopollenin using thiourea and a subsequent alkaline hydrolysis

For application to bromosporopollenin **15**, the protocol detailed in Section C-5.9.1.2 was adapted with different solvents. In a first instance, DMSO was used following Aoki *et al.*[324] Then reaction was attempted in methanol, as suggested by Bradshaw *et al.*[325] The expected reaction is illustrated in Figure 52.

Sulphur loadings in the product **28** were determined by combustion elemental analysis (see Table 111). The corresponding results, gathered in Table 57, showed that the reaction incorporated much less sulphur when performed in methanol as opposed to DMSO. It could be objected that DMSO might still be adsorbed to or absorbed in the final thiosporopollenin **28**, hence inducing a bias in the measurement. However, this seemed utterly improbable as DMSO, being highly water-soluble, must have been washed away by the several washing steps and overall by the alkaline hydrolysis. The lower level of sulphur was thus explained more likely by the difference in reaction temperature, since reflux takes place at 65°C in methanol and 189°C in DMSO. This was supported by the trial carried out at room temperature, which showed minimum thiolation. Refluxing at 65°C was still insufficient to generate high loadings. As a conclusion, DMSO, used in previous thiolations,[12,153] was confirmed as the solvent of choice.

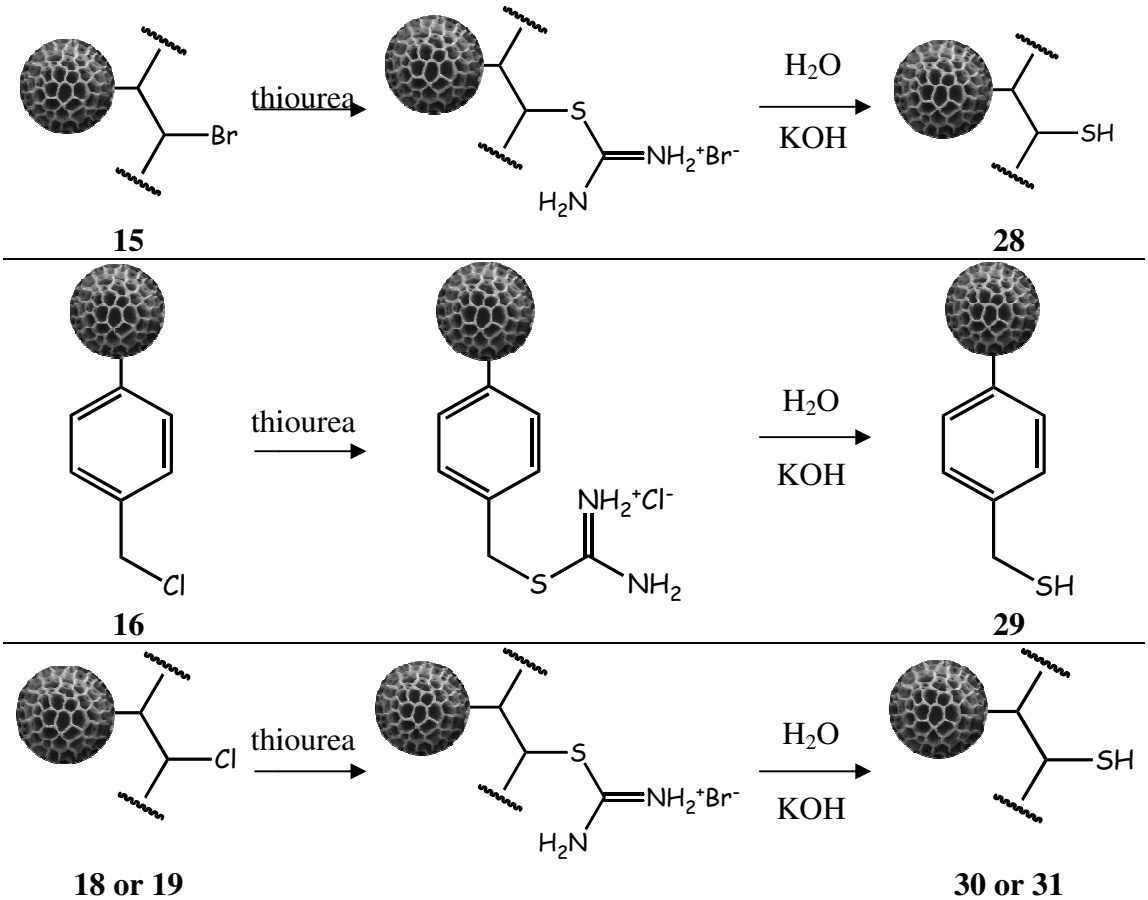

Figure 52 – Thiolation of halogenated sporopollenin with thiourea – Hypothesis highlighting the functional groups concerned by potential changes and the isothiouronium intermediate

Thiolation of chlorinated and chloromethylated sporopollenins **18** and **16** with

thiourea was thus performed in DMSO under reflux as described above and in Section C-5.9.1.2. The isothiouronium salt obtained was then hydrolysed in potassium hydroxide. The reaction principle was identical to that illustrated in Figure 52.

Sulphur loadings in the products **29**, **30** and **31** were determined by combustion elemental analysis (see Table 111). Two important comments can be made regarding the results collated in Table 57 and Table 58, and they are most probably linked. Firstly, similarly to sodium hydrogen sulphide (see Section B-5.5.2.1), the thiolating agent appeared to have introduced more sulphur than initially expected according to the substitution mechanism envisaged; however, in this case, no polymerisation of sulphides could explain the high level of sulphur. Secondly, nitrogen was present in thiosporopollenins **28**, **29**, **30** and **31** while initial halogenated sporopollenins **15**, **16**, **18** and **19** were virtually nitrogen-free; this could have two origins: incomplete hydrolysis of isothiouronium salts and side reactions.

Initial sporopollenin		**Ratio thiourea/Cl¶ (mol.mol^{-1})**	**Thiolated sporopollenin**			**Ratio S / Cl ‡ (%)**
Sample	**Chloride loading* (mmol.g^{-1})**		**Sample**	**Sulphur loading† (mmol.g^{-1})**	**Nitrogen loading† (mmol.g^{-1})**	
18	0.80 (0.30)	5	**30**	1.43 (0.86)	1.05 (0.64)	170
16	0.90	5	**29**	1.60	1.50	178
	0.80	3		0.68	0.92	85

Standard deviation is given in brackets after the results when available.
* determined by gravimetric analysis after hydrolysis in sodium hydroxide;
¶ equivalents of thiourea used vis-à-vis chloride loading; † determined by combustion elemental analysis; ‡ quotient of sulphur loading in final product by chloride loading in initial sample

Table 58 – Results of the thiolation of chloro- and chloromethyl sporopollenins using thiourea and a subsequent alkaline hydrolysis

Some of the nitrogen present in thiolated sporopollenins certainly reflected on only partial hydrolysis of isothiouronium salts by potassium hydroxide in the second step of the treatment. Steric hindrance and sporopollenin's intricate structure might explain it, as surprising as it can be. Even a second hydrolysis could not remove all nitrogen and only reduced its content in product **28** from 2.07mmol.g^{-1} (batch **2**) to 1.69mmol.g^{-1} (batch **2a**) (see Table 111).

Thiourea must also have induced secondary reactions with other functional groups of sporopollenin, hence explaining the some of the nitrogen and the high loading of sulphur. Carboxyls could form thioesters and Michael type additions could be envisaged on conjugated systems, but none of the products would withstand hydrolysis.

Speculative additions-cyclisations or cycloadditions yielding aminothiazole-type cycles could be a bit far-fetched. Ergo, hypothetical side reactions proposed are still very ill-defined and controversial. A rational explanation was even more difficult to rise after it had been verified that no sulphur could be loaded in underivatised sporopollenin (AHS, **1**), using the same conditions, if no prior halogenation had been performed (see Table 111, batch no. **0**).

The amount of unhydrolysed isothiouronium salts (and speculative by-products mentioned above) was directly determined by the nitrogen content (two nitrogen atoms were considered to be held per nitrogenous entity), and equated to the quantity of sulphur involved in them. Therefore, the level of free thiols could be estimated by difference with the total loading of sulphur. The data collated above were thus used to suggest the possible loadings of by-products and thiols in Table 59. Estimated loadings of thiols were found to match approximately the levels of halide in initial sporopollenin samples. This tended to show that all isothiouronium intermediate was hydrolysed and that most halide had been substituted by thiourea. This was however only a hypothetical evaluation and further chemical assays were develop to determine the loading of thiols really available to nucleophilic substitution (see Section B-5.5.4.1) and to disulphide bridge formation (see Section B-5.5.4.2).

Initial sporopollenin		**Thiolated sporopollenin**				
Type	**Halide loading*** **(mmol.g^{-1})**	**Type**	**Sulphur loading† (mmol.g^{-1})**	**Nitrogen loading† (mmol.g^{-1})**	**By-product loading (mmol.g^{-1})**	**Thiol loading (mmol.g^{-1})**
15	4.39	**28**	5.21	2.60	1.30	3.91
16	0.90	**29**	1.60	1.50	0.75	0.85
	0.80		0.68	0.92	0.46	0.22
18	0.80	**30**	1.43	1.05	0.53	0.91
19	0.60	**31**	0.82	0.59	0.30	0.52

* determined by gravimetric analysis after hydrolysis in sodium hydroxide;
† determined by combustion elemental analysis

Table 59 – Interpretation of the thiolation results in term of free thiol loading

In conclusion, thiourea could possibly have introduced thiol groups but this still required to be proven by such as formation of disulphide linkages (e.g. using Ellman's reagent or cysteine) and reaction with electrophiles (e.g. alkyl isothiocyanates). It was estimated that most of the halogens could have been converted as expected to thiols. However, part of it was attached to sporopollenin to yield functions that were not

accessible for further reaction. As a consequence, alternative reagents were sought to provide a cleaned product and enable confirmation of the generation of thiol groups on sporopollenin.

5.5.2.3 Thiolation with thioacetic acid

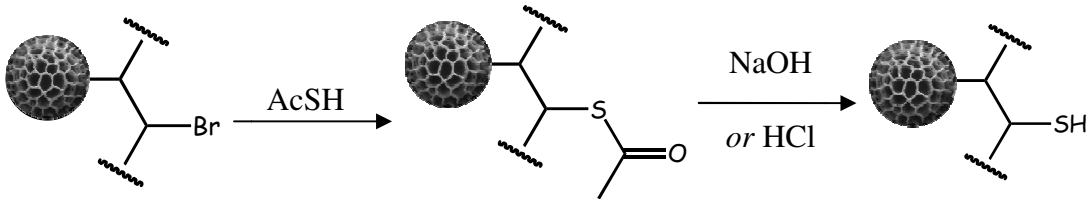

15 **32a** **32b**

Figure 53 – Thiolation of bromosporopollenin with thioacetic acid – Hypothesis highlighting the functional groups concerned by potential changes and the thioester intermediate

In order to avoid the problematic introduction of nitrogen, a nitrogen-free substitute was sought for thiourea. Potassium thioacetate is a thiolating agent used to form thioesters in tosylated positions of sugars.[326] A similar reaction was thus attempted on bromosporopollenin, to substitute bromine with thioacetic acid. Once again, this procedure, detailed in Section C-5.9.1.3, involved two steps: attachment of the thioacetate substituent, and then hydrolysis of the intermediate thioester. Hydrolysis could be performed under either acidic or basic conditions. The expected reaction is illustrated in Figure 53.

Bromosporopollenin 15 Bromine loading* (mmol.g^{-1})	**Hydrolysis**	**Thiosporopollenin 32b Sulphur loading† (mmol.g^{-1})**
1.85	none	0.80
	acidic	0.80
	basic	0.60

* determined by gravimetric analysis after hydrolysis in sodium hydroxide; † determined by combustion elemental analysis

Table 60 – Results of the thiolation of bromosporopollenin using thioacetic acid and subsequent hydrolysis

Results, gathered in Table 60, showed that the hypothesised reaction gave lower levels of sulphur in final thiolated sporopollenins than previously (see Sections B-5.5.2.1 and B-5.5.2.2). The fact that halogens are not as good leaving groups as sulphonyl ligands (such as tosyls) was a probable reason for poorer loadings. This reaction was however not repeated and the level of thiols was not chemically assayed by

disulphide bond formation or nucleophilic substitution. Consequently, thioacetic acid (or potassium thioacetate) could be given further consideration in the future as a viable thiolating agent for sporopollenin, which would yield a nitrogen free product.

5.5.2.4 Thiolation with sodium thiosulphate

A further thiolation pathway was studied involving Bunte salts, which are alkylthiosulphate type components.[327] They are readily obtained using sodium thiosulphate[328] and their further acidic hydrolysis yields thiols. Sodium thiosulphate could therefore constitute a cheap, non-toxic, non-pungent and nitrogen-free thiolating agent. The only drawback, when compared to sodium hydrogen sulphide, is the need for a hydrolysis step, but this is common with all other methods.

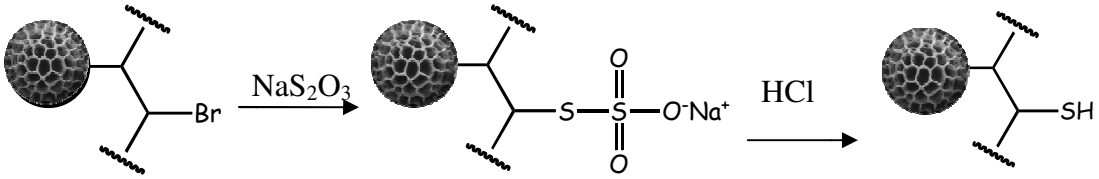

15 **33**

Figure 54 – Thiolation of bromosporopollenin with sodium thiosulphate – Hypothesis highlighting the functional groups concerned by potential changes and the Bunte salt intermediate

A procedure, detailed in Section C-5.9.1.4, was devised using hydro-alcoholic solution of sodium thiosulphate and subsequent treatment with hydrochloric acid. Expected reaction is illustrated in Figure 54.

The level of sulphur in the final product was evaluated by combustion elemental analysis (see Table 114). Results showed that no sulphur and therefore no thiol group was attached to sporopollenin **33**. The expected product was thus not achieved in this very limited trial. Repetition of this reaction is necessary before any definitive conclusion can be drawn.

5.5.2.5 Conclusion

The attempts to use thioacetic acid or thiosulphate as alternative thiolating agents either gave low or zero sulphur levels by combustion elemental analysis. However, both reactions need to be repeated and backed up. Additionally, a more extensive exploration of reaction conditions may yield higher levels of attached sulphur.

The highest levels of sulphur attachment were achieved by thiolation of

halogenated sporopollenins using either sodium hydrogen sulphide or thiourea. However both techniques exhibited drawbacks. Hydrogen sulphide ions tended to form polysulphides and thiourea introduced unwanted nitrogenous functions in sporopollenin.

To solve the problem of formation of polysulphides, it could be advised to implement a reduction step, using DTT for instance, to remove excess sulphides and recover the expected thiols. This could prove an easy and quick procedure to test in further investigation of thiosporopollenin.

The use of thiourea remains unsatisafactory though, because of the covalent attachment of nitrogen to thiosporopollenin. Basic hydrolysis of the isothiouronium intermediate did not remove all of it. An alternative acidic hydrolysis might be envisaged to possibly decrease the loading of unwanted nitrogenous function, and maybe eliminate them.

5.5.3 FTIR spectroscopy of thiosporopollenin

Investigation of thiosporopollenin by FTIR spectroscopy was performed with products **25**, **26a**, **26b**, **27**, **28**, **29**, **30** and **31**, and spectra are displayed in Appendices I-15 to 22. Results were not very meaningful since the spectra did not show any difference to those of starting materials (**15**, **16**, **18** and **19**). Indeed , removal of halogen by treatment with sodium hydrogen sulphide or thiourea could only be monitored by changes in the fingerprint region (550-800ppm), where a peak could still be observed in all of the thiosporopollenins' spectra. Thiol groups could also possibly show a band at 2550-2600ppm, although it was too weak to break through of the baseline noise.

5.5.4 Further reactions on thiosporopollenin

Many conventional analytical methods (e.g. liquid-phase NMR) were not possible with sporopollenin derivatives as they cannot be dissolved in solvents commonly used for NMR spectroscopy. Mass spectrometry cannot be used as the sporopollenin is too involatile. Therefore, combustion elemental analysis was regarded as a convenient means to follow reactions, since sporopollenin does not contain sulphur, despite a certain lack of repeatability regarding sulphur determination.[329] It is however not functional-group specific.

Consequently, alternative analytical means had to be implemented to specifically assess the loading of free thiols in the target thiosporopollenins. These analytical

methods involved different properties of thiols: their nucleophilicity and their ability to form disulphides. Both types of reactions were not only used for analysis but also to demonstrate the possibilities of further derivatisations of thiolated sporopollenin. In the present study, nucleophilic substitutions and oxidative disulphide attachments were carried out using thiolated sporopollenins **25** and **28** obtained from bromosporopollenin (**15**) by treatment with sodium hydrogen sulphide and with thiourea respectively.

5.5.4.1 Nucleophilicity

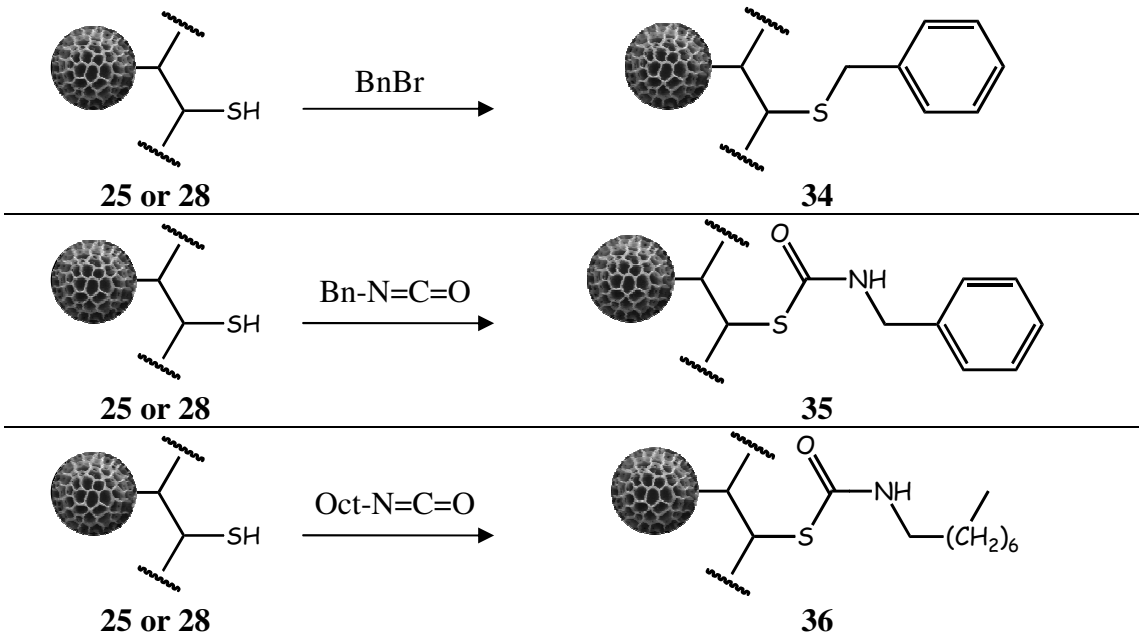

Figure 55 – Nucleophilic substitutions on thiols of thiosporopollenin with benzylbromide, benzylisocyanate and octylisocyanate

Thiols are known to react with electrophiles. Mercaptide ions exhibit a strong nucleophilicity due to the relatively large and highly polarisable sulphur atom. Industrial measurements, performed in the past on commercial resin **G** as catalogued in Section B-5.5.1, exemplify it when applied to analytical purposes.[279] Indeed, when this PS-thiophenol was sold by Argonaut Technologies Inc., the company used to analyse the thiol content based on its benzylbromide uptake, since the resin was known to scavenge alkylating reagents. Similarly, sulphur loading on commercial resin **E** was industrially evaluated after nucleophilic substitution.[281] In the same vein, nucleophilicity of thiosporopollenin was assessed in this study using the following compounds: benzylbromide, benzylisocyanate and octylisocyanate.

The scavenging capacities of thiolated sporopollenin were evaluated with benzylbromide according to the procedure detailed in Section C-5.9.4.1. The amount of

benzylbromide attached was assayed by weight difference based on the blank being the non-derivatised sporopollenin AHS **1**. The expected reaction is illustrated in Figure 55. According to the results gathered in Table 61, the data were not very coherent and standard deviations were found to be quite high. Ergo weight difference was considered biaised and uptake of an alkylating agent was not regarded as a good way to evaluate the loading of free thiols.

Sample	**Sulphur loading (mmol.g^{-1})***	**Benzylbromide uptake† (mmol.g^{-1})**
AHS (**1**)	0.00 (0.00)	3.86 (3.46)
25	2.90 (0.80)	1.62 (0.24)
28 (in DMSO)	4.43	2.10 (0.23)
28 (in ethanol)	1.20	5.02

Standard deviation is given in brackets where available.
* determined by combustion elemental analysis; † determined by weight difference

Table 61 – Benzylbromide uptake by sporopollenin (native and thiolated)

In order to avoid monitoring attachment by weight difference, nitrogenous electrophiles were then chosen such that combustion elemental analysis could be used (see results in Table 119 and Table 120). Isocyanates were good candidates since they present a suitably electrophilic carbon atom and the desired nitrogen. Reactions of benzylisocyanate and octylisocyanate with thiosporopollenins **25** and **28** were performed following the procedures described in Sections C-5.9.4.2 and C-5.9.4.3. Blanks were also carried out with underivatised AHS (**1**). The expected reaction is illustrated in Figure 55.

According to the results gathered in Table 62, isocyanates were readily attached covalently to non-derivatised sporopollenin (AHS, **1**) since they are very electrophilic. They can indeed undergo nucleophilic substitutions with hydroxyl groups present in AHS, whose loading had been evaluated at ca. 1mmol.g^{-1} in past studies.[12,13] This matched approximately the loadings of isocyanates bonded to native sporopollenin (**1**).

Isocyanates were also attached covalently to thiosporopollenins **25** and **28**, according to the data shown in Table 62. The loading level of isocyanate in sporopollenin was evaluated by combustion elemental analysis based on nitrogen. However, important inconsistencies were observed. It is also noteworthy that the presence of nitrogen in initial thiosporopollenin **28**, obtained by treatment of AHS (**1**)

with thiourea (see Section B-5.5.2.2), had to be taken into account (see total loading of isocyanate in Table 62). This showed some incoherence; for example, after the uptake of octylisocyanate in thiosporopollenin **28** without using triethylamine, the percentage of nitrogen was lower than in the starting material. In addition, when the three blanks, performed with underivatised sporopollenin (AHS, **1**), were also deduced from the results (see loading of isocyanate relative to blanks in Table 62) then only certain results were still meaningful, precisely the uptake of octylisocyanate by **25** (55%) and benzylisocyanate by **28** (50%).

Initial sporopollenin			**Sporopollenin isocyanate derivative**			
Product	**Sulphur loading* (mmol.g^{-1})**	**Nitrogen loading* (mmol.g^{-1})**	**Type of isocyanate**	**Loading of nitrogen (mmol.g^{-1})†**	**Loading of isocyanate (mmol.g^{-1})**	
					total§	**relative to blanks (1)**
1	0.00	0.00	Benzyl isocyanate	1.01		
			Octyl isocyanate	0.83		
			Octyl isocyanate‡	0.38		
25 (batch 1)	2.73	0.09	Benzyl isocyanate	1.02 [37%]	0.93 [34%]	N/d
			Octyl isocyanate	2.43 [89%]	2.34 [86%]	1.51 [55%]
			Octyl isocyanate‡	0.82 [30%]	0.73 [27%]	0.30 [11%]
28 (batch 2a)	2.42	1.60	Benzyl isocyanate	3.83	2.23 [92%]	1.22 [50%]
			Octyl isocyanate	2.13 [88%]	0.53 [22%]	N/d
			Octyl isocyanate‡	0.37 [15%]	N/d	N/d

Equivalent percent ratios of sulphur atoms involved in attachment of isothiocyanate are given in square brackets.
* determined by combustion elemental analysis; † based on combustion elemental analysis only; § data obtained by deduction of the nitrogen content initially present in **25** or **28**; ‡ reaction conditions were changed: no triethylamine was used.

Table 62 – Attachment of benzylisocyanate and octylisocyanate to sporopollenin (native and thiolated)

Attachment of octylisocyanate was attempted both with and without triethylamine, in order to verify that the base was necessary to obtain good loadings. According to the results shown in Table 62 and taking blanks and initial nitrogen into

account, as aforementioned, hardly any octylisocyanate was attached to sporopollenin without using triethylamine.

On the contrary, when it was used, up to more than 50% of the sulphur present in thiosporopollenins were found available for derivatisation with isocyanate. However, it seems surprising that octyl- and benzylisocyanates reacted selectively with **25** and **28** respectively. The most probable reason for such findings is that of problematic evaluation of the actual isocyanate uptake in **28** due to the presence of nitrogen in initial thiosporopollenin in large proportions.

Several phenomena could explain the partial loading observed. First, the intricated structure of sporopollenin might induce an important steric hindrance around the thiols, hence limiting their reactivity. Also, sulphur atoms of thiourea-treated sporopollenin could be involved in functions other than thiols as highlighted in Section B-5.5.2.2. This made evaluation of the real uptake of isocyanates relatively difficult.

5.5.4.2 Investigation into the formation of a disulphide linkage

In the early 1960s, an efficient method was designed to analyse thiol groups in proteins[330] and has been more recently applied to determine thiol loadings in resins.[331] The protocol is based on the reaction of DTNB (or Ellman's reagent)[332] with thiols *via* the oxidative formation of a disulphide bridge. Ellman's reagent was therefore used to assay free thiols in thiosporopollenin. Two methods were derived from the literature[331] to implement the procedure detailed in Section C-5.9.2. Reaction involved the cleavage of DTNB's disulphide bond in order to link one half to sporopollenin's thiols leaving the other moiety as a 2-nitro-5-thiobenzoate ion. That anion was then quantified by UV spectroscopy at 412nm, having a known absorption coefficient ε=13,600$dm^3.cm^{-1}.mol^{-1}$ at that wavelength. Expected reaction is illustrated in Figure 56. Assays were perfomed against blanks in which underivatised sporopollenin was used.

Results, displayed in Table 63, were unexpectedly low and did not match those obtained previously by nucleophilic substitution (see Section B-5.5.4.1). Use of a calibration curve could be envisaged in the future with hopefully more consistant results. However, since DTNB contains a nitro group, its attachment was confirmed by nitrogen combustion elemental analysis as shown in Table 63. The loading of Ellman's reagent, as determined by nitrogen elemental analysis, was still much lower than that of isocyanates that could be attached (see Table 62 in Section B-5.5.4.1). This could mean

that thiol groups reacted more readily by substitution than by disulphide bridge formation.

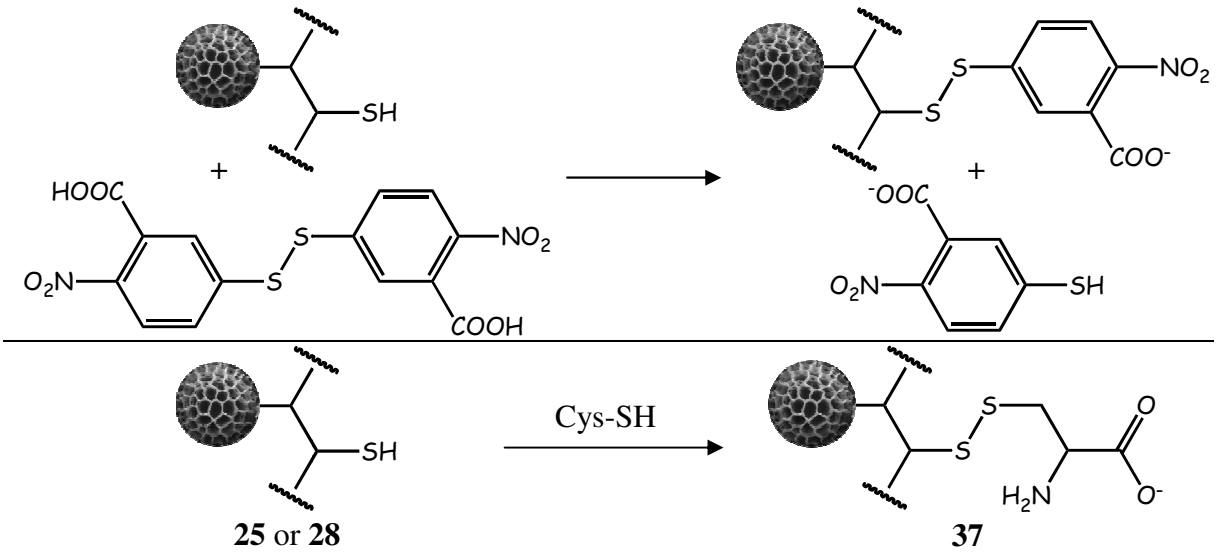

25 or **28** **37**

Figure 56 – Formation of disulphide bridges on thiosporopollenin – Reaction with Ellman's reagent and with cysteine

Creation of a disulphide bond to thiolated sporopollenin had already been investigated with cysteine in a previous study using DMSO and TFA as oxidising reagents.[153] Various methods are known to oxidise thiols into disulphides, including some catalytic routes.[333] Amongst them, hydrogen peroxide is one of the most widely used oxidising reagents[327] although this reagent also yields sulphonic acids as by-products.[334] Therefore, milder conditions involving oxidation by aerial oxygen in alkaline medium, as developed by Otto *et al.,*[335] were chosen to study the thiolated sporopollenins **25** and **28**.

Initial thiosporopollenin			Loading of DTNB (mmol.g^{-1})	
Sample	**Sulphur loading (mmol.g^{-1})***	**Nitrogen loading (mmol.g^{-1})***	**Spectroscopic assay**	**Nitrogen elemental analysis***
AHS **1**	0.00 (0.00)	0.00 (0.00)	0.013† 0.003‡	-
25	1.85	0.16	0.024† (0.005) 0.018‡ (0.001)	0.34
28	2.42	2.24	0.048‡ (0.037)	0.37

Standard deviation is given in brackets where available.
* determined by combustion elemental analysis; † analysis in methanol;
‡ analysis in methanol/THF

Table 63 - Attachment of Ellman's reagent to sporopollenin (native and thiolated) by disulphide bonds

Air was simply bubbled through the reaction mixture following the method described in Section C-5.9.3.1. This was expected to oxidatively bind cysteine's thiol group to the thiolated sporopollenins, as illustrated in Figure 56. In order to lead the reaction to completion, cysteine was used in excess and contact time varied to enable equilibrium to be reached. Most trials were conducted in an alkaline medium, dilute aqueous sodium bicarbonate, but reaction was also experimented in DMSO, following a protocol by Sanz *et al.*[336] Trials were carried out at room temperature in order to avoid the potential attachment of the amino group of cysteine. A parallel reaction of alanine with thiosporopollenin under similar conditions (see method in Section C-5.9.3.1) showed that no amino acid was covalently linked to the polymer by peptide bond: elemental analysis exhibited 0.00% nitrogen. Reaction of cysteine with underivatised sporopollenin constituted another blank to check that no secondary reactions occurred.

The determination of cysteine loading level by nitrogen elemental analysis (see Table 116) showed that attachment of cysteine by disulphide bridges under aerial oxidation was nearly as efficient as that of DTNB. The reaction parameter, the loading of cysteine and the proportion of thiols available in thiosporopollenin to form disulphide bonds are gathered in Table 64.

Initial sporopollenin		**Media**	**Ratio Cys/S (mol.mol^{-1})**	**Reaction time (days)**	**Cysteine loading (mmol.g^{-1})**	**Availability of thiols (%)**
Type	**Sulphur loading* (mmol.g^{-1})**					
AHS **1**	0.00	$NaHCO_3$	-	0.5	0.09†	-
25	1.85		7.0	0.5	0.49†	26
	3.68		3.5	5	0.28† 1.22‡ 1.29¶	8 33§ 35§
28	4.43		2.9	0.5	0.20†	5
			4.5	4	1.69†	38§
25	3.68	DMSO	5.4	2	0.23† 0.70‡	8§ 19§

* determined by combustion elemental analysis; † based on nitrogen combustion elemental analysis; ‡ determined by ninhydrin method after reduction in acetic acid; ¶ determined by ninhydrin method after reduction in acetic acid with zinc catalyst; § samples that were not washed with hydrochloric acid

Table 64 – Results of oxidative disulphide bonding of cysteine to sporopollenin

The results, displayed in Table 64, showed that up to ca. 30-40% of the sulphur was composed of thiols accessible to disulphide bond formation. This was however lower than the availability of thiols to nucleophilic substitution by isocyanates (see

Section B-5.5.4.1). The acidic washings performed during the treatment of the final samples were initially thought to break the newly formed disulphide bond. Indeed the reduction step, as developed in this study (see Section C-5.9.3.2), involved treatment in acid; therefore even dilute hydrochloric acid could have cleaved some of the disulphide bridges, hence lowering the cysteine loading. Nevertheless, a method was implemented that avoided the use of acid during the washings. The results, displayed in Table 64, indicate that whether the final sample was washed with dilute acid or not did not seem to change the availability of thiols. Results were found relatively inconsistent, ranging from 5% up to 38%.

Therefore, the data were backed up by other analytical methods. Reduction of the disulphide bridges was envisaged in order to quantify the cysteine released. Reduction was performed on two of the previous samples in dilute aqueous acetic acid following the method detailed in Section C-5.9.3.2. The amount of cysteine released was analysed by a method involving ninhydrin,[238] recently improved[337] and detailed in Section C-5.1.5. The results, displayed in Table 64, showed that a larger amount of cysteine was attached to thiosporopollenin than detected by combustion elemental analysis. The method of quantification involving the reductive release of cysteine was believed to be the most efficient to demonstrate the successful formation of disulphide bridges, since it involved the specific cleavage of sulphur-sulphur bonds. Incidentally, the use of zinc powder as a catalyst during the reduction step did not prove to change the release of cysteine (see Table 64).

5.5.5 Conclusion

Versatility of sporopollenin was used here to attach thiols and convert it into a solid support for such a functionality. Sporopollenin was initially halogenated in order to prepare it for subsequent substitution of halogens by thiol groups.

Different methods of thiolation were investigated including the use of sodium hydrogen sulphide, thiourea, thioacetic acid and sodium thiosulphate. The first two methods enabled to yield high loading levels of sulphur in target thiolated sporopollenin (2-4mmol.g^{-1}), despite some recurrent problems like the formation of polysulphide or the introduction of nitrogen in the structure, depending on the reagent used. Sodium hydrogen sulphide and thiourea have been largely used to make the desired thiolated sporopollenin that was investigated to establish that the loaded sulphur could be identified as thiol groups.

Thus, availability of thiols on thiosporopollenin was investigated with regard to their reactivity with electrophiles. Alkyl isocyanates were found to covalently bind to sporopollenin with various and inconsistent loading levels depending on the reagent used. Up to more than 50% of sulphur present in thiosporopollenin was available for nucleophilic substitution. However, it is noteworthy that other nucleophilic groups present in sporopollenin (e.g. hydroxyl groups) might compete with the thiols. A study was also devised with cysteine, to form oxidative disulphide bonds. It appeared that up to nearly 40% of the sulphur present in thiosporopollenin was available to form disulphides.

In conclusion, thiolation of sporopollenin, formed either by treatment with sodium hydrogen sulphide or with thiourea, generated a material which showed similar functional group properties to those expected from solid-supported thiol groups (e.g. thiolated polystyrene-based resins). Isocyanates and cysteine, for instance, were attached with loading levels (0.5-2.5mmol.g^{-1}) close to those found in commercial resins (1-5mmol.g^{-1}).

6 Conclusions

Relatively simple and convenient methods have been developed to isolate sporopollenin from pollen grains and spores. The resulting exines were then applied with two objectives: physical encapsulation of products within them and chemical derivatisation of the polymeric material itself. These different and complementary uses offered a wide scope of applications ranging from oral or topical drug delivery to food and cosmetic formulation, to novel solid resins for scavenging, ion-exchange or solid-phase organic synthesis. Several authors have proved that emptied pollen grains could be filled with various substances, although this was the first systematic study carried out on encapsulation within exines, especially those from the commercially available *Lycopodium clavatum* spores. However, sporopollenin derivatisation has been investigated over the past ten years, in this laboratory, and the present work presents more detailed and systematic study of both physical and chemical characteristics to demonstrate the potential both physical and chemical attachments and thus offer greater possibilities of its being exploited commercially.

Encapsulation of a compound inside exines by physical entrapment was possible thanks to the porous nature of sporopollenin. This yielded powdery formulations with high loadings. Important levels of encapsulated product (over $2g.g^{-1}$) could be reached by using neat liquids (such as oils). Solids had to be dissolved beforehand to very high concentrations in order to increase the final loading as much as possible; ergo saturated solutions were often sought for. In this case, the solvent had to be chosen to maximise on concentration levels and as a consequence loading levels. Also, important is the need to remove the solvent without losing loading or denaturing the loaded product through such as evaporation or freeze-drying. A wide range of products were physically attached in exines including small mineral and organic molecules as well as larger ones such as carbohydrates, nucleic acids or fats, or even macromolecules like proteins and oligonucleotides. By contrast, much lower loadings were obtained by chemical attachment of a compound to sporopollenin. This is because the inner cavity of the exines is comparatively vast in relation to the number of chemical groups on sporopollenin capable of being derivated to anchor the material to be loaded.

Encapsulation seemed the better means of loading for such as oral drug delivery since high loading could be achieved while minimal change is effected to the natural

product, *i.e.* sporopollenin. Therefore the natural sporopollenin has great universality of application which is important in potential future legislation through such as the FDA or MHRA. It has been observed that intact exine microcapsules readily entered the blood stream through the gut lining following oral uptake; hence offering the potential for direct oral uptake of a number of drugs if they can be suitably encapsulated and then transported with the exines.

Importantly, sporopollenin microcapsules could be used with proteins without any apparent denaturation of the latter, as illustrated with alkaline phosphatase. Furthermore, some interesting protective effects were observed on loaded oils. Exines partly shielded UV light and, overall, exhibited antioxidant properties, so that they limited greatly aerial and luminous oxidation of fats and even improved their condition with regard to rancidity, in some cases. The exact mechanism has not yet been fully defined and therefore further studies are needed. More extensive investigations on oils and cyclic voltammetry are currently in progress to determine the exact source of sporopollenin's antioxidant nature. Taste masking abilities of exines were also discovered and could open up on food applications with pungent fish oils or oral drug formulation with bitter medications such as ibuprofen.

Chemical derivatisation of sporopollenin offers possibilities for new types of bioconjugates. Once covalently bonded to sporopollenin, an active principle would form a protecting pro-drug that could potentially be more stable than encapsulation if the attached product and anchoring functionalities resist gastric conditions. Whether by physical or chemical attachment to sporopollenin, preparation of a drug for oral delivery is very attractive, as opposed to parenteral delivery, for the comfort and simplicity it offers to the patient, as well as the easiness in the fabrication and sterilisation.

Unfortunately, in order to applied newly derivatised sporopollenin to oral drug delivery, food industry or cosmetics, each one of them has to undergo a full pharmaceutical investigation so as to be legally recognised as safe (toxicity date showing harmlessness), and then accepted as a drug or a safe food additive (typically, FDA or HMRA approval). Pollen is already GRAS (generally recognised as safe) and sold in health food shops whereas sporopollenin, as such, has got to go through such legislation. However, in the past ten years extracts of pollen have been FDA-approved for neutraceutical products such as Femal®[338,339] and Prostat®.[340] Physical attachment being regarded as a formulation, no new compound is created by encapsulation in native sporopollenin microcapsules; ergo the legal process for the final mixture would be much

easier, more rapid (by years) and, consequently, cheaper.

However, chemically modified sporopollenins could be used for applications other than food, drug or cosmetics. Derivatising exines could aim at creating novel resins to replace synthetic ones made out of non-renewable starting materials. Sporopollenin-based derivatives can be used in replacement of modified polystyrenes as cheap ion-exchange resins, robust specialised scavengers for various chemicals or resistant support for solid-phase synthesis. To mimic artificial derivatised polymers, various functional groups have been introduced on sporopollenin, namely primary and secondary amides, primary amines, bromines, chlorines, chloromethyls, azides and thiols. Investigations were also carried out with most of them to involve them in further reaction. Succinic anhydride was attached to aminosporopollenin and a whole linker was synthesised. Substitutions of halogens for thiols or azides were systematically studied in halogenated sporopollenins. Azides were then reduced to primary amines. And finally, nucleophilic substitutions and oxidative disulphide bridging were performed with thiosporopollenin. All the reactions involved in sporopollenin derivatisation were classic and simple. However, more can be envisaged. Examples have been given of potential novel applications of aminated sporopollenins such as a solid mimic of triethylamine or a brominating resin; quaternisation of aminosporopollenin could also offer new perspective as anion-exchange resin or solid particular surfactant. Moreover, most functional groups of derivatised sporopollenin (e.g. carboxyls, amines, thiols) could chelate metallic ions and open up a whole new range of applications; apart from being ion-exchange resins and scavengers, they could form metallic active principles (e.g. with antimony against leishmaniasis,[341] gold against rheumatoid arthritis[342] or cisplatin against some cancers[343]), chromatography supports for protein purification (e.g. with nickel), or solid-supported catalysts (e.g. with palladium).

For all targeted applications, sporopollenin exines' interest lies in the fact that they offer potent properties competing with existing products, whether being microcapsules, ion-exchange resins, scavengers or solid supports for heterogeneous synthesis. These qualities are exines's high monodispersity (within one species), their chemical inertness, their mechanical stability, their biocompatibility and their commercial availability for rather low prices (especially when *Lycopodium clavatum* spores are used).

C. Experimental

Note: When centrifugation was used, the relative centrifugal force (*RCF*) applied was given in *g*-force, and calculated as: $RCF = 1.118\times10^{-5}\times r\times N^2$, with r being the radius from the central fulcrum to the centrifuge tube (in cm) and N the speed of the centrifuge spindle (in rotations per minute).

1 Material and apparatus

S-type *Lycopodium clavatum* L. spores were purchased from G. Baldwin & Co (London, UK), Unikem (Copenhagen, Denmark) and Tibrewala International (Katmandu, Nepal), L-type *Lycopodium* spec. spores from Post Apple Scientific (North East, USA) and Cedar Vale (USA) and *Ambrosia trifida* pollen from Sigma-Aldrich (Poole, UK). *Aspergillus niger* was generously provided by Tate & Lyle PLC (Selby, UK) and *Chlorella vulgaris* by maBitec Gmbh (Bruckmühl, Germany).

Cocoa butter, beeswax, carnauba wax and gum Arabic were supplied by Nestlé Ltd. (York, UK), echium oil by Springdale Crop Synergies Ltd. (Driffield, UK), rapeseed oil by Aarhus United Ltd. (Hull, UK), enfuvirtide (*Fuzeon*) by F. Hoffman-La Roche Ltd. (Basle, Switzerland), and growth hormones (1,097Da and 3,340Da) by Ipsen (Barcelona, Spain).

Integrin beta-1 antibody was provided by Leigh Madden (University of Hull, Hull, UK), fluorescein-tagged oligonucleotides by Tom Brown (University of Southampton, Southampton, UK), fish vaccines by Joseph Banoub (Memorial University of Newfoundland, St. John's, Canada), TSAO-T by Christophe Len and Pierre Villa (Université de Picardie Jules Verne, Amiens, France) and PL30-peptide-FITC and NU:UB 363-FITC by David Mincher (Napier University, Edinburgh, UK).

Cod liver oil and ethyl eicosapentenoate were purchased from Seven Seas Ltd. (Hull, UK), (+)-limonene (*Histoclear* II) from National Diagnostics Inc. (Atlanta, USA), *Lyc-O-Mato* from Vita Healthcare Ltd. (London, UK), sunflower and soybean oils from Tesco plc, alkaline phosphatase (ALP) and 9*H*-(1,3-dichloro-9,9-dimethylacridin-2-one-7-yl)phosphate diammonium salt (DDAO-phosphate) from Bio-Rad (Hercules, USA), *Humatrope* from Eli Lilly & Co (Indianapolis, USA).

Other chemical reagents were purchased from Sigma-Aldrich, Fisher Scientific UK Ltd., Lancaster Synthesis Ltd., Avocado Organics or Merck KGaA.

1.1 Combustion elemental analysis

Elemental analyses were performed on a Fisons instrument Carlo Erba EA 100 C H N S analyser. Analyses were carried out at the University of Hull by Carol Kennedy, Department of Chemistry, in duplicate for each sample and the elements percentages (*%C*, *%H*, *%N*, *%S*) shown were the mean values of the analyses.

The loadings of nitrogen and sulphur (mmol of element per gram of sporopollenin) were respectively calculated as follows: $loading_N = \frac{\%N \times 10}{14}$, as the molar weight of nitrogen is 14g.mol^{-1}, and $loading_S = \frac{\%S \times 10}{32}$, as the molar weight of sulphur is 32g.mol^{-1}.

1.2 Fourier transform infrared (FTIR)

IR spectrophotometry was carried out on a Perkin-Elmer Paragon 1000 Fourier Transform Infra Red Spectrometer. Samples were ground with anhydrous potassium bromide (spectrosol grade) to produce disks to a ratio of 1/9 (w/w). FTIR spectra were a result of 4 scans against a background.

1.3 Ultraviolet (UV) spectrophotometry

UV absorption spectra were recorded on a Perkin-Elmer Lambda 10 ultraviolet-visible double-beam spectrophotometer. Experiments were performed in single-use polymethyl methacrylate cells.

1.4 Microscopy

1.4.1 Scanning electron microscope (SEM)

Scanning electron micrographs were obtained using a Leica Cambridge Stereoscan 360 Scanning Electron Microscope (SEM). Tony Sinclair, Institute of

Chemistry for Industry, University of Hull, performed the SEM.

1.4.2 Laser confocal scanning microscope (LSCM)

Confocal images were obtained using a Bio-Rad Radiance 2100 laser scanning microscope equipped with Ar (488nm), Green HeNe (563nm) and Red diode (637nm) laser lines and connected to a Nikon TE-2000E inverted microscope from Nikon, Japan. Images were collected using LaserSharp2000.

1.4.3 Microtome sections

Spores were mixed with 2.5% glutaraldehyde using 0.1% cacodylate buffer, post fixed in 1% osmium tetroxide, dehydrated in aqueous ethanol starting with water/ethanol 7/3 (v/v), adding ethanol and decreasing water content. This last dehydration step was unnecessary for already dry exines.

Particles were then suspended in LR white (acrylic resin) in light vacuum then stained in toluidine blue. The resulting solid was finally sliced into slim translucent disks and mounted for TEM or LM observations. Microtome sections were performed at the University of Hull by Jan Halder, Department of Biological Sciences.

1.4.4 Light microscopy (LM)

Optical micrographs were obtained on a Nikon Upright Transmission Microscope, unless stated in the relevant experimental Sections (C-3.2 and C-3.4).

1.4.5 Transfer electron microscopy (TEM)

Transmission electron micrographs were obtained using a Jeol JEM 3010 Transmission Electron Microscope (TEM). Jan Halder, Department of Biological Sciences, University of Hull, performed the TEM.

1.5 Flame spectroscopy

1.5.1 Flame atomic absorption spectroscopy (FAAS)

Flame Atomic Absorption Spectroscopy was performed on a Perkin Elmer AAnalyst 100 instrument fuelled with acetylene oxygen gas and Hollow-Cathod lamps set for each metal ion to analyse.

1.5.2 Emission spectroscopy

Flame Atomic Emission Spectroscopy was carried out on a Corning 400 flame photometer fuelled with natural gas.

1.5.3 Inductively coupled plasma-optical emission spectrometry (ICP-OES)

Inductively Coupled Plasma-Optical Emission Spectrometry was performed on a Perkin Elmer Optima 5300DV Spectrometer by Robert Knight, Department of Chemistry, so as to determine ion concentrations and to carry out elemental analyses.

1.6 Solid-state magic angle spinning NMR (MAS NMR)

Samples were prepared for MAS NMR by packing exines (ca. 50mg) into 4mm MAS rotors. For ^{1}H NMR experiments, approximately water (50µl) was pipetted into the samples.

All NMR experiments were carried out on a Bruker Avance II 500MHz spectrometer using a 4mm MAS DVT probe, at a temperature of 293K. ^{1}H, ^{13}C, ^{15}N, ^{31}P measurements were acquired at operating frequencies of 500.1025MHz, 125.7546MHz, 50.697MHz and 202.456MHz, respectively. Samples were spun at 10kHz for ^{1}H measurements and 5kHz for ^{13}C, ^{15}N and ^{31}P detected measurements. Both ^{1}H and ^{13}C spectra were externally referenced to tetramethylsilane at 0ppm. ^{15}N and ^{31}P

measurements were externally referenced to *N*-acetyl leucine and phosphoric acid at 128.77ppm and 0ppm, respectively.

^{1}H experiments were conducted with a typical $\pi/2$ pulse length of 7μs, a relaxation delay of 4s and typically 256 scans. A Carr-Purcell-Meiboom-Gill (CPMG) pulse sequence with τ = 1.1ms and 8 loops was used as a T2 filter to remove very broad signals. CPMG spectra are the accumulation of 1024 scans. Water suppression was achieved using a presaturation pulse centred on the water peak.

Cross polarization (CP) experiments were performed with a 80-100% ramped proton pulse of typically 750μs for ^{15}N, 1.5ms for ^{13}C and 1ms for ^{31}P were used during the Hartmann-Hahn match. Hetero-nuclear proton decoupling of typically 70kHz was applied during 49ms acquisition time. The recycle delay time was 2s for ^{15}N, ^{13}C and ^{31}P.

All NMR data was processed using 'Topspin' Version 1.3 (Bruker Instruments, Karlsruhe, Germany).

2 Extraction of sporopollenin capsules

Development of extraction procedures is detailed in Section B-1.

2.1 *Lycopodium* spp. spores (S-type & L-type)

2.1.1 'Full treatment'

2.1.1.1 To obtain DFS

Raw *Lycopodium* spp. spores (200g) were suspended in acetone (900cm^3) and stirred under reflux for 4h. Defatted sporopollenin (DFS) was recovered by filtration (porosity grade 3 or 4), with 60% typical yield.

A strict control of temperature of the treatment at 60°C helped and kept L-type spores intact, without changing the yields significantly.

2.1.1.2 To obtain BHS

DFS (ca. 120g) was suspended in an aqueous alkaline solution [potassium or sodium hydroxide, 6% (w/v), 800cm^3] and stirred under reflux for 6h. After recovery of the particles by filtration (porosity grade 3 or 4), this treatment was repeated with renewed base. Particles were recovered by filtration and washed with hot water (5×100cm^3) and hot ethanol (5×100cm^3). The sample was then suspended in ethanol (800cm^3) and stirred under reflux for 2h. Base-hydrolysed sporopollenin (BHS) was recovered by filtration and dried in an oven at 60°C.

A strict control of temperature of the treatment at 80°C helped and kept L-type spores intact, without changing significantly yields and elemental analysis results.

Typical yields and combustion elemental analyses are gathered in Table 65.

	Base used	Typical yield (w/w)	Typical combustion elemental analysis (w/w)		
			%C	%H	%N
S-type BHS	KOH	30%	55%	7.5-8%	0.5%
	NaOH	30%	55%	7.5-8%	0%
L-type BHS	KOH	30%	45-50%	6.7-7%	0.5%
	NaOH	30%	50-55%	7-7.5%	0%

Table 65 – Results of extraction of BHS by 'full treatment' from *Lycopodium* spec.

2.1.1.3 To obtain AHS

BHS (ca. 60g) was suspended in 85% *ortho*-phosphoric acid (800cm^3) and stirred under reflux for 7 days. Particles were recovered by filtration (porosity grade 3 or 4), washed with water (5×100cm^3), ethanol (5×100cm^3) and dichloromethane (DCM, 3×50cm^3) and then finally suspended in DCM (750cm^3) with trifluoroacetic acid (5cm^3), stirred at room temperature overnight and recovered by filtration. The particles were washed with DCM (3×50cm^3), ethanol (3×50cm^3), water (3×50cm^3), 2M hydrochloric acid (3×50cm^3), 2M sodium hydroxide (3×50cm^3), water (3×50cm^3), ethanol (3×50cm^3) and DCM (3×50cm^3). Acid-hydrolysed sporopollenin (AHS) was finally recovered by filtration and then dried in an oven at 60°C.

A strict control of temperature of the treatment at 60°C and a shortening of reaction contact time to 5 days helped and kept L-type spores intact, without changing significantly yields and elemental analysis results.

Typical yields and combustion elemental analyses are gathered in Table 66.

	Typical yield (w/w)	Typical combustion elemental analysis (w/w)		
		%C	%H	%N
S-type AHS	20-25%	65%	7.5-8%	0.00%
L-type AHS	20-25%	60%	6.5-7.5%	0.00%

Table 66 – Results of extraction of AHS by 'full treatment' from *Lycopodium* spec.

2.1.2 'Hemi treatment'

2.1.2.1 To obtain 'one-pot BHS'

Raw *Lycopodium* spp. spores (200g) were suspended in an aqueous alkaline solution [potassium or sodium hydroxide, 6% (w/v), 800cm^3] and stirred under reflux for 6h. After recovery of the particles by filtration (porosity grade 3 or 4), this treatment was repeated with fresh base. Particles were recovered by filtration, washed with hot water (5×100cm^3) and hot ethanol (5×100cm^3), suspended in ethanol (750cm^3) and stirred under reflux for 2h. One-pot base-hydrolysed sporopollenin (1-pot BHS) was recovered by filtration and dried in an oven at 60°C.

A strict control of temperature of the treatment at 80°C helped and kept L-type spores intact, without changing significantly yields and elemental analysis results.

Typical yields and combustion elemental analyses are gathered in Table 67.

	Typical yield (w/w)	**Typical combustion elemental analysis (w/w)**		
		%C	**%H**	**%N**
S-type one-pot BHS	30-40%	50-55%	7.8%	0.0%
L-type one-pot BHS	40-50%	45-50%	6.5-7%	0.4%

Table 67 – Results of extraction of 'one-pot BHS' from *Lycopodium* spec.

2.1.2.2 To obtain 'two-pot AHS'

BHS (ca. 80g) was suspended in 85% *ortho*-phosphoric acid (500cm^3) and stirred under reflux for 7 days. Acid-hydrolysed sporopollenin (AHS) was recovered by filtration (porosity grade 3 or 4), washed with water (5×100cm^3), ethanol (5×100cm^3), 2M hydrochloric acid (3×100cm^3), 2M sodium hydroxide (3×100cm^3), water (3×50cm^3) and ethanol (3×50cm^3), and then suspended in ethanol (500cm^3) and stirred under reflux for 2h. AHS was finally recovered by filtration and then dried in an oven at 60°C.

A strict control of temperature of the treatment at 60°C and a shortening of reaction contact time to 5 days helped and kept L-type spores intact, without changing significantly yields and elemental analysis results.

Typical yields and combustion elemental analyses are gathered in Table 68.

	Typical yield (w/w)	Typical combustion elemental analysis (w/w)		
		%C	%H	%N
S-type two-pot AHS	20-30%	65%	7.5%	0.00%
L-type two-pot AHS	30%	65%	7%	0.00%

Table 68 – Results of extraction of 'two-pot AHS' from *Lycopodium* spec.

2.1.3 Acetolysis

Use of acetolysis in extracting spores was adapted from earlier studies.[87,88]

2.1.3.1 To obtain AcS

Raw *Lycopodium* spp. spores (10g) were suspended in an acetolytic solution [sulphuric acid/acetic anhydride 1/9 (v/v), 30cm^3] and stirred under reflux for 15min. Acetolysed sporopollenin (AcS) was recovered by filtration (porosity grade 3 or 4), washed with acetic acid (3×10cm^3), ethanol (3×10cm^3), water (3×10cm^3), ethanol (3×10cm^3) and DCM (3×10cm^3), and dried in an oven at 60°C.

Typical yields and combustion elemental analyses are gathered in Table 69.

	Yield (w/w)	Combustion elemental analysis (w/w)			
		%C	%H	%N	%S
S-type AcS	ca. 40%	53.47%	7.55%	2.08%	3.13%
L-type AcS	ca. 40%	52.75%	7.29%	1.75%	0.41%

Table 69 – Results of extraction of sporopollenin by acetolysis from *Lycopodium* spec.

2.2 *Ambrosia trifida* pollen grains

2.2.1 'Full treatment'

2.2.1.1 To obtain DFS

Sample 1: Raw *Ambrosia trifida* pollen (250mg) was suspended in acetone (40cm^3) and stirred under reflux for 1h. Defatted sporopollenin (DFS) was recovered by centrifugation (1000 *g*, 5min).

Sample 2: Raw *Ambrosia trifida* pollen (5g) was suspended in acetone (15cm^3) and stirred under reflux for 1h. Defatted sporopollenin (DFS) was recovered by filtration (porosity grade 5).

2.2.1.2 To obtain BHS

Sample 1: DFS (sample 1, ca. 150mg) was suspended in an aqueous solution of sodium hydroxide [0.2% (w/v), 40cm^3] and stirred at 80°C for 1h. Base-hydrolysed sporopollenin (BHS) was recovered by centrifugation (1000 *g*, 5min), washed with water (3×10cm^3) and ethanol (3×10cm^3), and dried in an oven at 60°C.

Sample 2: DFS (sample 2, ca. 3g) was suspended in an aqueous solution of sodium hydroxide [1% (w/v), 15cm^3] and stirred under reflux for 1h. Base-hydrolysed sporopollenin (BHS) was recovered by filtration (porosity grade 5). Due to poor filtration, sample was neutralised by addition of concentrated hydrochloric acid (5cm^3) and the aqueous suspension was readily used for next step. Particles were then suspended in ethanol (70cm^3), stirred under reflux for 1h, recovered by filtration, washed with water (3×10cm^3) and ethanol (3×10cm^3), and dried in an oven at 60°C.

2.2.1.3 To obtain AHS

Sample 1: BHS (sample 1, ca. 75mg) was suspended in *ortho*-phosphoric acid (85%, 40cm^3) and stirred at 90°C for 1h. Acid-hydrolysed sporopollenin (AHS) was recovered by centrifugation (1000 *g*, 5min), washed with water (3×10cm^3) and ethanol (3×10cm^3), and dried under vacuum.

Sample 2: BHS (sample 2, ca. 1.5g) was suspended in *ortho*-phosphoric acid (85%, 50cm^3) and stirred under reflux for 1h. Acid-hydrolysed sporopollenin (AHS)

was recovered by filtration (porosity grade 5) and washed with water (3×10cm^3) and ethanol (3×10cm^3). Sample was then suspended in ethanol (50cm^3) and stirred under reflux for 1h. AHS was recovered by filtration and dried under vacuum.

Typical yields and combustion elemental analyses are gathered in Table 70.

	Typical yield (w/w)	Typical combustion elemental analysis (w/w)		
		%C	%H	%N
AHS (sample 1)	40%	69.94%	9.41%	0.78%
AHS (sample 2)	40%	55.77%	8.60%	0.52%

Table 70 – Results of extraction of AHS by 'full treatment' from *A. trifida*

2.2.2 Acetolysis

Use of acetolysis in extracting spores was adapted from earlier studies.[87,88]

Raw *Ambrosia trifida* pollen (mass m) was suspended in acetic acid glacial (volume V_1) at room temperature and treated pollen was recovered by centrifugation (1000 g, 5min). Pollen was suspended in an acetolytic solution [1/9 (v/v) sulphuric acid/acetic anhydride, volume V_2] and left in boiling-water bath for 1 minutes. Acetolysed sporopollenin (AcS) was recovered by centrifugation, washed with acetic acid (3×10cm^3), water (3×10cm^3) and ethanol (3×10cm^3), and dried under vacuum.

Sample 3: m=200mg; V_1=10cm^3; V_2=1.2cm^3;

Sample 4: m=1g; V_1=50cm^3; V_2=5cm^3.

Typical yields and combustion elemental analyses are gathered in Table 71.

	Typical yield (w/w)	Typical combustion elemental analysis (w/w)		
		%C	%H	%N
AcS (sample 3)	40%	50.59%	7.20%	4.18%
AcS (sample 4)	40%	45.41%	7.48%	3.65%

Table 71 - Results of extraction of sporopollenin by acetolysis from *A. trifida*

2.2.3 Extraction with hydrochloric acid

This method of extraction was taken from Tawashi and Amer's patents.[92-94]

Sample 5: *Ambrosia trifida* pollen (2g) was suspended in 6M hydrochloric acid (10cm^3). The mixture was left at 110°C for 24h in a sealed thick-walled tube. Particles were recovered by filtration (porosity grade 4), washed with water (3×20cm^3) and with

ethanol (3×20cm^3) and freeze-dried.

	Yield (w/w)	Combustion elemental analysis (w/w)		
		%C	%H	%N
sample 5	ca. 40%	69.86%	8.19%	0.92%

Table 72 - Results of extraction of sporopollenin with hydrochloric acid from *A. trifida*

2.3 *Aspergillus niger* conidia

2.3.1 Acidic treatment

85% *ortho*-phosphoric acid (20cm^3) was mixed with *Aspergillus niger* culture medium (20cm^3) and the resulting reaction mixture was stirred under reflux for 6h and diluted with water. After centrifugation (1000 *g*, 5min), no particle could be recovered.

2.3.2 Alkaline treatment

Sodium hydroxide pellets (60g) were dissolved in *Aspergillus niger* culture medium (1dm^3) and the resulting reaction mixture was stirred under reflux for 4h. Solvent was evaporated under reduced pressure. Particles were split into four samples. Each part was washed with water (5×50cm^3), ethanol (2×50cm^3) and diethyl ether (50cm^3) using centrifugation (1000 *g*, 5min) as a recovery method. Particles were finally dried under vacuum over phosphorus pentoxide.

2.4 *Chlorella vulgaris* cells

2.4.1 Alkaline treatment

Chlorella vulgaris (50g) was suspended in acetone (150cm^3), stirred under reflux for 4h and recovered by filtration (porosity grade 4). Resulting particles were suspended in 6% sodium hydroxide (150cm^3) and stirred under reflux for 6h. Base-hydrolysed *C. vulgaris* was recovered by filtration (por. 4), washed with water (5×100cm^3) and ethanol (3×100cm^3) and finally dried under vacuum over phosphorus pentoxide.

2.4.2 Acidic treatment

Base-hydrolysed *Chlorella vulgaris* (50g) was suspended in 85% phosphoric acid (150cm^3), stirred under reflux for 1h, 3h or 24h. In any case, no particles could be recovered by filtration or centrifugation, but a paste was isolated and dried under vacuum over phosphorus pentoxide.

3 Physical properties

3.1 Resistance of spores to pressure

Fresh raw *L. clavatum* S-type spores (0.1g) were compressed into a pellet (diameter d = 13mm) under an increasing weight, in a press usually used to prepare potassium bromide discs for IR spectroscopy. When the spore shell was ruptured, particles burst open and released an oily liquid, leaking from the die: the pressure naturally decreased suddenly.

The maximal weight (w_{max}, kg) was then recorded. The corresponding pressure (Pa) was calculated as follows: $P = \frac{4 \times w_{max}}{\pi \times d^2}$. Result is given in Section B-2.2.

3.2 Wall thickness

AHS particles (from *Ambrosia trifida* L. pollen grains, *Lycopodium* spec. L-type or *L. clavatum* L. S-type spores) were mounted on a microscope slide after microtome section (see Section C-1.4.3). Optical transmission micrographs were then observed using an Olympus BX51 microscope with a 100X objective lens. Wall thickness was measured on the images using *Image-Plus Pro* software. Results are given in Section B-2.1.2, Table 26.

As the stain used (toluidine blue) did not dye properly the spores, difficulties faced to focus the pictures had to be addressed as detailed in Section B-2.1.2 and Table 25.

3.3 Density

3.3.1 Loose powder

Loose spore or sporopollenin powder (ca. 10g) was weighed exactly in a measuring cylinder. After decanting and compaction by tapping, the volume of powder was recorded.

Density ($g.cm^{-3}$) was the quotient of the mass of powder (g) by its volume (cm^3).

Results are gathered in Section B-2.3, Table 28.

3.3.2 Compressed tablets

Spores or sporopollenin particles (0.1g) were compressed for 2min into a 13mm-diametered tablet, in a press usually used to prepare potassium bromide discs for IR spectroscopy. Whole spores were crushed under 1 to 3 tonnes, *i.e.* subjected to a pressure lying between 75,000 and 226,000hPa; empty AHS were crumpled under 10 tonnes, *i.e.* subjected to a pressure of 753,000hPa.

Tablet mass (m, g) was recorded, while its diameter (d, cm) and thickness (h, cm) were measured with a vernier calliper in order to calculate its density (ρ_{tab}, g.cm^{-3}) as follows:

$$\rho_{tab} = \frac{m}{h \times \pi \times \left(\frac{d}{2}\right)^2}$$

Results determined with whole 25µm spores from *Lycopodium clavatum* are gathered in Section B-2.3, Table 29.

3.3.3 Pycnometry

The density of sporopollenin and spores was assessed by pycnometry in a measuring cylinder. A known volume (V ~40cm^{-3}) of compact powder (after decanting and tapping) was weighed (weight w, g) and suspended in ethanol up to a volume V_0 (~100cm^{-3}). The total weight was recorded (w_0, g).

The density of sporopollenin (ρ, g.cm^{-3}) was given by the following formula:

$$\rho = \frac{\rho_{EtOH} \times w}{V_0 \times \rho_{EtOH} - w_0 + w}$$

with ρ_{EtOH} being the density of ethanol (ρ_{EtOH}=0.78g.cm^{-3}). Results are gathered in Section B-2.3, Table 30.

3.4 Determination of sporopollenin's extinction coefficient

This method was implemented with the help of Prof. Paul Fletcher (Department of Chemistry, University of Hull) and experimental work was performed with the help of Vincent Panel (Ecole Nationale Supérieure de Chimie de Paris, France).

Three types of particles were used for this work: AHS from *A. trifida* pollen, from S-type *L. clavatum* spores and from L-type *Lycopodium* spores. The spore particles were spread evenly over a quartz plate (10×40mm), either as a dry powder or from a dispersion in ethanol with subsequent evaportation of the solvent. The cell was completed by attaching the upper quartz plate and fixing with plastic bands over the ends.

The exine monolayer within the cell was determined by recording an optical transmission micrograph image using an Olympus BX51 microscope. Area fractions A_f were derived from the images using *Image-Plus Pro* software. For more accuracy, only the surface hit by the spectrophotometer light beam was considered in the determination of A_f. Estimation of the beam projection induced a ±3% error.

Distance d between the quartz plates was determined using a microscope focus method. Results were obtained with a ±2% error, and found to be slightly smaller than the outer diameter of undistorted AHS shells.

The UV-visible spectra of sporopollenin particle monolayers were measured using a Unicam UV3 spectrophotometer. To record the spectra, the quartz cell was taped in place in the sample position on the front of standard cuvette holder of the spectrophotometer. Light transmittance T_m of the monolayer (including quartz plates) was then measured against air, on wavelengths ranging from 190-900nm and with a ±0.001% error. A blank transmittance T_{blank} was also recorded with only quartz plates.

Mathematical principle is given in Section B-4.2.3.1 and results in Section B-4.2.3.2.

4 Encapsulation

4.1 Encapsulation processes

4.1.1 Encapsulation processes for liquids

The loading of liquid was expressed in volume or mass unit of liquid per mass unit of sporopollenin ($cm^3.g^{-1}$ or $mg.g^{-1}$). Neat liquids encapsulated with the protocols described below were: water, ethanol, propanol, isopropanol, *n*-butanol, isobutanol, sunflower oil, rapeseed oil, soybean oil, cod liver oil, echium oil and eicosapentenoic acid, as detailed in Section B-3.2.

Alternatively, mixtures of liquids were encapsulated: a 9/1 oil/ethanol (v/v) emulsion was formed by mixing both components at 40°C for 30s immediately before encapsulation (described below).

4.1.1.1 Passive filling

Sporopollenin (0.1g to 2g) was mixed with the liquid ($0.1cm^3$ to $5cm^3$), stirred for about 30s to 1min into a homogeneous mixture and set aside for at least 1h.

4.1.1.2 Compression filling

Sporopollenin (0.5g to 1g) was compressed into a 13mm-diametered cylindrical tablet under 10 tonnes, by mean of a press commonly used in IR spectroscopy to make potassium bromide discs. The sporopollenin tablet was then immersed in the liquid. As the pellet soaked it up by swelling, the liquid was thus driven into the particles to the extent of $5cm^3.g^{-1}$.

4.1.1.3 Vacuum filling

Sporopollenin (0.1g to 2g) was mixed with the liquid ($0.1cm^3$ to $5cm^3$), stirred for about 1min and subjected to a vacuum (0.1mmHg) for 30min to 2h.

4.1.2 Encapsulation processes for melted fats

The loading of melted fats was expressed in mass unit of fat per mass unit of sporopollenin ($mg.g^{-1}$). Fats encapsulated with the protocols described below were melted beeswax, melted carnauba wax and melted cocoa butter, as detailed in Section B-3.2.

4.1.2.1 Passive filling

Sporopollenin (0.5g) was mixed with the melted fat (0.5g). Temperature was kept high enough so that the fat stayed in a liquid state (see Table 31 in Section B-3.2.1.4) and the mixture was stirred for about 30s to 1min until it was homogeneous and then set aside for at least 1h at the same temperature.

4.1.2.2 Compression filling

Sporopollenin (0.5g) was compressed into a 13mm-diametered cylindrical tablet under 10 tonnes, by mean of a press commonly used in IR spectroscopy to make potassium bromide discs. The sporopollenin tablet was then immersed in the melted fat (0.5g) and temperature was kept high enough so that the fat stayed in a liquid state (see Table 31 in Section B-3.2.1.4) while the pellet soaked it up by swelling.

4.1.2.3 Vacuum filling

Sporopollenin (0.5g) was mixed with the melt fat (0.5g), stirred for about 1min at a temperature high enough so that the fat stayed in a liquid state (see Table 31 in Section B-3.2.1.4) and then subjected to a vacuum (0.1mmHg) for 30min to 2h at room temperature.

4.1.3 Encapsulation processes for solids *via* solutions

The solid to be encapsulated was dissolved into a suitable solvent (as discussed in Section B-3.3 and summarised in Table 73, Table 74, Table 75 and Table 76) up to a certain concentration (also given in the same tables). The resulting solution was then loaded according to the same techniques as implemented for neat liquids (see Section

C-4.1.1): passive filling, compression filling or vacuum filling.

Proteins that were not stable at room temperature (growth hormones, enfuvirtide, somatropin, insulin, alkaline phosphatase and antibody) had to be encapsulated in a cold room kept at -10°C.

Solid to be encapsulated	Solvent	Concentration
methyl orange	water	0.5g.cm^{-3}
malachite green	water	3g.cm^{-3}
malachite green	ethanol	3g.cm^{-3}
Nile red	ethanol	3g.cm^{-3}
Evans blue	water	3g.cm^{-3}
Evans blue	ethanol	3g.cm^{-3}

Table 73 – Solvents and concentrations used to encapsulate various dyes

Solid to be encapsulated	Solvent	Concentration
bacitracin	water/ethanol 4/1 (v/v)	20mg.cm^{-3}
α-amylase	water	41mg.cm^{-3}
α-amylase	water/ethanol 4/1 (v/v)	70mg.cm^{-3}
β-D-galactosidase	water	52mg.cm^{-3}
β-D-galactosidase	water/ethanol 4/1 (v/v)	100mg.cm^{-3}
ovalbumin	water	50mg.cm^{-3}
insulin	PBS	20mg.cm^{-3}
somatropin	water	10mg.cm^{-3}
somatropin	water/ethanol 4/1 (v/v)	13mg.cm^{-3}
1,097Da growth hormone	water	14mg.cm^{-3}
1,097Da growth hormone	water/ethanol 4/1 (v/v)	29mg.cm^{-3}
1,097Da growth hormone	DMSO	82mg.cm^{-3}
3,340Da growth hormone	water	19mg.cm^{-3}
3,340Da growth hormone	water/ethanol 4/1 (v/v)	102mg.cm^{-3}
3,340Da growth hormone	DMSO	130mg.cm^{-3}
enfuvirtide	water	54mg.cm^{-3}
enfuvirtide	water/ethanol 4/1 (v/v)	130mg.cm^{-3}
enfuvirtide	DMSO	94mg.cm^{-3}
integrin beta-1 antibody	PBS	2mg.cm^{-3}
PL30-FITC	ethanol	6mg.cm^{-3}
NU:UB 363-FITC	ethanol	2mg.cm^{-3}

Table 74 – Solvents and concentrations used to encapsulate various proteins and peptides

Solid to be encapsulated	Solvent	Concentration
calf thymus DNA extract	ethanol	5mg.cm^{-3}
6,393Da fluorescein-tagged 19-mer oligonucleotide	ethanol	2.4mg.cm^{-3}
4,141Da fluorescein-tagged 12-mer oligonucleotide	ethanol	1.4mg.cm^{-3}
TSAO-T	acetone	3mg.cm^{-3}

Table 75 – Solvents and concentrations used to encapsulate various nucleic acids

gum Arabic	water	100mg.cm^{-3}
starch	water	200mg.cm^{-3}
ascorbic acid	water	500mg.cm^{-3}
glycine	WE41	500mg.cm^{-3}
β-alanine	WE41	500mg.cm^{-3}
α-histidine	WE41	500mg.cm^{-3}
α-phenylalanine	WE41	500mg.cm^{-3}
tryptophan	WE41	500mg.cm^{-3}
tyrosine	WE41	500mg.cm^{-3}
ibuprofen	water	250mg.cm^{-3}
fish vaccines	water	1mg.cm^{-3}

Table 76 – Solvents and concentrations used to encapsulate various products

4.1.3.1 Encapsulation of proteins using DMSO as a solvent

The protein to be encapsulated (artificial growth hormone or enfuvirtide) was dissolved in DMSO up to a concentration indicated in Table 74. The solution (3cm^3) was then mixed with loose sporopollenin (0.3g). The mixture was stirred for 1h and subjected to a vacuum for a further 1h. Particles were than suspended in diethyl ether (20cm^3), stirred for 1h, recovered by filtration (porosity grade 3), washed with diethyl ether (10×20cm^3) and dried under vacuum over phosphorus pentoxide.

4.2 Evaluation of sporopollenin's properties towards fats

4.2.1 UV irradiation

A test portion (either neat fat or encapsulated in sporopollenin) was spread on a

watch glass or in a Petri dish, exposed under a UV lamp held at a distance of 13cm and irradiated for a given period of time. That lamp used was a Philips Original Home Solaria type HB 171/A, 220-230 volt 50Hz, 75W possessing 4 Philips CLEO 15W UV type 30 bulbs.

PVs of the irradiated and non-irradiated samples were then compared (see Section C-4.2.2).

4.2.2 Peroxide value (PV) titration

4.2.2.1 Normal procedure

This protocol follows IUPAC method 2.501.[246,247] A test portion (either neat fat or encapsulated in sporopollenin) was mixed into chloroform ($10cm^3$) and stirred so that all its fatty content (0.1g to 2g) dissolved. Acetic acid ($15cm^3$) was added followed by saturated aqueous potassium iodide ($1cm^3$). The flask was then stoppered, shaken for 1min and set aside away from light for exactly 5min at RT. The reaction was quenched by dilution with water ($75cm^3$). The liberated iodine was titrated against a 0.01N sodium thiosulphate solution (volume *V*), using a starch indicator.

A blank test was carried out simultaneously where the volume V_0 of titrating solution did not exceed $0.05cm^3$.

The peroxide value, expressed in milliequivalents of active oxygen per kg, was given by the formula:

$$PV = \frac{(V - V_0) \times T}{m} \times 1000$$

with *V* and V_0 respectively being the volumes of titrating solution for the sample and for the blank, *T* the concentration of titrating solution and m the mass of fat in the test portion.

4.2.2.2 Modified PV titration: filtration adjunct

A test portion (either neat fat or encapsulated in sporopollenin) was mixed into chloroform ($10cm^3$) and stirred so that all its fatty content (0.1g to 2g) dissolved. The mixture was then filtered (porosity grade 3) and acetic acid ($15cm^3$) was added to the filtrate, followed by saturated aqueous potassium iodide ($1cm^3$). The rest of the procedure was identical to the initial protocol given above.

4.2.2.3 Modified PV titration: addition of iodine

A test portion of sporopollenin exines (0.5g) was mixed into chloroform (10cm^3) and acetic acid (15cm^3). Saturated aqueous potassium iodide (1cm^3) was added. The flask was then stoppered, shaken for 1min and set aside away from light for exactly 5min at RT. The reaction was quenched by dilution with water (75cm^3). Iodine solution (0.02M) in saturated iodide (1cm^3) was then added. The total iodine in solution was titrated against a 0.01N sodium thiosulphate solution (volume *V*), using a starch indicator.

4.2.3 Evaluation of the capacities of sporopollenin to refine oils

Cod liver oil (1g to 2g) of known PV (see Section C-4.2.2) was mixed with sporopollenin (0.1g to 0.8g). The mixture was stirred for 1min at room temperature and filtered by centrifugation (porosity grade 3). PV of the recovered oil was then titrated (see Section C-4.2.2).

4.2.4 Rancimat

Rancimat apparatus was generously made available by Croda International plc (Hull, UK) and their standard procedure was modified and adapted to use with sporopollenin particles.[250]

A test portion (pure fat, or fat loaded in sporopollenin) was suspended in glass wool with as much dispersion as possible. The glass wool pad was then set in the middle of a glass test tube. A Metrohm 743 Rancimat version 1.0 was set up with eight similar tubes of different samples; the heating blocks were warmed at 50°C; and air was blown through the samples at a flow rate of 20$dm^3.h^{-1}$, while volatile oxidation products were collected in a measuring vessel filled with water (90cm^3). The conductivity of the latter was followed by a cell in order to determine the oxidative induction time (OIT) as follows: OIT was theoretically reached when the second derivative of conductivity is maximal. Practically, the conductivity grew slowly until the OIT was reached, then its slope became steeper; so the OIT was deduced from the intersection of the tangents to the curve.

4.2.5 Taste trial

Five samples were prepared with cod liver and sunflower oils encapsulated in AHS extracted from *L. clavatum* L. S-type spores. Oil (resp. cod liver oil 0.5g, 1.0g, 2.0g, 4.0g and sunflower oil 0.5g) was filled in loose AHS powder (1.0g) using the vacuum technique for 2h. Water ($5cm^3$) was mixed with sporopollenin (1.0g) to constitute a blank.

The samples were randomly pulled out of an opaque envelope by a third person and labelled alphabetically as they came (see Table 77).

Twenty volunteers tasted ca. 10 milligrams of each one of the previous samples (with mouth rinsing between) in a random order. Firstly, the volunteers were informed that the samples possibly contained water, sunflower oil, cod liver oil, olive oil or cocoa butter. Secondly, they were challenged to identify which product was encapsulated in each sample on the basis of taste. Thirdly, they scored the samples on a scale one, for the mildest or most palatable, to five, for the strongest or most pungent. Results of the test are gathered in Section B-4.5.

A fish oil/ sporopollenin 4/1 (w/w)	**B** blank (placebo)	**C** fish oil/ sporopollenin 0.5/1 (w/w)
D fish oil/ sporopollenin 1/1 (w/w)	**E** sunflower oil/ sporopollenin 2/1 (w/w)	**F** fish oil/ sporopollenin 2/1 (w/w)

Table 77 – Labelling of samples for taste trial

Statistical treatment of the data was performed by Dr. Alan Rigby (Postgraduate Medical Institute, University of Hull).[344]

4.3 Alkaline phosphatase activity

4.3.1 Assay of enzyme activity

This method was devised with the help of Dr. Leigh Madden (Postgraduate Medical Institute, University of Hull).

Alkaline phosphatase (ALP) activity was measured on a UNICAM 8625 UV/Vis Spectrometer, set up at a wavelength λ=650nm, a water bath and heating block

temperature of 22°C or 37°C. The UV cuvettes used were 1cm-long PMMA cells.

To maintain alkaline conditions suitable for ALP, the solvent of reaction was phosphate buffered saline solution (PBS) (pH=7.4). The quantities of reagents used in the cell were standardized by several initial trials as such: PBS ($1cm^3$), DDAO-phosphate ($2mm^3$), and enzyme solution in glycerol ($2mm^3$).

Sample solution (ca. $1cm^3$) was place in a PMMA cell. DDAO-phosphate ($2mm^3$) was added and UV absorption was followed against time. Sample solution was either a filtrate of released enzyme (see Section C-4.3.2) or a fresh solution of enzyme made up by dissolving commercial ALP solution in glycerol ($2mm^3$) in PBS ($1cm^3$). In order to obtain a baseline, neat PBS ($1cm^3$) was used instead of a sample solution and it was verified that UV absorption was constant in time over 1min.

4.3.2 Encapsulation and release

ALP solution in glycerol ($2mm^3$) was mixed with S-type AHS (0.001g) at 4°C for a few ten seconds and then encapsulated by centrifugation (10,000 *g*; 10min; 4°C). After encapsulation, ALP was released from loaded AHS by re-suspension of the powder in PBS ($1cm^3$), shaking for half a minute and filtration through a 0.45µm-porosity syringe-tip filter. The activity of the filtrate was assessed as described in above Section C-4.3.1.

In order to control the tenacity of enzyme attachment to sporopollenin exines, further flushes were carried out by running PBS ($1cm^3$) through filter again and assessing the activity of the filtrate.

4.3.3 Mathematical principle

Activity of ALP (*a*, in units of enzyme) was the quantity of substrate DDAO-phosphate dephosphorylated (*n*, µmol) per unit of time (*t*, min): $a = \frac{n}{t} = \frac{c \times V}{t}$, with *V* ($cm^3$) the constant volume of the reaction vessel, and *c* the concentration of DDAO produced by dephosphorylation ($\mu mol.cm^{-3}$ *i.e.* $mmol.dm^{-3}$).

To obtain the activity *a* of the enzyme, the concentration *c* of DDAO produced was thus followed by UV absorption. In a UV cell (path length *l*, cm), UV absorption (*Abs*) of a solution of DDAO-phosphate in contact with ALP was measured at a

wavelength of λ=650nm over a certain period of time: this corresponded to assessing the increase of the product (DDAO) concentration (c, mmol.dm^{-3}). According to Beer-Lambert law, $Abs = \varepsilon \times l \times c \times 10^{-3}$ with ε being the molar extinction coefficient of DDAO at 650nm. Thus, the concentration of DDAO was: $c = \frac{Abs \times 10^3}{\varepsilon \times l}$. As a result, the activity was obtained from the variation of the absorption as follows: $a = \frac{Abs \times V \times 10^3}{\varepsilon \times l \times t}$.

5 Chemical derivatisation

The work of chemical derivatisation of sporopollenin was supported by several co-workers who provided some experimental data presented here:

- Vanessa Le Poupon was involved in the reactions of sporopollenin with amines, the halogenation of sporopollenin and the azidation and thiolation of halogenated sporopollenins;
- Andreas Löbbert[222] was involved in the construction of the linker arm on sporopollenin and the azidation of bromosporopollenin;
- Maria Leigh[66] was involved in the halogenation of sporopollenin and the thiolation of halogenated sporopollenins;
- Étienne Baco[302] was involved in the thiolation of bromosporopollenin and the derivatisation of thiosporopollenins.

5.1 Assays and analytical methods

5.1.1 Sodium (or potassium) assay

This method was developed from Vogel's textbook.[319]

Potentially derivatised sporopollenin (0.1g) was stirred overnight in 2M sodium hydroxide (10cm^3) at RT, recovered by filtration (por. 3), washed with water (3×10cm^3), ethanol (10cm^3) and DCM (10cm^3) and dried at 60°C to constant weight. The dry solid (mass w_0 ~0.1g accurate to 1mg) was then stirred overnight in 2M hydrochloric acid (10cm^3) at RT, recovered by filtration (por. 3) and washed with water (3×10cm^3). Both filtrate and aqueous washings were collected quantitatively in a 100cm^3 volumetric flask, which was then filled up with distilled water.

Sodium concentration c (mmol.dm^{-3}) was finally assayed by flame atomic emission spectroscopy (see Section C-1.5.2) against a calibration curve. Standard solutions were made up with sodium chloride from a 200ppm stem solution *i.e.* 508.37mg$_{NaCl}$.dm^{-3} (8.70mmol.dm^{-3}).

Sodium loading in the original sample (mmol.g^{-1}) was obtained as follows:

$loading = \frac{c \times 0.1}{w}$.

Alternatively, this assay was performed with potassium salts and the standard solutions were made up from a 200ppm stem solution *i.e.* 381.33$mg_{KCl}.dm^{-3}$ (5.12$mmol.dm^{-3}$).

5.1.2 Assay of chloride salts by gravimetric analysis

This method was developed from Vogel's textbook.[319]

Potentially derivatised sporopollenin (0.1g) was stirred overnight in 2M hydrochloric acid (10cm^3) at RT, recovered by filtration (por. 3), washed with water (3×10cm^3), ethanol (10cm^3) and DCM (10cm^3) and dried at 60°C to constant weight. The dry solid (mass w_0 ~0.1g accurate to 1mg) was then stirred overnight in 2M sodium hydroxide (10cm^3) at RT, recovered by filtration (por. 3) and washed with water (3×10cm^3).

Both filtrate and aqueous washings were collected quantitatively, mixed and acidified by 6M nitric acid (5cm^3). A 0.1M silver nitrate solution (5cm^3) was added to the mixture, which was immediately protected from light and set aside overnight. Silver chloride was coagulated by heating nearly to boiling, with constant stirring, then cooled down for 1h, recovered by filtration in an oven-dry, pre-weighed funnel (por. 4), washed with dilute nitric acid (3×10cm^3) and dried at 120°C away from light.

Loading of chloride in the original sample ($mmol.g^{-1}$) was calculated as such: $loading = \frac{w_{AgCl}}{M_{AgCl} \times w_0}$, with w_{AgCl} the weight of precipitate (mg) and M_{AgCl} the molecular mass of silver chloride (*i.e.* 143.3$g.mol^{-1}$).

5.1.3 Halogen assay by gravimetric analysis

This method was developed from various textbooks.[345,346]

Dry brominated, chlorinated or chloromethylated sporopollenin (mass w_0 ~0.1g accurate to 1mg) was stirred overnight in 2M sodium hydroxide (10cm^3) under reflux, recovered by filtration (por. 3) and washed with water (3×10cm^3).

Both filtrate and aqueous washings were collected quantitatively, mixed and

acidified by 6M nitric acid (5cm^3). A 0.1M silver nitrate solution (5cm^3) was added to the mixture, which was immediately protected from light and set aside overnight. Silver halide was coagulated by heating nearly to boiling, with constant stirring, then cooled down for 1h, recovered by filtration in an oven-dry, pre-weighed funnel (por. 4), washed with dilute nitric acid (3×10cm^3) and dried at 120°C away from light.

Loading of halogen (bromine or chlorine) in the original sample was calculated as such: $loading = \frac{w_{ppt}}{M_{ppt} \times w_0}$, with w_{ppt} the weight of precipitate (mg) and M_{ppt} its molecular mass (*i.e.* 187.8g.mol^{-1} for silver bromide and 143.3g.mol^{-1} for silver chloride).

5.1.4 Tollens' test

The method described in the literature[346] was directly applied to sporopollenin particles.

Two stock aqueous solutions were prepared: silver nitrate (2.5g in 42cm^3, solution A) and potassium hydroxide (3.0g in 42cm^3, solution B). Tollens' reagent was prepared *in situ* by adding concentrated 0.880 ammonia to solution A (3cm^3) until the initial brown precipitate had almost redissolved to give a greyish slightly cloudy solution; solution B (3cm^3) was added to it, as well as extra 0.880 ammonia until the solution was clear again. Sporopollenin (0.2g) was suspended in Tollens' reagent (2.5cm^3), shaken for a while, recovered by filtration (por. 3), washed with water (20cm^3), 6M nitric acid (3×20cm^3), water (3×20cm^3) and ethanol (20cm^3), and dried at 60°C.

Particles were then submitted to an ICP-OES silver assay (see Section C-1.5.3). The loading (mmol.g^{-1}) of functions sensitive to this test (aldehydes) in sporopollenin exines was: $loading_{aldehyde} = \frac{x_{Ag}}{MW_{Ag}}$, with x_{Ag} the loading of silver given by ICP-OES (mg.g^{-1}) and MW_{Ag} the molar weight of silver (107.87g.mol^{-1}).

NB: Tollens' reagent tends to form explosive silver fulminate that should be quenched with water and dilute nitric acid.

5.1.5 Ninhydrin test for cysteine quantification

5.1.5.1 Reaction of ninhydrin

This method was developed from Plummer's textbooks.[238]

A 4mol.dm^{-3} sodium acetate buffer solution was prepared from sodium hydroxide by addition of glacial acetic acid. Ninhydrin (0.8g) and hydrindantin (0.12g) were dissolved in DMSO (30cm^3) under a stream of nitrogen gas. The solution was diluted with sodium acetate buffer solution (10cm^3) and nitrogen was bubbled through the mixture for at least 2min. The final solution was sealed and stored at 4°C.

The unknown amino acid solution (1cm^3) and the previous ninhydrin solution (1cm^3) were mixed, heated in a boiling water bath for 10min and immediately cooled in ice. Then aqueous methanol [50% (v/v), 5cm^3] was added and the mixture was thoroughly mixed with a vortex mixer for 15s.

Solution absorbance was measured against aqueous methanol [50% (v/v)] at 570nm. Concentration of cysteine (c, mmol.dm^{-3}) in the unknown solution was determined against a calibration curve obtained following the procedure described in Section C-5.1.5.2.

5.1.5.2 Calibration curve

Standards were prepared using a similar protocol developed elsewhere.[302]

A stem aqueous solution of cysteine (1.0mmol.dm^{-3}) was made up with cysteine hydrochloride salt (0.158g.dm^{-3}), and then diluted with water into 10 standard solutions, down to 0.1mmol.dm^{-3}.

Each cysteine solution (1cm^3) and the previous ninhydrin solution (1cm^3) were mixed, heated in a boiling water bath for 10min and immediately cooled in ice. Then aqueous methanol [50% (v/v), 5cm^3] was added and the mixture was thoroughly mixed with a vortex mixer for 15s.

Absorbance of each standard solution was measured against aqueous methanol [50% (v/v)] at 570nm in order to design a calibration curve.

5.2 Reaction of sporopollenin with aqueous ammonia

Attachment of ammonia to sporopollenin was adapted from previous investigations.[12,13,149]

S-type AHS (mass m_1) was suspended in 0.880 ammonia (volume V). Ammonium chloride (mass m_2) was added and the mixture was stirred at temperature T for time t. Particles were then recovered by filtration (por. 3), washed with water ($10cm^3$), 2M hydrochloric acid ($3\times10cm^3$), water ($3\times10cm^3$), ethanol ($10cm^3$) and DCM ($10cm^3$) and dried under vacuum over phosphorus pentoxide to a constant weight, to yield the product **2**.

Reaction parameters are gathered in the following Table 78.

Product 2 Batch no.	AHS Mass m_1 (g)	Ammonia Volume V (cm^3)	NH_4Cl Mass m_2 (g)	Temp. T (°C)	Time t (h)
ATS 1	5	100	0	22	12
ATS 2	1	150	0	22	24
ATS 3	1	150	0	22	72
ATS 4	0.1	20	0	22	96
ATS 5	0.1	5	0	22	96
ATS 6	0.1	6	0.1	22	12
ATS 7	0.1	20	0.1	22	12
ATS 8	0.1	2	0.1	22	12
ATS 9	0.1	20	0.1	22	96
ATS 10	0.1	5	0.25	22	96
ATS 11	0.1	2	0.1	120	12
ATS 12	0.1	2	0.2	120	12

Table 78 – Reaction of AHS with ammonia – parameters of reaction

Note 1: Reactions at 120°C were performed in a thick-walled sealed tube, under pressure.

Note 2: In batches 9, 10, 11 and 12, the resulting ammonia-treated sporopollenin (**2**) was enriched in ^{15}N by addition of ^{15}N-labelled ammonium chloride ($^{15}NH_4Cl$) to the reaction mixture (1%), for the purpose of solid-state NMR.

The loading of ammonia in the resulting ammonia-treated sporopollenin (ATS) **2** was determined by nitrogen combustion elemental analysis (see Section C-1.1). Data are displayed in Table 79 and results are discussed in Section B-5.2.2.

Product 2 Batch no.	Combustion elemental analysis (w/w)			Nitrogen loading ($mmol.g^{-1}$)
	%C	%H	%N	
ATS 1	70.54%	7.29%	0.57%	0.41
ATS 2	62.74%	7.70%	0.63%	0.45
ATS 3	67.99%	9.81%	0.71%	0.51
ATS 4	75.41%	7.99%	1.07%	0.76
ATS 5	74.14%	7.77%	0.88%	0.63
ATS 6	70.03%	7.31%	1.00%	0.71
ATS 7	71.75%	7.81%	0.89%	0.64
ATS 8	65.15%	8.20%	0.74%	0.53
ATS 9	58.51%	8.10%	1.49%	1.06
ATS 10	74.50%	7.87%	0.87%	0.62
ATS 11	68.63%	8.82%	2.59%	1.85
ATS 12	74.60%	9.58%	1.24%	0.89

Table 79 – Ammonia-treated sporopollenin – elemental analysis

5.3 Reaction with monoamines

Procedures of attachment of aliphatic amines to sporopollenin were adapted from previous studies.[12,13] Reaction of aniline used here was investigated elsewhere.[154]

5.3.1 With 1-butylamine, diethylamine or triethylamine

S-type AHS (0.5g) was suspended in toluene ($10cm^3$) and 1-butylamine, diethylamine or triethylamine ($1cm^3$) was added. The mixture was stirred for 12h under reflux in a Dean-Stark apparatus. Cooled particles were recovered by filtration (por. 3), washed with toluene ($6\times50cm^3$), ethanol ($6\times50cm^3$), acetic acid ($6\times50cm^3$), water ($10\times50cm^3$), 2M hydrochloric acid ($10\times50cm^3$), water ($10\times50cm^3$), ethanol ($3\times50cm^3$) and DCM ($3\times50cm^3$) and dried under vacuum over phosphorus pentoxide to a constant weight.

The resulting sporopollenins **6a**, **6b** and **6c** were submitted to combustion elemental analysis (see Section C-1.1) and chloride gravimetry (see Section C-5.1.2). Data are displayed in Table 80 and results are discussed in Section B-5.2.3.1.

Product	Amine	Combustion elemental analysis (w/w)			Chloride loading ($mmol.g^{-1}$)
		%C	%H	%N	
6a	1-*n*-butylamine	72.41	8.69	1.27	0.00
6b	diethylamine	71.21	7.15	0.73	0.00
6c	triethylamine	72.98	8.01	0.37	0.00

Table 80 – Attachment of saturated aliphatic amines to AHS – analytical data

Each one of the previous samples (0.1g) was re-suspended in 2M hydrochloric acid ($10cm^3$) and stirred at room temperature overnight. The particles were recovered by filtration (por. 3), washed with water ($5\times30cm^3$), ethanol ($3\times30cm^3$) and DCM ($3\times30cm^3$), and dried under vacuum over phosphorus pentoxide to a constant weight.

The resulting sporopollenins were submitted to combustion elemental analysis (see Section C-1.1). Data are displayed in Table 81 and results are discussed in Section B-5.2.3.1.

Product	Amine	Combustion elemental analysis (w/w)		
		%C	%H	%N
6a	1-*n*-butylamine	70.13	8.13	0.76
6b	diethylamine	69.34	7.17	0.38
6c	triethylamine	70.98	8.03	0.00

Table 81 – Amine-treated sporopollenins, after acidic washing – analytical data

5.3.2 With allylamine or propargylamine

S-type AHS (1g) was suspended in toluene ($30cm^3$) and either allylamine or propargylamine ($1cm^3$) was added. The mixture was stirred for 12h under reflux in a Dean-Stark apparatus. Cooled particles were recovered by filtration (por. 3), washed with toluene ($6\times50cm^3$), ethanol ($6\times50cm^3$), acetic acid ($6\times50cm^3$), water ($10\times50cm^3$), 2M hydrochloric acid ($10\times50cm^3$), water ($10\times50cm^3$), ethanol ($3\times50cm^3$) and DCM ($3\times50cm^3$) and dried under vacuum over phosphorus pentoxide to a constant weight.

The resulting sporopollenins **6d** and **6e** were submitted to combustion elemental analysis (see Section C-1.1) and chloride gravimetry (see Section C-5.1.2). Data are displayed in Table 82 and results are discussed in Section B-5.2.3.1.

Product	Amine	Combustion elemental analysis (w/w)			Chloride loading ($mmol.g^{-1}$)
		%C	%H	%N	
6d	allylamine	70.69	7.79	1.55	0.00
6e	propargylamine	69.02	7.51	1.60	0.00

Table 82 – Attachment of unsaturated aliphatic amines to AHS – analytical data

Each one of the previous samples (0.1g) was re-suspended in 2M hydrochloric acid ($10cm^3$) and stirred at room temperature overnight. The particles were recovered by filtration (por. 3), washed with water ($5\times30cm^3$), ethanol ($3\times30cm^3$) and DCM ($3\times30cm^3$), and dried under vacuum over phosphorus pentoxide to a constant weight.

The resulting sporopollenins were submitted to combustion elemental analysis (see Section C-1.1). Data are displayed in Table 83 and results are discussed in Section B-5.2.3.1.

Product	Amine	Combustion elemental analysis (w/w)		
		%C	%H	%N
6d	allylamine	70.04	7.76	1.12
6e	propargylamine	70.75	7.61	1.27

Table 83 – Amine-treated sporopollenins, after acidic washing – analytical data

5.3.3 With aniline

S-type AHS (1g) was suspended in neat aniline (50cm^3) and the dispersion was diluted with toluene (volume *V*). The mixture was stirred under reflux for 12h. Cooled particles were recovered by filtration (por. 3), washed with toluene (6×50cm^3), ethanol (6×50cm^3), acetic acid (6×50cm^3), water (10×50cm^3), 2M hydrochloric acid (10×50cm^3), water (10×50cm^3), ethanol (3×50cm^3) and DCM (3×50cm^3) and dried under vacuum over phosphorus pentoxide to a constant weight.

The resulting sporopollenin **7** was submitted to combustion elemental analysis (see Section C-1.1) and chloride gravimetry (see Section C-5.1.2). Data are displayed in Table 84 and results are discussed in Section B-5.2.3.2.

Product	Toluene Volume *V* (cm^3)	Combustion elemental analysis (w/w)			Chloride loading (mmol.g^{-1})
		%C	%H	%N	
7a	50	71.56	7.77	1.97	0.00
7b	0	72.32	7.30	2.83	0.00

Table 84 – Attachment of aniline to AHS – analytical data

The previous sample (0.1g) was re-suspended in 2M hydrochloric acid (10cm^3) and stirred at room temperature overnight. The particles were recovered by filtration (por. 3), washed with water (5×30cm^3), ethanol (3×30cm^3) and DCM (3×30cm^3), and dried under vacuum over phosphorus pentoxide to a constant weight.

The resulting sporopollenin was submitted to combustion elemental analysis (see Section C-1.1). Data are displayed in Table 85 and results are discussed in Section B-5.2.3.2

Product	Toluene Volume *V* (cm^3)	Combustion elemental analysis (w/w)		
		%C	%H	%N
7a	50	72.62	7.78	1.58
7b	0	72.48	7.28	2.35

Table 85 – Aniline-treated sporopollenins, after acidic washing (RT) – analytical data

Alternatively, freshly obtained aniline-treated sporopollenin **7a** (0.1g) was re-suspended in 2M hydrochloric acid (10cm^3) and stirred at 50°C overnight. The particles were recovered by filtration (por. 3), washed with water (5×30cm^3), ethanol (3×30cm^3) and DCM (3×30cm^3), and dried under vacuum over phosphorus pentoxide to a constant weight.

The resulting sporopollenin was submitted to combustion elemental analysis (see Section C-1.1). Data are displayed in Table 86 and results are discussed in Section B-5.2.3.2

Product	Toluene Volume *V* (cm^3)	Combustion elemental analysis (w/w)		
		%C	%H	%N
7a	50	71.95	7.45	0.81

Table 86 – Aniline-treated sporopollenin, after hot acidic treatment – analytical data

5.3.4 With 1-dodecylamine

S-type AHS (0.1g) was suspended in toluene (2cm^3) and ^{15}N-labelled 1-dodecylamine (0.1cm^3) was added. The mixture was stirred for 12h under reflux. Cooled particles were recovered by filtration (por. 3), washed with toluene (5×10cm^3), ethanol (5×10cm^3), water (5×10cm^3), 2M hydrochloric acid (5×10cm^3), water (3×10cm^3), ethanol (3×10cm^3) and DCM (3×10cm^3) and dried under vacuum over phosphorus pentoxide to a constant weight.

The resulting sporopollenin **6f** was submitted to combustion elemental analysis (see Section C-1.1) and data are displayed in Table 87.

Product	Combustion elemental analysis (w/w)		
	%C	%H	%N
6a	77.11	11.84	1.61

Table 87 – Attachment of dodecylamine to AHS – analytical data

5.4 Building a linker arm

Results concerning the construction of a spacer are gathered in Section B-5.2.4.1 and the following protocols were developed in order to mimic a linker already synthesised on polystyrene.[299]

5.4.1 Formation of compound 8: reaction of sporopollenin 1 with ethylenediamine

This procedure of was adapted from two extensive studies regarding the chemical attachment of ω-diamines to sporopollenin.[154,297]

S-type AHS **1** (2) was suspended in ethylenediamine (10cm^3), diluted with toluene (30cm^3). The mixture was stirred under reflux for 24h in a Dean-Stark apparatus. The cooled particles were recovered by filtration (por. 3), washed with toluene (3×30cm^3), 2M hydrochloric acid (3×30cm^3), water (5×30cm^3), ethanol (3×30cm^3) and DCM (3×30cm^3) and dried under vacuum over phosphorus pentoxide to a constant weight.

The resulting sporopollenin **8** was submitted to combustion elemental analysis (see Section C-1.1), sodium test (see Section C-5.1.1) and chloride gravimetry (see Section C-5.1.2). Data are gathered in Table 88.

Product 8 Batch no.	Combustion elemental analysis (w/w)			Sodium loading (mmol.g^{-1})	Chloride loading (mmol.g^{-1})
	%C	%H	%N		
1	60.18%	7.40%	4.89%	0.00	1.420
2	63.50%	7.54%	5.71%	0.00	1.182
3	60.09%	11.51%	5.57%	0.00	N/d

Table 88 – Attachment of ethylenediamine to sporopollenin – analytical data

5.4.2 Formation of compound 9: succinylation of product 8

Ethylenediamine-treated sporopollenin **8** (3g) was suspended in anhydrous toluene (40cm^3) and succinic anhydride (20g) was added. The mixture was stirred overnight at room temperature under nitrogen. The cooled particles were recovered by filtration (por. 3), washed with toluene (3×30cm^3), 2M hydrochloric (3×30cm^3), water (3×30cm^3), ethanol (3×30cm^3) and DCM (3×30cm^3), and dried under vacuum over phosphorus pentoxide to a constant weight.

The resulting sporopollenin **9** was submitted to combustion elemental analysis (see Section C-1.1), sodium test (see Section C-5.1.1) and chloride gravimetry (see Section C-5.1.2). Data are gathered in Table 89.

Product 9 Batch no.	Combustion elemental analysis (w/w)			Sodium loading (mmol.g^{-1})	Chloride loading (mmol.g^{-1})
	%C	%H	%N		
1	64.15	6.75	4.24	2.29	0.569
2	62.67	6.72	4.25	N/d	0.501
3	59.23	10.46	4.41	N/d	0.497

Table 89 – Succinylation of sporopollenin – analytical data

5.4.3 Formation of compound 10: reaction of product 9 with 6-amino-1-(*tert*-butyl-dimethyl)silyloxyhexane

Succinylated aminosporopollenin **9** (3g) was suspended in toluene (50cm^3) and 1-amino-6-(*tert*-butyldimethyl)silyloxyhexane (3.15g) was added. The mixture was stirred under reflux overnight in a Dean Stark apparatus. The cooled particles were recovered by filtration (por. 3), washed with ethanol (5×50cm^3) and DCM (3×30cm^3), and dried under vacuum over phosphorous pentoxide to a constant weight.

The resulting sporopollenin **10** was submitted to combustion elemental analysis (see Section C-1.1), sodium test (see Section C-5.1.1) and chloride gravimetry (see Section C-5.1.2). Data are gathered in Table 90.

Product 10 Batch no.	Combustion elemental analysis (w/w)			Sodium loading ($mmol.g^{-1}$)	Chloride loading ($mmol.g^{-1}$)
	%C	%H	%N		
1	68.27	8.03	4.27	0.14	0.00
2	60.64	11.27	4.82	N/d	0.00

Table 90 – Attachment of 1-amino-6-(*tert*-butyldimethyl)silyloxyhexane to sporopollenin – analytical data

5.4.4 Formation of compound 11: acetylation of product 10

Acetylation of sporopollenin derivatives was adapted from previous investigations.[12,13]

Silylated compound **10** (2g) was suspended in a solution of pyridine ($6cm^3$) in DCM ($100cm^3$). A solution of acetyl chloride ($1cm^3$) in DCM ($10cm^3$) was added dropwise at 0°C to the previous suspension. The reaction mixture was stirred for 1h at 0°C and for 2.5h at room temperature. The particles were recovered by filtration (por. 3), washed with ethanol ($5\times50cm^3$) and DCM ($3\times30cm^3$), and dried under vacuum over phosphorus pentoxide to a constant weight.

The resulting sporopollenin **11** was submitted to combustion elemental analysis (see Section C-1.1), sodium test (see Section C-5.1.1) and chloride gravimetry (see Section C-5.1.2). Data are gathered in Table 91.

Product 11 Batch no.	Combustion elemental analysis (w/w)			Sodium loading ($mmol.g^{-1}$)	Chloride loading ($mmol.g^{-1}$)
	%C	%H	%N		
1	65.41	8.31	4.39	0.00	0.00
2	66.26	9.14	4.48	0.00	0.00
3	60.25	10.11	4.09	0.00	0.00

Table 91 – Acetylation of sporopollenin – analytical data

5.4.5 Formation of compound 12: deprotection of silylated hydroxyls in product 11

Silylated and acetylated compound **11** (mass m_1) was suspended in THF (volume V) and tetrabutylammonium fluoride (TBAF) (mass m_2) was added. The dispersion was stirred for 2 days at room temperature. The particles were recovered by filtration (por. 3), washed with ethanol (5×50cm^3) and DCM (3×30cm^3), and dried under vacuum over phosphorus pentoxide to a constant weight. Solvent in the filtrate was evaporated under reduced pressure, the residue was redissolved in water (50cm^3) and its silicon content was determined by ICP-OES (see method in Section C-1.5.3 and results in Figure 42 in Section B-5.2.4.1). Reaction parameters are given in the following Table 92.

Product 12 Batch no.	Sporopollenin Mass m_1 (g)	THF Volume V (cm^3)	TBAF Mass m_2 (g)
1	0.1	10	0.1
2	1.5	100	1.1
3	3.62	150	1

Table 92 – Deprotection of silylated sporopollenin – reaction parameters

The resulting sporopollenin **12** was submitted to combustion elemental analysis (see Section C-1.1), sodium test (see Section C-5.1.1) and chloride gravimetry (see Section C-5.1.2). Data are gathered in Table 93.

Product 12 Batch no.	Combustion elemental analysis (w/w)			Sodium loading (mmol.g^{-1})	Chloride loading (mmol.g^{-1})
	%C	%H	%N		
1	64.47	8.31	4.39	0.45	0.00
2	69.19	9.49	4.72	0.64	0.00
3	61.68	10.42	4.27	N/d	0.00

Table 93 – Deprotection of silylated sporopollenin – analytical data

5.4.6 Formation of compound 13: nucleophilic substitution on product 12

Derivatised sporopollenin **12** (0.1g) was suspended in a solution of pyridine (0.3cm^3) in DCM (10cm^3). A solution of phenylsulfonyl chloride (0.1g) in DCM (5cm^3) was added dropwise to the previous dispersion at 0°C. The reaction mixture was stirred

for 2.5 hours at room temperature. The particles were recovered by filtration (por. 3), washed with ethanol (5×30cm^3) and DCM (2×30 cm^3) and dried under vacuum over phosphorous pentoxide to a constant weight.

The resulting sporopollenin **13** was submitted to combustion elemental analysis (see Section C-1.1), sodium test (see Section C-5.1.1) and chloride gravimetry (see Section C-5.1.2). Data are given in Table 94.

Product 13 Batch no.	Combustion elemental analysis (w/w)			Sodium loading (mmol.g^{-1})	Chloride loading (mmol.g^{-1})
	%C	%H	%N		
1	63.77	6.77	4.32	0.22	0.00
2	63.15	7.22	4.10	N/d	0.00
3	59.80	9.75	4.05	N/d	0.00

Table 94 – Reaction of phenylsulfonyl chloride with sporopollenin – analytical data

5.4.7 Removal of the linker arm

Linker-armed sporopollenin **13** (0.1g) was suspended in 2M sodium hydroxide (30cm^3) and stirred for 2 days under reflux. The cooled particles were recovered by filtration (por. 3), washed with 2M hydrochloric acid (5×30cm^3), water (5×30cm^3), ethanol (5×50 cm^3) and DCM (3×30 cm^3), and dried under vacuum over phosphorus pentoxide to a constant weight. Solvent in the filtrate was evaporated under reduced pressure, the residue was redissolved in water (50cm^3) and its sulphur content was determined by ICP-OES (see method in Section C-1.5.3 and results in Figure 42 in Section B-5.2.4.1).

The resulting sporopollenin **14** was submitted to combustion elemental analysis (see Section C-1.1) and data are given in Table 95.

Product	Combustion elemental analysis (w/w)			
	%C	%H	%N	%S
14	57.7	10.30	3.38	0.00

Table 95 – Removal of linker arm – analytical data

5.5 Reduction of derivatised sporopollenin

Reduction protocol was initially developed elsewhere.[12,13]

Derivatised sporopollenin (mass m_1) was suspended in sodium-dried 1,4-dioxane (volume V) and lithium aluminium hydride (LAH, mass m_2) was added. The mixture was stirred for 4 days under reflux in nitrogen. The reaction vessel was then cooled to 0°C and LAH was successively quenched dropwise with ethyl acetate (100cm^3), ethanol (50cm^3), water (100cm^3) and 2M sulphuric acid (200cm^3). Particles were recovered by filtration (por. 3), washed with water (3×50cm^3), ethanol (3×30cm^3) and DCM (2×30cm^3) and dried under vacuum over phosphorus pentoxide to a constant weight. Reaction parameters are gathered in Table 96.

Batch	Final product	Initial sporopollenin		1,4-Dioxane	LAH
		Type	Mass m_1 (g)	Volume V (cm^3)	Mass m_2 (g)
1	**3**	ATS (**2**)	0.45	50	0.8
2	**3**	ATS (**2**)	0.45	50	0.8
3	**3**	ATS (**2**)	1	100	1.5
4	**3**	ATS (**2**)	1	100	1.5
5	**3**	ATS (**2**)	0.7	70	1.3
6	**21**	**20**	0.45	50	0.8

Table 96 – Reduction of derivatised sporopollenin – reaction parameters

The resulting sporopollenin **3** or **21** was submitted to combustion elemental analysis (see Section C-1.1), sodium test (see Section C-5.1.1) and chloride gravimetry (see Section C-5.1.2). Data are given in Table 97.

Batch no.	Product	Combustion elemental analysis (w/w)			Chloride loading (mmol.g^{-1})
		%C	%H	%N	
1	**3**	50.25	7.25	4.04	N/d
2	**3**	53.65	5.23	0.26	N/d
3	**3**	51.87	7.05	1.27	0.711
4	**3**	50.84	6.90	1.32	0.498
5	**3**	59.81	7.86	0.49	N/d
6	**21**	64.15	6.75	2.15	1.43

Table 97 – Reduction of derivatised sporopollenin – analytical data

5.6 Dehydration of ammonia-treated sporopollenin

Results of the dehydration of sporopollenin are discussed in Section B-5.2.2.4.

5.6.1 With phosphorus oxychloride

Ammonia-treated sporopollenin **2** (0.1g) was suspended in chloroform (5cm^3). Triethylamine (1cm^3) was added to the resulting dispersion, followed by phosphorus oxychloride (0.7cm^3), and the mixture was stirred under reflux overnight. The cooled particles were filtered (por. 3), washed with chloroform (3×30cm^3), ethanol (3×30cm^3) and DCM (3×30cm^3) and dried under vacuum over phosphorus pentoxide to a constant.

The resulting sporopollenin **5a** was submitted to combustion elemental analysis (see Section C-1.1) and chloride gravimetric assay (see Section C-5.1.3). Data are given in Table 98.

Product	Combustion elemental analysis (w/w)			Chloride loading (mmol.g^{-1})
	%C	%H	%N	
5a	70.03	7.31	1.00	0.26

Table 98 – Dehydration of sporopollenin using phosphorus oxychloride – analytical data

5.6.2 With phosphorus pentachloride

Ammonia-treated sporopollenin **2** (0.1g) was suspended in chloroform (5cm^3). Triethylamine (1cm^3) was added to the resulting dispersion, followed by phosphorus pentachloride (1cm^3), and the mixture was stirred under reflux overnight. The cooled particles were filtered (por. 3), washed with chloroform (3×30cm^3), ethanol (3×30cm^3) and DCM (3×30cm^3) and dried under vacuum over phosphorus pentoxide to a constant.

The resulting sporopollenin **5b** was submitted to combustion elemental analysis (see Section C-1.1) and chloride gravimetric assay (see Section C-5.1.3). Data are displayed in Table 99.

Product	Combustion elemental analysis (w/w)			Chloride loading ($mmol.g^{-1}$)
	%C	%H	%N	
5b	67.28	6.02	0.88	0.52

Table 99 – Dehydration of sporopollenin using phosphorus pentachloride – analytical data

5.6.3 With ethyldichlorophosphate in presence of 1,8-diazabicyclo[5.4.0]undec-7-ene (DBU)

Ammonia-treated sporopollenin **2** (0.1g) was suspended in DCM (50cm^3) and DBU (0.45g) was added, followed by ethyldichlorophosphate (0.33g). The resulting mixture was stirred at room temperature for one day. The particles were recovered by filtration (por. 3), washed with ethanol (5×50cm^3) and DCM (3×30cm^3), and dried under vacuum over phosphorus pentoxide to a constant weight.

The resulting sporopollenin **5c** was submitted to combustion elemental analysis (see Section C-1.1) and chloride gravimetric assay (see Section C-5.1.3). Data are given in Table 100.

Product	Combustion elemental analysis (w/w)		
	%C	%H	%N
5c	55.96	10.10	2.04

Table 100 – Dehydration of sporopollenin using DBU – analytical data

The sample was washed again with water (10×50cm^3), ethanol (10×50cm^3) and DCM (3×30cm^3) and dried under vacuum over phosphorus pentoxide to a constant weight.

The resulting sporopollenin was submitted to combustion elemental analysis (see Section C-1.1) and chloride gravimetric assay (see Section C-5.1.3). Data are given in Table 101.

Product	Combustion elemental analysis (w/w)		
	%C	%H	%N
5c	54.63	9.29	1.95

Table 101 – Dehydrated sporopollenin, after washings – analytical data

5.7 Halogenations

5.7.1 Direct bromination

Bromination method was adapted from earlier studies.[12,13,53]

Sporopollenin (mass *m*) was suspended in a solution of dibromine (concentration *c*, volume *V*) and stirred overnight at room temperature. Bromosporopollenin was recovered by filtration (por. 3), washed extensively with DCM (10×100cm^3) until the filtrate was colourless, methanol (10×50cm^3) until the filtrate was colourless again, water (3×30cm^3), methanol (3×30cm^3) and DCM (3×30cm^3), and dried under vacuum over phosphorus pentoxide to a constant weight. Reaction parameters are gathered in the following Table 102.

Product 15 Batch no.	Sporopollenin		Bromine solution		
	Type	Mass *m* (g)	Solvent	Concentration *c* (% (v/v))	Volume *V* (cm^3)
1	S-type AHS	20	chloroform	10	250
2	S-type AHS	5	chloroform	10	100
3	S-type AHS	5	chloroform	30	75
4	S-type AHS	5	glacial acetic acid	30	100
5	L-type AHS	5	glacial acetic acid	30	100

Table 102 – Bromination of sporopollenin – reaction parameters

The resulting sporopollenin **15** was submitted to combustion elemental analysis (see Section C-1.1) and the dropping of carbon level gave a rough estimation of the loading of bromine ($loading_{Br}$, mmol.g^{-1}) by comparison with initial sporopollenin, as follows:

$$loading_{Br} = \frac{(100 - \%C_1 - \%H_1 - \%N_1) \times \%C_0 - (100 - \%C_0 - \%H_0 - \%N_0) \times \%C_1}{7.99 \times \%C_0}$$

with $\%C_0$, $\%H_0$ and $\%N_0$ (resp. $\%C_1$, $\%H_1$, $\%N_1$) the respective wt. percentages of carbon, hydrogen and nitrogen in initial sporopollenin (resp. brominated sporopollenin).

A more precise value of the level of bromine in the product **15** was then determined by gravimetry (see Section C-5.1.3). Data are gathered in Table 103 and the results discussed in Section B-5.3.2.

Product 15 Batch no.	Combustion elemental analysis (w/w)			Loading of bromine (mmol.g^{-1})	
	%C	%H	%N	estimation	gravimetry
1	39.73	3.37	0.00	5.97	1.85
2	30.13	3.01	0.00	6.76	4.43 (0.20)
3	34.43	2.76	0.00	5.24	4.04 (0.26)
4	38.53	3.45	0.00	4.63	1.05 (0.01)
5	36.78	3.46	0.00	5.35	5.13 (3.06)

Standard deviation is given in brackets where available.

Table 103 – Bromination of sporopollenin – analytical data

5.7.2 Chloromethylation

Chloromethylation protocol was developed from the literature[347] and adapted to sporopollenin in a previous study.[12]

Sporopollenin (1g) was stirred in dimethoxymethane (20cm^3) for 1h at 35°C. The mixture was cooled to 0°C and thionyl chloride (2g *i.e.* 1.3cm^3) was added dropwise, followed by a solution of zinc chloride (0.5g) in dimethoxymethane (5cm^3). The mixture was stirred at 35°C for 20h and particles were collected by filtration (por. 3), washed with water (10×30cm^3) until no chloride was detected in the filtrate after by addition of 0.1M silver nitrate solution, 1,4-dioxane (3×30cm^3), methanol (3×30cm^3) and DCM (3×30cm^3), and dried under vacuum over phosphorus pentoxide to a constant weight.

The loading of chlorine in the resulting products **16** and **17** was determined by gravimetry (see Section C-5.1.3). Data are gathered in Table 104 and results are discussed in Section B-5.3.3.

Product	Batch no.	Initial sporopollenin type	Loading of chlorine (mmol.g^{-1})
16a	**1**	S-type AHS	0.90 (0.10)
16a	**2**	S-type AHS	1.01 (1.00)
17	**3**	Aniline-treated sp. **7b**	0.49 (0.19)
16b	**4**	L-type AHS	0.34 (0.01)

Standard deviation is given in brackets.

Table 104 – Chloromethylation of sporopollenin – analytical data

5.7.3 Direct chlorination

5.7.3.1 With phosphorus pentachloride

Chlorination of sporopollenin by nucleophilic substitution of hydroxyl groups using phosphorus pentachloride was developed from previous studies[348] and adapted to sporopollenin elsewhere.[12]

Phosphorus pentachloride (1.32g) was dissolved in dry DCM (35cm^3) at 0°C. Potassium carbonate (0.88g) was then added followed by sporopollenin (1g). The mixture was then stirred for 10min at 0°C. Particles were recovered by filtration (por. 3), washed with DCM (3×30cm^3), methanol (30cm^3), water (10×30cm^3) until no chloride was detected in the filtrate by addition of 0.1M silver nitrate solution, methanol (3×30cm^3) and DCM (3×30cm^3), and dried under vacuum over phosphorus pentoxide to a constant weight.

The loading of chlorine in the resulting product **18** was determined by gravimetry (see Section C-5.1.3). Data are gathered in Table 105 and results are discussed in Section B-5.3.4.

Product 18 Batch no.	Initial sporopollenin type	Loading of chlorine (mmol.g^{-1})
1	S-type AHS	0.65 (0.37)
2	S-type AHS	0.89 (0.70)
3	L-type AHS	0.35 (0.01)
4	L-type AHS	1.05 (0.69)

Standard deviation is given in brackets.

Table 105 – Reaction of sporopollenin with phosphorus pentachloride – analytical data

5.7.3.2 With thionyl chloride

Chlorination of sporopollenin by nucleophilic substitution of hydroxyl groups using thionyl chloride was developed from previous studies[349] and adapted to sporopollenin elsewhere.[12]

To a suspension of sporopollenin (1g) in diethyl ether (40cm^3) at room temperature thionyl chloride (1.3cm^3) was added dropwise. The mixture was then stirred under reflux for 1h then at room temperature for a further 1h. Particles were

recovered by filtration (por. 3), washed with diethyl ether (3×30cm^3), water (10×30cm^3) until no chloride was detected in the filtrate by addition of 0.1M silver nitrate solution, methanol (3×30cm^3) and DCM (3×30cm^3), and dried under vacuum over phosphorus pentoxide to a constant weight.

The loading of chlorine in the resulting product **19** was determined by gravimetry (see Section C-5.1.3). Data are gathered in Table 106 and results are discussed in Section B-5.3.4.

Product 19 Batch no.	Initial sporopollenin type	Loading of chlorine (mmol.g^{-1})
1	S-type AHS	0.59 (0.01)
2	L-type AHS	0.45

Standard deviation is given in brackets where available.

Table 106 – Reaction of sporopollenin with thionyl chloride – analytical data

5.8 Azidation

S-type halogenated sporopollenin (0.3g) was suspended into a solution of sodium azide (0.4g) in DMSO (20cm^3). The resulting mixture was stirred for 1 day at 60°C. The cooled particles were collected by filtration (por. 3), washed with DMSO (2×40cm^3), water (8×50cm^3), ethanol (2×40cm^3) and DCM (2×40cm^3) and dried under vacuum over phosphorus pentoxide to a constant weight.

The loading of nitrogen was determined by combustion elemental analysis (see Section C-1.1). Data are gathered in Table 107 and results are discussed in Section B-5.4.

Final product	Initial sporopollenin	Combustion elemental analysis (w/w)			Cl loading (mmol.g^{-1})
		%C	%H	%N	
20	Bromosp. **15**	48.12%	4.11%	7.39%	N/a
22a	Chlorosp. **18**	63.52%	7.31%	0.01%	0.91
22b	Chlorosp. **19**	69.26%	8.00%	0.50%	0.48
23	Chloromethyl sp.**16**	51.85%	5.67%	0.99%	0.70
24	Chloromethyl aniline-treated sp. **17**	63.61%	6.38%	3.00%	N/d

Table 107 – Azidation of halogenated sporopollenin – analytical data

5.9 Reactions with thiols

5.9.1 Thiolation

5.9.1.1 With sodium hydrogen sulphide

The thiolation method involving sodium hydrogen sulphide was adapted from previous studies[320] and initially developed on sporopollenin elsewhere.[153]

S-type derivatised sporopollenin (mass m_1) was suspended in DMSO (volume V). Crushed sodium hydrogen sulphide (mass m_2) was added and the mixture was stirred under reflux overnight. Particles were recovered by filtration (por. 3), washed with water (5×50cm^3), 2M hydrochloric acid (5×50cm^3), water (5×50cm^3), ethanol (5×50cm^3) and DCM (3×30cm^3), and dried under vacuum over phosphorus pentoxide to a constant weight.

Reaction parameters are gathered in the following Table 108.

Final product	**Batch no.**	**Initial sporopollenin**		**DMSO**	**Sodium hydrogen sulphide**
		Type	**Mass m_1 (g)**	**Volume V (cm^3)**	**Mass m_2 (g)**
-	**0**	AHS **1**	0.5	10	0.4
25	**1**	bromosp. **15**	0.2	5	0.4
25	**2**		0.4	25	0.7
25	**3**	bromosp. **15**	5	100	1.9
25	**4**		3	75	1.3
27	**5**	chloromethylsp. **16**	0.5	10	0.4
26a	**6**	chlorosp. **18**	0.5	10	0.4
26b	**7**	chlorosp. **19**	0.5	10	0.4

Table 108 – Thiolation of sporopollenin using sodium hydrogen sulphide – reaction parameters

The loading of sulphur in the resulting sporopollenins **25**, **26** and **27** was determined by sulphur combustion elemental analysis (see Section C-1.1) and data are gathered in Table 109. The level of available thiols was evaluated by various means detailed in Section B-5.5.

Final product	Batch no.	Combustion elemental analysis (w/w)			
		%C	%H	%N	%S
-	0	62.34	7.89	0.00	0.00
25	1	32.82	3.27	0.13	8.74
25	2	43.99	2.98	0.19	10.65
25	3	48.85	3.75	0.23	5.93
25	4	47.96	3.11	0.10	11.76
27	5	67.00	7.68	0.16	1.87
26a	6	65.76	7.25	0.13	2.98
26b	7	66.28	7.25	0.14	3.27

Table 109 – Thiolation of sporopollenin using sodium hydrogen sulphide – analytical data

5.9.1.2 With thiourea

The thiolation method involving thiourea was adapted from previous studies[320,325] and initially developed on sporopollenin elsewhere.[153]

S-type derivatised sporopollenin (mass m_1) was suspended in solvent (volume V_1). Thiourea (mass m_2) was added and the mixture was stirred at temperature T overnight. Particles were recovered by filtration (por. 3), washed with water (5×50cm^3), 2M hydrochloric acid (5×50cm^3), water (5×50cm^3), methanol (5×50cm^3) and DCM (3×30cm^3).

They were then stirred in an aqueous solution of potassium hydroxide (25% (m/v), volume V_2) under reflux for 6h, recovered by filtration (por. 3), washed with water (5×50cm^3), 2M hydrochloric acid (5×50cm^3), water (5×50cm^3), methanol (5×50cm^3) and DCM (3×30cm^3), and dried under vacuum over phosphorus pentoxide to a constant yield.

Reaction parameters are gathered in the following Table 110.

Product	Batch	Sporopollenin		Solvent			Thio-urea	Base
		Initial sp.	Mass m_1 (g)	Type	Volume V_1 (cm^3)	Temp. T (°C)	Mass m_2 (g)	Volume V_2 (cm^3)
-	**0**	AHS **1**	0.5	DMSO	10	189	1.00	20
28	**1**	bromosp. **15**	5	DMSO	60	189	4.56	100
28	**2**	bromosp. **15**	5	DMSO	60	189	4.56	100
28	**2a**	thiosp. **28** batch **2**	5	n/a	n/a	n/a	n/a	100
28	**3**	bromosp. **15**	0.2	methanol	20	22	0.36	20
28	**4**	bromosp. **15**	0.2	methanol	20	22	1.21	20
28	**5**	bromosp. **15**	0.2	methanol	20	22	2.42	20
28	**6**	bromosp. **15**	0.2	methanol	10	65	0.2	20
28	**7**	bromosp. **15**	5	ethanol	60	78	4.56	100
29	**8**	chloro-methylsp. **16**	0.3	DMSO	10	189	0.45	20
30	**9**	chlorosp. **18**	0.3	DMSO	10	189	0.45	20
31	**10**	chlorosp. **19**	0.3	DMSO	10	189	0.45	20

Table 110 – Thiolation of sporopollenin using thiourea – reaction parameters

Note: Batch no. **2a** was obtained from batch **2** by treating thiosporopollenin with a second hydrolysis in potassium hydroxide to try and remove more isothiouronium salt.

The loading of sulphur in the resulting sporopollenins was determined by sulphur combustion elemental analysis (see Section C-1.1) and data are gathered in Table 111.The level of available thiols was evaluated by various means detailed in Section B-5.5.

Product	Batch no.	Combustion elemental analysis (w/w)			
		%C	%H	%N	%S
-	0	63.56	7.67	0.00	0.00
28	1	46.10	3.20	4.38	19.14
28	2	52.89	3.73	2.90	14.18
28	2a	53.06	3.81	2.24	7.75
28	3	59.68	4.91	1.07	1.98
28	4	56.32	5.02	1.27	2.68
28	5	56.87	5.11	1.29	2.89
28	6	54.50	5.07	1.53	2.62
28	7	55.75	4.77	2.36	3.83
29	8	62.03	6.14	2.08	5.12
30	9	62.84	5.87	2.10	6.51
31	10	67.05	7.43	0.82	2.63

Table 111 – Thiolation of sporopollenin using thiourea – analytical data

5.9.1.3 With thioacetic acid

The thiolation method involving thioacetic acid was adapted from previous studies.[326]

Sporopollenin (0.5g) was suspended in 1,4-dioxane (20cm^3) under nitrogen. Thioacetic acid (0.8g) was added and the mixture was then stirred for 24h under reflux. Particles were recovered by filtration (por. 3), washed with ether (3×10cm^3), 2M sodium hydroxide (10×10cm^3), water (10×10cm^3), 2M hydrochloric acid (10×10cm^3), water (10×10cm^3), ethanol (10×10cm^3) and DCM (10×10cm^3), and dried at 60°C.

The resulting sporopollenin **32a** was submitted to combustion elemental analysis (see Section C-1.1) and data are given in Table 112.

Product	Combustion elemental analysis (w/w)			
	%C	%H	%N	%S
32a	49.49	4.38	0.38	2.60

Table 112 – Thiolation of sporopollenin using thioacetic acid – analytical data before hydrolysis

Thioacetic acid-treated sporopollenin (0.1g) was stirred in 2M hydrochloric acid or 2M sodium hydroxide (5cm^3) overnight under reflux. Particles were recovered by filtration (por. 3), washed with water (5×50cm^3), 2M hydrochloric acid (5×20cm^3), water (5×20cm^3), ethanol (5×20cm^3) and DCM (3×20cm^3), and dried at 60°C.

The loading of sulphur in the resulting sporopollenin **32b** was determined by sulphur combustion elemental analysis (see Section C-1.1) and data are gathered in

Table 113.

Product 32b Batch no.	Treatment	Combustion elemental analysis (w/w)			
		%C	%H	%N	%S
1	acid	52.55	4.56	0.36	2.59
2	base	59.28	5.11	0.65	2.08

Table 113 – Thiolation of sporopollenin using thioacetic acid – analytical data before hydrolysis

5.9.1.4 With sodium thiosulphate (Bunte salts)

The thiolation method involving sodium thiosulphate was adapted from Bunte[350] and other studies.[351-353]

Sporopollenin (3g) was suspended in a 3/1 (v/v) water/methanol (40cm^3). Sodium thiosulphate (4.9g) was added and the mixture was stirred overnight under reflux. Particles were recovered by filtration (por. 3), washed with water (10×50cm^3), ethanol (5×50cm^3) and DCM (5×50cm^3), and dried at 60°C.

Sodium thiosulphate-treated sporopollenin (1g) was stirred in 4M hydrochloric acid (100cm^3) overnight at room temperature. Particles were recovered by filtration (por. 3), washed with 2M hydrochloric acid (5×50cm^3), water (10×50cm^3), methanol (5×50cm^3) and DCM (5×50cm^3), and dried at 60°C.

The loading of sulphur in the resulting sporopollenin **33** was determined by sulphur combustion elemental analysis (see Section C-1.1) and data are given in Table 114.

Product	Combustion elemental analysis (w/w)			
	%C	%H	%N	%S
33	43.47	3.77	0.28	0.00

Table 114 – Reaction of sporopollenin with sodium thiosulphate – analytical data

5.9.2 Reaction of sporopollenin with Ellman's reagent (DTNB)

Ellman's reagent method to assay thiols was adapted from previous studies[332] and developed on resins elsewhere.[331]

Sporopollenin (mass w_0 ~0.01g accurate to 1mg) was weighed in a 10cm^3

volumetric flask, and then mixed to a solution of DTNB (2.5×10^{-3}mol.L^{-1}, 4cm^3) in methanol. Diisopropyl ethylamine (5mm^3) was added. The mixture was stirred for 30 minutes then set aside overnight at room temperature. After removal of the magnetic bar, the solution was diluted to V=10cm^3 with methanol.

Supernatant absorbance A was measured against methanol at 412nm. Amount of thiols (n_{SH}, mmol) in the 10cm^3-flask was determined using Beer-Lambert's law, with ε=13,600dm^3.cm^{-1}.mol^{-1} being the absorption coefficient of DTNB at 412nm:

$$n_{SH} = \frac{A \times V}{\varepsilon \times l}$$

The loading of free thiols in sporopollenin (mmol.g^{-1}) was then calculated as:

$$loading_{SH} = \frac{n_{SH}}{w_0}$$

5.9.3 Reaction of sporopollenin with cysteine

Oxidative attachment of cysteine to sporopollenin was adapted from other investigations.[320,336,354]

5.9.3.1 Formation of disulphide bridges with cysteine

Sporopollenin (0.5g) was suspended in a solvent (volume V). L-Cysteine hydrochloride (mass m) was added and the mixture was stirred at room temperature for a time t while a stream of compressed air bubbled through the solution. Particles were recovered by filtration (por. 3), washed with water (10×10cm^3), 2M hydrochloric acid (10×10cm^3) in some cases, water (10×20cm^3), ethanol (10×10cm^3) and DCM (5×10cm^3), and dried at 60°C or under vacuum over phosphorus pentoxide.

Reaction parameters are gathered in the following Table 115.

Product 37 Batch no.	Initial sp.	Solvent		Cys Mass *m* (g)	Reaction time *t* (h)	Acid washing
		Type	Volume *V* (cm^3)			
1	thiosp. **25**	0.5M $NaHCO_3$	25	0.8	12	yes
2	AHS (**1**)	0.5M $NaHCO_3$	25	0.8	12	yes
3	thiosp. **28**	0.5M $NaHCO_3$	25	0.8	12	yes
4	thiosp. **25**	0.5M $NaHCO_3$	25	0.8	12	yes
5	thiosp. **28**	0.5M $NaHCO_3$	25	1.2	96	no
6	thiosp. **25**	0.5M $NaHCO_3$	25	1.2	120	no
7	thiosp. **25**	DMSO	30	1.2	48	no

Table 115 – Oxidative attachment of cysteine to sporopollenin – reaction parameters

The resulting sporopollenins were submitted to combustion elemental analysis (see Section C-1.1) and data are gathered in Table 116.

Product 37 Batch no.	Combustion elemental analysis (w/w)			
	%C	%H	%N	%S
1	48.79	3.49	0.77	5.58
2	73.20	9.25	0.32	0.00
3	49.77	3.66	3.22	9.86
4	49.38	3.64	0.72	5.67
5	39.68	2.64	2.37	7.08
6	38.38	2.72	0.54	11.38
7	45.36	3.28	0.45	13.21

Table 116 – Oxidative attachment of cysteine to sporopollenin – analytical data

Two blanks, one with sodium hydrogen sulphide-treated sporopollenin (**25**) and the other with thiourea-treated sporopollenin (**28**), were also performed with the same procedure. Sporopollenin (0.5g) was suspended in 0.5M aqueous sodium bicarbonate ($25cm^3$). L-Alanine (0.8g) was added and the mixture was stirred at room temperature for 12h while a stream of compressed air bubbled through the solution. Particles were recovered by filtration (por. 3), washed with water ($10\times10cm^3$), 2M hydrochloric acid ($10\times10cm^3$), water ($10\times20cm^3$), ethanol ($10\times10cm^3$) and DCM ($5\times10cm^3$), and dried

under vacuum over phosphorus pentoxide.

The resulting samples were submitted to combustion elemental analysis (see Section C-1.1) and data are gathered in Table 117.

Initial thiosporopollenin	Combustion elemental analysis (w/w)			
	%C	%H	%N	%S
25	49.89	4.11	0.00	10.43
28	53.10	4.01	2.08	7.05

Table 117 – Oxidative attachment of alanine to thiosporopollenin – analytical data

5.9.3.2 Reduction of disulphide bridges

Oxidised sporopollenin (0.06g) was suspended in aqueous acetic acid [5% (v/v), 10cm^3]. In some cases, zinc powder (mass *m*) was added and the mixture was stirred overnight at room temperature. Particles were recovered by filtration (por. 4), washed with acetic acid [5% (v/v), 3×10cm^3] and water (5×10cm^3), and filtrate and washings were collected quantitatively, gathered in a 100cm^3 volumetric flask completed with water, and submitted to a ninhydrin test (see Section C-5.1.5).

Reaction parameters and results are gathered in the following Table 118.

Batch no.	Batch no. of initial sp. 37	Zinc Mass *m* (mg)	Cysteine concentration (mmol.L^{-1})	Initial loading of cysteine (mmol.g^{-1})
1	**7**	0	0.422	0.70
2	**6**	0	0.730	1.22
3	**6**	2	0.775	1.29

Table 118 – Reductive cleavage of cysteine-sporopollenin bond

5.9.4 Nucleophilic substitutions

5.9.4.1 With benzylbromide

Benzylbromide (w_0~0.2g, accurately weighed) and sporopollenin (w_1~0.1g, accurately weighed) were suspended in DCM (20cm^3). The mixture was stirred under reflux overnight. Particles were recovered by filtration (por. 3), washed with DCM (10×5cm^3) and dried under vacuum over phosphorus pentoxide to a constant weight (w_2). Solvent was evaporated from the filtrate under reduced pressure and the residue weighed accurately (w_3).

The loading L of benzylbromide (in mmol.g^{-1}) in sporopollenin **34** was approximated (due to material loss during filtration) as being:

$$L = \frac{w_2 - w_1}{w_1 \times MW}$$ with w_1 and w_2 in g, and MW=171.04g.mol^{-1} being the molecular weight of benzylbromide.

This value was backed up by calculation from the residue, as follows:

$$L = \frac{w_0 - w_3}{w_1 \times MW}$$ with w_0, w_1 and w_3 in g, and MW=171.04g.mol^{-1} being the molecular weight of benzylbromide.

5.9.4.2 With benzylisocyanate

Attachment of benzylisocyanate to thiosporopollenin was adapted from previous works[355,356] and initially developed on sporopollenin elsewhere.[153]

Sporopollenin (0.1g) was suspended in dichloromethane (25cm^3) under nitrogen. Benzylisocyanate (0.4g) and triethylamine (1cm^3) were added and the mixture was stirred under reflux overnight. Particles were recovered by filrtation (por. 3), washed with DCM (20cm^3), methanol (5×20cm^3) and DCM (5×20cm^3), and dried under vacuum over phosphorus pentoxide.

The resulting sporopollenins were submitted to combustion elemental analysis (see Section C-1.1) and data are given in Table 119.

Initial sporopollenin	Batch no.	Combustion elemental analysis (w/w)		
		%C	%H	%N
AHS 1	**1**	70.97	7.55	1.42
25	**2**	52.17	4.24	1.43
28	**3**	59.80	4.68	5.36

Table 119 – Attachment of benzylisocyanate to sporopollenin – analytical data

5.9.4.3 With octylisocyanate

The method of attachment of octylisocyanate to thiosporopollenin was derived from that reported in the previous Section.

Sporopollenin (0.1g) was suspended in dichloromethane (25cm^3) under nitrogen. Octylisocyanate (0.465g) and triethylamine (volume V) were added and the mixture was stirred under reflux overnight. Particles were recovered by filtration (por. 3), washed with methanol (5×20cm^3) and DCM (5×20cm^3), and dried at 60°C.

The resulting sporopollenins were submitted to combustion elemental analysis

(see Section C-1.1). Reaction parameters and analytical data are gathered in Table 120.

Initial sporopollenin	Batch no.	NEt_3 Volume V (cm^3)	Combustion elemental analysis (w/w)		
			%C	%H	%N
AHS 1	**1**	1	68.78	8.07	1.16
25	**2**	1	51.13	4.94	3.41
28	**3**	1	48.51	4.72	2.98
AHS 1	**4**	0	70.91	8.24	0.53
25	**5**	0	51.44	4.11	2.97
28	**6**	0	52.79	4.34	2.62

Table 120 – Attachment of octylisocyanate to sporopollenin

Glossary

Note: Irregular plurals are given in brackets.

Angiosperm:[1] A flowering plant, therefore a spermatophyte.

Anther:[1,4] The male sporangium of flowering plants, that produces pollen, born by a filament to compose a stamen.

Aperture:[2] A specialized region of the sproroderm, that is thinner than the remainder of the sporoderm and generally differs in ornamentation and/or in structure. Various types of apertures are recognised on the basis of their position (pole, equator), their depth (layer) or their shape. In living pollen grains or spores, the apertures usually function as sites of germination, as well as water transfer routes.

- **Colpus (-i)**: An elongated longitudinal aperture with a length/breadth ratio greater than 2;
- **Laesura (-ae)**: A proximal scar of a monolete or trilete spore;
- **Pore**: A round to elliptic aperture with a length/breadth ratio less than 2;
- **Sulcus (-i)**: An elongated aperture with a length/breadth ratio greater than 2, parallel to equator;
- **Ulcus (-i)**: A round aperture.

Baculum (-a): cf. infratectum

Binary name:[21] A formal method of naming species in botany. It consists of the combination of two terms:

- A genus name: italicised and capitalised; may be shortened to its first letter, in context;
- A specific descriptor: italicised and never capitalised.

They are generally followed by the surname of the scientist who first published the classification. Botanist names are systematically abbreviated[357] and a standardised index, first published by the Royal Botanic Gardens, Kew (U.K.) in 1992,[22] is kept updated.[1] (See below the list of botanists appearing in this study)

The abbreviation "spec." is used when the actual specific name cannot or need not be specified. The abbreviation "spp." (plural) indicates several species.

A **ternary name** enables to indicate section (sect.), subspecies (subsp.), varieties

(var.), subvarieties (subvar.), forms (f.), subforms (subf.), and cultivars or cultivated variety (cv.).

Botanists appearing in this study (by abbreviation):[357]

- Aiton: William Aiton (1731-1793), United Kingdom;
- Á.Löve & D.Löve: Áskell Löve (1916-1994) and Doris Benta Maria Löve, née Wahlen (1918-2000), Iceland;
- Baker: John Gilbert Baker (1834-1920), United Kingdom
- Beij.: Martinus Willem Beijerinck (1861-1931), The Netherlands;
- B. Øllg.: Benjamin Øllgaard (1943-), Denmark;
- Callen: Eric Ottleben Callen (1912-1970), Canada;
- Cass.: Alexandre Henri Gabriel de Cassini (1781-1832), France;
- Duchesne: Antoine Nicolas Duchesne (1747-1827), France;
- Fr.: Elias Magnus Fries (1794-1878), Sweden;
- Kütz.: Friedrich Traugott Kützing (1807-1893), Germany;
- L.: Carolus Linnaeus (1707-1778), Sweden;
- Sibth.: John Sibthorp (1758-1796), United Kingdom;
- Sm.: James Edward Smith (1759-1828), United Kingdom;
- Thunb.: Carl Peter Thunberg (1743-1828), Sweden;
- Tiegh.: Philippe Édouard Léon van Tieghem (1839-1914), France;
- Torr.: John Torrey (1796-1873), USA;
- Turra: Antonio Turra (1730-1796), Italy.

Examples:

- *Ambrosia trifida* L. [Genus + species + botanist (Carolus Linnaeus)]
- *Lycopodium* spec. [Genus + unknown species]
- *A. niger* [Genus abbreviation + species]
- *L. clavatum* subsp. *contiguum* B. Øllg. [Genus abbreviation + species + subspecies + botanist (Benjamin Øllgaard)]
- *Tulipa gesneriana* cv. "Apeldoorn" [Genus + species (garden tulip) + infraspecific type (cultivar)]

Bisaccate: cf. saccus

Callose:[6] A linear 1,3-β-D-glucan found in certain plant cell walls, especially present in some phases of spore production.

Caput (-ita): cf. infratectum

Colpus (-i): cf. aperture

Columella (-ae): cf. infratectum

Conidium (-a):[1] A type of asexual reproductive spore of fungi (like *Aspergillus* spp.) usually produced at the conidial heads.

Conidial head *or* **conidiophore**:[1] The tip or side of the hyphae of a mould (like *Aspergillus* spp.), where spores (*conidia*) are sprouting.

Cryptogam:[1,6] A non-seed-bearing plant (as opposed to a spermatophyte). Cryptogams reproduce by spores. They include ferns, mosses and fungi.

Decorations: cf. tectal elements

Distal: cf. polarity

Echinate: cf. tectal elements

Ectexine: cf. layers

Endexine: cf. layers

Endocytosis:[6] For a cell, a way of internalisation of substances from the external environment.

Endospore: Either a synonym of *intine*[2] or a type of *spore*.[1,6] To avoid confusion, this term was not used in this study.

Epithelium (-a):[1,6] The purely cellular layer covering all free surfaces of the body, cutaneous, mucous, and serous, and devoid from lymph or blood vessels.

Equator *and* **equatorial plane**:[2] The virtual dividing line *and* plane between the distal and proximal faces of a palynomorph. (cf. polarity)

Exine *or* **exospore**:[2] The outer layer of the wall of a palynomorph, which is highly resistant to strong acids and bases, and is composed primarily of sporopollenin. (cf. layers)

Foot layer: cf. layers

Gemma (-ae): cf. infratectum

Gymnosperm:[1] A non-flowering spermatophyte. Gymnosperms are mainly represented by conifers and their allies.

Hypha (-ae):[1] A filament that make up the body of moulds like *Aspergillus* spp. and that ends with conidial heads or conidiophores.

HypoGel™:[278] A TentaGel™ derivatised with oligo ethylene glycols (5 or 10 monomer units).

Infratectum:[2] A general term for the spore wall layer beneath the tectum, which may

be *alveolar* (foam-like), *granular* (with grains), *columellar* (with *columellae*), or structureless. (cf. layers)

- **Baculum (-a)**: A cylindrical, free standing infractectal element, supporting no tectum or a caput.
- **Caput (-ita)**: The expanded head of a columella, left-over from a tectum.
- **Columella (-ae)**: A rod-like element of the sexine/ectexine, either supporting a tectum or a caput.
- **Gemma (-ae)**: A round element of the infratectum.
- **Pilum (-a)**: An element of the infratectum constituted of a columella and its caput.

Intine *or* **endospore**:[2] The innermost of the major layers of the pollen grain wall underlying the exine and bordering the surface of the cytoplasm. The intine is composed of polysaccharides, mainly cellulose, and is therefore not acetolysis resistant. (cf. layers)

Laesura (-ae): cf. aperture *and* trilete

Layers:[2] A general term applied to the distinct strata of the sporoderm (or palynoderm). The main layers (from the innermost) are *intine*, *exine*, in some cases *perine*, and *pollenkitt*. The presence of each layer or sublayer depends on the species of palynomorph. Exine itself is divided into subdivisions described by two systems:

- **The 'Faegri' system**: *ectexine* (outer part of exine, stained by fuschin) and *endexine* (inner part of exine, relatively unstained by fuschin – with no or little sporopollenin);
- **The 'Erdtman' system**: *sexine* (outer part of exine, sculptured) and *nexine* (inner part of exine, non-sculptured).

Finer divisions are (from the outermost): *tectal elements* (sexine 3), *tectum* (sexine 2), *infratectum* (sexine 1), *footlayer* (nexine 1), all of that being the *ectexine*, and *endexine* (nexine 2).

Loculus (-i):[4] The internal cavity of sporangium that holds spores or pollen grains during their maturation.

Microsporidian:[6] A parasitic protozoan that invades arthropods, annelids and fishes cells. It has minute spores (2-20µm) that sprout rapidly, infect the host cells and eventually destroy them. In silkworms, the species *Nosema bombycis* causes the disease *pébrine*.

Monolete:[2] Describing a spore with one laesura left by the tetrad separation on its proximal face. (cf. also trilete)

Nexine: cf. layers

Oblate: cf. shape classes

Orbicule *or* **Ubisch body**:[8,65,68] A spherical 6-8µm-sized granule formed in the tapetum of some angiosperms by accumulation of sporopollenin precursors in early developmental stages. Orbicules cross the loculus to deposit on the external template of growing microspores where sporopollenin polymerises. Eventually, excess sporopollenin concretes in extra orbicules left on the tapetal surface.

Ornamentation: cf. tectal elements

Palynoderm:[2] The entire wall of a pollen grain. (cf. also sporoderm)

Palynology:[2] The study of palynomorphs, pollen grains and spores, as well as some similar particles. The subdisciplines include *paleopalynology* (study of fossil palynomorphs), *aeropalynology* (study of palynomorphs found in the atmosphere), *melissopalynology* (study of palynomorphs found in honey or collected by bees) and *pollen analysis* (study of assemblages of dispersed palynomorphs such as those isolated from samples of peat).

Palynomorph:[2] A general term for all entities found in palynological preparations, mainly pollen grains and spores.

Parenteral:[6] Strictly speaking, describing a drug delivery route avoiding the gastro-intestinal tract; most generally, describing a mode of drug administration by injection (subcutaneous, intramuscular, intravenous, etc.).

Perine *or* **perispore**:[2] A sporoderm layer that is not always acetolysis resistant and is situated around the exine of some spores.

Peroblate *and* **perprolate**: cf. shape classes

Pilum (-a): cf infratectum

Pistil:[1] The female sexual organ of flowers, holding the ovary at its base, surmounted by the style and tipped by the stigma.

Polarity:[2] The condition of having distinct poles. The polarity of palynomorphs may be determined from their orientation in tetrads, or from the distribution of apertures and other features. The *equatorial plane* crosses the *polar axis* perpendicularly, and separates the *distal* side that faces outward in the tetrad stage and the *proximal* side that faces towards the centre of the tetrad during development.

Pollen:[2] The reproductive particle carrying gametes of seed plants (spermatophytes).

Pollen grains develop from microspores in male sporangia (anthers or male cones).

Pollenkitt:[2,49] A fatty coating covering entomophilous (insect-borne) pollen grains. This cement, composed of sticky waxes and volatile lipids originating from the tapetum, helps and holds the dispersal unit together, attracts pollinator insects and makes pollen adheres to them and to the stigma during fecundation.

Pollen tube:[1] The conduit grown through the style by a pollen grain when it lands on the stigmata of a flower, to deliver sperm cells (male gametes) to the ovaries, for fecundation.

Pore: Either a type of aperture[2] (cf. aperture), or a nano-sized channel that crosses the layers of exine and are parts of its constituting elements;[221] this second meaning is referred to as *nanopores* or *nanochannels* to avoid confusion. (See Section A-3.5)

Prolate: cf. shape classes

Proximal: cf. polarity

Psilate: cf. tectal elements

Reticulate: cf. tectal elements

Rugulate: cf. tectal elements

Saccate: cf. saccus

Saccus (-i):[1] A sac or bladder, sometimes called wing, formed on a pollen grain by expansion of the sexine detached from the nexine. Sacci are at least partly filled with an alveolar infratectum. A pollen grain exhibiting sacci is called *saccate*.

- **Bisaccate**: Describing pollen with two sacci (e.g. *Pinus* spec. pollen);
- **Corpus (-i)**: The body of a saccate pollen grain;
- **Monosaccate**: Describing pollen with one saccus.

Saprophytic:[1] Describing an organism, fungus, bacterium or protozoon, which feeds on non-living organic material, usually dead and decaying plant or animal matter.

Sculpturing:[2] A sculptured entity of exine layers, either internal (sexine) or external (tectal elements).

Sexine: cf. layers

Shape classes:[2] The categories of pollen and spore shape based on the relations between polar axis (P) and equatorial diameter (E).

	Shape name	P/E ratio
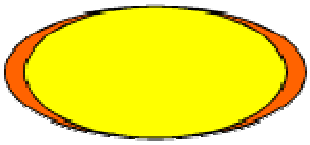	peroblate	<0.50
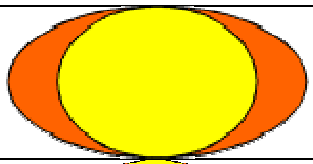	oblate	0.50-0.75
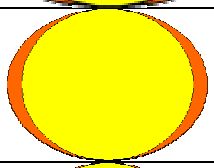	suboblate	0.75-0.88
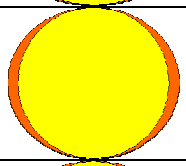	oblate spheroidal	0.88-1.00
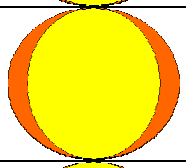	spheroidal	~1.00
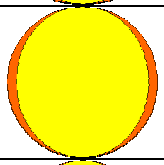	prolate spheroidal	1.00-1.14
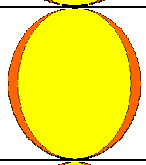	subprolate	1.14-1.33
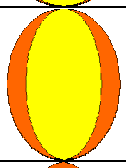	prolate	1.33-2.00
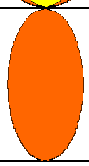	perprolate	>2

Spermatophyte:[1] A seed-bearing plant. Spermatophytes are traditionally subdivided into angiosperms and gymnosperms.

Spheroidal: cf. shape classes

Sporangium (-a):[1,4] The sexual organ of plant, internally carpeted by the *tapetum*, which produces spores or pollen grains within its cavity called *loculus*.

Spore: The term encompasses different meanings, more precisely the following ones:

- The minute, single- or few-celled, asexual reproductive unit of cryptogams and

fungi.[2] In this study, the general term *spore* is extensively used with this acceptation. With regard to its size, botanists and palynologists sometimes name it **megaspore, miospore**, **isospore** or **microspore**;[2] these names were however not used in this work.

- The sexual cell resulting in the fusion of two asexual spores in some fungi and more precisely named **ascospore** or **zygospore**, depending on the species.[1,6]
- In seed-bearing plants, the microscopic particle present in the sporangium as a precursor of a pollen grain (**microspore** in anther or male cone) or an ovule (**megaspore** in ovary or female cone).[1,2]
- The resistant cellular inclusion developed by some bacteria, mainly of *Bacillus* or *Clostridium* genera, in their dormant stages and also called **endospore**.[1,6] This acceptation is not used in this study, to avoid any confusion.
- By extension, the resistant cellular inclusion developed by some unicellular algae (**cyst**).[14]

Sporoderm:[2] The entire wall of a spore (or a pollen grain, by extension).

Sporoplasm:[1] The living part (protoplasm) of a spore (or a pollen grain, by extension).

Sporopollenin:[1,4,5] The name given to the acetolysis resistant biopolymers which make up most of the material of the exine.

Stamen:[1] The male sexual organ of flowers, composed of filaments holding up anthers.

Stigma (-):[1] The tip of the pistil, atop the style.

Striate: cf. tectal elements

Strobilus (-i):[16,18-20] A high leaf developed by certain fern allies (mainly *Lycopodium* spp.) and bearing the sporangia.

Style:[1] The stem of the pistil, atop the ovary and capped by the stigma.

Suboblate *and* **subprolate**: cf. shape classes

Sulcus (-i): cf. aperture

Tapetum (-a):[1,4] The internal tissue of sporangia which spores and pollen grains are made from.

Tectal elements:[2] The external sculptured ornamentations on the exine surface. They can have different shapes.

- **Echinate** *and* **microechinate**: Describing an ornamentation comprising **spines**.
- **Psilate**: Describing a palynomorph with a smooth surface.
- **Reticulate** *and* **microreticulate**: Describing an ornamentation comprising a

reticulum, consisting of a honey-comb-like pattern composed of ridges (**muri**) separating hollows (**lumina**).

- **Rugulate**: Describing an ornamentation comprising elongated elements arranged in an irregular pattern.
- **Striate**: Describing an ornamentation comprising **striae**, parallel elongated elements separated by grooves.
- **Verrucate**: Describing an ornamentation comprising **verrucae**, wart-like elements.

Tectum: cf. layers

TentaGel™:[278] A trade name given by Rapp Polymere GmbH to a derivatised copolymer consisting of a low cross-linked polystyrene matrix on which polyethylene glycol (PEG) is attached.

Tetrad:[2] A general term for a group of four united pollen grains or spores, either as a dispersal unit or as a developmental stage.

The *tetrad stage* is the period during post-meiotic development when the four spores are united by the presence of a temporary wall which is destroyed when the mature spores are freed. When the four particles that constituted the tetrad separate, they are sometimes marked by laesurae forming trilete or monolete scars, depending on the shape of the tetrad.

Tricolporate:[2] Describing pollen grains with three compound apertures (pores and colpi).

Trilete:[2,358] Describing a spore with three laesurae, thus showing a trilete mark (Y-shaped scar) left by the tetrad separation on its proximal face. (cf. also monolete)

Tryphine:[2,49] Debris (proteins and lipids) from the senescent tapetum coating the mature spore or pollen grain.

Ubisch body: cf. orbicule

Ulcus (-i): cf. aperture

Verrucate: cf. tectal elements

Viscin thread: An acetolysis resistant, sporopollenin cord-shaped strands arising from the exine of a pollen grain, usually from the proximal surface,[2] which crosses the loculus to join the tapetum. Viscin threads especially occur of *Ericaceae* and *Onagraceae*.[47]

Zygospore: cf spore

References

1. *Encyclopædia Britannica* (2006) Chicago: Encyclopædia Britannica, Inc. Available from: http://search.eb.com [accessed March 2007].
2. W. Punt, S. Blackmore, S. Nilsson and A. Le Thomas, *Glossary of Pollen and Spore Terminology*. P. Hoen (ed.) (1999) Utrecht: Laboratory of Palaeobotany and Palynology. Available from: http://www.bio.uu.nl/~palaeo/glossary/glos-int.htm [accessed March 2007].
3. A. Traverse, *Paleopalynology*. (1988) Boston: Unwin Huyman, 600 pp.
4. R. Kessler and M. Harley, *Pollen. The hidden sexuality of flowers*. (2004) London: Papadakis, 264 pp.
5. J. Heslop-Harrison, *"Sporopollenin in the biological context."* in J. Brooks *et al.* (eds.) *Sporopollenin*. (1971) London & New York: Academic Press, p. 1-30.
6. *Stedman's online medical dictionary*. (2006) Hagerstown: Lippincott Williams & Wilkins. Available from: www.stedmans.com/section.cfm/45 [accessed March 2007].
7. P. D. Moore, J. A. Webb and M. E. Collinson, *Pollen analysis*. 2nd ed. (1991) Oxford: Blackwell Scientific Publications, 216 pp.
8. J. Rozema, A. J. Noordijk, R. A. Broekman, A. van Beem, B. M. Meijkamp, N. V. J. de Bakker, J. W. M. van de Staaij, M. Stroetenga, S. J. P. Bohncke, M. Konert, S. M. Kars, H. Peat, R. I. L. Smith and P. Convey, *Plant Ecology*, **154** (2001) 11-26.
9. I. Orhan, E. Küpeli, B. Şener and E. Yesilada, *Journal of Ethnopharmacology*, **109** (2007) 146-150.
10. G. O. W. Kremp, *"Lycopodium clavatum."* in *The spores of the Pteridophytes*. (1972) Tokyo: Hirokawa, p. 144.
11. *"Pteridofitos."* (2002) Lima: Universidad Peruana Cayetano Heredia. Available from: http://www.geocities.com/fanerogamas/UPCH/Cripto/Pteridofitos/clase_iii.htm [accessed July 2007].
12. S. J. Kettley, *Ph.D. thesis*, University of Hull, UK (2001).
13. A. J. Boasman, *Ph.D. thesis*, University of Hull, UK (2003).
14. J. Brooks, P. R. Grant, M. Muir, P. Van Gijzel and G. Shaw (eds.)

Sporopollenin. (1971) London & New York: Academic Press, 718 pp.

15. J. Brooks and W. C. Elsik, *Grana*, **14** (1974) 85-91.
16. C. Linnaeus, *"Lycopodium clavatum."* in *Species Plantarum*. (1753) Stockholm: Laurentius Salvius, p. 1101.
17. H. Braconnot, *Annales de Chimie et de Physique*, **2** (1829) 91-105.
18. B. Oellgaard, *Opera Botanica*, **92** (1987) 153-178.
19. C. Jérôme, *Bulletin Annuel-Association des Amis du Jardin Botanique du Col de Saverne* (2004) 10-14.
20. C. Jérôme, *Le Monde des Plantes*, **483** (2004) 11.
21. *International Code of Botanical Nomenclature (Saint Louis Code)*, International Association for Plant Taxonomy (2001). Available from: http://www.bgbm.org/iapt/nomenclature/code/SaintLouis/0001ICSLContents.htm [accessed March 2007].
22. *"The International Plant Names Index."* (2004) IPNI. Available from: http://www.ipni.org [accessed March 2007].
23. M. Deprost, *"Mobilisation contre l'ambroisie."* in *Le Progrès* (Lyon, France) **2 Aug.** (2004) p. 5.
24. O. K. Davis, *"Ambrosia (Asteraceae)."* (1999) Tucson: University of Arizona. Available from: http://geo.arizona.edu/palynology [accessed March 2007].
25. *"Ambrosia trifida."* (2003) Bisbee (Arizona): Southwest School of Botanical Medicine. Available from: http://www.swsbm.com/NGSImages/Ambrosia_trifida.jpg [accessed July 2007].
26. D. W. Denning, J.-P. Latgé, P. E. Verweij, M. J. Day, D. Graybill, W. J. Steinbach, J. Frisvad, M. A. Peñalva, G. Atherton, J. Bartholomew and P. Giles, *"The Aspergillus Website."* K. Knight (ed.) (2007). Available from: http://www.aspergillus.org.uk [accessed March 2007].
27. W. Gardener, *personnal communication*, Tate & Lyle PLC, Selby, UK (2006).
28. S. S. Tsay and K. Y. To, *Biotechnology and Bioengineering*, **29**(*3*) (1987) 297-304.
29. *"Aspergillus niger."* Manual de Sanidade de Sementes. Available from: www.patologiadesementes.com.br [accessed July 2007].
30. D. Scharf, *"Stock images: yeast and fungi."* Scharf Photo. Available from: http://www.scharfphoto.com/stockphotos/archives/cat_yeast_and_fungi.php [accessed July 2007].

31. *"Genomics: Aspergillus niger."* (2007) DSM Food Specialties. Available from: http://www.dsm.com/en_US/html/dfs/genomics_aniger.htm [accessed July 2007].
32. D. Ellis, *"Aspergillus niger."* (2006) Adelaide: University of Adelaide. Available from: http://www.mycology.adelaide.edu.au [accessed March 2007].
33. E. P. Feofilova, D. V. Nemsted, V. M. Tereshina and A. S. Memorskaya, *Applied Biochemistry and Microbiology*, **42**(*6*) (2006) 545-549.
34. J. Brooks and G. Shaw, *Grana*, **17** (1978) 91-97.
35. J. Brooks and G. Shaw, *Transactions of the Bose Research Institute*, **40**(*2*) (1977) 19-38.
36. G. Shaw, *"The chemistry of sporopollenin."* in J. Brooks *et al.* (eds.) *Sporopollenin*. (1971) London & New York: Academic Press, p. 305-348.
37. J. Brooks and G. Shaw, *Chemical Geology*, **10**(*1*) (1972) 69-87.
38. *"Chlorella."* (2007) Nutrimart.com. Available from: http://www.nutrimart.com/Bulk/Description/chlorell.htm [accessed July 2007].
39. *"Order Chlorella."* (2005) Nature's balance. Available from: http://www.natures-balance.com/Catalog/Chlorella_Home/ChlorellaOrder/chlorellaorder.html [accessed July 2007].
40. R. Kay, *Critical Reviews in Food Science and Nutrition*, **30**(*6*) (1991) 555-573.
41. P. F. van Bergen, P. Blokker, M. E. Collinson, J. S. Sinninghe Damsté and J. W. De Leeuw, *"Structural biomacromolecules in plants: what can be learnt from the fossil record?"* in A. R. Hemsley and I. Poole (eds.) *The Evolution of Plant Physiology. From wholes plants to ecosystems.* Chapter 8 (2004) London: Elsevier Academic Press, p. 133-154.
42. A. Maack, *"Sporopollenin - A new versatile biopolymer."* in *Polymerix*, held in Rennes, France (2003).
43. A. W. Atkinson, Jr., B. E. S. Gunning and P. C. L. John, *Planta*, **107** (1972) 1-32.
44. D. D. Fernando and D. D. Cass, *American Journal of Botany*, **81**(*12*) (1994) 1592-1600.
45. W. G. Chaloner and G. Orbell, *"A palaeobiological definition of sporopollenin."* in J. Brooks *et al.* (eds.) *Sporopollenin*. (1971) London & New York: Academic Press, p. 273-294.

46. K. Faegri and J. Iversen, *Textbook of Pollen Analysis*. 2nd ed. (1964) Oxford: Blackwell, 237 pp.
47. R. Wiermann and S. Gubatz, *International Review of Cytology-a Survey of Cell Biology*, **140** (1992) 35-72.
48. S. Gubatz, S. Herminghaus, B. Meurer, D. Strack and R. Wiermann, *Pollen et Spores*, **28**(*3-4*) (1986) 347-354.
49. P. Echlin, *"Production of sporopollenin by the tapetum."* in J. Brooks *et al.* (eds.) *Sporopollenin*. (1971) London & New York: Academic Press, p. 220-247.
50. J. W. De Leeuw and C. Largeau, *"A review of macromolecular compounds that comprise living organisms and their role in kerogen, coal and petroleum formation."* in M. H. Engel and S. A. Macko (eds.) *Organic Geochemistry, Principles and Applications*. (1993) New York: Plenum Press, p. 23-72.
51. J. W. De Leeuw, G. J. M. Versteegh and P. F. Van Bergen, *Plant Ecology*, **182**(*1-2*) (2006) 209-233.
52. J. F. John, *Journal für Chemie und Physik*, **12**(*3*) (1814) 244-252.
53. F. Zetzsche and K. Huggler, *Justus Liebigs Annalen der Chemie*, **461** (1928) 89-108.
54. F. Zetzsche, P. Kalt, J. Lietchi and E. Ziegler, *Journal Für Praktische Chemie*, **148** (1937) 267-286.
55. F. Zetzsche and O. Kälin, *Helvetica Chimica Acta*, **14**(*63*) (1931) 517-519.
56. F. Zetzsche and H. Vicari, *Helvetica Chimica Acta*, **14** (1931) 62-67.
57. G. Shaw, *"Sporopollenin."* in J. B. Harborne (ed.) *Phytochemical Phylogeny*. Chapter 3 (1970) London & New York: Academic Press, p. 31-35.
58. J. Burczyk and J. Dworzanski, *Phytochemistry*, **27**(*7*) (1988) 2151-2153.
59. A. Kadouri, S. Derenne, C. Largeau, E. Casadevall and C. Berkaloff, *Phytochemistry*, **27**(*2*) (1988) 551-557.
60. C. Berkaloff, E. Casadevall, C. Largeau, P. Metzger, S. Peracca and J. Virlet, *Phytochemistry*, **22**(*2*) (1983) 389-397.
61. P. Blokker, S. Schouten, J. W. De Leeuw, J. S. Sinninghe Damsté and H. Van den Ende, *Planta*, **207** (1999) 539-543.
62. G. W. Gooday, P. Fawcett, D. Green and G. Shaw, *Journal of General Microbiology*, **74** (1973) 233-239.
63. U. Brunner and R. Honegger, *Canadian Journal of Botany*, **63**(*12*) (1985) 2221-2230.

64. P. F. van Bergen, M. E. Collinson, D. E. G. Briggs, J. W. De Leeuw, A. C. Scott, R. P. Evershed and P. Finch, *Acta Botanica Neerlandica*, **44**(*4*) (1995) 319-342.

65. R. G. Stanley and H. F. Linskens (eds.) *Pollen: biology, biochemistry, management*. (1974) Berlin, Heidelberg & New York: Springer-Verlag, 307 pp.

66. M. Leigh, *M.Chem. thesis*, University of Hull, UK (2007).

67. J. R. Rowley and J. J. Skvarla, *American Journal of Botany*, **62**(*5*) (1975) 479-485.

68. P. Echlin and H. Godwin, *Journal of Cell Science*, **3**(*3*) (1968) 161-174.

69. P. Echlin and H. Godwin, *Journal of Cell Science*, **3**(*3*) (1968) 175-186.

70. N. I. Gabarayeva, *Review of Palaeobotany and Palynology*, **85** (1995) 123-152.

71. J. R. Rowley, *Grana*, **13** (1973) 129-138.

72. J. Brooks and G. Shaw, *"Recent developments in the chemistry, biochemistry, geochemistry and post-tetrad ontogeny of sporopollenins derived from pollen and spore exines."* in J. Heslop-Harrison (ed.) *Pollen: development and physiology*. (1971) London: Butterworths, p. 99-114.

73. J. Brooks and G. Shaw, *Grana Palynologica*, **8**(*2-3*) (1968) 227-234.

74. C. M. Rogers and B. D. Harris, *American Journal of Botany*, **56**(*10*) (1969) 1209-1211.

75. M. Takahashi and J. J. Skvarla, *American Journal of Botany*, **78**(*8*) (1991) 1063-1069.

76. W. A. Taylor, *American Journal of Botany*, **80**(*2*) (1993) 165-171.

77. W. A. Taylor, *Pollen et Spores*, **31**(*3-4*) (1989) 251-288.

78. A. R. Hemsley, *Courier Forschung-Institute of Senckenberg*, **147** (1992) 93-107.

79. A. R. Hemsley and A. C. Scott, *Review of Palaeobotany and Palynology*, **69** (1991) 337-351.

80. J. R. Rowley, J. J. Skvarla and G. El-Ghazaly, *Canadian Journal of Botany*, **81**(*11*) (2003) 1070-1082.

81. M. A. Morbelli and J. R. Rowley, *Sexual Plant Reproduction*, **6** (1993) 98-107.

82. G. Shaw and A. Yeadon, *Journal of the Chemical Society* (1966) 16-22.

83. D. Green, *Ph.D. thesis*, University of Bradford, UK (1973).

84. W. J. Guilford, D. M. Schneider, J. Labovitz and S. J. Opella, *Plant Physiology*, **86**(*1*) (1988) 134-136.

85. G. Shaw and D. C. Apperley, *Grana*, **35**(*2*) (1996) 125-127.
86. G. Shaw and A. Yeadon, *Grana Palynologica*, **5**(*2*) (1964) 247-252.
87. G. Erdtman, *Svensk Botanisk Tidskrift*, **54**(*4*) (1960) 561-564.
88. M. Hesse and M. Waha, *Plant Systematics and Evolution*, **163**(*3-4*) (1989) 147-152.
89. E. Domínguez, J. A. Mercado, M. A. Quesada and A. Heredia, *Grana*, **37**(*2*) (1998) 93-96.
90. K. Schulze Osthoff and R. Wiermann, *Journal of Plant Physiology*, **131**(*1-2*) (1987) 5-15.
91. A. R. Hemsley, A. C. Scott, P. J. Barrie and W. G. Chaloner, *Annals of Botany*, **78**(*1*) (1996) 83-94.
92. M. S. Amer and R. Tawashi (Amer Particle Technologies Inc.), USA, *Patent* **US 5,013,552** (1991).
93. M. S. Amer and R. Tawashi (Amer Particle Technologies Inc.), USA, *Patent* **US 5,275,819** (1994).
94. R. Tawashi, USA, *Patent* **US005648101A** (1997).
95. F. A. Loewus, B. G. Baldi, V. R. Franceschi, L. D. Meinert and J. J. McCollum, *Plant Physiology*, **78**(*3*) (1985) 652-654.
96. K. E. Espelie, F. A. Loewus, R. J. Pugmire, W. R. Woolfenden, B. G. Baldi and P. H. Given, *Phytochemistry*, **28**(*3*) (1989) 751-753.
97. M. Couderchet, J. Schmalfuß and P. Böger, *Pesticide Biochemistry and Physiology*, **55**(*3*) (1996) 189-199.
98. B. G. Baldi, V. R. Franceschi and F. A. Loewus, *Protoplasma*, **141**(*1*) (1987) 47-55.
99. D. Southworth, *American Journal of Botany*, **72**(*8*) (1985) 1274-1283.
100. D. Southworth, *Grana*, **24** (1985) 161-166.
101. E. Duhoux, *Zeitschrift für Pflanzenphysiology*, **99** (1980) 207-214.
102. S. Herminghaus, S. Gubatz, S. Arendt and R. Wiermann, *Zeitschrift Für Naturforschung C-a Journal of Biosciences*, **43**(*7-8*) (1988) 491-500.
103. F. Ahlers, J. Lambert and R. Wiermann, *Zeitschrift Für Naturforschung C-a Journal of Biosciences*, **54**(*7-8*) (1999) 492-495.
104. S. Gubatz, M. Rittscher, A. Meuter, A. Nagler and R. Wiermann, *Grana*, **Suppl. 1** (1993) 12-17.
105. C. Jungfermann, F. Ahlers, M. Grote, S. Gubatz, S. Steuernagel, I. Thom, G.

Wetzels and R. Wiermann, *Journal of Plant Physiology*, **151**(*5*) (1997) 513-519.

106. J. R. Rowley, J. J. Flynn and M. Takahashi, *Botanica Acta*, **108** (1995) 300-308.
107. D. Southworth, *American Journal of Botany*, **61**(*1*) (1974) 36-44.
108. J. Wittborn, K. V. Rao, G. El-Ghazaly and J. R. Rowley, *Annals of Botany*, **82**(*2*) (1998) 141-145.
109. J. R. Rowley, *Plant Systematics and Evolution*, **Suppl. 5** (1990) 13-29.
110. J. M. Pettitt, *Protoplasma*, **88** (1976) 117-131.
111. J. Rozema, R. A. Broekman, P. Blokker, B. B. Meijkamp, N. de Bakker, J. van de Staaij, A. van Beem, F. Ariese and S. M. Kars, *Journal of Photochemistry and Photobiology B-Biology*, **62**(*1-2*) (2001) 108-117.
112. P. Blokker, P. Boelen, R. Broekman and J. Rozema, *Plant Ecology*, **182** (2006) 197-207.
113. J. Brooks and G. Shaw, *Nature*, **220** (1968) 678-679.
114. J. Brooks and G. Shaw, *Nature*, **223** (1969) 754-756.
115. J. Brooks and G. Shaw, *Grana*, **11** (1971) 1-8.
116. K. Faegri, *"The preservation of sporopollenin membranes under natural conditions."* in J. Brooks *et al.* (eds.) *Sporopollenin*. (1971) London & New York: Academic Press, p. 256-272.
117. H. Ahokas, *Experientia*, **32**(*2*) (1976) 175-177.
118. L. J. Blackwell, *Ph.D. thesis*, University of Hull, UK (2008).
119. B. P. Binks, J. H. Clint, G. Mackenzie, C. Simcock and C. P. Whitby, *Langmuir*, **21**(*18*) (2005) 8161-8167.
120. I. W. Bailey, *Journal of the Arnold Arboretum*, **41** (1960) 141-151.
121. F. Ahlers, J. Lambert and R. Wiermann, *Zeitschrift Für Naturforschung C-a Journal of Biosciences*, **58**(*11-12*) (2003) 807-811.
122. A. Maack, Germany, *Patent* **WO 03/094942** (2003).
123. A. Maack, Germany, *Patent* **US 7,182,965** (2005).
124. A. Diego Taboada, *personnal communication*, University of Hull, UK (2007).
125. D. Southworth, *Canadian Journal of Botany*, **64** (1986) 983-987.
126. M. Kedves, *Review of Palaeobotany and Palynology*, **64** (1990) 181-186.
127. A. R. Hemsley, M. E. Collinson, W. L. Kovach, B. Vincent and T. Williams, *Philosophical Transactions of the Royal Society of London, Series B*, **345** (1994) 163-173.
128. A. R. Hemsley, P. D. Jenkins, M. E. Collinson and B. Vincent, *Botanical*

Journal of the Linnean Society, **121** (1996) 177-187.

129. A. R. Hemsley, B. Vincent, M. E. Collinson and P. C. Griffiths, *Annals of Botany*, **82** (1998) 105-109.
130. M. E. Collinson, A. R. Hemsley and W. A. Taylor, *Grana*, **Suppl. 1** (1993) 31-39.
131. A. R. Hemsley, M. E. Collinson and A. P. R. Brain, *Botanical Journal of the Linnean Society*, **108** (1992) 307-320.
132. J. Wittborn, K. V. Rao, G. El-Ghazaly and J. R. Rowley, *Grana*, **35** (1996) 185-198.
133. B. M. Gullvåg, *Grana Palynologica*, **6**(*3*) (1966) 435-475.
134. I. Thom, M. Grote, J. Abraham-Peskir and R. Wiermann, *Protoplasma*, **204** (1998) 13-21.
135. M. Kawase and M. Takahashi, *Grana*, **34**(*4*) (1995) 242-245.
136. D. Southworth, *Grana Palynologica*, **9**(*1-3*) (1969) 5-15.
137. J. Brooks and G. Shaw, *Nature*, **219** (1968) 532-533.
138. C. S. Cockell and J. Knowland, *Biological Reviews*, **74**(*3*) (1999) 311-345.
139. P. Blokker, D. Yeloff, P. Boelen, R. A. Broekman and J. Rozema, *Analytical Chemistry*, **77** (2005) 6026-6031.
140. M. Geisert, T. Rose, R. K. Zahn, G. Shaw and J. Brooks, *Journal Für Praktische Chemie*, **330**(*3*) (1988) 476-478.
141. H. Bubert, J. Lambert, S. Steuernagel, F. Ahlers and R. Wiermann, *Zeitschrift Für Naturforschung C-a Journal of Biosciences*, **57**(*11-12*) (2002) 1035-1041.
142. C. Grimshaw, *"Sir John Cornforth in conversation with Prof. T.W. Goodwin, 11 October 1989."* (1990) UK. Interview: 134min 33s. Available from: http://edina.ac.uk/purl/isan/0028-0000-2505-0000-0-0000-0000-0 [accessed August 2007].
143. E. Domínguez, J. A. Mercado, M. A. Quesada and A. Heredia, *Sexual Plant Reproduction*, **12**(*3*) (1999) 171-178.
144. R. Hollyhead, *Ph.D. thesis*, University of Bradford, UK (1972).
145. K. Wehling, C. Niester, J. J. Boon, M. T. M. Willemse and R. Wiermann, *Planta*, **179**(*3*) (1989) 376-380.
146. R. G. Achari, G. Shaw and R. Holleyhead, *Chemical Geology*, **12**(*3*) (1973) 229-234.
147. M. M. Mulder, E. R. E. Van der Hage and J. J. Boon, *Phytochemical Analysis*, **3**

(1992) 165-172.

148. J. S. Watson, M. A. Sephton, S. V. Sephton, S. Self, W. T. Fraser, B. H. Lomax, I. Gilmour, C. H. Wellman and D. J. Beerling, *Photochemical and Photobiological Sciences*, **6** (2007) 689-694.
149. L. Galbraith, *personnal communication*, University of Hull, UK (2003).
150. P. Fawcett, D. Green, R. Holleyhead and G. Shaw, *Grana*, **10** (1970) 246-247.
151. J. Barkauskas and M. Dervinyte, *Journal of the Serbian Chemical Society*, **69**(*5*) (2004) 363-375.
152. H. P. Boehm, *Advances in Catalysis*, **16** (1966) 179-274.
153. B. Dinneweth, *M.Sc. thesis*, University of Hull, UK (2002).
154. L. Maillet, *M.Sc. thesis*, University of Hull, UK (2002).
155. A.-K. Prahl, H. Springstubbe, K. Grumbach and R. Wiermann, *Zeitschrift Für Naturforschung C-a Journal of Biosciences*, **40**(*9-10*) (1985) 621-626.
156. S. Gubatz and R. Wiermann, *Botanica Acta*, **105** (1992) 407-413.
157. S. Gubatz and R. Wiermann, *Zeitschrift Für Naturforschung C-a Journal of Biosciences*, **48**(*1-2*) (1993) 10-15.
158. A. Meuter-Gerhards, S. Riegert and R. Wiermann, *Journal of Plant Physiology*, **154**(*4*) (1999) 431-436.
159. A. Meuter-Gerhards, C. Schwerdtfeger, S. Steuernagel, S. Wilmesmeier and R. Wiermann, *Zeitschrift Für Naturforschung C-a Journal of Biosciences*, **50**(*7-8*) (1995) 487-492.
160. F. Ahlers, H. Bubert, S. Steuernagel and R. Wiermann, *Zeitschrift Für Naturforschung C-a Journal of Biosciences*, **55**(*3-4*) (2000) 129-136.
161. S. Wilmesmeier, S. Steuernagel and R. Wiermann, *Zeitschrift Für Naturforschung C-a Journal of Biosciences*, **48**(*9-10*) (1993) 697-701.
162. R. Hayatsu, R. E. Botto, R. L. McBeth, R. G. Scott and R. E. Winans, *Energy and Fuels*, **2** (1988) 843-847.
163. A. R. Hemsley, W. G. Chaloner, A. C. Scott and C. J. Groombridge, *Annals of Botany*, **69**(*6*) (1992) 545-549.
164. A. R. Hemsley, P. J. Barrie, W. G. Chaloner and A. C. Scott, *Grana*, **Suppl. 1** (1993) 2-11.
165. A. Fasano, *Journal of Pharmaceutical Sciences*, **87**(*11*) (1998) 1351-1356.
166. F. Delie and M. J. Blanco-Príeto, *Molecules*, **10**(*1*) (2005) 65-80.
167. F. Ahlers, I. Thom, J. Lambert, R. Kuckuk and R. Wiermann, *Phytochemistry*,

50(*6*) (1999) 1095-1098.

168. M. Rittscher and R. Wiermann, *Sexual Plant Reproduction*, **1** (1988) 125-131.
169. M. Rittscher and R. Wiermann, *Sexual Plant Reproduction*, **1** (1988) 132-139.
170. J. H. Ford, *"Pollen wall development in epacridaceae."* in J. Brooks *et al.* (eds.) *Sporopollenin*. (1971) London & New York: Academic Press, p. 130-173.
171. R. Potonié and K. Rehnelt, *"Aspects of sporin."* in J. Brooks *et al.* (eds.) *Sporopollenin*. (1971) London & New York: Academic Press, p. 295-304.
172. T. Liu and Z. Zhang, *Biotechnology and Bioengineering*, **85**(*7*) (2004) 770-775.
173. W. Jorde and H. F. Linskens, *Acta Allergologica*, **29**(*3*) (1974) 165-175.
174. D. Southworth, M. B. Singh, T. Hough, I. J. Smart, P. Taylor and R. B. Knox, *Planta*, **176** (1988) 482-487.
175. *Wikipedia* (2007). Available from: http://en.wikipedia.org [accessed July 2007].
176. M. L. Weiner, *Food and Chemical Toxicology*, **26**(*10*) (1988) 867-880.
177. G. Fabian, *Lymphology*, **16**(*1*) (1983) 43-48.
178. G. Volkheimer, *Pathologe*, **14**(*5*) (1993) 247-252.
179. G. Volkheimer, *Zeitschrift für Gastroenterologie*, **2** (1964) 57-64.
180. G. Volkheimer, F. H. Schulz, H. Wendland and E. D. Hausdorf, *Maroc Médical*, **47**(*506*) (1967) 626-633.
181. G. Volkheimer and F. H. Schultz, *Digestion*, **1** (1968) 213-218.
182. G. Volkheimer and F. H. Schultz, *Qualitas Plantarum et Materiae Vegetabilies*, **17** (1968) 17-30.
183. G. Volkheimer, F. H. Schulz, H. Lehmann, I. Aurich, M. Hübner, A. Hallmayer, H. Münch, H. Oppermann and S. Strauch, *Medicina Experimentalis. International Journal of Experimental Medicine*, **18** (1968) 103-108.
184. G. Volkheimer, *Acta Hepato-Gastroenterologica*, **20**(*5*) (1973) 361-362.
185. C. L. Wells, M. A. Maddaus, S. L. Erlandsen and R. L. Simmons, *Infection and Immunity*, **56** (1988) 278-282.
186. L. T. Canham, R. S. Saffie, S. E. Connor and R. Aston, *Drug Delivery World*, **Winter**(*2*) (2001) 56-63.
187. W. A. Walker and K. J. Bloch, *The New York Academy of Science* (1983) 593-602.
188. D. E. Bockman and W. B. Winborn, *Anatomical Record*, **155** (1996) 603-622.
189. E. Sanders and C. T. Ashworth, *Experimental Cell Research*, **22** (1961) 137-145.

190. M. Thomasson, *personnal communication*, University of Hull, UK (2007).

191. D. H. Robinson and J. W. Mauger, *American Journal of Hospital Pharmacy*, **48**(*10*) (1991) S14-S23.

192. A. Leone-Bay, D. R. Paton and J. J. Weidner, *Medicinal Research Reviews*, **20**(*2*) (2000) 169-186.

193. S. L. Atkin, S. Barrier, S. T. Beckett, T. Brown, G. Mackenzie and L. Madden, *Collection Symposium Series*, **7** (2005) 307-311.

194. G. Orive, R. M. Hernández, A. Rodríguez Gascón, A. Domínguez-Gil and J. L. Pedraz, *Current Opinion in Biotechnology*, **14**(*6*) (2003) 659-664.

195. P. Forssell, R. Partanen and K. Poutanen, *Food Science & Technology*, **20**(*3*) (2006) 18-20.

196. L. Brannon-Peppas, *Medical Plastics & Biomaterials*, **Nov.-Dec.** (1997) 34-44.

197. R. Z. B. Desamero, H. Cheng, S. Cahill, M. Girvin, H. Deng, R. Callender, P. Rath, B. Variano and J. E. Smart, *Biopolymers*, **67**(*1*) (2002) 26-40.

198. V. V. Ranade, *Journal of Clinical Pharmacology*, **31**(*1*) (1991) 2-16.

199. T. M. Dando and C. M. Perry, *Drugs*, **63**(*24*) (2003) 2755-2766.

200. J. Staniforth, R. M. Bannister, J. C. Gilbert, D. A. V. Morton and A. J. M. Richards, UK, *Patent* **WO 01/76575** (2001).

201. J. L. Jorizzo, *Journal of Cutaneous Medicine and Surgery*, **8**(*Suppl. 3*) (2004) 13-21.

202. J. L. Jorizzo, *Journal of Drugs in Dermatology*, **3**(*1*) (2004) 21-26.

203. J. L. Jorizzo, D. Stewart, A. Bucko, S. A. Davis, P. Espy, P. Hino, D. Rodriguez, R. Savin, D. Stough, K. Furst, M. Connolly and S. Levy, *Cutis*, **70**(*6*) (2002) 335-339.

204. C. A. Tabrizi, P. Walcher, U. B. Mayr, T. Stiedl, M. Binder, J. McGrath and W. Lubitz, *Current Opinion in Biotechnology*, **15**(*6*) (2004) 530-537.

205. K. Coupland, *personnal communication*, University of Hull, UK (2007).

206. Z. H. Wu, Q. N. Ping, Y. Wei and J. M. Lai, *Acta Pharmacologica Sinica*, **25**(*7*) (2004) 966-972.

207. J. R. P. Bishop, G. Nelson and J. Lamb, *Journal of Microencapsulation*, **15**(*6*) (1998) 761-773.

208. P. Berressem, *Chemistry in Britain*, **35**(*2*) (1999) 29-32.

209. S. J. Jackson and K. Lee, *Lebensmittel-Wissenschaft & Technologie*, **24**(*4*) (1991) 289-297.

210. M. Tsukada, A. Shirata and S. J. Hayasaka (Director General of National Institute of Sericultural and Entomological Sciences, Japanese Ministery of Agriculture, Forestry and Fisheries), USA, *Patent* **US 6,156,330** (2000).
211. M. Thomasson, *Literature review*, University of Hull, UK (2005).
212. J. A. Ko, H. J. Park, Y. S. Park, S. J. Hwang and J. B. Park, *Journal of Microencapsulation*, **20**(*6*) (2003) 791-797.
213. L. W. Chan, L. T. Lim and P. W. S. Heng, *Journal of Microencapsulation*, **17**(*6*) (2000) 757-766.
214. P. T. Tayade and R. D. Kale, *AAPS PharmSci*, **6**(*1*) (2004).
215. J. Whelan, *Drug Discovery Today*, **6**(*23*) (2001) 1183-1184.
216. G. De Rosa, F. Quaglia, M. I. La Rotonda, M. Besnard and E. Fattal, *International Journal of Pharmaceutics*, **242**(*1-2*) (2002) 225-228.
217. M. Saravanan, K. Bhaskar, G. S. Rao and M. D. Dhanaraju, *Journal of Microencapsulation*, **20**(*3*) (2003) 289-302.
218. F. Delie, *Advanced Drug Delivery Reviews*, **34**(*2-3*) (1998) 221-233.
219. S. R. Hall, H. Bolger and S. Mann, *Chemical Communications*, **22** (2003) 2784-2785.
220. Y. J. Wang and F. Caruso, *Chemical Communications*, **13** (2004) 1528-1529.
221. G. Bohne, E. Richter, H. Woehlecke and R. Ehwaldi, *Annals of Botany*, **92**(*2*) (2003) 289-297.
222. A. Löbbert, *personnal communication*, University of Hull, UK (2007).
223. *Everything added to food in the U.S.*, Food and Drug Administration (2007). Available from: http://vm.cfsan.fda.gov/~dms/eafus.html [accessed 18/05/2007].
224. E. Andrews, *personnal communication*, Nestlé PTC, York, UK (2005).
225. P. Fletcher, *personnal communication*, University of Hull, UK (2005).
226. B. Binks and T. Dunstan, *personnal communication*, University of Hull, UK (2005).
227. J. Emberlin, B. Adams-Groom and J. Tidmarsh, *Report commissioned by the Soil Association*, National Pollen Research Unit, Worcester, UK (1999).
228. A. Osol and R. Pratt (eds.) *The United States Dispensatory*. 27th ed. (1973) Philadelphia: Lippincott.
229. R. Otton, F. Graziola, J. de Souza, T. Curi, M. Hirata and R. Curi, *Cell Biochemistry and Function*, **16** (2000) 253-259.
230. M. E. Surette (Pilot Therapeutics, Inc.), USA, *Patent* **US 6,667,064** (2001).

231. *"Prolea, la filière française des huiles et protéines végétales."* (2007) Prolea. Available from: http://www.prolea.com/ [accessed July 2007].

232. British Pharmacopoeia Commission, *British Pharmacopoeia*. (2005) Norwich: The Stationery Office.

233. B. D. Llewellyn, *"Index of dyes."* (2005) StainsFile. Available from: http://stainsfile.info/StainsFile/dyes/dyes.htm [accessed July 2007].

234. V. N. Paunov, G. Mackenzie and S. D. Stoyanov, *Journal of Materials Chemistry*, **17** (2007) 609-612.

235. R. W. Griffiths and G. J. Gleich, *The Journal of Biological Chemistry*, **247**(*14*) (1972) 4543-4548.

236. G. Schultz and A. K. Solomon, *Journal of General Physiology*, **44** (1961) 1189-1199.

237. M. Sutter, S. Oliveira, N. N. Sanders, B. Lucas, A. Hoek, M. A. Hink, A. J. W. G. Visser, S. C. Smedt, W. E. Hennink and W. Jiskoot, *Journal of Fluorescence*, **17**(*2*) (2007) 181-192. .

238. D. T. Plummer (ed.) *An Introduction to Practical Biochemistry*. 2nd ed. (1978) London: McGraw-Hill, 362 pp.

239. W. L. Chu, *"Nucleic acid drug market to reach €161bn?"* in *Drug Reasearcher*, **19th Jan.** (2005). Available from: http://www.drugresearcher.com/news/ng.asp?n=57462-nucleic-acid-drug [accessed August 2007].

240. N. Gabarayeva and A. R. Hemsley, *Review of Palaeobotany and Palynology*, **138**(*2*) (2006) 121-139.

241. J. R. Rowley and J. J. Skvarla, *Review of Palaeobotany and Palynology*, **140** (2006) 91-112.

242. J. Rozema, P. Boelen and P. Blokker, *Environmental Pollution*, **137** (2005) 428-442.

243. D. Berry, *"Fats' chance."* in *Food Product Design* (2003). Available from: http://www.foodproductdesign.com/articles/0603AP.html [accessed March 2007].

244. S. Cérantola, F. Breton, E. Ar Gall and E. Deslandes, *Botanica Marina*, **49**(*4*) (2006) 347-351.

245. C. Leray, *"Cyberlipid center."* (2007) Cyberlipid. Available from: http://www.cyberlipid.org/index.htm [accessed September 2007].

246. *Peroxide value - acetic acid-chloroform method*, American Oil Chemists' Society (2003).
247. *Peroxide value*, IUPAC (1971).
248. *Peroxide value (PV)*, Croda Chemicals Europe Ltd. (2003).
249. *Anisidine value (PAV)*, Croda Chemicals Europe Ltd. (2004).
250. Y. Raoul, *personnal communication*, Croda, Hull, UK (2007).
251. C. Paquot and J. Mercier, *Journal of the American Oil Chemists' Society*, **36** (1959) 20-21.
252. A. V. A. Resurreccion and A. E. Reynolds, *Journal of Food Science*, **55**(*3*) (1990) 629-&.
253. A. J. Young and G. M. Lowe, *Archives of Biochemistry and Biophysics*, **385**(*1*) (2001) 20-27.
254. A. Kontush, B. Finckh, B. Karten, A. Kohlschutter and U. Beisiegel, *Journal of Lipid Research*, **37**(*7*) (1996) 1436-1448.
255. J. Cherfas, *New Scientist*, **1674** (1989).
256. *"Health effects of UV radiation."* (2007) World Health Organisation. Available from: http://www.who.int/uv/health/en/ [accessed July 2007].
257. H. Davies, G. R. Bignell and C. Cox, *Nature*, **417** (2002) 949-954.
258. T. A. Day and S. M. Demchik, *Environmental and Experimental Botany*, **36**(*4*) (1996) 447-454.
259. F. S. Xiong, J. Komenda, J. Kopecký and L. Nedbal, *Physiologia Plantarum*, **100**(*2*) (1997) 378-388.
260. *Food grade d-limonene: MSDS*, Florida Chemical Company Inc. (2006). Available from: http://www.floridachemical.com/302000_Food_Grade_d-Limonene_MSDS.pdf [accessed July 2007].
261. R. C. Weast (ed.) *Handbook of Chemistry and Physics*. 55th ed. (1974) Cleveland: CRC Press.
262. M. Leja, A. Mareczek, G. Wyżgolik, J. Klepacz-Baniak and K. Czekońska, *Food Chemistry*, **100**(*1*) (2007) 237-240.
263. T. Nagai, R. Inoue, N. Suzuki, T. Myoda and T. Nagashima, *International Journal of Molecular Medicine*, **15**(*2*) (2005) 259-263.
264. G. Miliauskas, P. R. Venskutonis and T. A. van Beek, *Food Chemistry*, **85**(*2*) (2004) 231-237.
265. P. McGuigan, *"Taking the 'fishy' out of fish oil."* in *Functional Foods and*

Nutraceuticals Magazine, **Sept.** (2005) p. 32-33. Available from: www.ffnmag.com.

266. H. Bays, *The American Journal of Cardiology*, **98**(*4A*) (2006) 71-76.
267. X. Zhu and A. Taneja, *"The trouble with omega-3 oils."* in *Functional Foods and Nutraceuticals Magazine*, **Sept.** (2006) p. 26. Available from: www.ffnmag.com.
268. S. C. Johnson and T. Cesario, *"How to fine-tune your flavours?"* in *Functional Foods and Nutraceuticals Magazine*, **Sept.** (2004). Available from: www.ffnmag.com.
269. J. Szejtli and L. Szente, *European Journal of Pharmaceutics and Biopharmaceutics*, **61**(*3*) (2005) 115-125.
270. B. Albertini, C. Cavallari, N. Passerini, D. Voinovich, M. L. Gonzalez-Rodriguez, L. Magarotto and L. Rodriguez, *European Journal of Pharmaceutical Sciences*, **21**(*2-3*) (2004) 295-303.
271. J. H. Cheng and H. W. Ockerman, *Meat Science*, **49**(*1*) (1998) 65-78.
272. S. M. Jafari, E. Assadpoor, B. Bhandari and Y. He, *Food Research International*, **41** (2008) 172-183.
273. W. Klaypradit and Y.-W. Huang, *LWT - Food Science and Technology*, **41** (2008) 1133-1139.
274. C. Dean and J. F. Lawless, *Journal of the American Statistical Association*, **84** (1989) 467-462.
275. C. Dean, *Journal of the American Statistical Association*, **87** (1992) 451-457.
276. D. A. Williams, *Applied Statistics*, **31** (1982) 144-148.
277. B. Francis, M. Green and C. Payne (eds.) *The GLIM System*. in *Release 4 Manual*. (1994) Oxford: Clarendon Press.
278. *"Polymers, resins and supports."* Rapp Polymere GmbH. Available from: www.rapp-polymere.com [accessed July 2007].
279. *"Polymer reagents and scavengers for parallel solution phase synthesis & purification."* Argonaut Technologies. Available from: http://www.yamato-net.co.jp/products/bio/solphaswp2.pdf [accessed July 2007].
280. *"Biotage."* (2005) Uppsala, Sweden: Biotage AB. Available from: http://www.biotage.com/ [accessed July 2007].
281. *"Novabiochem."* (2007) Merck KGaA. Available from: www.merckbiosciences.co.uk/html/NBC/home.html [accessed July 2007].

282. P. Fawcett, D. Green and G. Shaw, *Radiochemical and Radioanalytical Letters*, **9**(*5-6*) (1972) 321-327.

283. R. T. Conley, *Infrared Spectroscopy*. (1966) Boston: Allyn and Bacon, Inc.

284. R. Adamson, S. Gregson and G. Shaw, *International Journal of Peptide and Protein Research*, **22**(*5*) (1983) 560-564.

285. W. M. Dehn and K. E. Jackson, *Journal of the American Chemical Society*, **55** (1933) 4284-4287.

286. G. Shaw, M. Sykes, R. W. Humble, G. Mackenzie, D. Marsden and E. Pehlivan, *Reactive Polymers*, **9**(*2*) (1988) 211-217.

287. R. B. Merrifield, *Journal of the American Chemical Society*, **85** (1963) 2149-2154.

288. J. B. Lambert, H. F. Shurvell, D. A. Lightner and R. G. Cooks, *Introduction to organic spectroscopy*. (1987) New York: Macmillan Publishing Company, 454 pp.

289. R. M. Silverstein, C. G. Bassler and T. C. Morrill, *Spectrometric identification of organic compounds*. 3rd ed. (1974) New York: John Wiley & Sons, 340 pp.

290. D. H. Williams and I. Fleming, *"Infrared and Raman Spectra."* in *Spectroscopic methods in organic chemistry*. Chapter 3 (1966) London: McGraw-Hill Publishing Company Ltd., p. 40-76.

291. C. Steelink, *"Application of N-15 NMR Spectroscopy to the Study of Organic Nitrogen in Humic Substances in the Soil."* in N. Senesi and T. M. Miano (eds.) *Humic Substances in the Global Environment and Implications for Human Health*. (1994) Amsterdam: Elsevier, p. 405-426.

292. *"NMR chemical shifts in diamagnetic molecules."* in *Tables of Chemical and Physical Constants*, S. Bennett *et al.* (ed.) (2007) Hook: Kaye and Laby National Physical Laboratory. Available from: http://www.kayelaby.npl.co.uk/chemistry/3_8/3_8_2c.html [accessed July 2007].

293. *"Waite solid-state NMR facility."* University of Adelaide. Available from: http://www.waite.adelaide.edu.au/NMR/nmrlistn.html [accessed July 2007].

294. G. C. Levy and R. L. Lichter, *^{15}N NMR Spectroscopy*. (1979) New York: Wiley.

295. B. Kamieński, W. Schilf, T. Dziembowska, Z. Rozwadowski and A. Szady-Chełmieniecka, *Solid State Nuclear Magnetic Resonance*, **16**(*4*) (2000) 285-289.

296. D. H. Williams and I. Fleming, *"Nuclear Magnetic Resonance Spectra."* in

Spectroscopic methods in organic chemistry. Chapter 4 (1966) London: McGraw-Hill Publishing Company Ltd., p. 77-129.

297. P. Andreou, *M.Sc. thesis*, University of Hull, UK (2006).
298. H. C. Kolb, M. G. Finn and K. B. Sharpless, *Angewandte Chemie International Edition*, **40**(*11*) (2001) 2004-2021.
299. F. Ferreira, A. Meyer, J.-J. Vasseur and F. Morvan, *Collection Symposium Series*, **7** (2005) 149-152.
300. R. B. Merrifield, *Angewandte Chemie (International ed.)*, **24**(*10*) (1985) 799-810.
301. G. Mackenzie and G. Shaw, *International Journal of Peptide and Protein Research*, **15** (1980) 298-300.
302. É. Baco, *M.Sc. thesis*, University of Hull, UK (2007).
303. F. A. Carey, *Organic Chemistry*. 4th ed. (2001) Montreal: McGraw-Hill.
304. H. Shirakawa and S. Ikeda, *Journal of Polymer Science*, **2** (1971) 231.
305. R. Menon, *Current Science*, **79**(*12*) (2000) 1632-1635.
306. R. C. D. Brown, *Contemporary Organic Synthesis*, **4**(*3*) (1997) 216-237.
307. I. Parrot, C.-G. Wermuth and M. Hibert, *Tetrahedron Letters*, **40**(*45*) (1999) 7975-7978.
308. R. C. D. Brown, *Journal of the Chemical Society-Perkin Transactions 1*, **19** (1998) 3293-3320.
309. I. Vlattas, J. Dellureficio, R. Dunn, I. I. Sytwu and J. Stanton, *Tetrahedron Letters*, **38**(*42*) (1997) 7321-7324.
310. X. Li, T. Kawakami and S. Aimoto, *Tetrahedron Letters*, **39**(*47*) (1998) 8669-8672.
311. E. Bayer, *Angewandte Chemie (International ed.)*, **30**(*2*) (1991) 113-129.
312. L. M. Gayo and M. J. Suto, *Tetrahedron Letters*, **38**(*2*) (1997) 211-214.
313. S. Kobayashi, I. Hachiya and M. Yasuda, *Tetrahedron Letters*, **37**(*31*) (1996) 5569-5572.
314. S. Kobayashi, M. Moriwaki, R. Akiyama, S. Suzuki and I. Hachiya, *Tetrahedron Letters*, **37**(*43*) (1996) 7783-7786.
315. C. L. Gibson, S. La Rosa and C. J. Suckling, *Tetrahedron Letters*, **44**(*6*) (2003) 1267-1270.
316. M. Katoh and M. Sodeoka, *Bioorganic and Medicinal Chemistry Letters*, **9**(*6*) (1999) 881-884.

317. R. J. Booth and J. C. Hodges, *Accounts of Chemical Research*, **32**(*1*) (1999) 18-26.

318. S. J. Shuttleworth, S. M. Allin and P. K. Sharma, *Synthesis-Stuttgart*, **11** (1997) 1217-1239.

319. A. I. Vogel, *Vogel's textbook of quantitative chemical analysis*. 5th ed. (1991) London: Longman Scientific & Technical, 877 pp.

320. J. McMurry (ed.) *Organic Chemistry*. 5th ed. (2000) Pacific Grove: Brooks/Coole.

321. W. W. Cleland, *Biochemistry*, **3**(*4*) (1964) 480-482.

322. W. L. Zahler and W. W. Cleland, *Journal of Biological Chemistry*, **243**(*4*) (1968) 716-719.

323. I. L. Finar (ed.) *Organic Chemistry*. 6th ed. (1973) London: Longman.

324. N. Aoki, K. Fukushima, H. Kurakata, M. Sakamoto and K. Furuhata, *Reactive and Functional Polymers*, **42** (1999) 223-233.

325. J. S. Bradshaw, K. E. Krakowiak, R. M. Izatt, R. L. Bruening and B. J. Tarbet, *Journal of Heterocyclic Chemistry*, **27**(*2*) (1990) 347-349.

326. Y.-L. Fu and M. Bobek, *Journal of Organic Chemistry*, **41**(*24*) (1976) 3831-3834.

327. J. March, *Advanced Organic Chemistry - Reactions, mechanisms and structure*. 4th ed. (1992) New York: J. Wiley & Sons, Inc., 1495 pp.

328. H. Distler, *Angewandte Chemie (International ed.)*, **6** (1967) 544-553.

329. C. Kennedy, *personnal communication*, University of Hull, UK (2007).

330. G. Bulaj, T. Kotemme and D. P. Goldenberg, *Biochemistry*, **37**(*25*) (1998) 8965-8972.

331. J. P. Badyal, A. M. Cameron, N. R. Cameron, D. M. Coe, R. Cox, B. G. Davis, L. J. Oates, G. Oye and P. G. Steele, *Tetrahedron Letters*, **42**(*48*) (2001) 8531-8533.

332. G. L. Ellman, *Archive of Biochemistry and Biophysics*, **82**(*1*) (1959) 70-77.

333. M. A. Walters, J. Chaparro, T. Siddiqui, F. Williams, C. Ulku and A. L. Rheingold, *Inorganica Chimica Acta*, **359**(*12*) (2006) 3996-4000.

334. B. J. Evans, J. T. Doi and W. K. Musker, *Journal of Organic Chemistry*, **55**(*8*) (1990) 2337-2344.

335. S. Otto, R. L. E. Furlan and J. K. M. Sanders, *Journal of the American Chemical Society*, **122**(*48*) (2000) 12063-12064.

336. R. Sanz, R. Aguado, M. R. Pedrosa and F. J. Arnáiz, *Synthesis*, **7** (2002) 856-858.

337. S.-W. Sun, Y.-C. Lin, Y.-M. Weng and M.-J. Chen, *Journal of Food Composition and Analysis*, **19**(*2-3*) (2006) 112-117.

338. K. Winther, E. Rein and C. Hedman, *Climacteric*, **8** (2005) 162-170.

339. K. Winther and C. Hedman, *Current Therapeutic Research*, **63** (2002) 344-353.

340. J. Elist, *Urology*, **67** (2006) 60-63.

341. J. Soto and J. T. Toledo, *Lancet Infectious Diseases*, **7**(*1*) (2007) 7.

342. P. Emery and M. Suarez-Almazor, *Clinical Evidence*, **10** (2002) 1454–1476.

343. R. A. Alderden, M. D. Hall and T. W. Hambley, *Journal of Chemical Education*, **83** (2006) 728-724.

344. A. Rigby, *personnal communication*, University of Hull, UK (2007).

345. L. H. Harwood, C. J. Moody and J. M. Percy, *Experimental organic chemistry - Standard and microscale*. 2nd ed. (1999) Oxford: Blackwell Science, 728 pp.

346. A. I. Vogel, *Vogel's textbook of practical organic chemistry*. 5th ed. (1989) London: Longman Scientific & Technical.

347. J. P. C. Bootsma, B. Eling and G. Challa, *Reactive Polymers*, **3**(*1*) (1984) 17-22.

348. R. M. Carman and I. M. Shaw, *Australian Journal of Chemistry*, **29** (1976) 133-143.

349. L. A. Brooks and H. R. Snyder, *Organic Syntheses*, **25** (1945) 84-86.

350. H. Bunte, *Berichte der deutschen chemischen Gesellschaft*, **7**(*1*) (1874) 646-648.

351. D. L. Klayman and W. F. Gilmore, *Journal of Medicinal Chemistry*, **7**(*6*) (1964) 823-824.

352. D. L. Klayman, M. M. Grenan and D. P. Jacobus, *Journal of Medicinal Chemistry*, **12**(*3*) (1969) 510-512.

353. D. L. Klayman, J. W. Lown and T. R. Sweeney, *Journal of Organic Chemistry*, **30**(*7*) (1965) 2275-2278.

354. A. Otaka, K. Takaki, A. Shide and N. Fujii, *Tetrahedron Letters*, **32**(*9*) (1991) 1223-1226.

355. D. Podhradský, Ľ. Drobnica and P. Kristian, *Experientia*, **35**(*2*) (1979) 154-155.

356. P. Desnuelle and M. Rovery, *Biochimica et Biophysica Acta* **3**(1949) 26-33.

357. R. K. Brummitt and C. E. Powell, *Authors of Plant Names*. (1992) London: Royal Botanic Gardens, Kew.

358. J. R. Rowley, *"Implications on the nature of sporopollenin based upon pollen*

development." in J. Brooks *et al.* (eds.) *Sporopollenin*. (1971) London & New York: Academic Press, p. 174-219.

Appendix A - Review of solid-state ^{13}C NMR spectra of sporopollenin

Appendix A (cont.)

↓ species		chemical shift δ (ppm) →	Ref.	Extr.
Gymnosperms	Pinophyta	*Pinus thunbergiana* L.	2	A
		Pinus sylvestris L.	3	B
			4, 5	B
		Cedrus atlantica L.	4	B
	Cycadophyta	*Dion edule* Lindl.	4, 5	B
		Encephalartos altensteinii Lehm.	4	B
		Cycas circinalis L.	7	A
			5	B

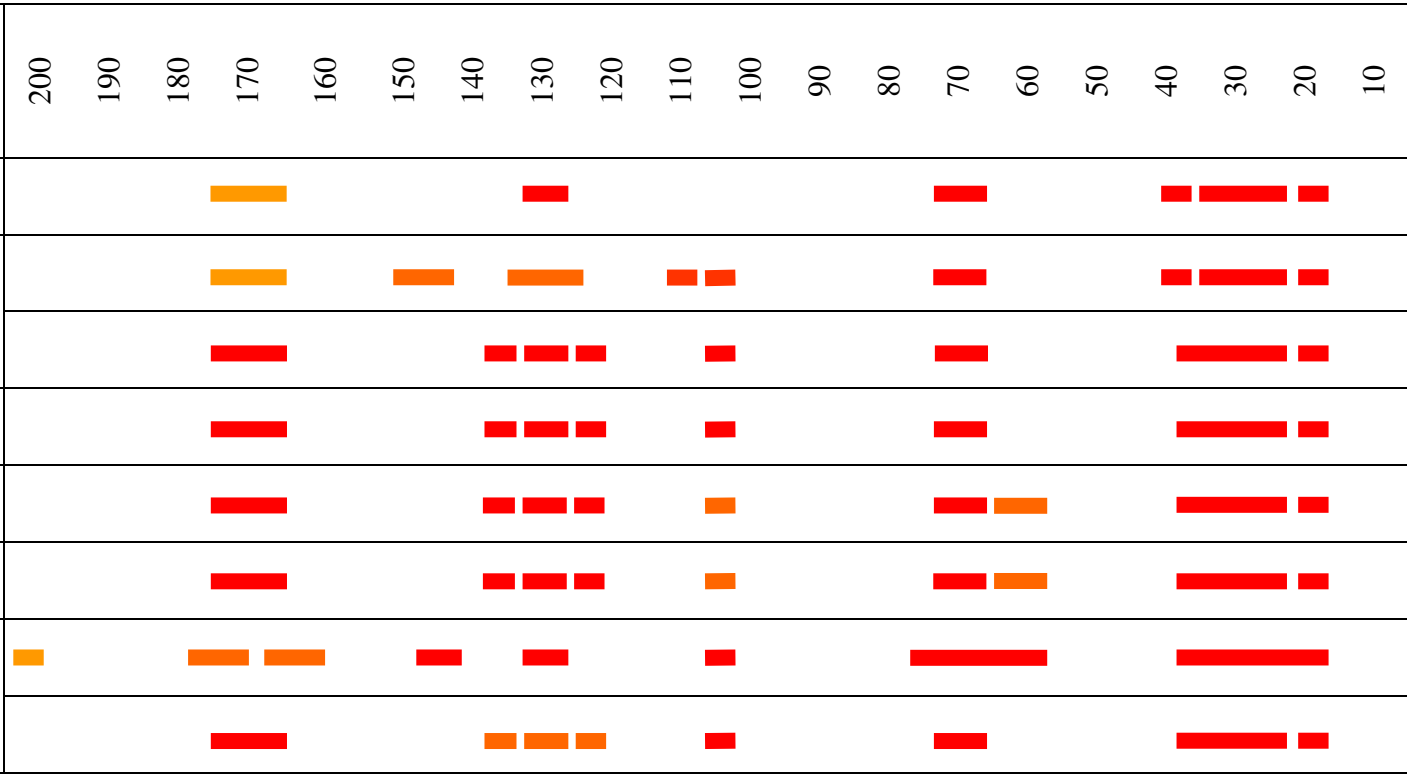

Appendix A (cont.)

↓ species	chemical shift δ (ppm) → 200 190 180 170 160 150 140 130 120 110 100 90 80 70 60 50 40 30 20 10	Ref.	Extr.
polymerised β-carotene		6	n/a
Angiosperms — *Triticum astivum* L.		2	A
Ambrosia trifida L.		2	A
Lilium longiflorum Thunb.		8	C
Betula pubescens L.		3	B
Cyclamen persicum L.		4	B
Garrya elliptica Dougl. ex Lindl.		4	B
Narcissus pseudonarcissus L.		4	B
Typha angustifolia L.		4	B
		7	A
		9	D
		10	D
Tulipa cv. “Apeldoorn”		7	A

Appendix A (cont.)

Extraction method (Extr.)

A. Full protocol (acetone, potassium hydroxide, phosphoric acid)
B. Erdtman acetolysis
C. Mild extraction with 4-methylmorpholine-*N*-oxide
D. Enzymatic extraction

References (Ref.)

1. C. Berkaloff, E. Casadevall, C. Largeau, P. Metzger, S. Peracca, and J. Virlet, *Phytochemistry*, **22** (*2*) (1983) 389-397.
2. W. J. Guilford, D. M. Schneider, J. Labovitz, and S. J. Opella, *Plant Physiology*, **86** (*1*) (1988) 134-136.
3. A. R. Hemsley, W. G. Chaloner, A. C. Scott, and C. J. Groombridge, *Annals of Botany*, **69** (*6*) (1992) 545-549.
4. A. R. Hemsley, P. J. Barrie, W. G. Chaloner, and A. C. Scott, *Grana*, **Suppl. 1** (1993) 2-11.
5. A. R. Hemsley, A. C. Scott, P. J. Barrie, and W. G. Chaloner, *Annals of Botany*, **78** (*1*) (1996) 83-94.
6. G. Shaw and D. C. Apperley, *Grana*, **35** (*2*) (1996) 125-127.
7. S. Wilmesmeier, S. Steuernagel, and R. Wiermann, *Zeitschrift Für Naturforschung C-a Journal of Biosciences*, **48** (*9-10*) (1993) 697-701.
8. K. E. Espelie, F. A. Loewus, R. J. Pugmire, W. R. Woolfenden, B. G. Baldi, and P. H. Given, *Phytochemistry*, **28** (*3*) (1989) 751-753.
9. H. Bubert, J. Lambert, S. Steuernagel, F. Ahlers, and R. Wiermann, *Zeitschrift Für Naturforschung C-a Journal of Biosciences*, **57** (*11-12*) (2002) 1035-1041.
10. F. Ahlers, H. Bubert, S. Steuernagel, and R. Wiermann, *Zeitschrift Für Naturforschung C-a Journal of Biosciences*, **55** (*3-4*) (2000) 129-136.

Appendix B

Overview of protocols for the extraction of microcapsules (exine/intine) from pollen/spores

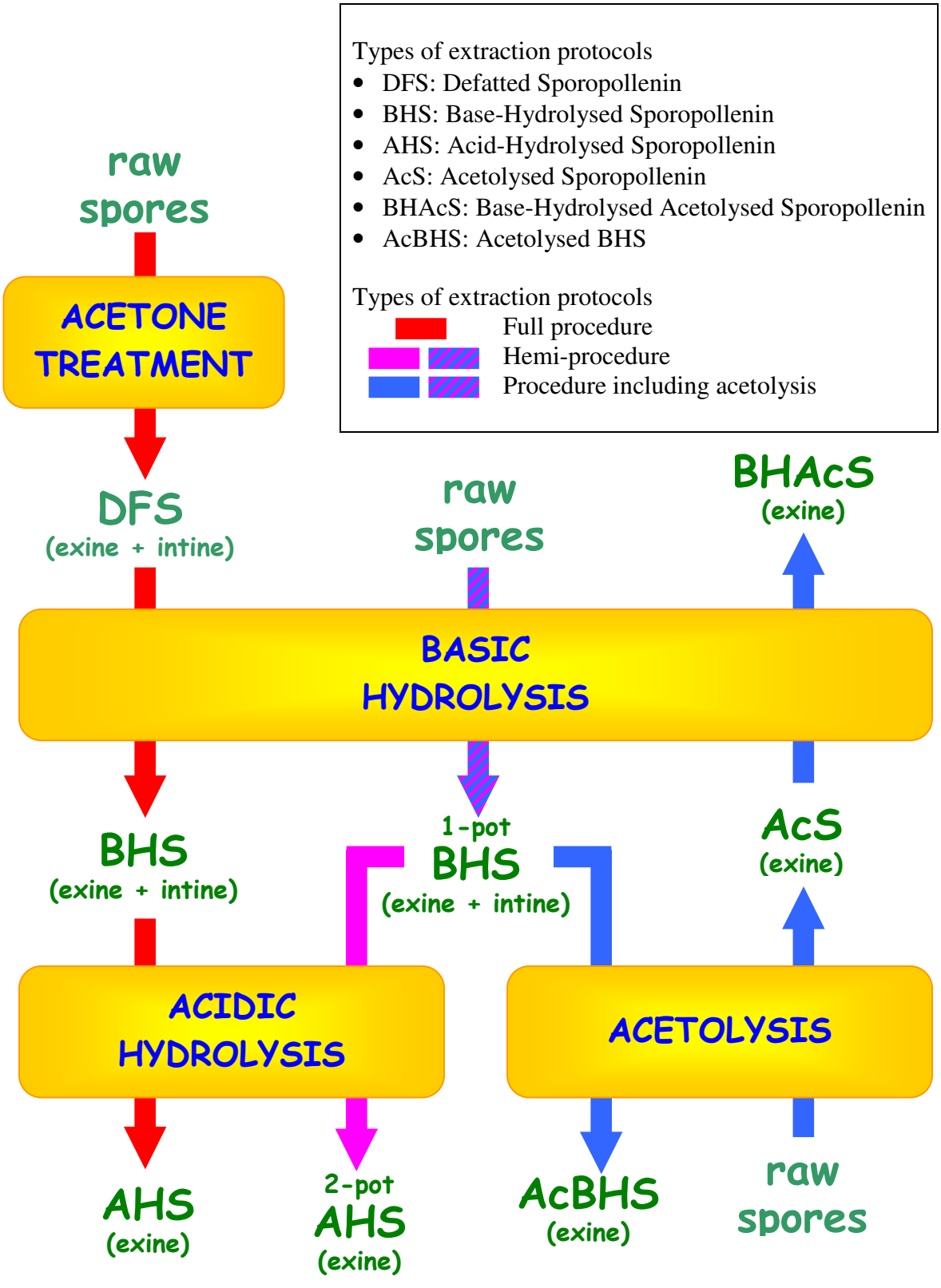

Appendix C - Refining properties of *Lycopodium* spp. sporopollenin on UV-damaged cod liver oil

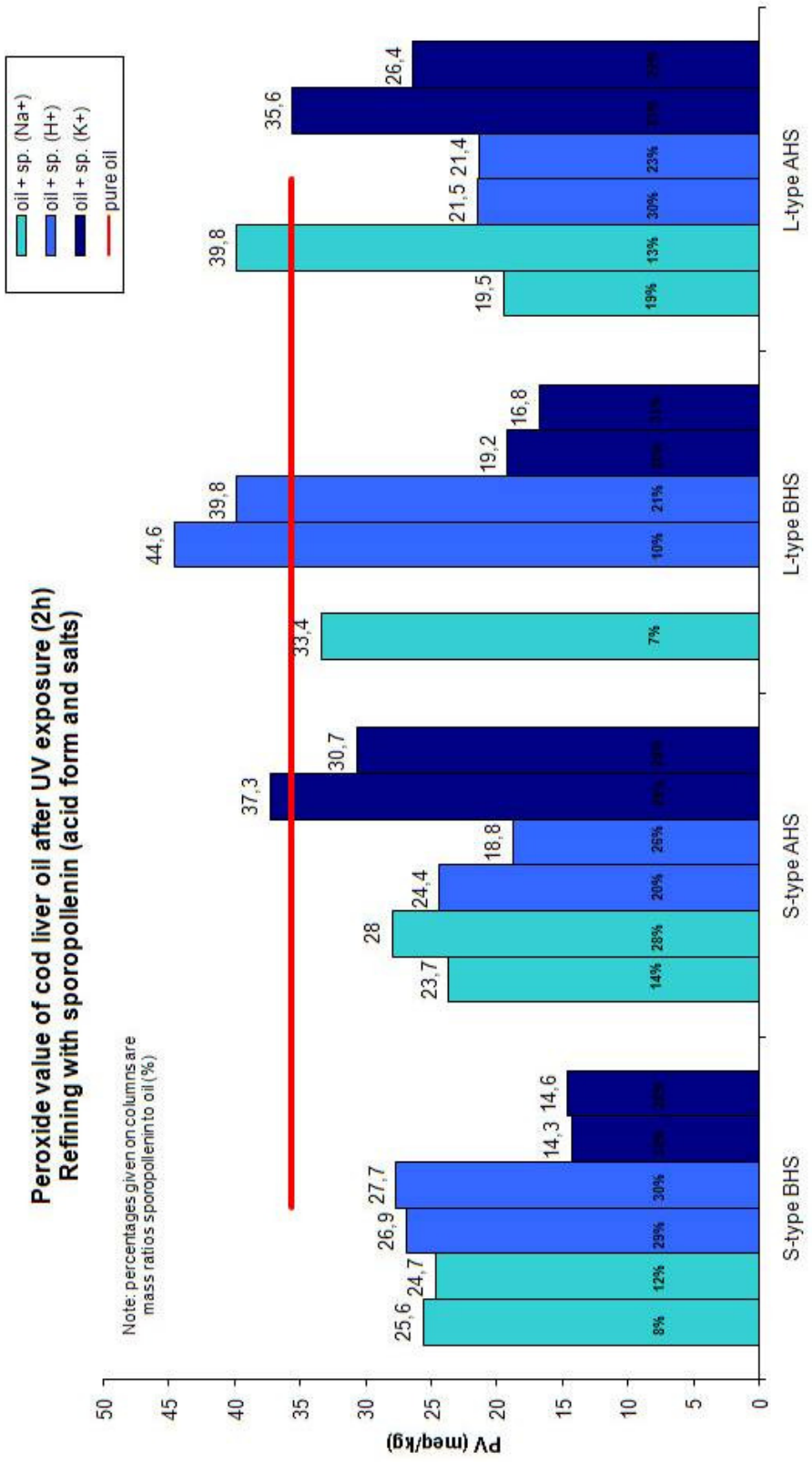

Appendix D - Refining properties of *Lycopodium* spp. sporopollenin on fresh cod liver oil

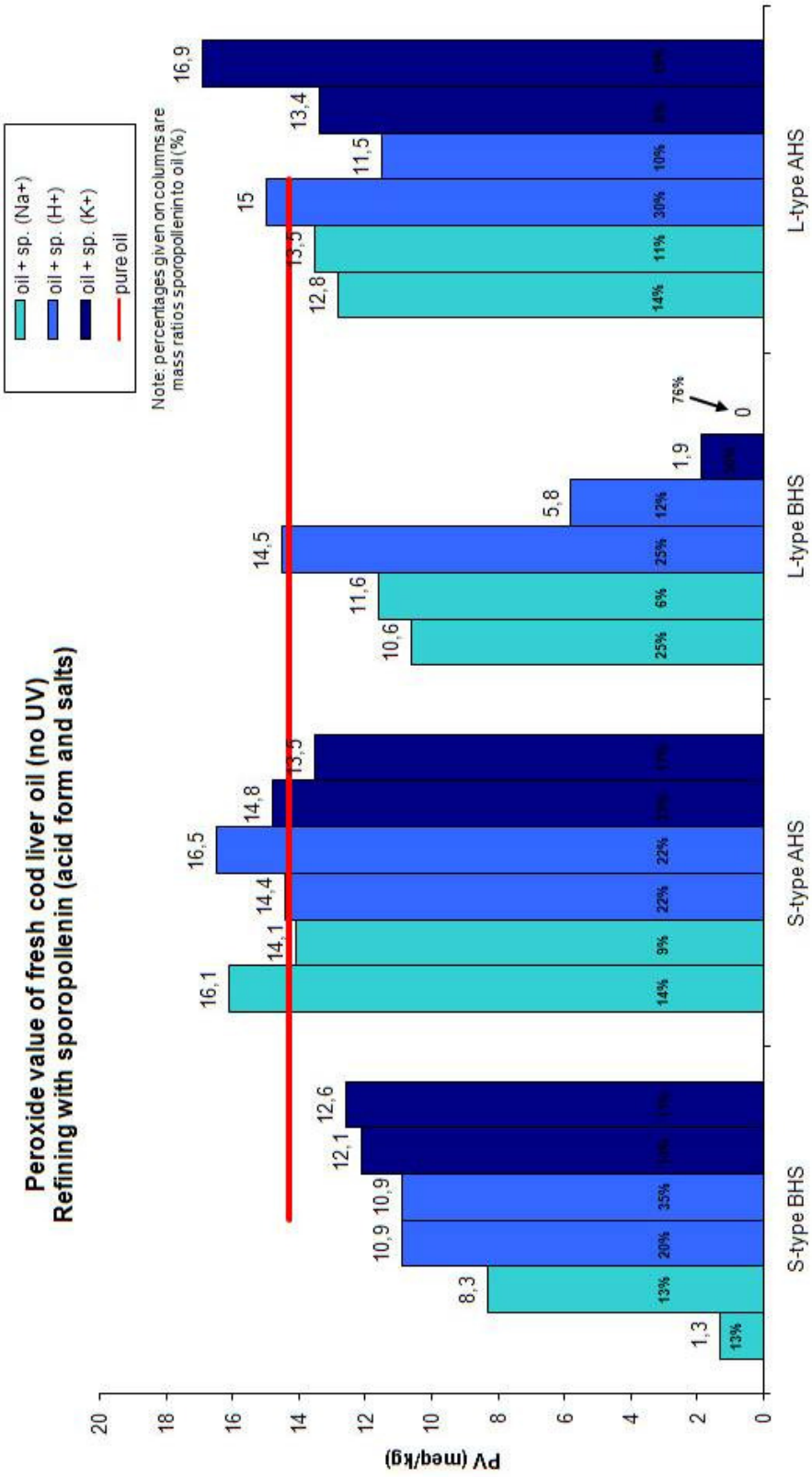

Appendix E - Refining properties of *Lycopodium* spp. sporopollenin on fresh cod liver oil- Reproducibility study

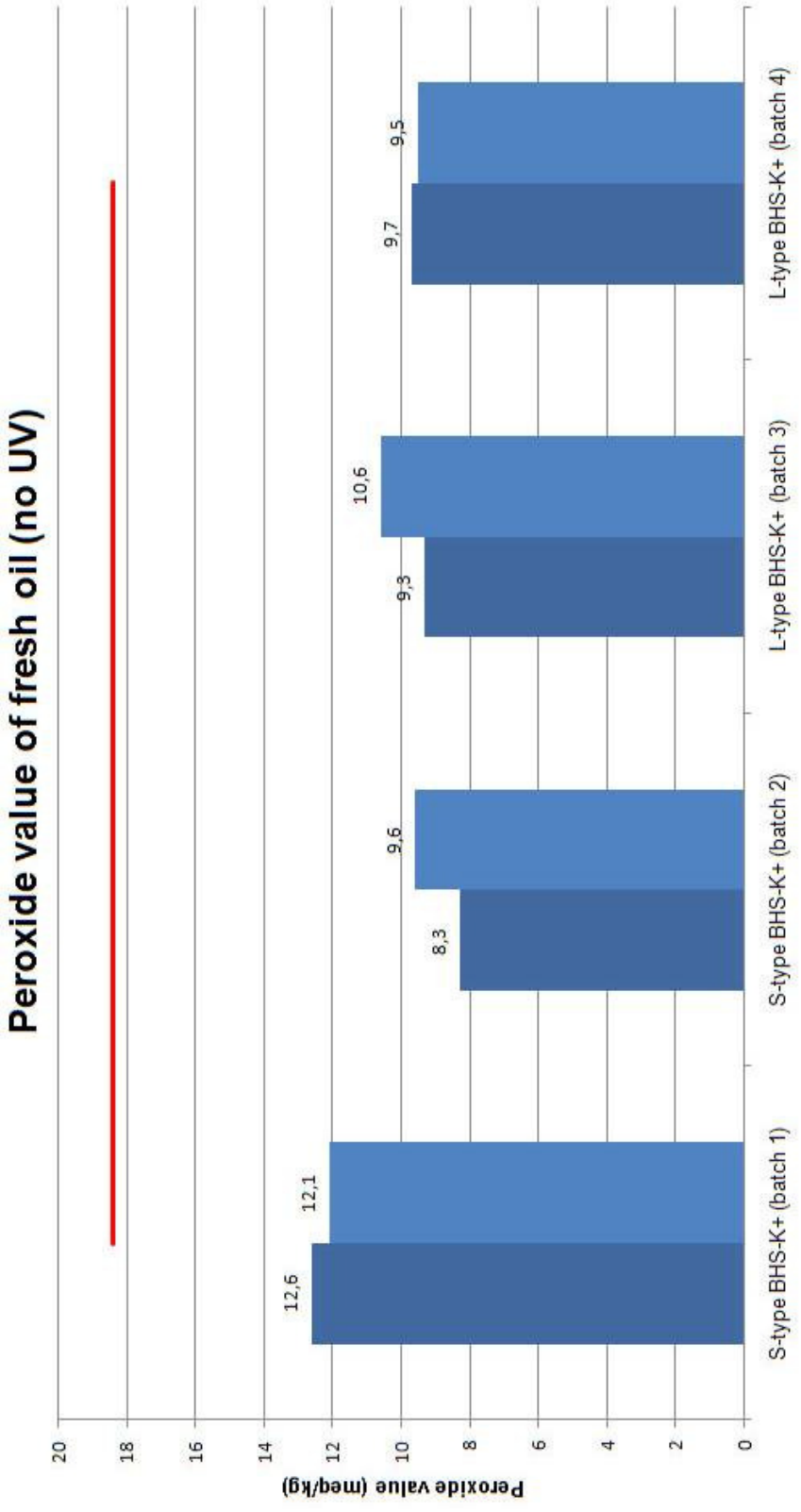

Appendix F – Resistance of oil to aerial oxidation – Effects of sporopollenin

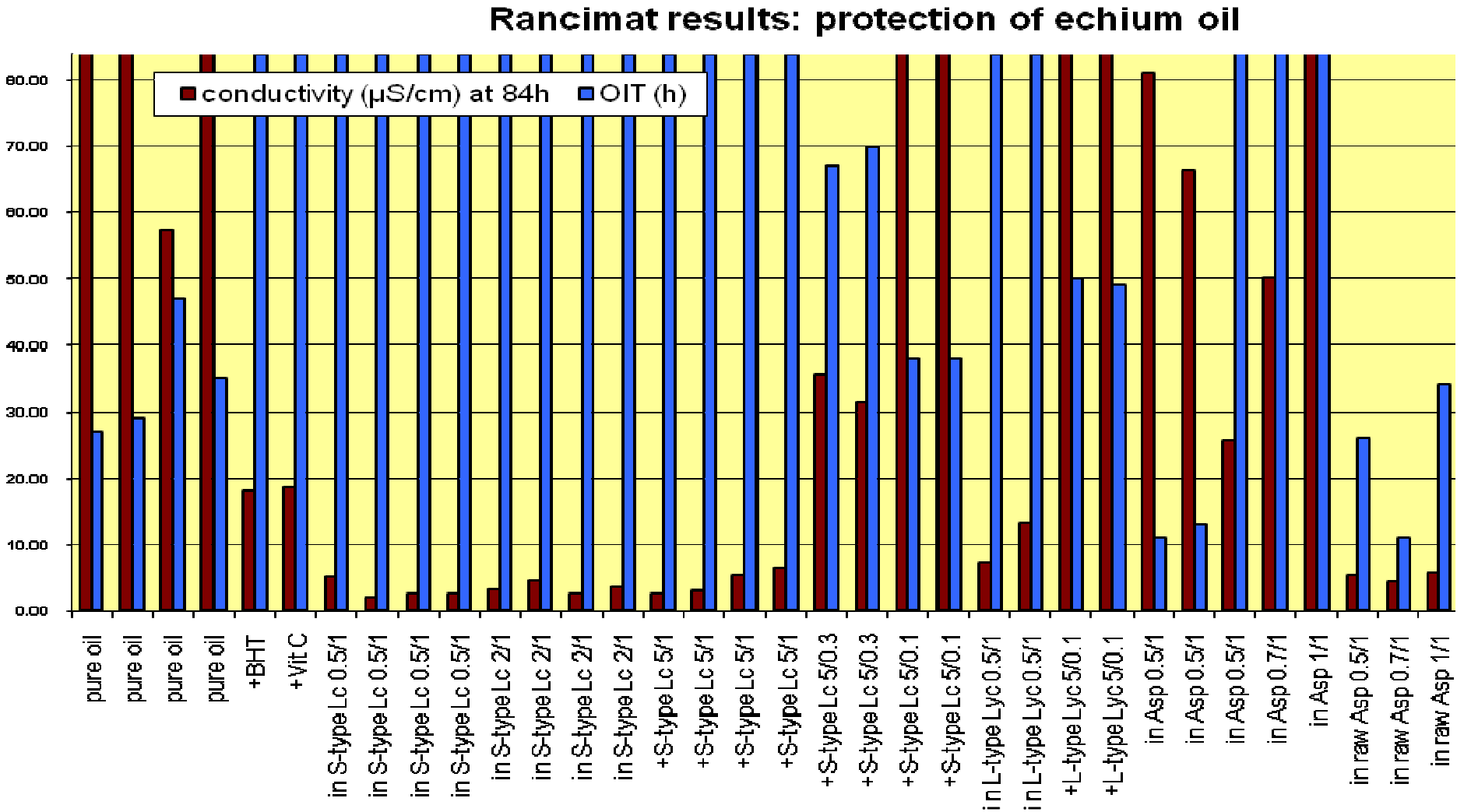

Abbreviations:
BHT: butylated hydroxytoluene
Vit C: vitamin C
Asp: extracted *Aspergillus niger* conidia
raw Asp.: non-extracted *A. niger* conidia

Symbols:
+ simple contact with oil
in encapsulation of oil

Ratios are given as oil/additive (w/w)

Appendix G

Oxidation inductive time of echium oil

Protection of *Aspergillus niger*

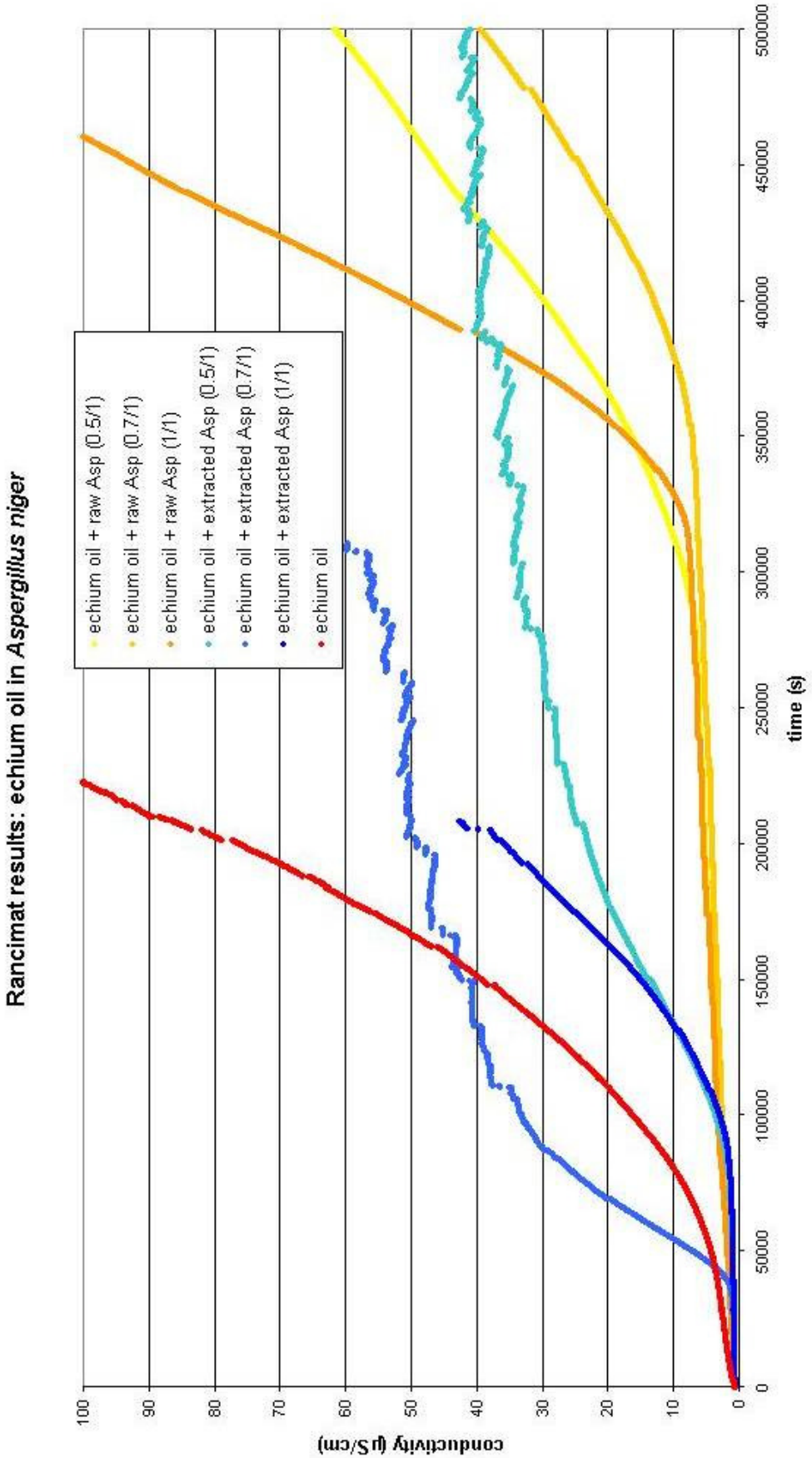

Appendix H

Oxidation inductive time of echium oil

Protection of *Lycopodium* spp.

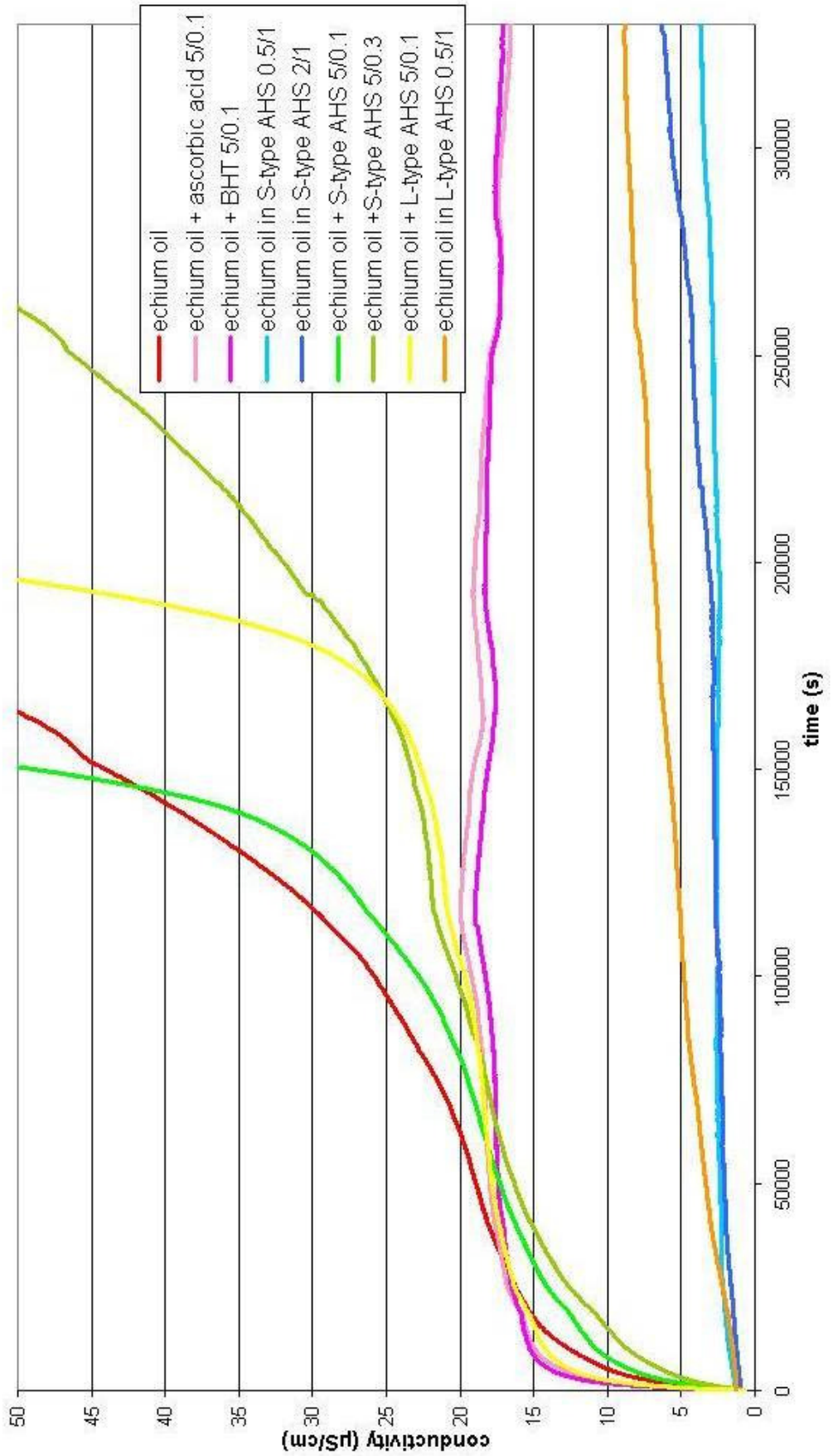

Appendix I, 1 – FTIR spectrum of underivatised sporopollenin (S-type AHS) 1

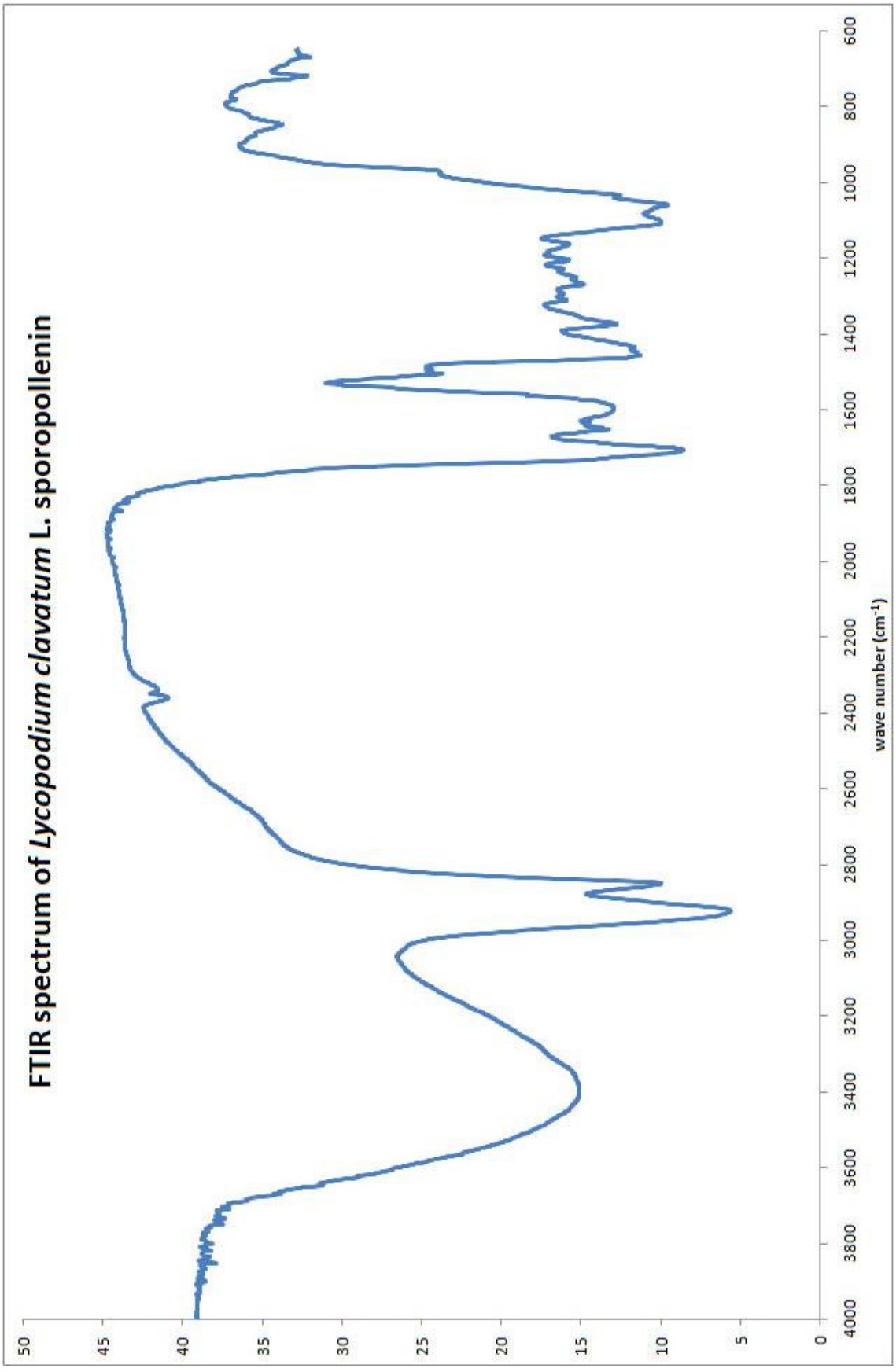

Appendix I, 2 – FTIR spectrum of ammonia-treated sporopollenin (ATS) 2

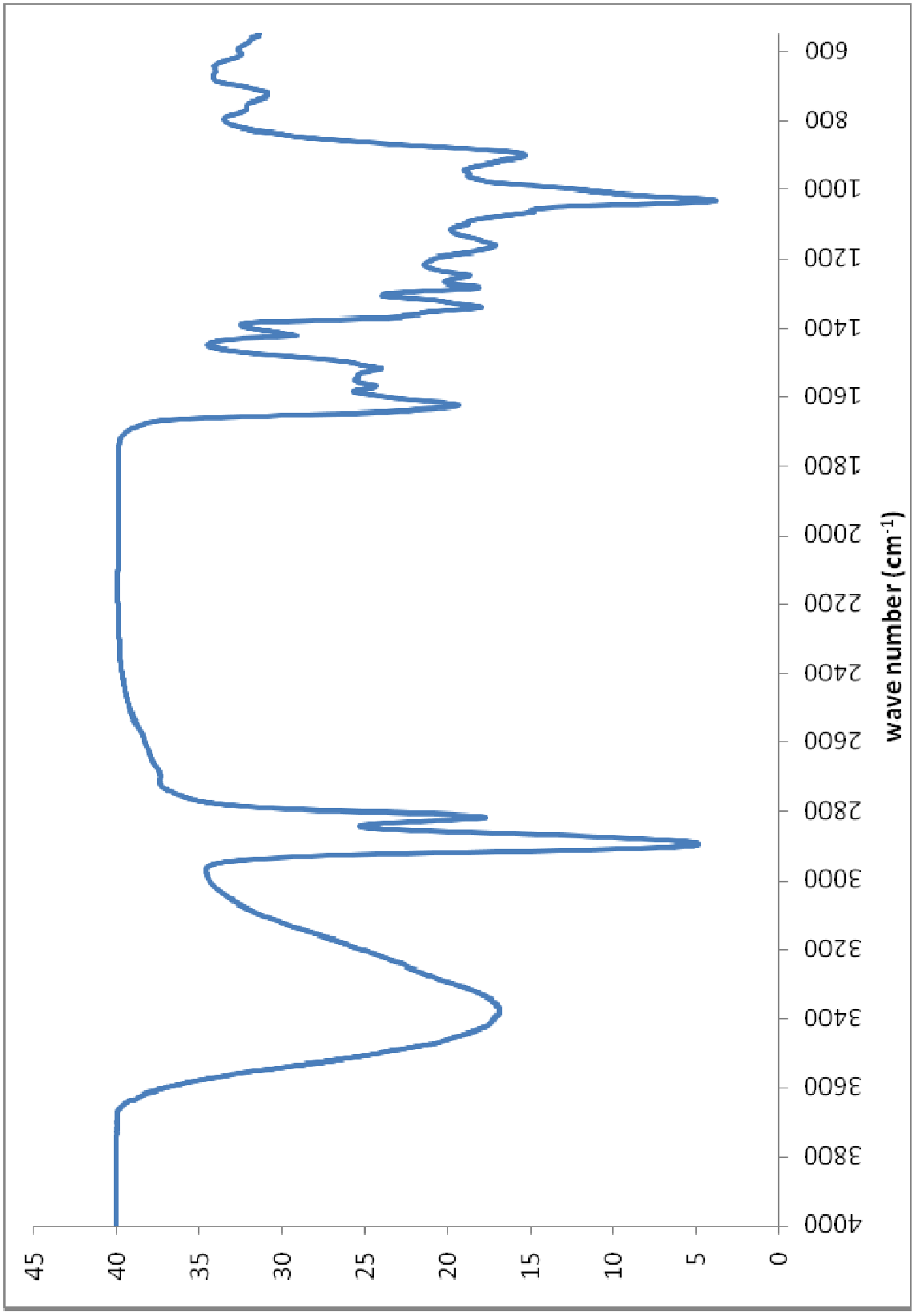

Appendix I, 3 – FTIR spectrum of reduced ATS 3

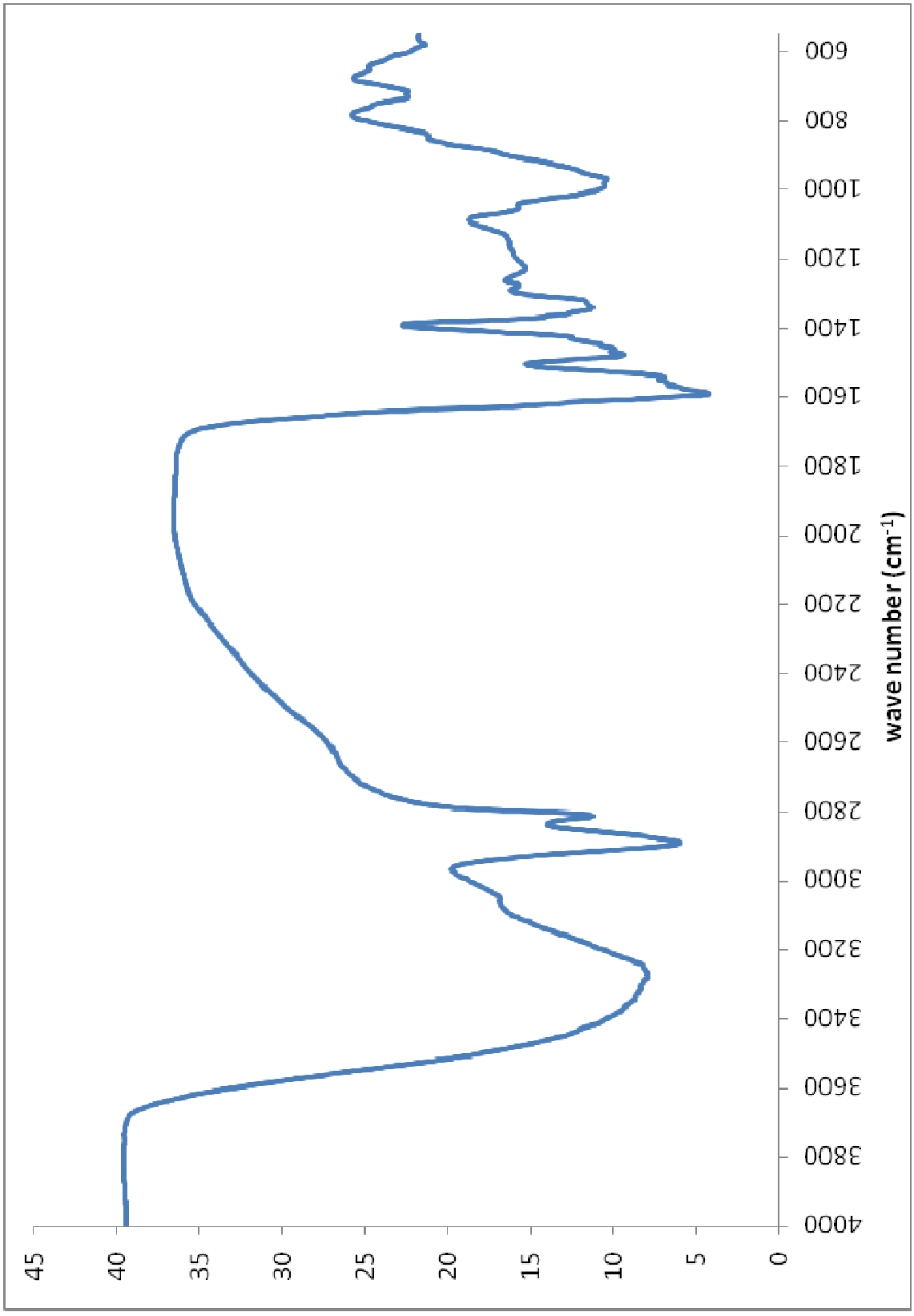

Appendix I, 4 – FTIR spectrum of butylamine-treated sporopollenin <u>6a</u>

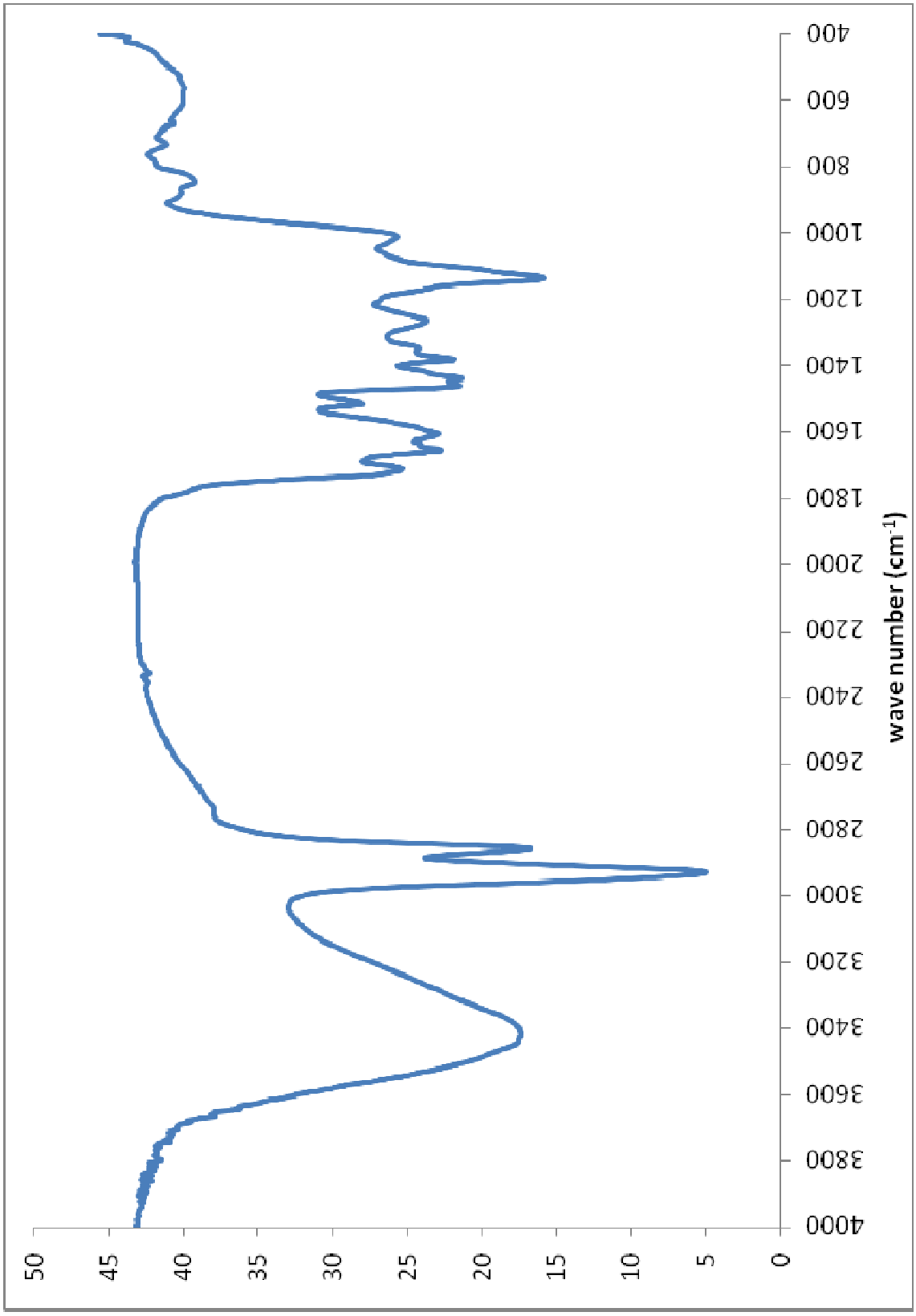

Appendix I, 5 – FTIR spectrum of aniline-treated sporopollenin 7b

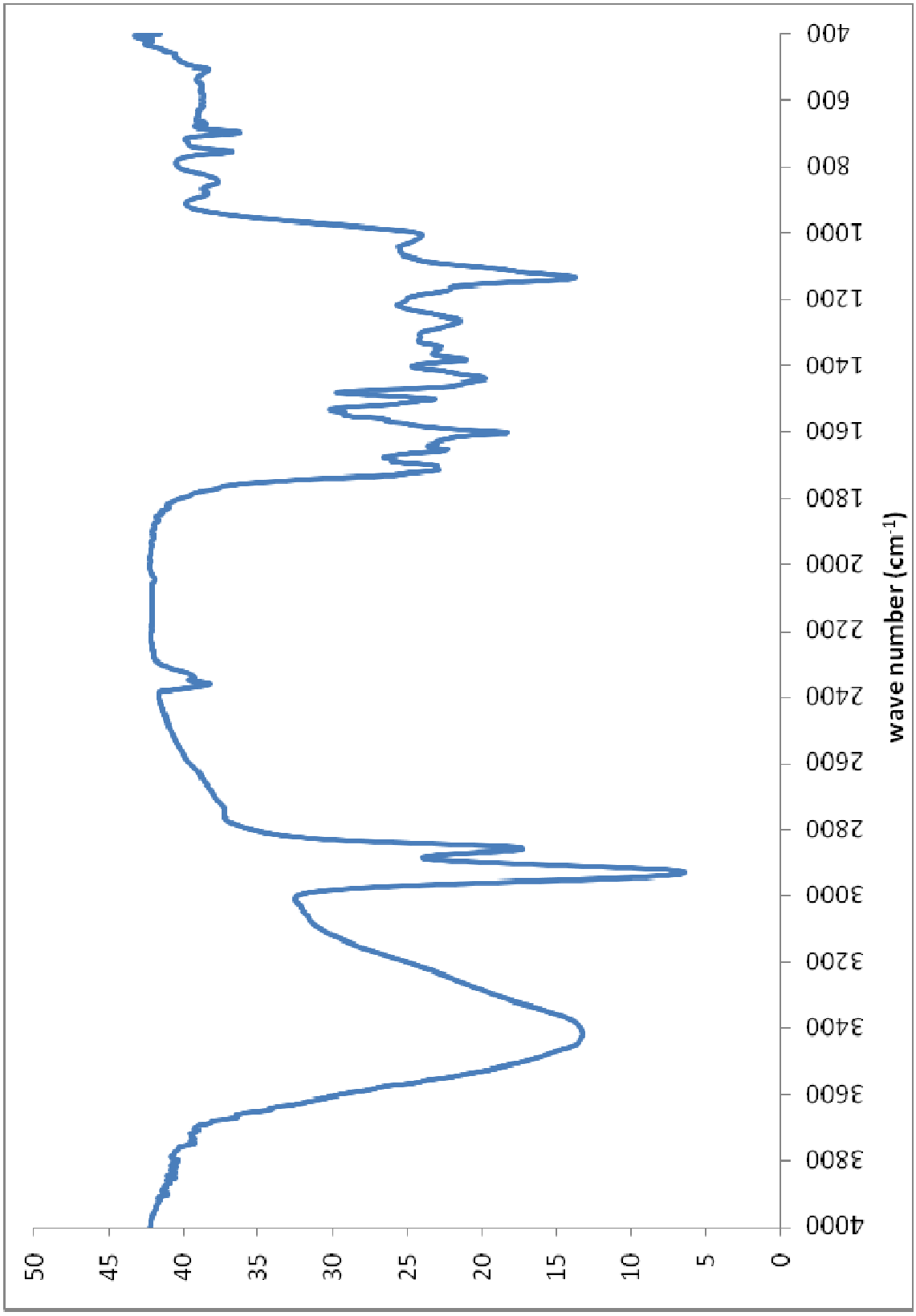

Appendix I, 6 – FTIR spectrum of bromosporopollenin <u>15</u>

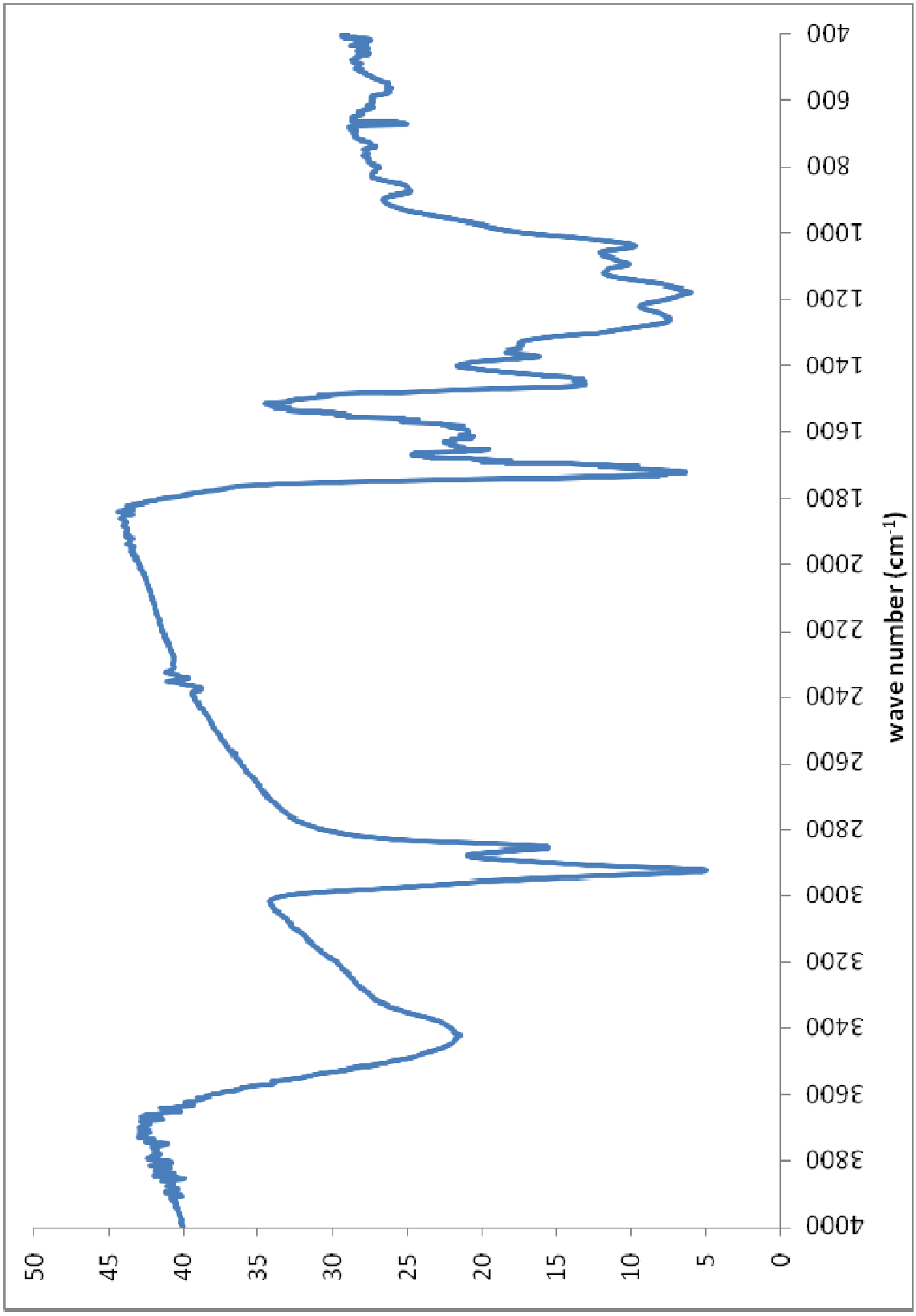

Appendix I, 7 – FTIR spectrum of chloromethyl sporopollenin **16**

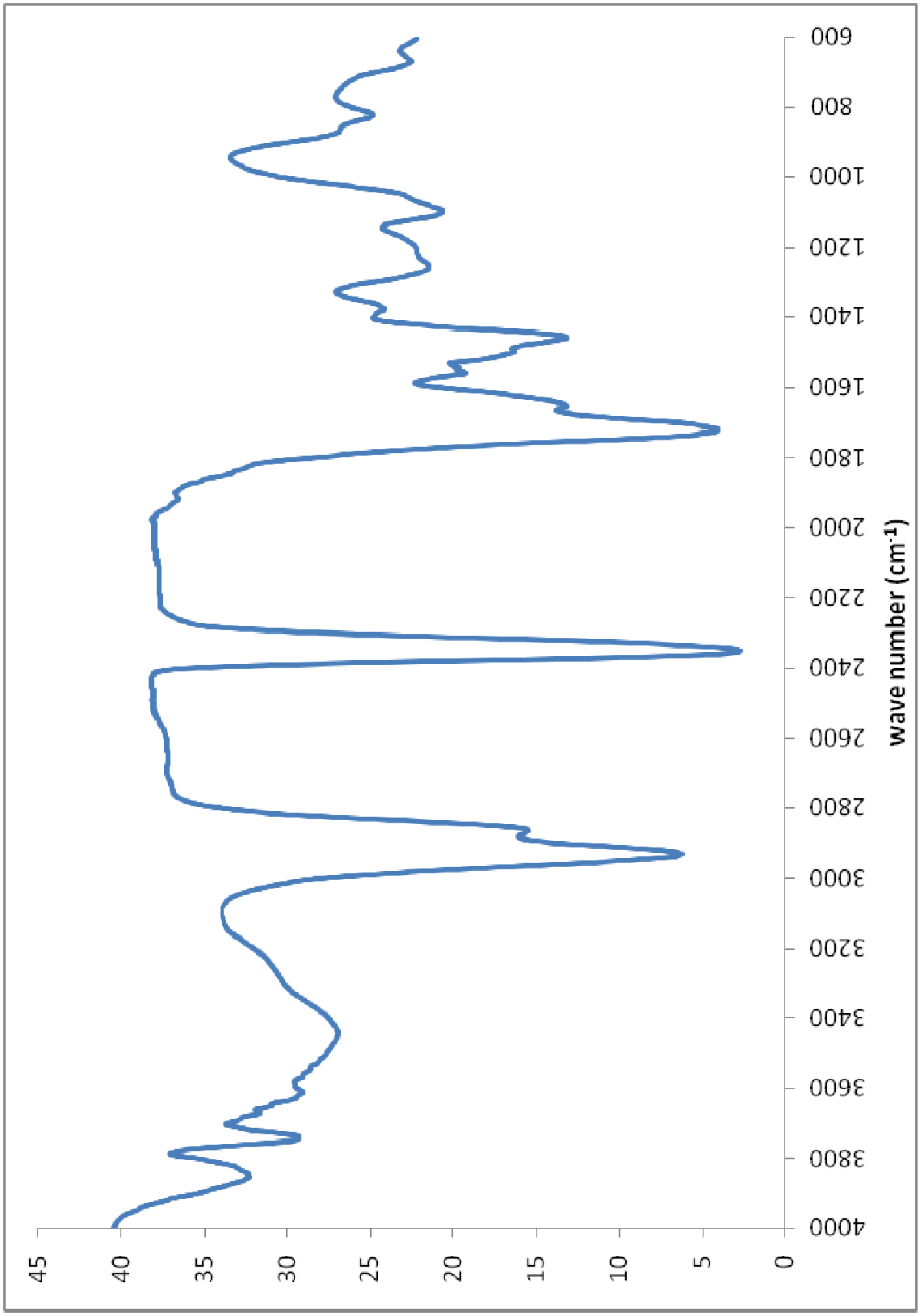

Appendix I, 8 – FTIR spectrum of chloromethyl anilido sporopollenin <u>17</u>

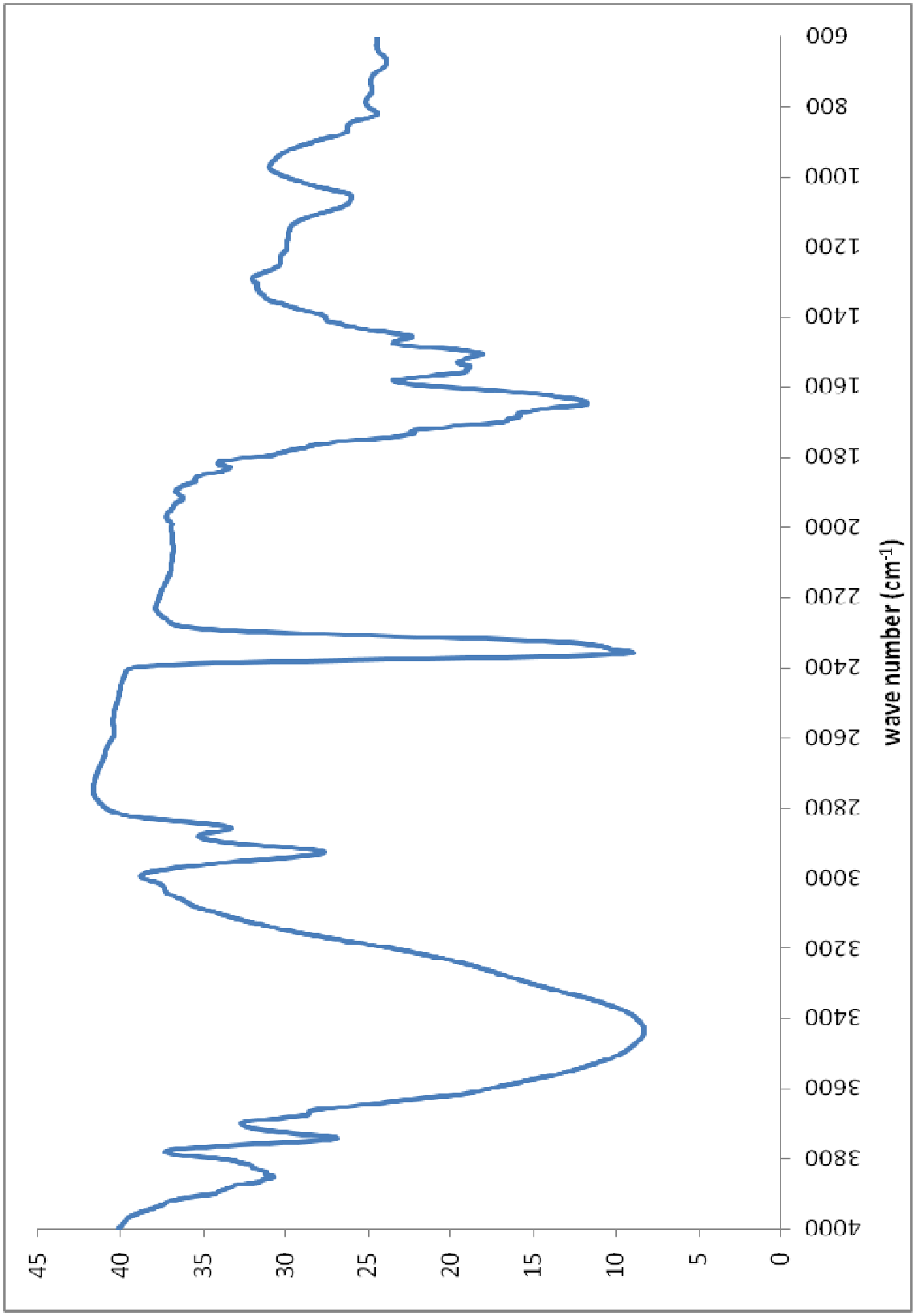

Appendix I, 9 – FTIR spectrum of chlorosporopollenin <u>18</u>

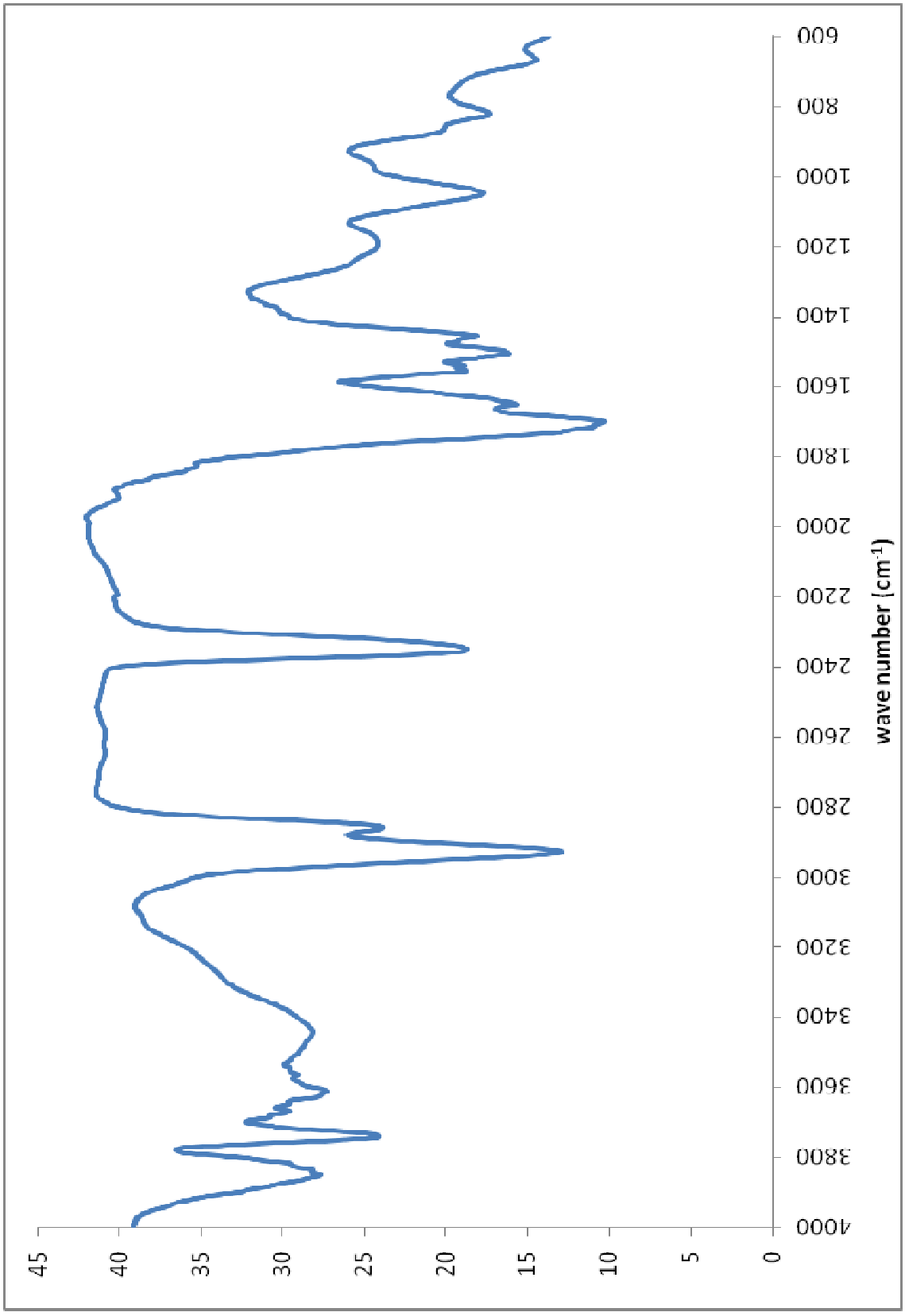

Appendix I, 10 – FTIR spectrum of chlorosporopollenin 19

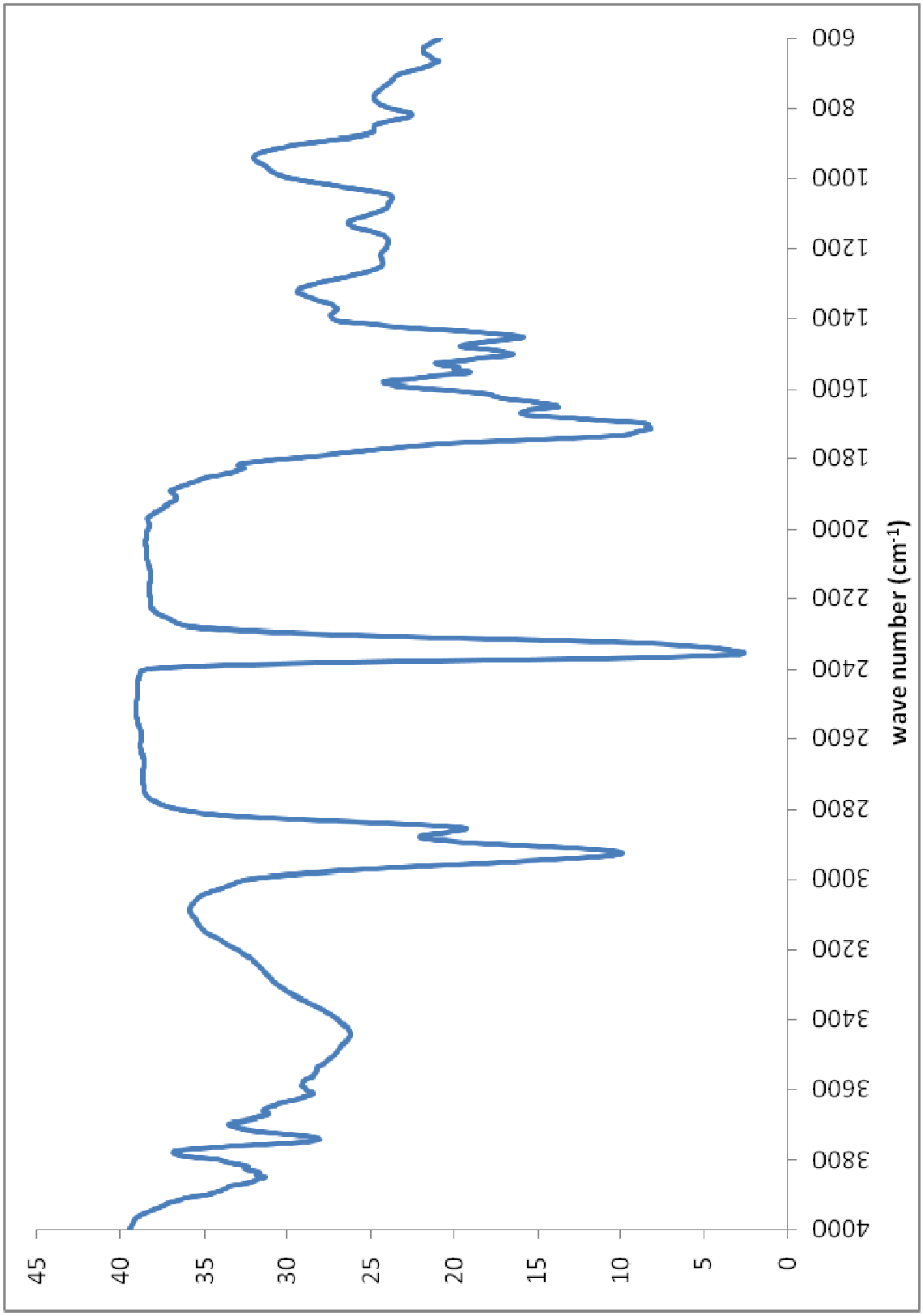

Appendix I, 11 – FTIR spectrum of azidosporopollenin 20

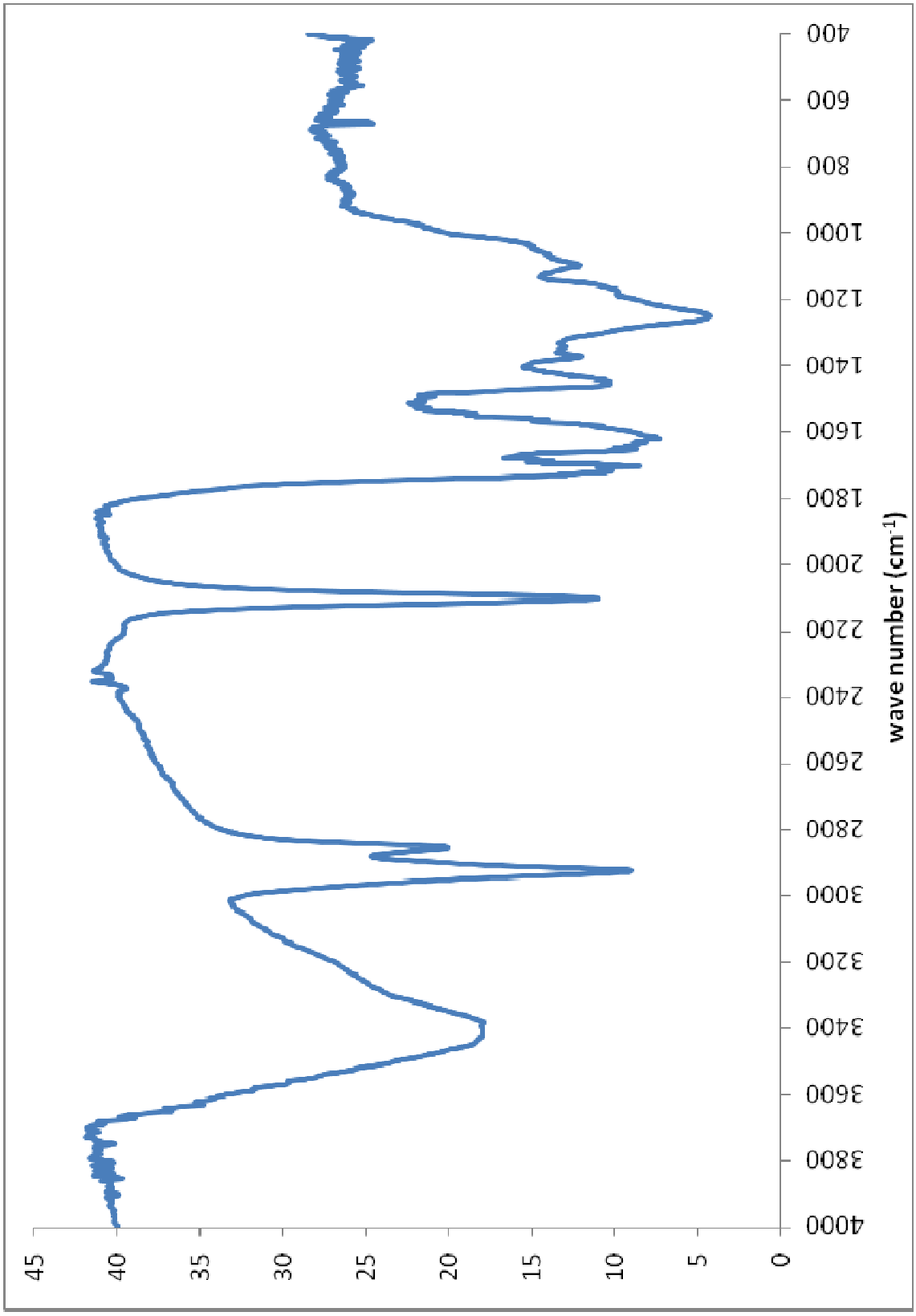

Appendix I, 12 – FTIR spectrum of reduced azidosporopollenin 21

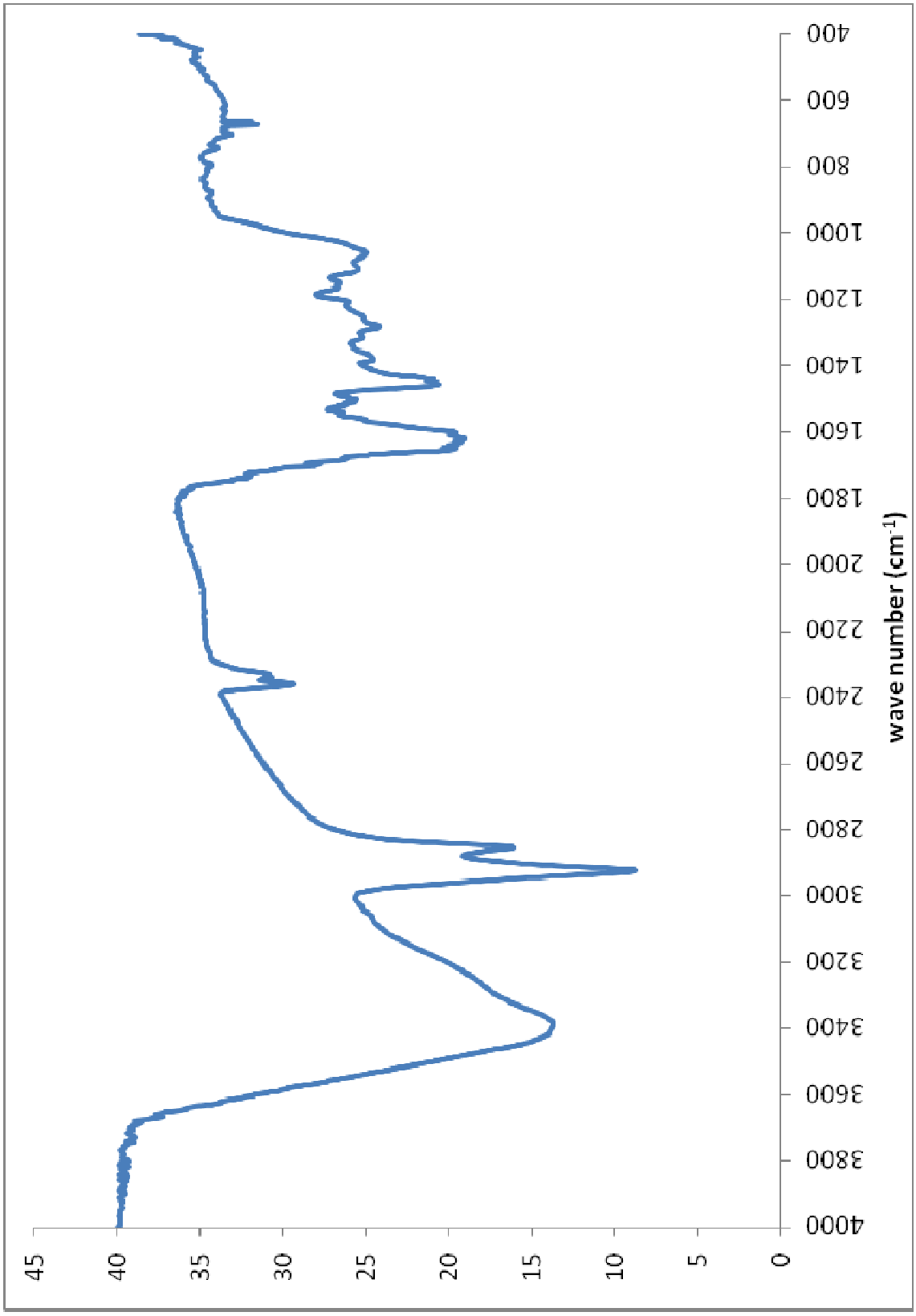

Appendix I, 13 – FTIR spectrum of azidosporopollenin 22b

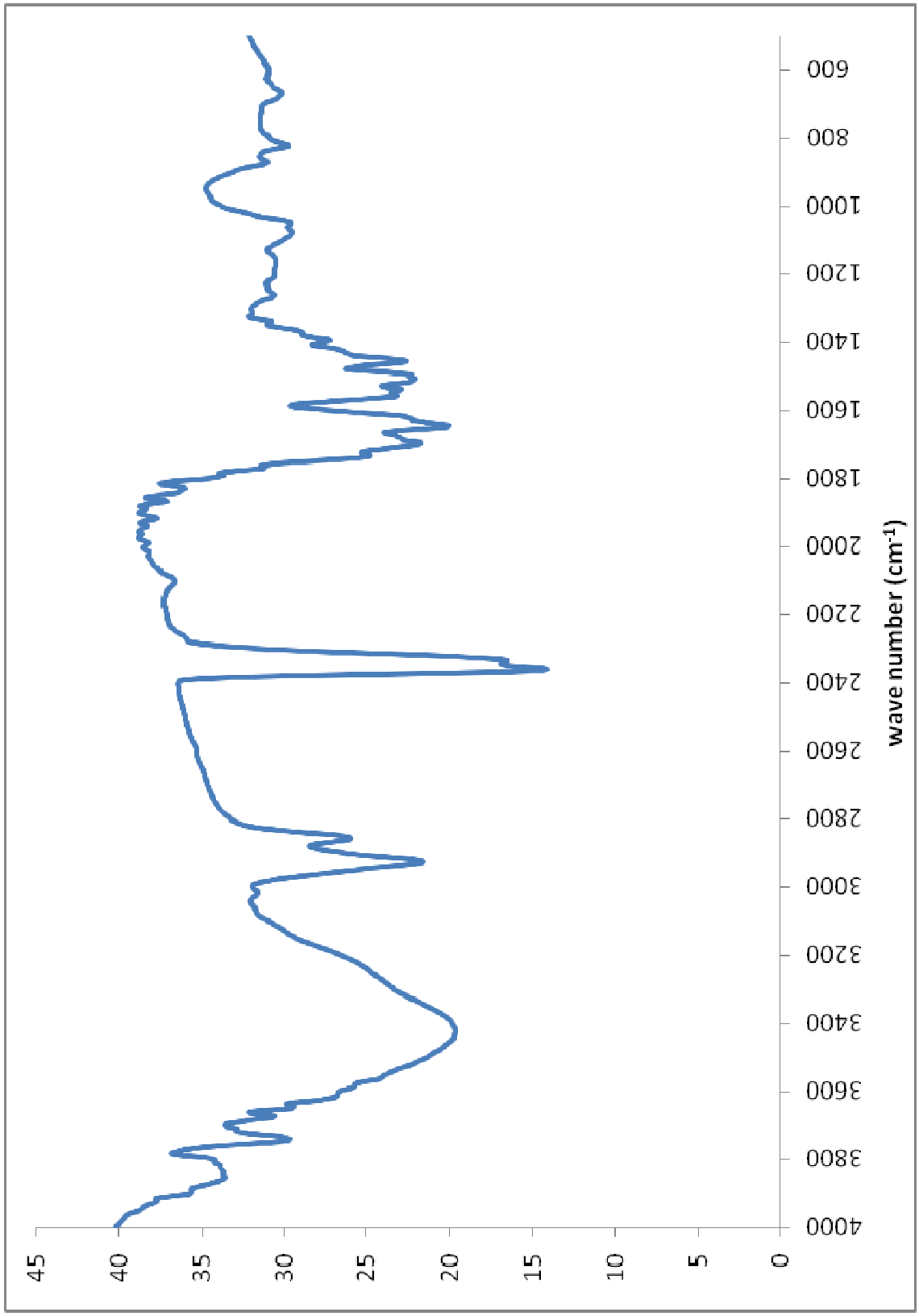

Appendix I, 14 – FTIR spectrum of azidosporopollenin <u>23</u>

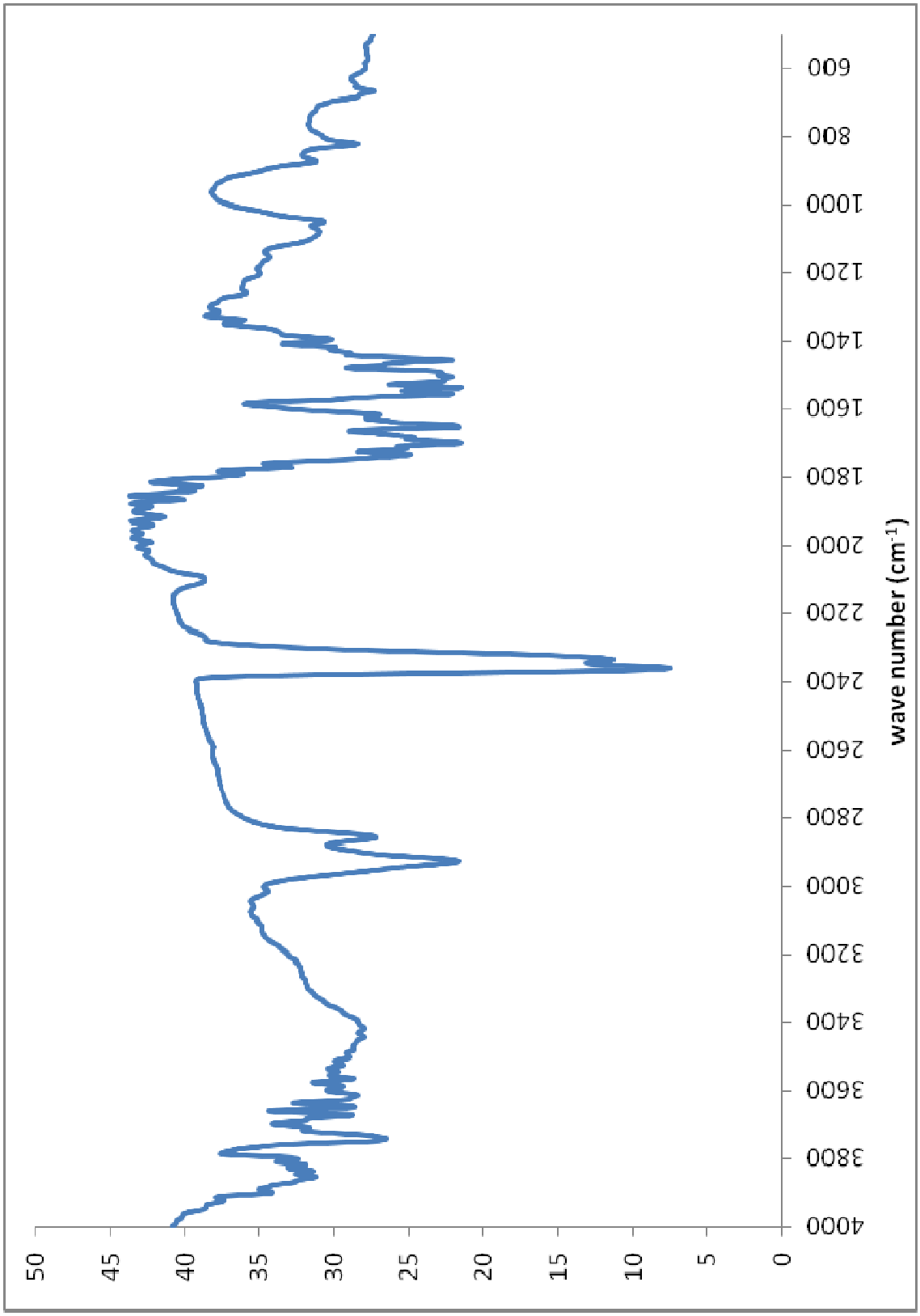

Appendix I, 15 – FTIR spectrum of thiosporopollenin 25

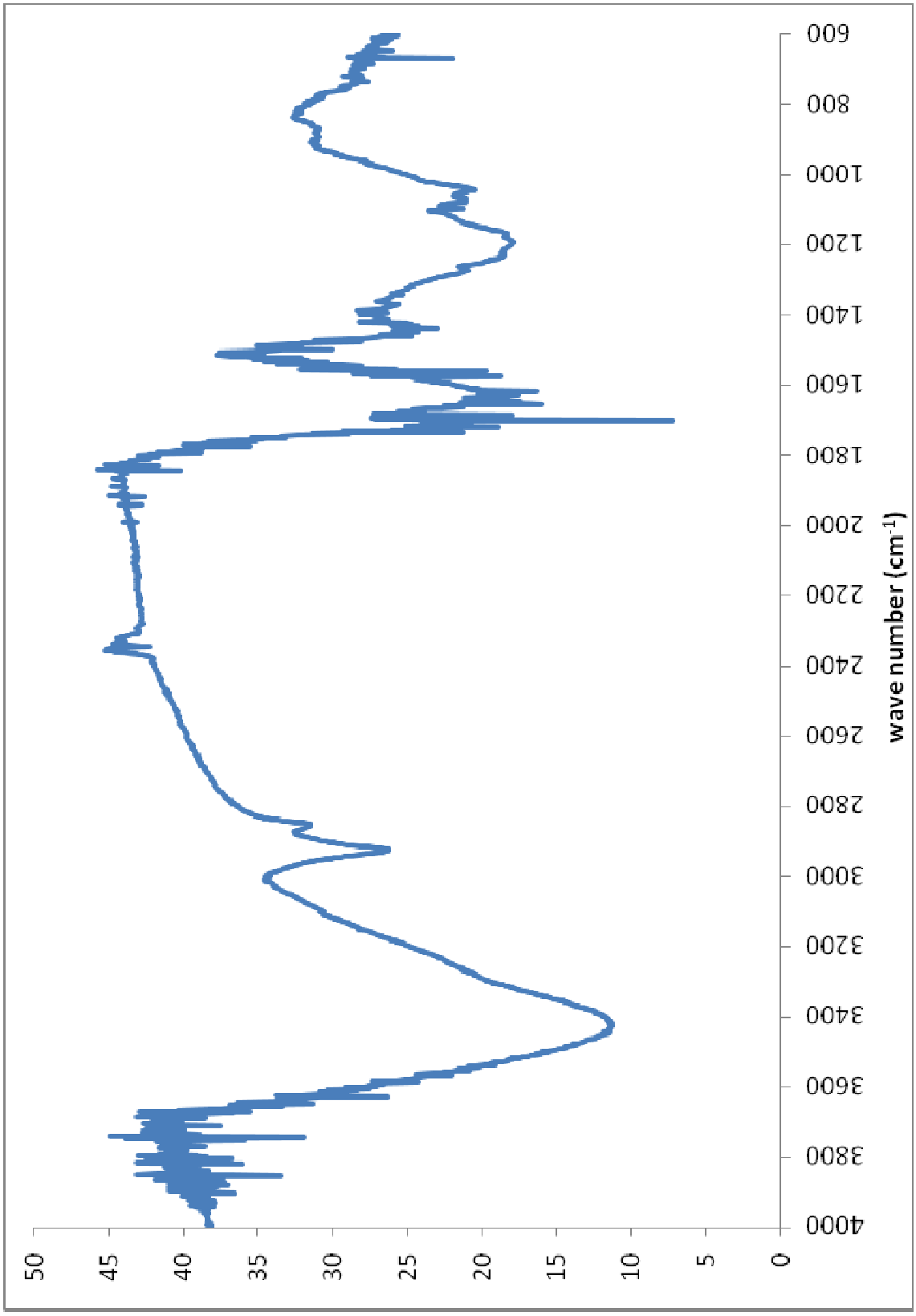

Appendix I, 16 – FTIR spectrum of thiosporopollenin <u>26a</u>

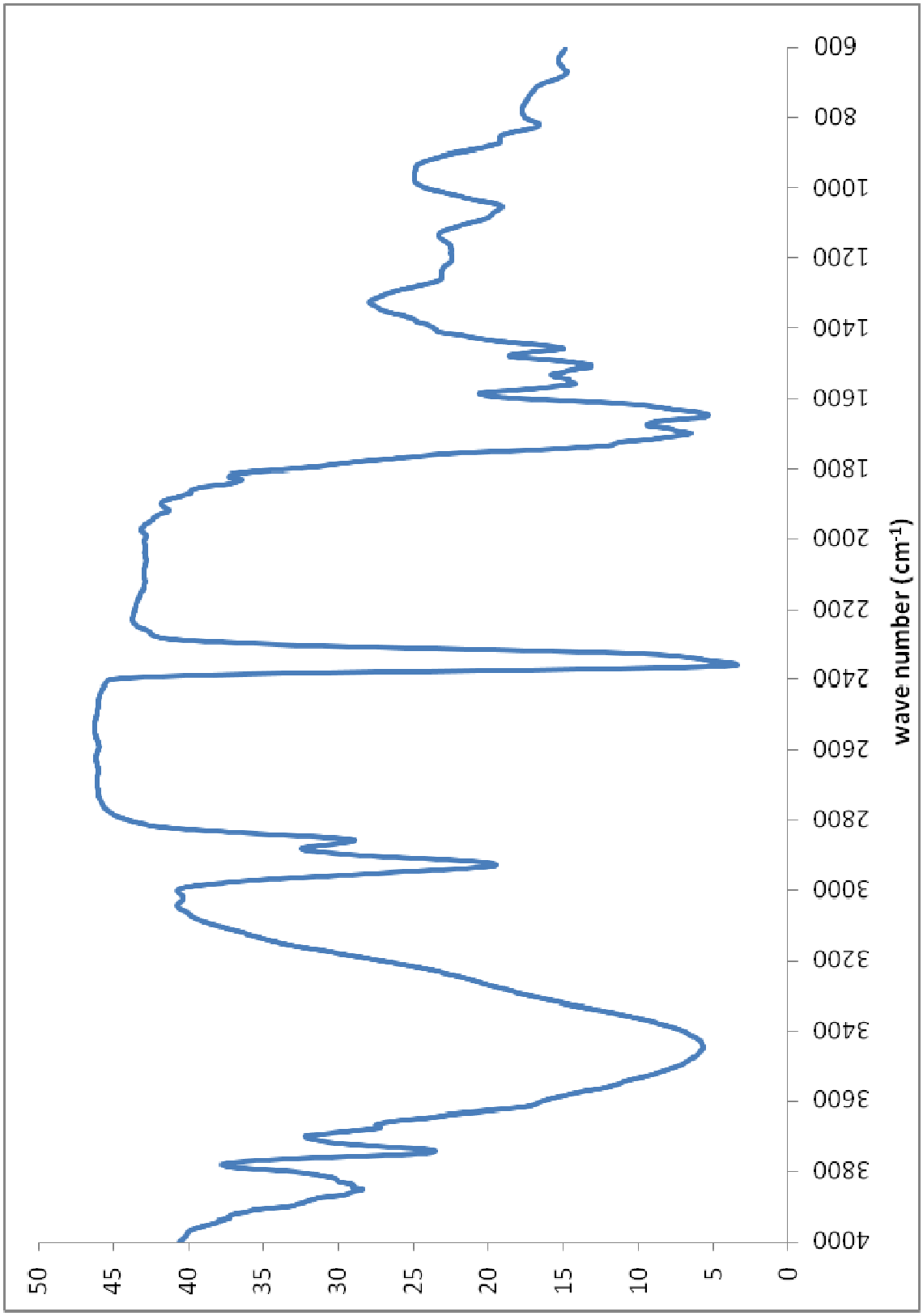

Appendix I, 17 – FTIR spectrum of thiosporopollenin <u>26b</u>

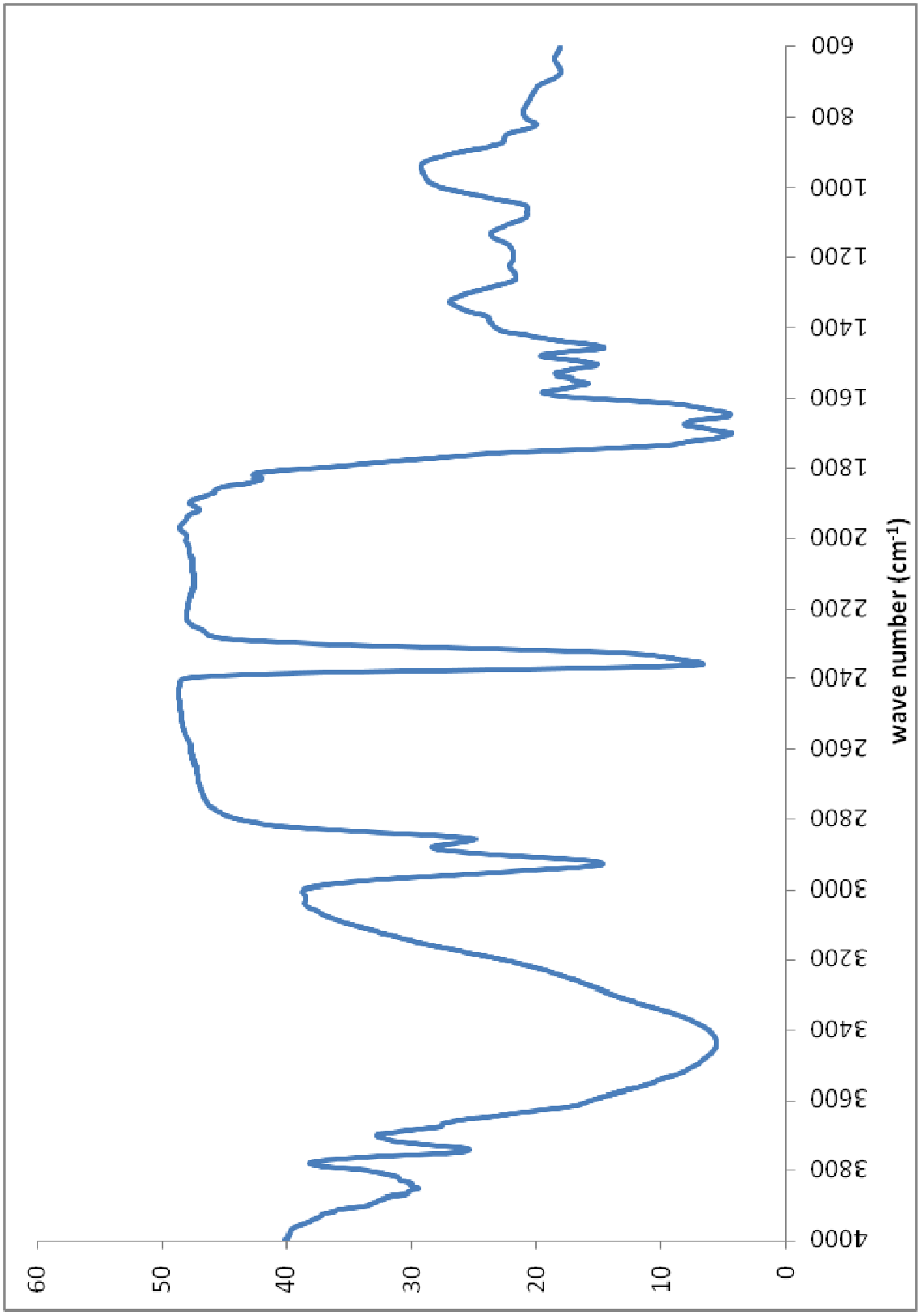

Appendix I, 18 – FTIR spectrum of thiosporopollenin 27

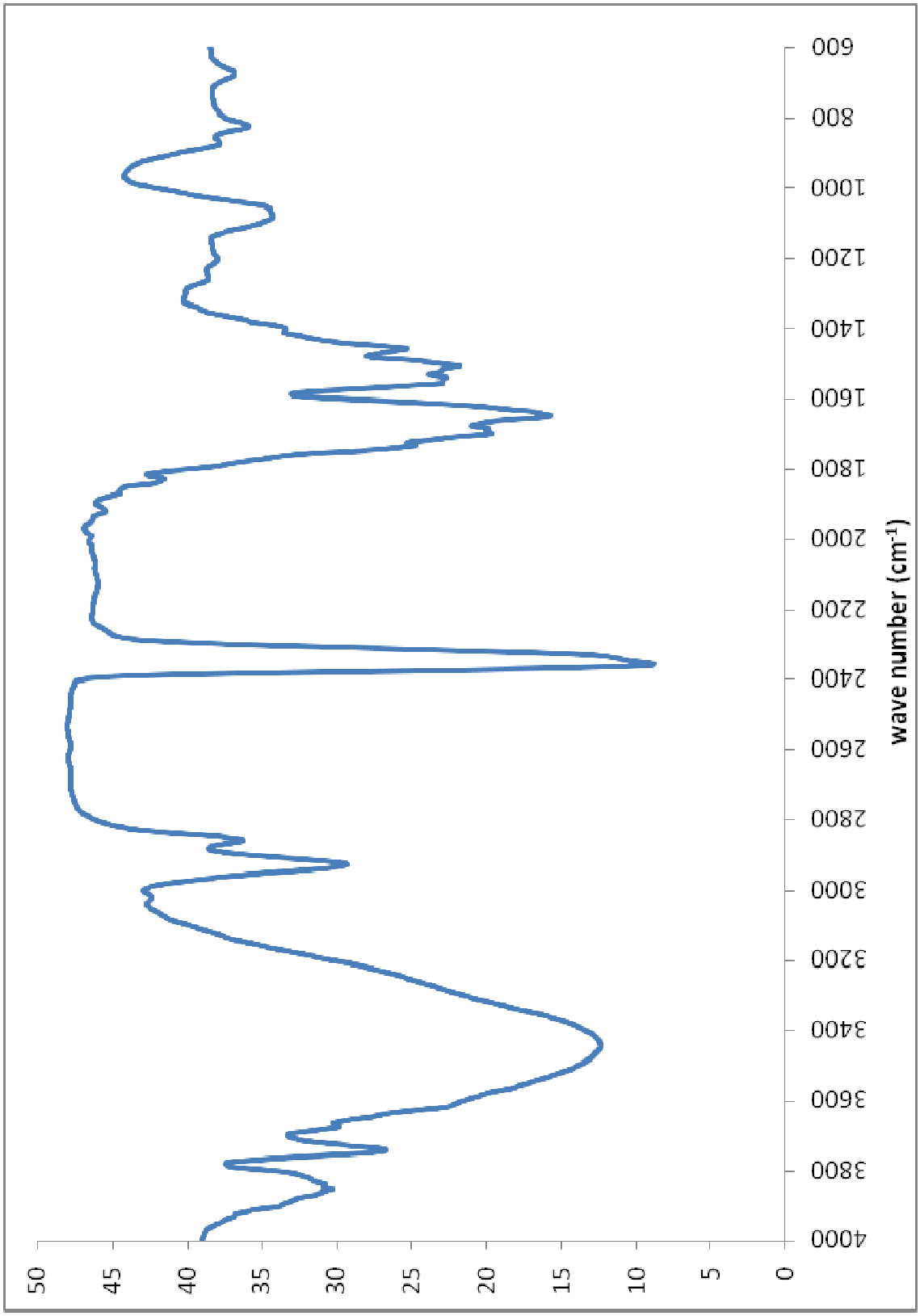

Appendix I, 19 – FTIR spectrum of thiosporopollenin <u>28</u>

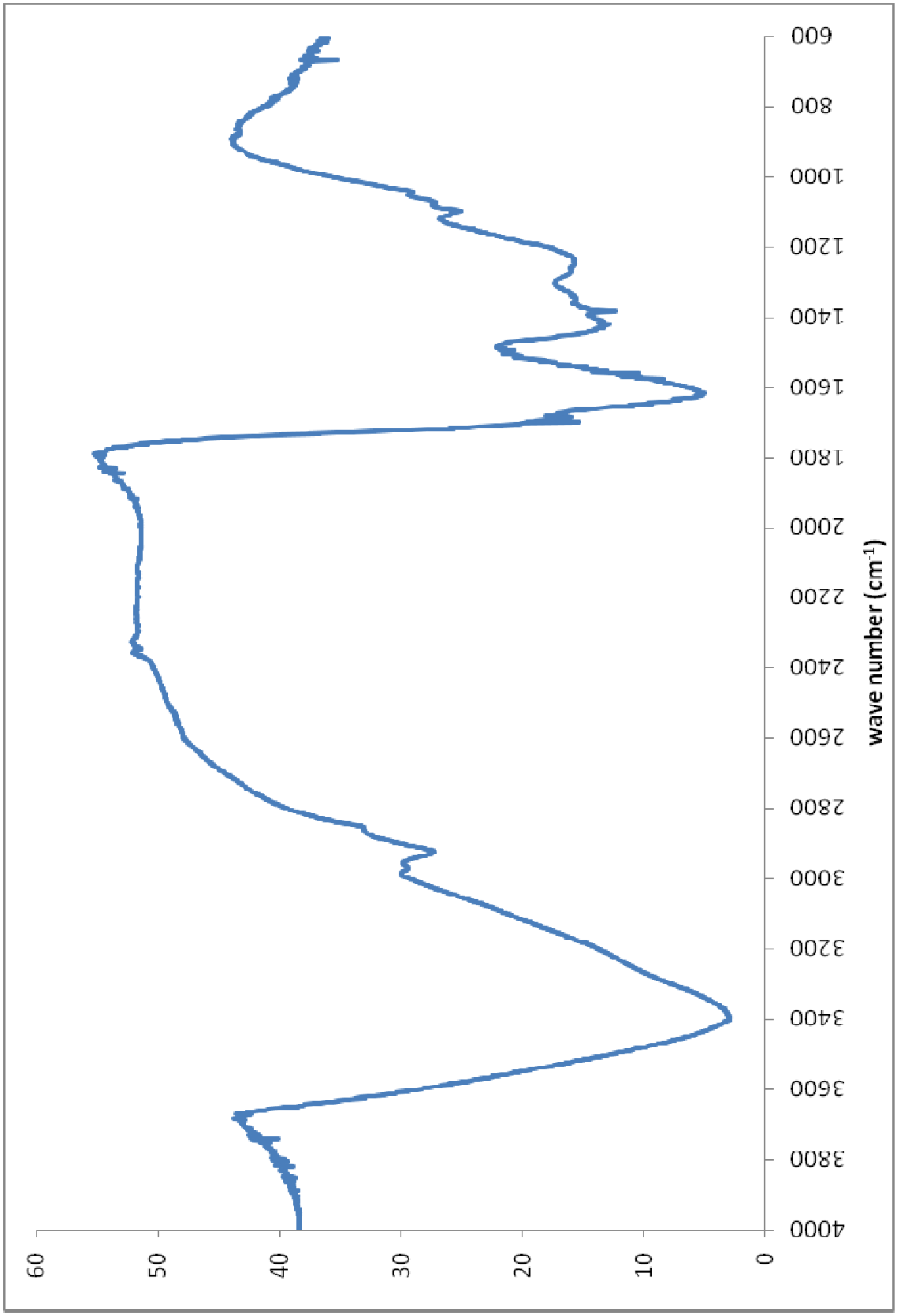

Appendix I, 20 – FTIR spectrum of thiosporopollenin 29

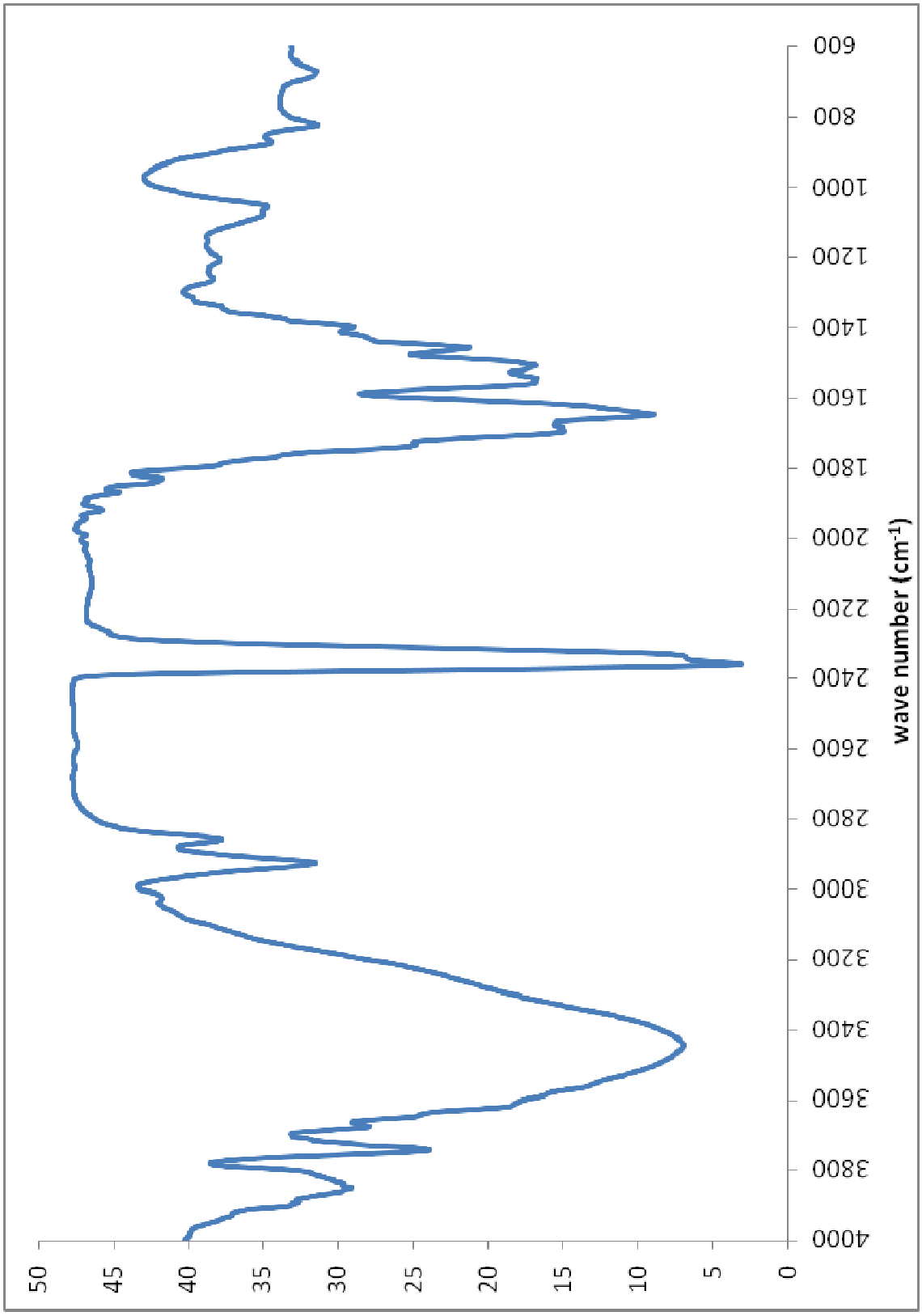

Appendix I, 21 – FTIR spectrum of thiosporopollenin 30

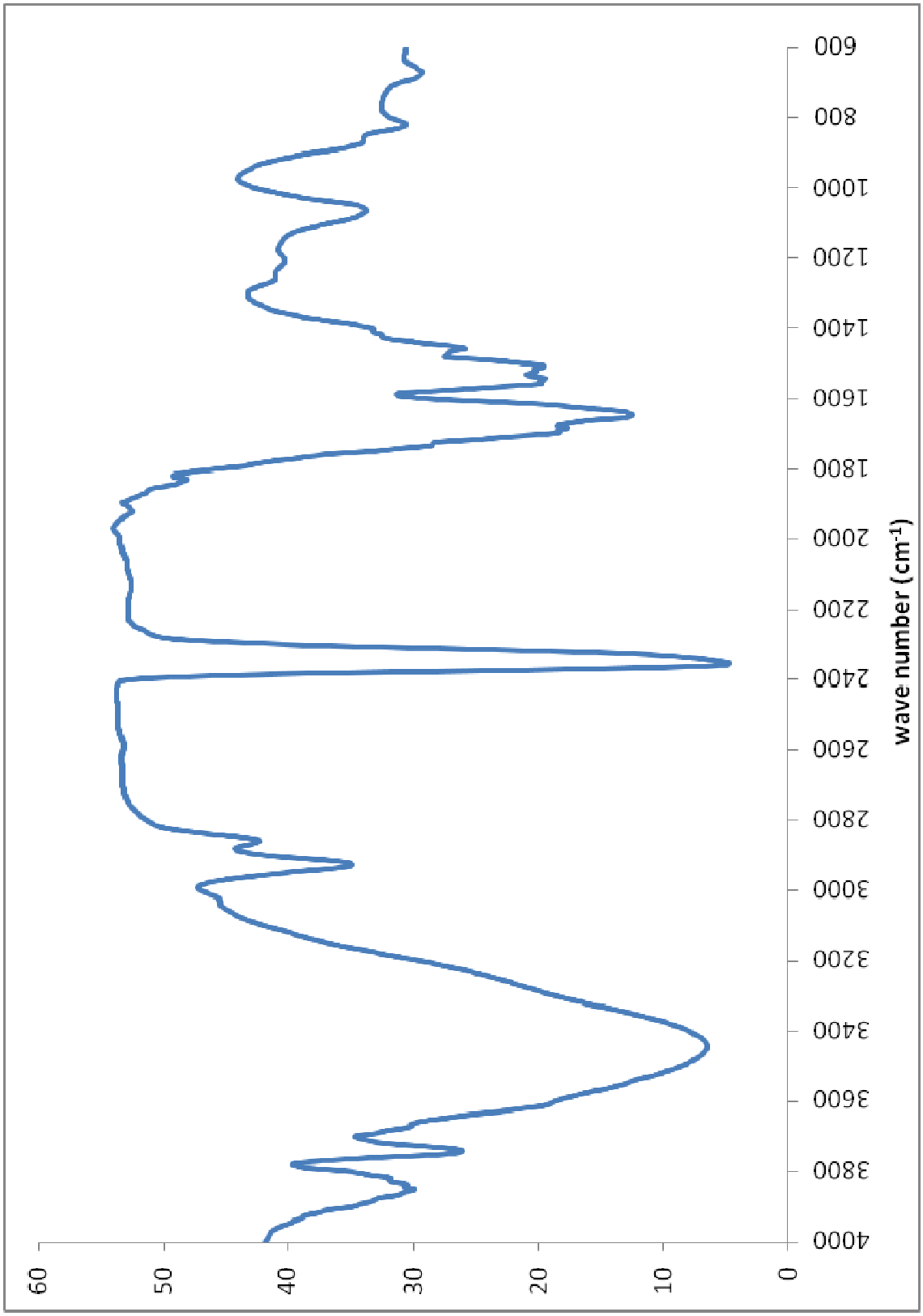

Appendix I, 22 – FTIR spectrum of thiosporopollenin (from thiourea) 31

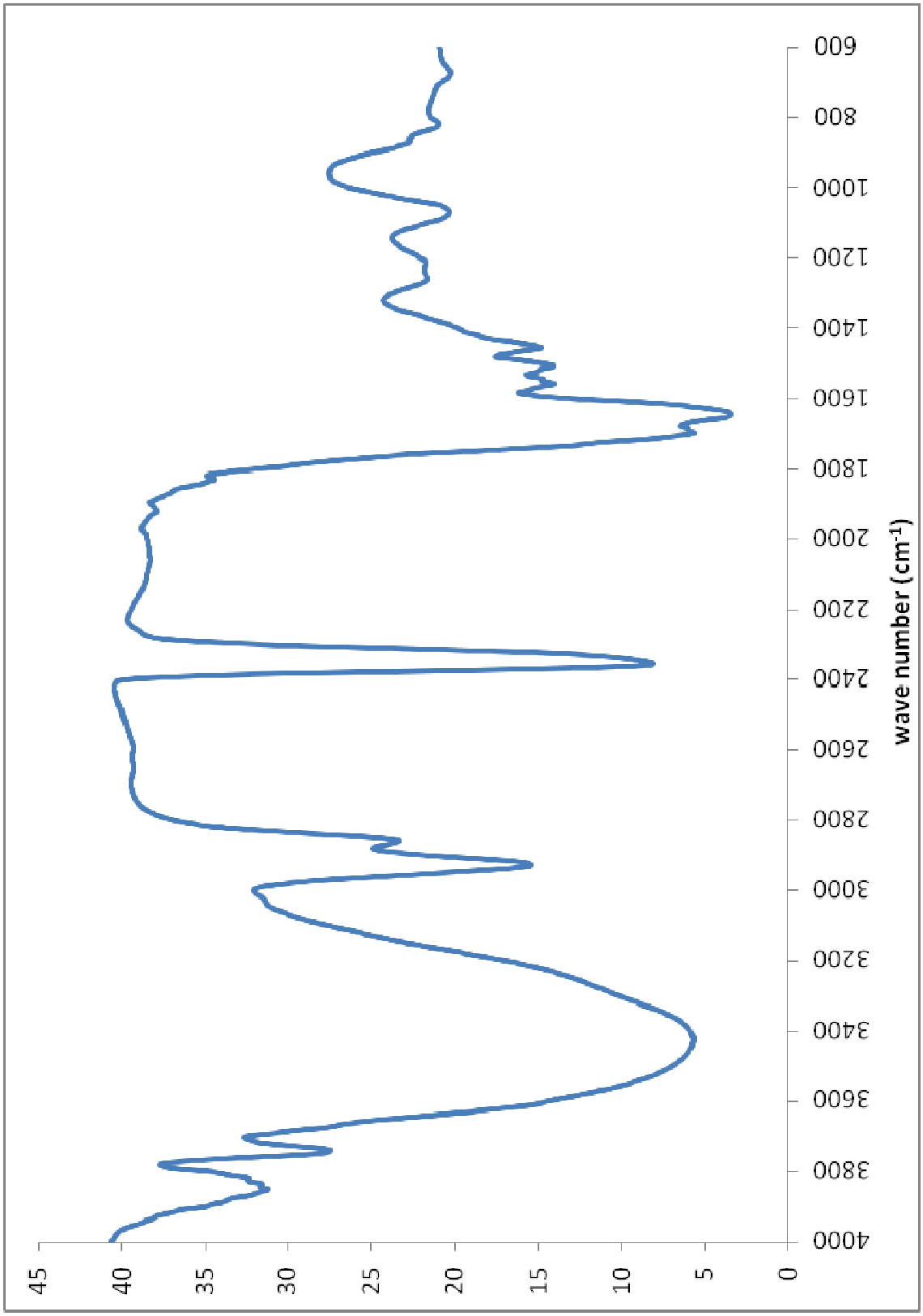

Appendix J-1 – Solid-state ^{13}C NMR spectrum of underivatised sporopollenin (S-type AHS) 1

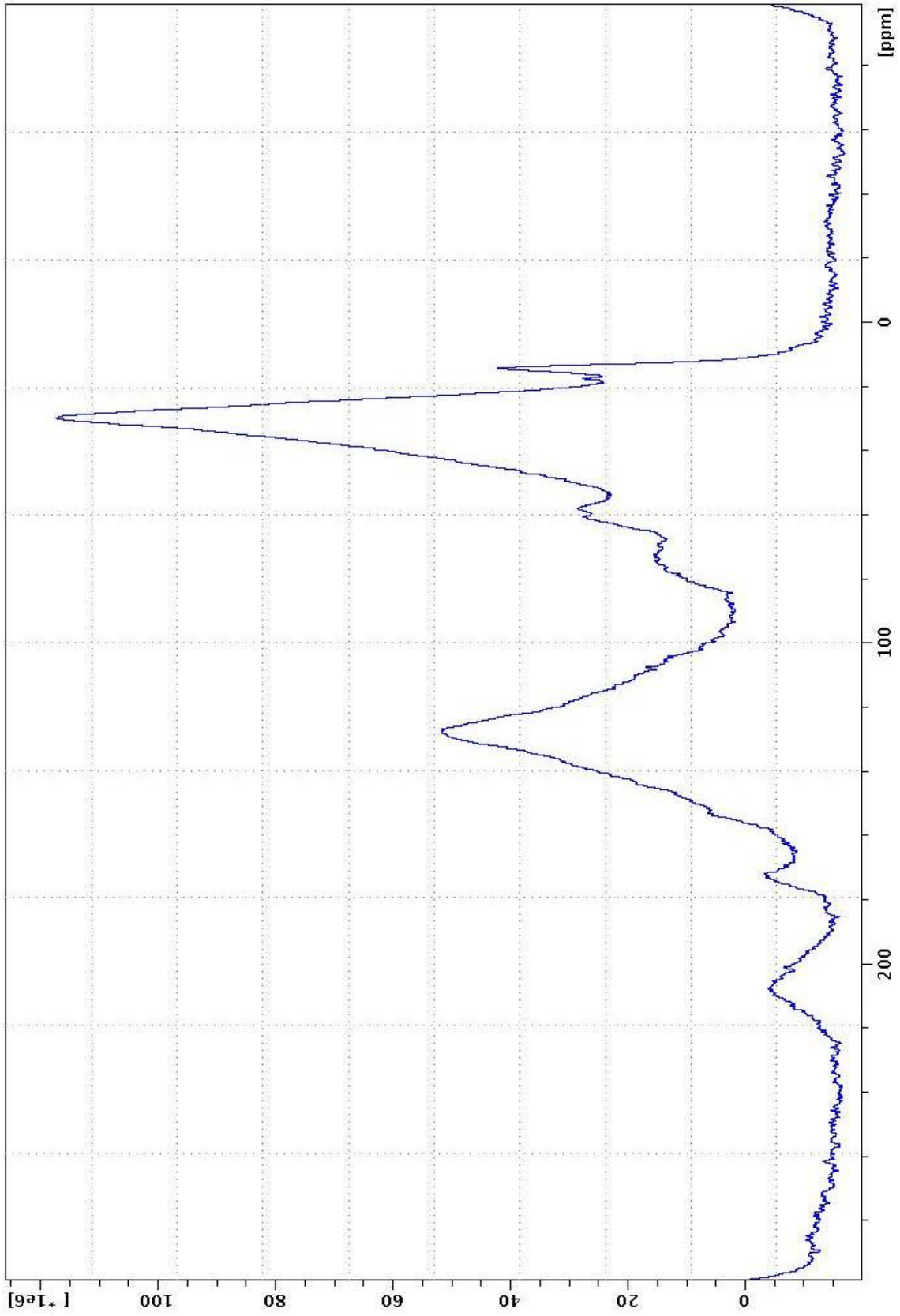

Appendix J-2 – Solid-state ^{1}H NMR spectrum of AHS <u>1</u>

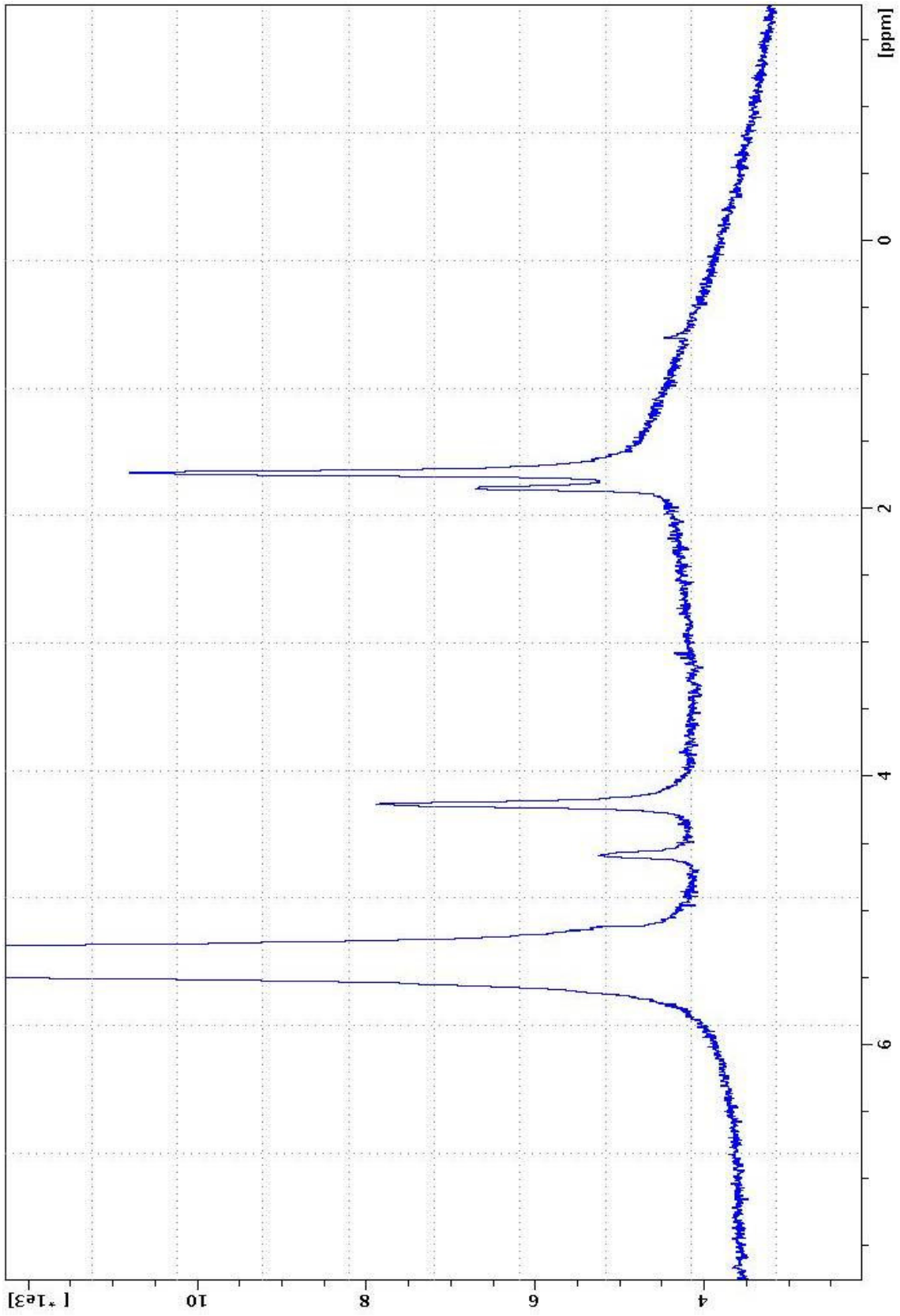

Appendix J-3 – Solid-state ^{13}C NMR spectra of AHS 1, ATS 2 and reduced ATS 3

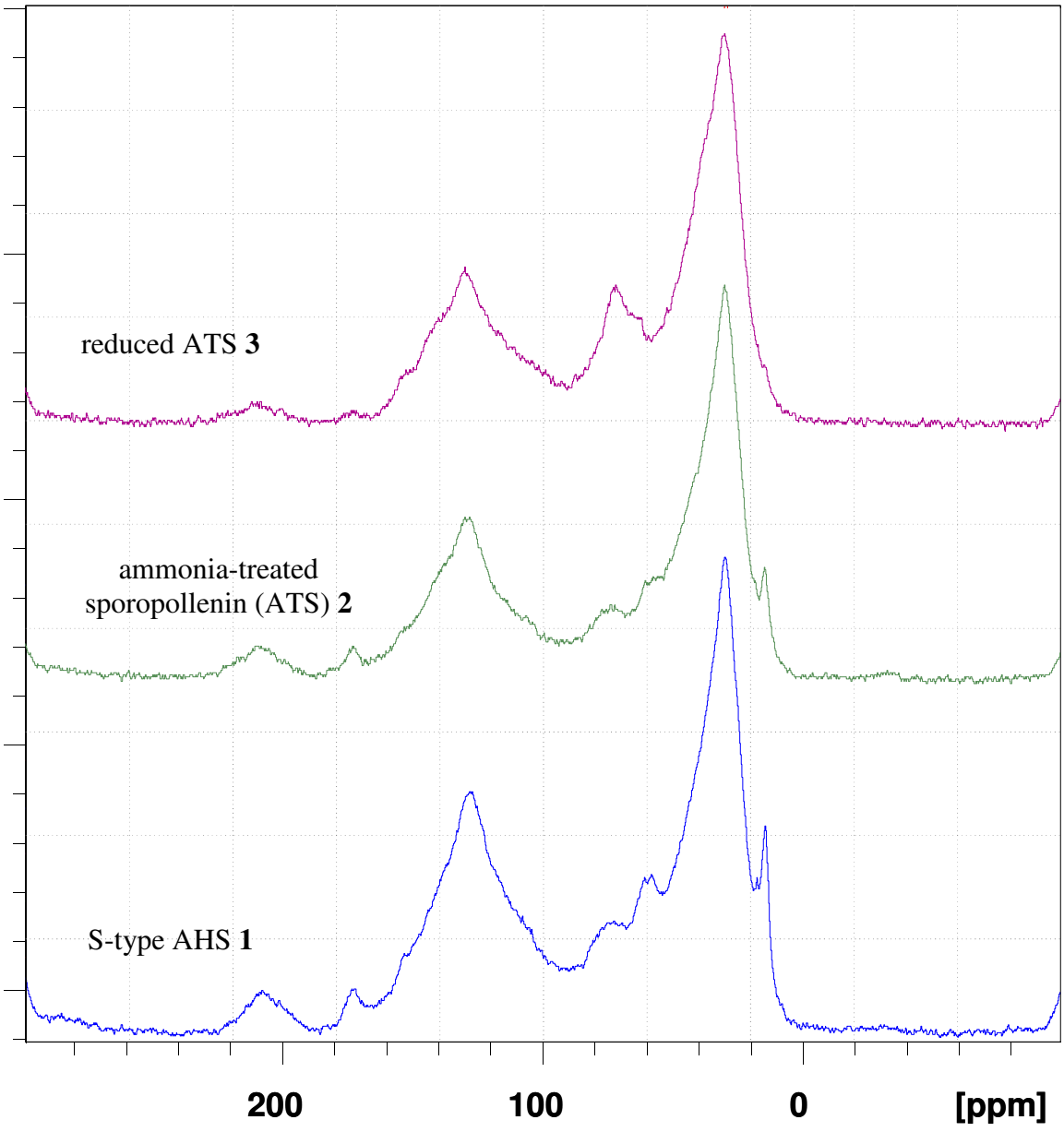

Appendix J-4 – Solid-state ^{15}N NMR spectra of ammonia-treated sporopollenin and its reduced counterpart

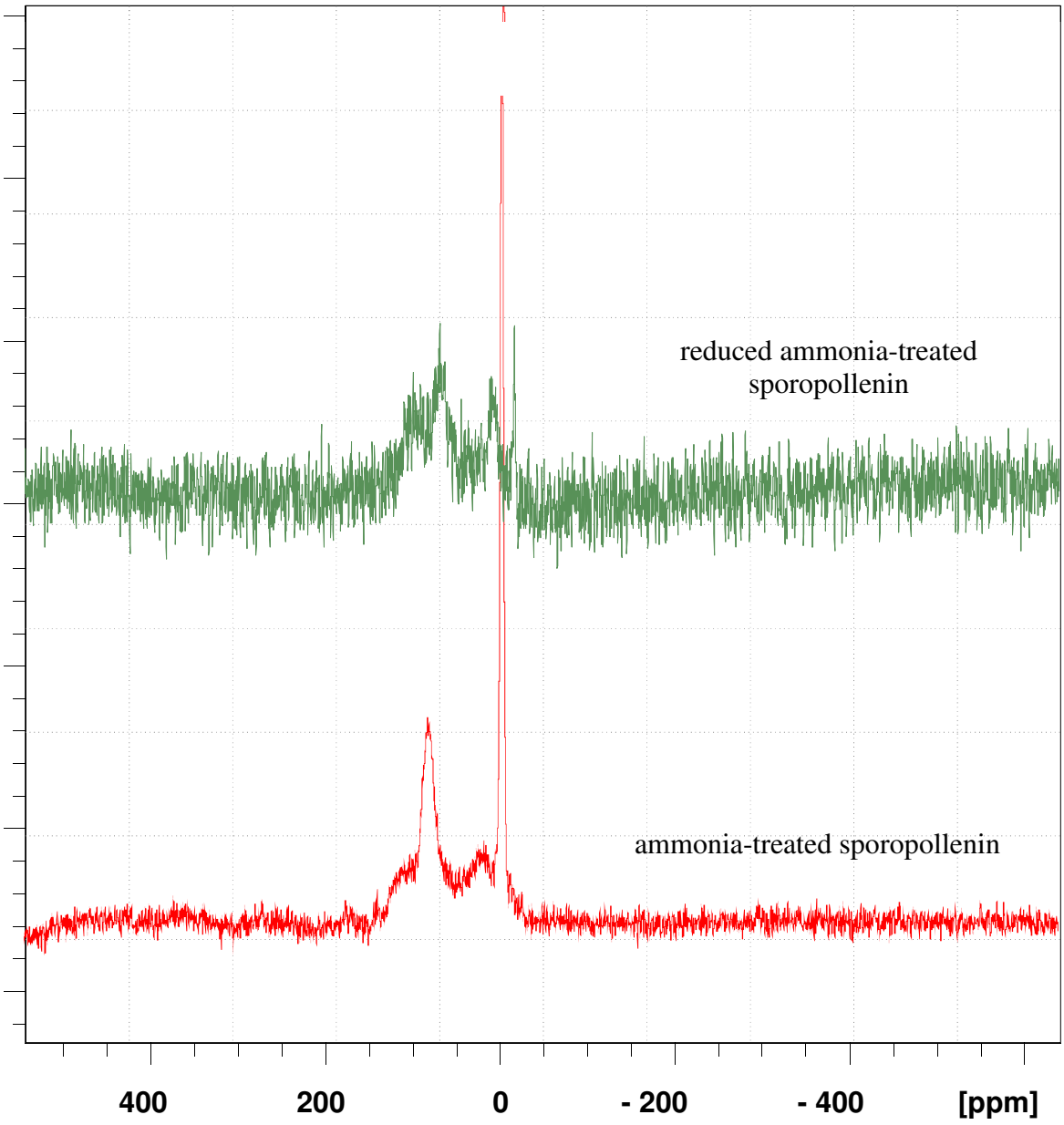

Appendix J-5 – Solid-state ^{15}N NMR spectra of dodecylamine-treated sporopollenin and its reduced counterpart

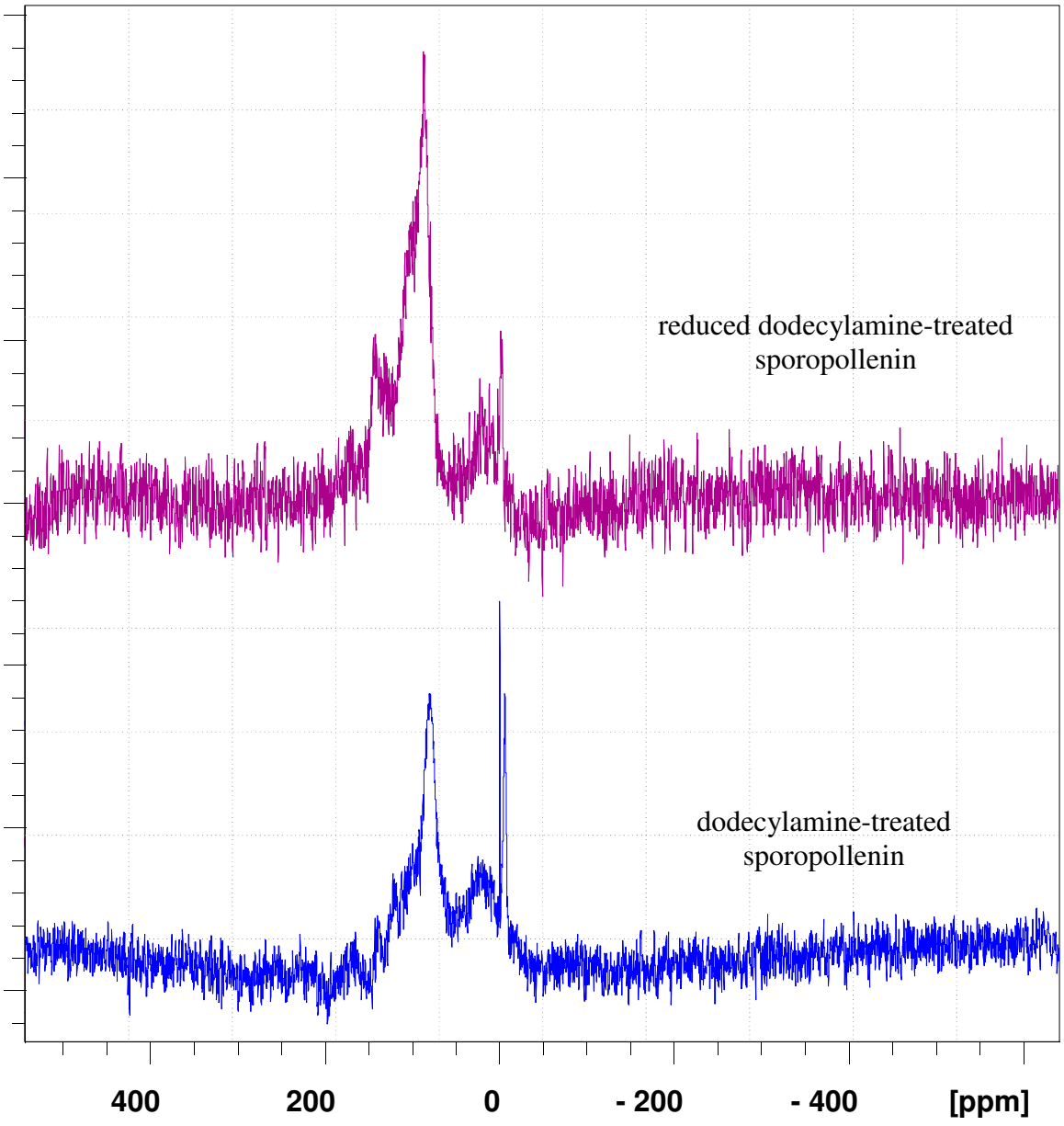

Appendix J-6 – Solid-state ^{13}C NMR spectra of amine-treated sporopollenins